

## Tu-Pos21

A LINEAR MOTOR - A FURTHER FUNDAMENTAL FOR SOLUTE TRANSPORT ELUCIDATED WITH THE ADP/ATP CARRIER (M. Klingenberg) Institute of Physical Biochemistry, University of Munich, Goethestrasse 33, 80336 Munich.

The ADP/ATP carrier (AAC) has been a key element in elucidating fundamentals of transport through biomembranes, such as demonstrating for the first time on the molecular level the single-binding centre-gated pore mechanism (SBCGP, 1969) and the induced transition fit (ITF) of carrier catalysis (1983). Also in structure information the AAC had a pioneering role being the first carrier of which the primary structure became known (1978), and it was the first example for evidence for non-helical intrachannel loops (1986). The high density of charged residues noted in the AAC early suggested a key role of many of these residues in various elements of the translocation machinery. Several conspicuously positioned charges and charge clusters are repeated threefold in the three repeat domains of the AAC. In the three domain structure these charges form rings around the translocation channel. The charge rings appear to be alternating positive and negative. Site-directed mutagenesis on residues located in these charge rings proves that they are essential for transport. So far, mutational neutralization of the intrahelical arginine charge ring (R96, R204, R294) at the matrix site, of R-clusters (R252 to 4) and of helix terminal negative residues (E45, D149) strongly inhibit AAC activity (Klingenberg, M., Nelson, D.R., BBA 1187, 241-244). Based on a previously applied concept of alternating charge pairing in nucleotide binding and in gating, a model for the translocation of charged solutes is developed. Positive charges along the channel are controlled by negative background charges in alternate charge pairing. The energy trap relief of solute binding is thus obtained as well as the propagation of binding. This energy trap relief by the ITF at the central binding site as well as substrate steering by vestibule charges are elements which cooperate in an electro-mechanical machinery which we term a "linear motor" for solute transport. The conditions differ fundamentally from the ion displacement mechanism in  $\text{Cl}^-$  (CFTR) and  $\text{Ca}^{2+}$  channels.

## Tu-Pos23

INHIBITION OF THE MITOCHONDRIAL PERMEABILITY TRANSITION PORE BY CYCLOSPORIN A IS MEDIATED BY MITOCHONDRIAL CYCLOPHILIN AND DOES NOT INVOLVE CALCINEURIN. ((A. Nicolli, E. Basso, V. Petronilli and P. Bernardi)) CNR and Department of Biomedical Sciences, University of Padova, 35121 Padova, Italy (Spon. by M. Zoratti)

The mitochondrial permeability transition pore (MTP) is a voltage-dependent mitochondrial channel inhibited by cyclosporin A (CsA) (see Bernardi et al., 1994, *J. Bioenerg. Biomembr.*, Oct. issue, for a recent review). We have investigated the still debated mechanism of MTP inhibition by CsA with a series of CsA derivatives with different affinities for cyclophilin and calcineurin. We show that the relative potency of all the tested derivatives at inhibiting the MTP and the peptidyl-prolyl-cis-trans-isomerase (PPIase) activity of both cyclophilin A and mitochondrial cyclophilin is similar. The match between MTP inhibition and PPIase activity is particularly good for mitochondrial cyclophilin, strongly indicating that this cyclophilin is the endogenous mediator of CsA inhibition of the pore. Interestingly, the N-MethylVal-4 derivative of CsA was as effective as CsA itself. Since the complex of cyclophilin with this derivative cannot bind calcineurin and is therefore devoid of immunosuppressive activity, these experiments indicate that calcineurin is not involved in CsA inhibition of the MTP. These findings provide a unique tool to discriminate calcineurin-dependent and -independent effects at the cellular level, and might expand our knowledge of MTP-related functions in intact cells.

## Tu-Pos25

BUTYLATED HYDROXYTOLUENE (BHT) AND INORGANIC PHOSPHATE ( $\text{P}_i$ ) PLUS  $\text{Ca}^{2+}$  ACTIVATE THE MITOCHONDRIAL PERMEABILITY TRANSITION PORE (PTP) via MUTUALLY EXCLUSIVE MECHANISMS. ((P.M. Sokolove and L.M. Haley)) Department of Pharmacology & Experimental Therapeutics, University of Maryland Medical School, Baltimore, MD 21201.

Mitochondria undergo a permeability transition (PT), i.e., become non-selectively permeable to small solutes, in response to a wide range of conditions/compounds. In general, PTP opening is  $\text{Ca}^{2+}$ - and  $\text{P}_i$ -dependent and is blocked by ADP, cyclosporin A (CsA), and trifluoperazine (TFP). Guduz and coworkers have reported [(1992) 7th European Bioenergetics Conference, EBEC Short Reports, 7, 125], however, that BHT induces PTP opening that may not share all of these characteristics. We have used mitochondrial swelling, followed as a decrease in apparent absorption at 540 nm, to compare the PTs induced by BHT and  $\text{P}_i$  +  $\text{Ca}^{2+}$  with the following results. (1) BHT effects depend on the ratio of BHT to mitochondrial protein. (2) At concentrations > 75 nmol/mg mitochondrial protein, BHT induces swelling that is relatively insensitive to EGTA and N-ethylmaleimide (NEM) and is stimulated by ADP, CsA, and TFP. (3) Lower BHT concentrations inhibit swelling triggered by  $\text{P}_i$  +  $\text{Ca}^{2+}$ . (4) A  $\text{P}_i$  concentration > 100  $\mu\text{M}$  is required to support swelling triggered by  $\text{Ca}^{2+}$ ; this swelling is eliminated by EGTA or NEM. (5)  $\text{P}_i$  concentrations < 100  $\mu\text{M}$  inhibit BHT-induced PTP opening. (6) TFP (< 25  $\mu\text{M}$ ) inhibits the PT triggered by  $\text{Ca}^{2+}$  + 200  $\mu\text{M}$   $\text{P}_i$ ; higher TFP concentrations enhance the BHT-induced PT. We propose that BHT and  $\text{P}_i$  +  $\text{Ca}^{2+}$  induce the PT by mutually exclusive mechanisms; several agents are identified that favor one mechanism while blocking the other. [Supported by a Grant-in-Aid (#94007080) from the American Heart Association and its MD Affiliate]

## Tu-Pos22

TYPE-1 HUMAN PORIN BIOTINYLATED AT OUTER SURFACES OF TRY PAN BLUE EXCLUDING B LYMPHOCYTES. ((Ch. Jakob, H. Goetz, S. Reymann, and F.P. Thinnies)) MPI Exper. Med., Hermann-Rein-Str.3, 37075 Göttingen, Germany (Spon. by C.A. Manella).

In 1989 we presented the first immuno-topological evidence on the expression of the TYPE-1 VDAC "Porin 31HL" in the plasmalemma of human B lymphocytes. Meanwhile, data from different laboratories accumulated indicating a multi-topological expression of VDAC (Thinnies et al., *Biol.Chem.Hoppe-Seyler* 375, 315-322, 1994).

We now show by two-dimensional SDS-PAGE in combination with Western and Avidin blotting that part of the TYPE-1 human porin of proven living B lymphocytes can be biotinylated at their outer cell surfaces.

These results prove expression of VDAC in the plasmalemma of mammalian cells. They will be discussed in the context of results from different approaches supporting plasmalemma-integrated VDAC, putatively forming part of a chloride channel complex.

## Tu-Pos24

TWO CLASSES OF THIOL GROUPS MODULATE VOLTAGE SENSING BY THE MITOCHONDRIAL PERMEABILITY TRANSITION PORE. ((P. Costantini, V. Petronilli and P. Bernardi)) CNR and Department of Biomedical Sciences, University of Padova, 35121 Padova, Italy (Spon. by K.D. Garlid)

The mitochondrial permeability transition pore (MTP) is a voltage-dependent mitochondrial channel inhibited by cyclosporin A (see Bernardi et al., 1994, *J. Bioenerg. Biomembr.*, Oct. issue, for a recent review). We have shown that a dithiol-disulfide interconversion plays an important role in the regulation of voltage sensing by the MTP: a higher open probability is associated with the disulfide, while a lower open probability is associated with the dithiol. The effect of thiol oxidants can be prevented by substitution with N-ethylmaleimide (NEM) and can be reverted by reduction with dithiothreitol, suggesting that this site is modulated by redox mediators and is potentially important in pathophysiology (Petronilli et al., 1994, *J. Biol. Chem.* 269, 16638). Since NEM also inhibits a variety of transport systems, including the  $\text{P}_i$  carrier, we have screened a series of sulfhydryl reagents to find a more specific inhibitor of the MTP at the voltage sensor. We describe here for the first time the effects of monobromobimane (MBM) on MTP voltage sensing and  $\text{P}_i$  transport in mitochondria. We show that (i) MBM blocks the effects of dithiol oxidants and crosslinkers at the voltage sensor but does not inhibit the  $\text{P}_i$  carrier; and (ii) that based on the differential sensitivity to MBM and NEM two classes of sulfhydryl groups affecting MTP voltage sensing can be defined.

## Tu-Pos26

TWO ATP-SENSITIVE ANION CHANNELS ARE PRESENT IN THE INNER MEMBRANE OF YEAST MITOCHONDRIA. ((C. Ballarin and M.Catia Sorgato)) Dipartimento di Chimica Biologica, Università di Padova, 35121 Padova, Italy.

We applied the patch clamp technique to yeast mitoplasts isolated from *Saccharomyces cerevisiae* wild type and VDAC-less strains, in order to investigate the electric activity of the inner mitochondrial membrane (IMM). In our experimental conditions we found that such activity was different from that displayed by mammalian mitoplasts, primarily for the absence, in the yeast IMM, of the voltage dependent anionic 107 pS channel which is considered the marker channel of IMM in mammalian tissues. On the contrary, in all yeast strains examined two other types of slightly anionic channels were identified, in both "mitoplast"-attached and excised patches. One type of channel, showing infrequent (~15 per minute) and brief openings (at 40 mV the mean open time is 10 msec) at both positive and negative (matrix) potentials, had a mean conductance of approximately 45 pS (in 150 mM KCl) which rectified slightly at positive potentials. The open probability showed only a marginal voltage dependence and the activity was insensitive to various inhibitory agents of known inner mitochondrial membrane proteins. Conversely, mM concentrations of ATP, added to the matrix side of the membrane, completely blocked the channel activity ( $\text{IC}_{50} = 0.24$  mM). The other type of channel found had a much higher conductance which also rectified at positive potential (375 pS at -40mV; 720 pS at 40 mV). The open probability was markedly dependent upon voltage in such a way that closures were enhanced at negative potentials. In this case also, matrix ATP affected the channel behaviour, albeit by a different mechanism, in that it abolished the voltage sensitivity by inducing a permanent open state at all applied voltages.

## Tu-Pos27

**UNCOUPLERS AS PROBES FOR MITOCHONDRIAL CHANNELS** ((M.L. Campo<sup>1</sup>, H. Tedeschi<sup>2</sup>, C. Muro<sup>1</sup> and K. W. Kinnally<sup>3</sup>)) <sup>1</sup>Dpto Bioquímica y Biol. Molecular, Univ. Extremadura, Cáceres, Spain, <sup>2</sup>Biology, SUNY Albany, N.Y., <sup>3</sup>Wadsworth Center, New York State Department of Health, Albany, N.Y.

Probes, e.g. sulfhydryl reagents, are used to identify important protein domains by evaluating their effects on activity. We had reported the respiratory uncouplers FCCP and CCCP perturb the two predominant channel activities in patch-clamp studies of mouse liver mitoplasts. These agents appear to act as slow blockers of mitochondrial Centum picoSiemen activity at  $\mu$ M. At similar  $\mu$ M, uncouplers also influence the open probability of Multiple Conductance Channel. While the effects on both channels are sometimes reversible by perfusion with medium (no uncoupler), reversibility is seen in all the excised patches tested by perfusion with the uncoupler plus 1 mM dithiothreitol (DTT). CCCP and DTT are known to affect sulfhydryl groups. While alternative interpretations are possible, these findings suggest sulfhydryl groups may be involved in the uncoupler effects. In addition, the  $\mu$ M IC<sub>50</sub>s suggest that these sites are distinct from those involved in classical uncoupling. This study was supported in part by Spanish DGICYT PB92-0720 and National Science Foundation Grant MCB 9117658.

## Tu-Pos29

**TEMPERATURE PLAYS A CRITICAL ROLE IN MODULATION OF THE MITOCHONDRIAL INNER MEMBRANE ANION CHANNEL (IMAC).** ((A.D. Beavis, G. Liu, M. Powers and H. Davatol-Hag)) Medical College of Ohio, Toledo, OH 43699

IMAC is an anion channel which at 25°C is inhibited by matrix Mg<sup>2+</sup> (IC<sub>50</sub> = 40  $\mu$ M) and by matrix protons (pIC<sub>50</sub> = 7.8). At pH 7.4, the activity is strongly dependent on matrix volume especially in isotonic salt (= 150 mM KCl). Increasing the temperature to the physiological range 35°-40°C markedly changes all of these properties and at pH 7.4, transport rates are increased more than 5-fold, the IC<sub>50</sub> values for Mg<sup>2+</sup> and H<sup>+</sup> are substantially increased, and the volume dependence is diminished. Arrhenius plots of the temperature dependence are nonlinear and are consistent with a model in which the open probability (P<sub>o</sub>) of IMAC increases with temperature. This model may be described by the equation:

$$\ln v = A + \ln T - \frac{\Delta H^\ddagger}{RT} + \frac{\Delta S^\ddagger}{R} - \ln \left( 1 + \exp \left( \frac{\Delta H}{RT} - \frac{\Delta S}{R} \right) \right)$$

where  $\Delta H^\ddagger$  and  $\Delta S^\ddagger$  are the enthalpy and entropy of activation for the transport step and  $\Delta H$  and  $\Delta S$  are the changes in enthalpy and entropy associated with opening of the channel at equilibrium. At pH 8.4,  $\Delta H^\ddagger$  = 29 kJ/mol, which is in the same range as values reported for the single channel conductance of other ion channels. The ratio  $\Delta H/\Delta S$  gives the temperature at which P<sub>o</sub> = 0.5 and this increases from 16°C at pH 8.4 to 29°C at pH 7.4 as a consequence of an increase in  $\Delta H$  from 158 to 170 kJ/mol. These findings indicate that at physiological temperatures, the activity of IMAC is very much greater than predicted by its behavior at 25°C. (This work was supported by NIH grant HL/GM 47735).

## Tu-Pos31

**PROGRESS TOWARD IDENTIFICATION AND PURIFICATION OF THE MITOCHONDRIAL INNER MEMBRANE ANION CHANNEL (IMAC).** ((G. Liu, Y. Lu and A.D. Beavis)) Medical College of Ohio, Toledo, OH 43699

The mitochondrial inner membrane anion channel is an anion transport pathway, which is reversibly inhibited by matrix Mg<sup>2+</sup> and H<sup>+</sup>, and irreversibly inhibited by dicyclohexylcarbodiimide (DCCD). We now present evidence that reaction of DCCD with IMAC requires protonation of a site with a pK of 7.8. We have also shown that proteins with MW values of 69 kD, 50 kD plus four close to 30 kD are labeled by <sup>14</sup>C-DCCD in intact mitochondria in a pH-sensitive manner. When mitochondrial proteins are solubilized with Triton X-100, reconstituted into proteoliposomes and fused with planar lipid bilayers, an anion channel can be observed which has a conductance of around 100 pS with salt gradient (600 mM KCl cis:60 mM KCl trans) across the bilayer. We also observe the activity of this channel in the flow-through of a hydroxylapatite column. We have repeated this fractionation using mitochondrial proteins treated with <sup>14</sup>C-DCCD at high and low pH, and find one or more bands are labeled in a pH-sensitive manner. When proteins extracted from submitochondrial particles are passed through a DEAE-cellulose column, we find the channel activity is eluted by 100 mM KCl together with a K<sup>+</sup> channel. Passage of this fraction through a Mono Q HPLC column appears to separate the two channels. The anion channel fraction contains at least two bands with the same molecular weight as bands eluted from the hydroxylapatite column. (This work was supported by NIH Grant HL/GM 47735).

## Tu-Pos28

**MULTIPLE CONDUCTANCE CHANNEL ACTIVITY FROM WILD-TYPE AND VDAC-LESS YEAST MITOPLASTS** ((Timothy Lohret and Kathleen Kinnally)) Dept. Biol. Scie. SUNY at Albany, Albany, N.Y. and Wadsworth Center for Laboratories and Research, NYS Dept. of Health, Albany, N.Y.

A multiple conductance channel activity (MCC) is found in wild-type yeast mitoplasts that is very similar to that previously described by us in mammalian mitoplasts using patch clamp techniques. This activity was found to be present but with an altered voltage dependence in mitoplasts of a VDAC-deletion mutant yeast. These results suggest that while VDAC is not required for MCC activity, VDAC may play some role in modifying MCC gating. MCC activity reconstituted in liposomes from detergent solubilized inner membranes is subject to modulation by physiological effectors, e.g. pH. Preliminary results indicate this activity is also influenced by a mitochondrial addressing leader peptide and comparisons with PSC activity are underway. This study was supported in part by National Science Foundation Grant MCB 9117658.

## Tu-Pos30

**THE MITOCHONDRIAL INNER MEMBRANE ANION CHANNEL (IMAC) IS INHIBITED BY DIDS.** ((A.D. Beavis and H. Davatol-Hag)) Medical College of Ohio, Toledo, OH 43699.

DIDS (4,4'-diisothiocyanostilbene-2,2'-disulfonic acid) is a potent irreversible inhibitor of the Cl<sup>-</sup>/HCO<sub>3</sub><sup>-</sup> exchanger and also inhibits many Cl<sup>-</sup> channels. We have now shown that this compound inhibits IMAC in intact mitochondria. IMAC is an anion channel which is regulated by Mg<sup>2+</sup> and protons and conducts a wide variety of anions ranging from small monovalent anions such as Cl<sup>-</sup>, HCO<sub>3</sub><sup>-</sup> and NO<sub>3</sub><sup>-</sup> up to large anions such as ATP<sup>4-</sup>. Many inhibitors have been identified which block this channel in intact mitochondria. DIDS completely blocks the transport of malonate and other anions of equal or larger size with an IC<sub>50</sub> of 17  $\mu$ M and a Hill coefficient of about 0.8. In contrast, inhibition of Cl<sup>-</sup> transport is minimal. The IC<sub>50</sub> value is decreased by N-ethylmaleimide and almost insensitive to pH. These and other properties are similar to those of other inhibitors such as the nucleotide analog Cibacron blue, 3GA and palmitoyl CoA. Combined inhibitor titrations indicate that DIDS and Cibacron blue may in fact compete for the same binding site. This is not surprising, since their structures have certain similarities. The IC<sub>50</sub> for DIDS is in the same range observed for other Cl<sup>-</sup> channels in which inhibition is reversible. These findings suggest that these agents cause IMAC to enter a subconductance state with altered anion selectivity, and raise the question as to whether other DIDS-sensitive Cl<sup>-</sup> channels may be blocked by Cibacron blue and palmitoyl CoA. (This work was supported by NIH grant HL/GM 47735).

## Tu-Pos32

**CHARACTERIZATION AND PARTIAL PURIFICATION OF A MULTI-CONDUCTANCE K<sup>+</sup> CHANNEL FROM SUBMITOCHONDRIAL PARTICLES.** ((Y. Lu and A.D. Beavis)) Medical College of Ohio, Toledo, OH 43699

Several K<sup>+</sup> channels can be observed following extraction of submitochondrial particles with Triton X-100, reconstitution into proteoliposomes and fusion with planar lipid bilayers. We now present a preliminary report on one of them. This channel is characterized by the presence of several conductance states. The most frequently observed have conductances of about 200 pS and 380 pS, less frequently conductance levels of about 600 pS and 800 pS are observed. Under gradient conditions, 600 mM KCl cis:60 mM KCl trans, the selectivity, P<sub>K+</sub>/P<sub>Cl-</sub>, calculated using the Goldman, Hodgkin, Katz equation is about 2.8; however, this increases to 5.5 for the 380 pS transition. Below the reversal potential, only the 200 pS conductance level is observed and the open probability decreases from > 30% down to < 1%. Preliminary data indicate that the conductance is decreased by propranolol and that the channel may be blocked by mersalyl. When the solubilized proteins are fractionated on a DEAE-cellulose column, this channel can be found in the fraction eluted with 100 mM KCl. The channel in this fraction binds to a mercurial affinity column and can be eluted with mercaptoethanol. In addition, this fraction can be further fractionated by passage through a Mono Q HPLC column. We are in the process of employing these and other procedures to purify and identify the channel. (This work was supported by NIH grant HL 36573).

## Tu-Pos33

POTASSIUM CHANNEL OPENER, RP 66471, INDUCES MEMBRANE DEPOLARIZATION OF RAT LIVER MITOCHONDRIA. ((A. Szewczyk, G. Wójcik and M.J. Nalecz)) Nencki Inst. of Exp. Biol., Warsaw, Poland. (Spon. by A. Azzi)

The potassium channel sensitive to ATP ( $K_{ATP}$ ) has been described in the inner membrane of rat liver mitochondria. Activation of this channel should lead to the depolarization of the inner mitochondrial membrane. Hence, effect of potassium channel openers on membrane potential of rat liver mitochondria were studied. It was shown that potassium channel opener RP 66471 induces depolarization of the mitochondrial membrane. The depolarization of mitochondrial membrane was induced exclusively by RP 66471 and not by other related compounds (nicorandil, apykalim, minoxidil sulfate, Ro 31-6930 and KRN 2391). Amplitude of depolarization was significantly larger in the presence of  $K^+$  and  $Rb^+$  ions than in the presence of  $Li^+$  and  $Na^+$  ions. The effect of RP 66471 appears specific since neither the inhibition of mitochondrial respiration nor the uncoupling of mitochondria was observed concomitantly. It was shown that effect of RP 66471 on membrane potential was caused by increasing permeability of inner mitochondrial membrane to potassium ions. Summarizing, our results suggest that mitochondrial  $K_{ATP}$  channel is involved in regulation of membrane potential of liver mitochondria and, as consequence, in regulation of substrate transport into mitochondria.

## Tu-Pos35

INDICATIONS OF A COMMON FOLDING PATTERN FOR VDAC CHANNELS FROM ALL SOURCES. ((J.M. Song, M. Colombini)) Dept. Zoology, Univ. of Maryland, College Park, MD 20742. (Spon. by S. Gupta)

VDAC (mitochondrial porin) is a large channel found in the outer membrane of mitochondria. The structure of the open channel isolated from yeast (*S. cerevisiae*), as mapped by site-directed mutations, consists of 1 alpha helix and 12 beta strands. The functional properties of VDAC isolated from mitochondria of very diverse organisms is highly conserved. This includes single-channel conductance, ion selectivity and voltage dependence. Analysis of the primary sequences now available for VDAC from higher plants, fungi, invertebrates, and mammals indicate that all form channels using homologous regions of the primary sequence. The transmembrane regions are constrained by the necessity to form sided structures, one surface facing the hydrophobic regions of the membrane interior and the other the aqueous pore. The constraints on the beta strands preclude the presence of adjacent charged residues or proline residues. The regions with the appropriate constraints are also those that have homology with the corresponding regions in the sequences from other species. Competing proposals utilizing 16 transmembrane beta strands are in conflict with experimental observations. (Supported by ONR grant # N00014-90-J-1024)

## Tu-Pos37

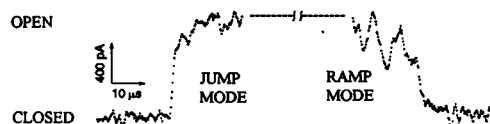
EXPERIMENTAL AND COMPUTATIONAL APPROACHES TO DETERMINING HOW VDAC FOLDS. ((C.A. Mannella<sup>1</sup>, E. Dolginova<sup>1</sup>, S. Stanley<sup>1</sup>, D. D'Arcangelis<sup>1</sup>, C.E. Lawrence<sup>2</sup>, A.F. Neuwald<sup>2</sup>)) <sup>1</sup>The Wadsworth Center, Empire State Plaza, Albany, New York, 12201-0509; <sup>2</sup>National Center for Biotechnology Information, NLM, NIH, Bethesda, MD 20894.

While there is no obvious homology between the primary structures of bacterial and mitochondrial porins, circular dichroism (CD) indicates the two classes of membrane proteins have similar secondary structure (Shao et al. 1994, *Biophys. J.* 66:A21). Proposals for the number of  $\beta$ -strands in VDAC's putative  $\beta$ -barrel range from 12 to 19. Constraints on modeling VDAC are being provided by low-resolution molecular envelopes from electron crystallography and by immunotopological studies, along with CD studies of short peptides representing subsequences in VDAC. Also, we have detected regions in VDAC sequences that are similar to an 11-residue model (identified using a new local multiple alignment algorithm, the Gibbs sampler, Lawrence et al., 1993, *Science* 262:208) corresponding to amphipathic  $\beta$ -strands tilted 30° in bacterial porins of known structure. (Supported in part by NSF grant MCB9219353.)

## Tu-Pos34

OPENING AND CLOSING TRANSITIONS OF A LARGE MITOCHONDRIAL CHANNEL WITH MICROSECOND TIME RESOLUTION. ((J.M. Tang, R.A. Levis, K.G. Lynn, and Bob Eisenberg)) Department of Physiology, Rush Medical College, Chicago, IL 60612 and Department of Physics, Brookhaven National Laboratory, Upton, NY 11973.

We have investigated the single channel current of a large conductance channel from the outer mitochondrial membrane. The gating characteristics of the channel were studied with the tip-dip technique and high bandwidth recording. This channel has a maximum conductance of 7 to 8 nS when recorded in symmetrical 3M KCl solution at room temperature. The channel has several distinct sets of conductance states. It shows different modes of opening and closing behaviors. The time course of opening and closing of the channel has been studied, with resolution of 1.2  $\mu$ sec at a bandwidth of about 300 kHz. Initial data showed the channel able to open and close in less than 1.2  $\mu$ sec. Occasionally, this channel appears to gate in a ramp mode (see figure). The time course is then much slower, often many  $\mu$ sec.



## Tu-Pos36

TOWARDS CRYSTALLIZATION OF THE MITOCHONDRIAL CHANNEL PROTEIN, VDAC ((D. Koppel<sup>1</sup>, P. Masters<sup>1</sup>, L. Shao<sup>2</sup>, C.A. Mannella<sup>1,2</sup>)) <sup>1</sup>The Wadsworth Center, Empire State Plaza, Albany, NY 12201-0509; <sup>2</sup>Departments of Biomedical Sciences and Physics, The University at Albany.

Attempts at crystallizing the mitochondrial porin, VDAC, have been hampered by limiting amounts of the purified protein and by lack of knowledge of its structure in detergents under varying conditions. We have been able to express yeast and fungal VDAC genes (gift of M. Forte, Oregon Health Sciences Univ.) in *E. coli* as fusion proteins with maltose binding protein, using the pMAL expression system. Conditions that optimize cleavage by factor Xa are found to differ for fusion proteins containing the yeast and fungal proteins. Yields of pure yeast VDAC of 20-40 mg/L of bacterial culture are obtained, compared to 0.1-0.2 mg/L of pure VDAC from fungal cultures. Circular dichroism (CD) of VDAC isolated from fungal mitochondria indicates that a high  $\beta$ -sheet structure, characteristic of VDAC's open state in liposomes, is preserved in detergents like octylglucoside and LDAO over a wide range of temperature (4-25°), pH (6-11) and ionic strength. Low pH induces a reversibly closed state with lower  $\beta$ -sheet content, having a CD spectrum like that observed in SDS at pH 7. (Supported by NSF grant MCB9219353.)

## Tu-Pos38

PHYSIOLOGICAL AND PHARMACOLOGICAL ACTIVATORS OF THE MITOCHONDRIAL  $K_{ATP}$  CHANNEL. ((P. Paucek, V. Yarov-Yarovoy, X. Sun, and K. D. Garlid)) Dept. of Chemistry, Biochemistry, and Molecular Biology, Oregon Graduate Institute of Science & Technology, Portland, OR 97291-1000.

The mitochondrial  $K_{ATP}$  channel is inhibited by ATP ( $K_i \approx 50 \mu$ M) in the presence of  $Mg^{2+}$ , which raises the question of how the channel is opened in vivo [Paucek et al. (1992) *J. Biol. Chem.* 267, 26062]. We now report physiological and pharmacological activation of this  $K_{ATP}$  channel. For these experiments, the partially purified, reconstituted  $K_{ATP}$  channel was inhibited by 500  $\mu$ M ATP in 2 mM  $Mg^{2+}$ . (i)  $K^+$  flux was completely reactivated by GTP ( $K_a \approx 7 \mu$ M) and GDP ( $K_a \approx 140 \mu$ M). Guanine nucleotides were without effect on the active state in the absence of ATP. GTP also activated the ATP-inhibited  $K_{ATP}$  channel in intact mitochondria respiring in  $K^+$  + succinate media ( $K_a \approx 3 \mu$ M in 60  $\mu$ M ATP). GTP- $\gamma$ S was as effective as GTP. (ii)  $K^+$  flux was completely reactivated by smooth muscle relaxants known to be  $K^+$  channel openers. Potent pharmacological activators of the mitochondrial  $K_{ATP}$  channel include diazoxide ( $K_a \approx 3 \mu$ M), cromakalim ( $K_a \approx 1 \mu$ M), and two developmental derivatives of cromakalim obtained from E. Merck ( $K_a \approx 7$  nM). Hill slopes are consistent with tetrameric structure. (iii) The mitochondrial  $K_{ATP}$  channel is regulated by nucleotides only on the cytosolic side. (Supported by NIH Grant GM 31086)

## Tu-Pos39

**ELECTROPHYSIOLOGICAL CHARACTERISTICS OF PHOE PORIN CHANNELS. IMPLICATIONS FOR THE EXISTENCE OF A SUPER-FAMILY OF ION CHANNELS.** ((C. Berrier, M. Besnard and A. Ghazi)) Biomembrane lab. URA CNRS 1116, Bat 432, Université Paris-Sud, 91405, Orsay, France.

Bacterial porins are generally described as voltage-dependent pores with two states (open and closed) governed by slow kinetics. A patch-clamp study of purified PhoE from *E. coli* (courtesy of Dr. F. Pattus), reconstituted in giant liposomes, confirms and extends our previous findings with OmpF and OmpC (Berrier et al. 1992. FEBS Lett. 306, 251) and reveals the following characteristics: 1) Channels are fully open at 0 mV and close at positive and negative potentials. However, channels behave asymmetrically in response to positive and negative potentials. 2) Channels exhibit fast and slow kinetics. 3) Channels reach an inactivated state in response to high negative potentials. PhoE channels have at least four different states: an open state, a short-lived closed state, a long-lived closed state and an inactivated state. 4) multiple conductances are observed which might correspond to cooperative transitions and/or to substates. Strikingly, all of these characteristics have been described for the mitochondrial VDAC and for "maxi-chloride" channels of the plasma membrane of animal cells. These common properties might reflect a similar structure. There is no sequence homology between VDAC and bacterial porins. But there is no sequence homology between the porin of *R. capsulatus* and OmpF and PhoE from *E. coli* which share nevertheless the same structure (as revealed by X-ray diffraction). In view of their common electrophysiological properties, we propose that bacterial and mitochondrial porins and maxi-chloride channels are members of a super-family of ion channels whose structure (rather than sequence) has been conserved through evolution.

## Tu-Pos41

**ALTERED VOLTAGE SENSITIVITY IN MUTANT OmpC PORIN CHANNELS** (Nicola D. Bishop and Edward J.A. Lea), School of Biological Sciences, University of East Anglia, Norwich, NR4 7TJ, UK

The outer membrane of *Escherichia coli* K-12 contains aqueous channels, porins which control the diffusion of nutrients and small molecules across it. Besides general diffusion porins, OmpF and OmpC, there is a number of other ones which assist the uptake of specific nutrients. In particular, LamB allows uptake of maltodextrins. In the absence of LamB, the cells do not grow readily on maltodextrins larger than maltotriose, as the larger ones are excluded by OmpC and OmpF on account of their size. By growing a strain expressing solely OmpC on media with maltodextrins as the only carbon source, Misra & Benson<sup>1</sup> obtained mutants involving mutations of the OmpC gene itself, called OmpC (Dex) mutants. The wild type OmpC porin, when incorporated into planar bilayer membranes induces single channel activity largely insensitive to membrane p.d. below 200 mV. The OmpC (Dex) mutants studied<sup>2</sup> show increased channel size and greater voltage sensitivity, closing completely at 200 mV. From structural studies<sup>3</sup> it has been shown that porins have a largely unobstructed lumen except for an internal loop which creates the *eyelet* region. The (Dex) mutants are in this region. By oligonucleotide directed mutagenesis, we have prepared a single point mutation, W56C in the lumen opposite the loop. Incorporated into planar bilayers from one side, the porin exhibits trimeric channel behaviour. The single channel conductivity (one third of a trimer) is approximately 320 pS in 1 M NaCl 10 mM CaCl<sub>2</sub> Hepes pH 7.4. This is much smaller than that of the wild type, 512 pS, measured under similar conditions. The behaviour with respect to the sign of the applied p.d. appears to be completely symmetrical, but the channel has voltage gating characteristics opposite to other porins, i.e. channels close at low p.d. (100-150 mV) and open at high p.d. (250-300 mV). The results imply that a conformational change of the channel results from this single point mutation which may be a key one in understanding the control of the voltage gating and filtration properties. 1. Misra, R. and Benson, S.R. (1988) J. Bacteriol. 170, 3611-3617. 2. Lakey, J.H., Lea, E.J.A. and Pattus, F. (1991). FEBS Lett 278, 31-34. 3. Cowan, S.W. et al. (1992). Nature 358, 727-733.

## Tu-Pos40

**A POLYETHYLENE GLYCOL WATER-SOLUBLE CONJUGATE OF PORIN: REFOLDING TO THE NATIVE STATE.** ((G. Fasman and J. Weil)) Grad. Dept. Biochem., Brandeis Univ., Waltham, MA 02254

Porin, from *R. capsulatus*, was chemically modified with methoxypolyethylene glycol succinimidyl carbonate to yield methoxypolyethylene glycol-porin (PEG-SC Porin50), a water soluble conjugate. The conformation of the conjugate in water, as determined by circular dichroism (CD) spectroscopy, was largely the random coil structure. It was predominately the  $\beta$ -sheet structure, by CD, in 0.6% octyltetraoxyethylene and 0.3 M LiCl, as was porin. A proteoliposome, containing the porin conjugate, was prepared and its permeability to sugars, i.e. stachyose, was measured. Both porin and a PEG-SC-porin incorporated in a proteoliposome maintained the permeability for stachyose. The swelling rate of the conjugate vs. sugar was lower than porin. This indicated that the pore in the conjugate existed, but probably with a narrower cross section. The refolding of the porin conjugate was studied by stepwise addition of trifluoroethanol (TFE) to lower the dielectric constant, simulating the insertion of porin into a membrane. The conjugate of porin formed an  $\alpha$ -helical structure and the helical content increased with increasing concentrations of TFE. The PEG-SC-Porin50 could be stepwise refolded to the native conformation, the  $\beta$ -sheet conformation, by the addition of hexafluoroisopropanol in the 5-10% concentration range, simulating the insertion of the porin into the phospholipid bilayer. Beyond 10% of HFIP, an  $\alpha$ -helical structure was formed. This indicated that the folding and insertion of porin requires a specific environment, i.e. that found in the membrane. PEG-SC-Porin50 could also be crystallized. Supported by a grant from the U.S. Lab Command Army Research office.

## Tu-Pos42

**POLYAMINE-INDUCED CLOSING ACTIVITY IN *ESCHERICHIA COLI* PORIN CHANNELS.** ((A.L. delaVega, B. Dowlati, A.H. Delcour)) Department of Biology, University of Houston. Houston, TX 77204.

Although bacterial porins are traditionally believed to be permanently open pores, electrophysiological experiments have demonstrated that they are mostly open but can be regulated by voltage and membrane-derived oligosaccharides. Here we present patch-clamp data which document that the behavior of *E. coli* porin channels can be modulated by the polyamines cadaverine and spermidine. Studies conducted on inside-out patches of outer membrane of *E. coli* in reconstituted liposomes provide evidence that bath-applied cadaverine and spermidine increase the frequency of channel closures in a concentration-, pH-, and voltage-dependent manner. Cooperative closures of more than one channel are increased in number and duration, indicating that the polyamines act as pore blockers as well as modifiers of gating and cooperativity. These effects are not readily reversible, but over time there is a distinct decrease in modulatory activity after the polyamines are removed. When cadaverine is present in the pipette, the measured patch resistance after seal formation increases greatly in comparison with control pipettes, which suggests that the drug permanently closes a number of porins and thereby reduces total current. It is known that polyamines are components of the outer membrane of *E. coli*, but their functional role remains to be determined. The present study suggests that they may serve as natural regulators of outer membrane permeability. Supported by grants from the Oak Ridge Associated Universities and NIH AI34905.

## CHANNEL DIVERSITY

## Tu-Pos43

**SEVERAL ION CHANNELS FROM CHOLINERGIC SYNAPTIC VESICLES RECONSTITUTED INTO BILAYERS.** ((Marie Kelly and Dixon J. Woodbury)) Department of Physiology, Wayne State University School of Medicine, Detroit, MI 48201.

Synaptic vesicles were isolated from the electric organ of *Torpedo californica*. Membrane proteins from synaptic vesicles were reconstituted into planar lipid bilayers by the Nystatin/Ergosterol fusion technique. Following fusion, a variety of conductances were observed. The most prominent conductance was 6-8 pS and was slightly cation-selective. This channel opens in bursts but has a low open probability.

Other channels were also observed, but less frequently. The largest channel had a conductance between 80-90 pS and was anion selective. Two additional anion channels had conductances of 6-8 and 17 pS. Conductances were also observed at 12.5 and 25 pS, although these channels may be multiples of the 6-8 pS channels. There is some evidence that the 25 pS channel is a separate channel and not a multiple, since it has been observed to open to 25 pS in the absence of a 6-8 pS or 12.5 pS state. Also, the 12.5 pS channel and 25 pS channel were seen simultaneously and had different reversal potentials under the same ionic conditions. A non-selective channel was observed at 28-30 pS. None of these channels were observed following addition of vesicles made from plasma membrane fragments.

## Tu-Pos44

**IDENTIFICATION OF A HIGH CONDUCTANCE CHANNEL FROM RAT SYNAPTIC VESICLES.** ((F.S. Scornik\*, G. Rodriguez de Lores Arnaiz\*, C. Sánchez Antelo\*, G.J. Pérez\* and O.D. Uchitel\*)) \*Instituto de Biología Celular, Fac. de Medicina, UBA, Argentina, \*Fac. de Farmacia y Bioquímica, UBA, Argentina.

Calcium entry to the synaptic terminal is a key step for neurotransmitter release. Its mechanism of action is not well understood but there are some evidence that one possible target is the synaptic vesicle. In the last years many transmembrane proteins from the synaptic vesicles have been identified, some of which show characteristics of ion channels. In the present work, the reconstitution in lipid bilayers technic was used to incorporate ion channels from rat synaptic vesicles. The experimental solution contained 500 mM BaCl<sub>2</sub> in the *cis* chamber and 50 mM BaCl<sub>2</sub> in the *trans* chamber. In this condition, a channel of 200 pS of conductance was observed. This channel is slightly voltage dependent. It seems to be cation selective since the addition of 450 mM choline chloride to the *trans* chamber did not affect the I-V curve. In addition, channel open probability, which was around 0.9 at all the voltages studied, was dramatically reduced after addition of 100  $\mu$ M CdCl<sub>2</sub>. The fact that Ba<sup>2+</sup> permeate through this channel and that it was blocked by cadmium strongly suggest the identity of this channel to be a calcium selective channel. Further experiments are need to characterize this high conductance channel, its modulation and its possible role in the process of neurotransmitter release.

## Tu-Pos45

MODULIN 26 ION CHANNEL ACTIVITY: EFFECT OF PHOSPHORYLATION AND MUTAGENESIS OF SER 262 ((J.W. Lee<sup>1</sup>, C.D. Weaver<sup>1</sup>, N.H. Shomer<sup>2</sup>, C.F. Louis<sup>2</sup>, and D.M. Roberts<sup>1</sup>)) <sup>1</sup>Dept. Biochem., Univ. Tenn., Knoxville, TN 37996; <sup>2</sup>Dept. Biochem. Vet. Biol., Univ. Minn., St Paul, MN 55108.

Nodulin 26 is a major integral membrane protein of the soybean symbiosome membrane (SM), and is a member of the major intrinsic protein (MIP) family. Recently, we purified nodulin 26 from SM, and showed that it forms single channels with large conductance (3.1 nS in 1 M KCl) upon reconstitution into planar lipid bilayers. However, the channel exhibited voltage sensitivity, and occupies lower conductance states at high applied voltages (>60 mV) (J. Biol. Chem. 269, 17858, 1994). In this study, recombinant nodulin 26 was expressed as a his-tag fusion protein in *E. coli*. Upon purification and reconstitution into planar lipid bilayers, recombinant nodulin 26 also exhibits channel activity with a maximum single channel conductance similar to that of native soybean nodulin 26. However, in contrast to the native protein, recombinant nodulin 26 did not show any tendency to occupy lower conductance states at high applied voltages. Previously, we have shown that nodulin 26 is phosphorylated specifically on ser<sup>262</sup> by a calcium-dependent protein kinase in the SM. Phosphorylation of recombinant nodulin 26 by this protein kinase restores voltage sensitivity. A nodulin 26 mutant with an ala<sup>262</sup> substitution is resistant to phosphorylation and exhibits channel activity that is not voltage sensitive. However, the introduction of a negative charge by the substitution of asp<sup>262</sup> results in a single channel activity that is now sensitive to voltage. Overall, the data suggest that phosphorylation of ser 262 controls the voltage sensitivity of the channel. (Supported by USDA grant 94-37305-0619).

## Tu-Pos47

MOLECULAR MODELING OF LIGAND SPECIFICITY OF CYCLIC NUCLEOTIDE GATED CHANNEL ((S-P Scott<sup>1</sup>, R. W. Harrison<sup>1</sup>, I. T. Weber<sup>1</sup>, and J. C. Tanaka<sup>2</sup>)) <sup>1</sup>Dept. of Biochemistry and Biophysics, University of Pennsylvania, <sup>2</sup>Dept. of Pharmacology, Thomas Jefferson University, Philadelphia, Pa. 19107, <sup>3</sup>Dept. of Pathology, University of Pennsylvania, Pa. 19104.

The cyclic nucleotide gated channel (CNGC) is activated by nucleotide binding which promotes ion access to the channel pore. CNGCs comprise a family whose members vary in their nucleotide selectivity and  $K_{0.5}$  values for current activation. The preference for cGMP over cAMP in homologously expressed CNGCs ranges from 1:1 for catfish olfactory cDNA channel clones to 1:40 for rat and bovine olfactory and bovine retinal clones. The  $K_{0.5}$  values for cyclic nucleotides range from 1.4  $\mu$ M for cGMP with bovine olfactory channels to 1200  $\mu$ M for cAMP with retinal bovine channels.

Molecular models of the nucleotide binding sites were computed from the crystal structure of catabolic activating protein (CAP) based on the amino acid sequence of rat, catfish, and bovine olfactory CNGCs using AMMP (Another Molecular Modeling Program), a program for molecular mechanics and dynamics. The peptide backbone was restrained to the CAP structure and the side chains were allowed to move to lowest energy using an all-atom potential. No cutoff was used for the electrostatic and non bonded terms. The models were further refined by hand using Insight II (Biosym<sup>TM</sup>) to adjust the side chains. The amino acids predicted to be important for contacts with the purine ring are residues 61, 93, 119, and position 127 (CAP numbering sequence). The amino acid residing in position 61 is either a TYR or PHE, which interacts with the N1 and C6 position of the purine rings. Invariant THR 93 is predicted to interact with the N2 of cGMP and ARG 119, invariant in olfactory CNGCs, is predicted to interact with the N1 of cAMP.

Supported by NIH EY06640.

## Tu-Pos49

A CA-BLOCKABLE MONOVALENT CATION CHANNEL OF THE ECTODERM OF THE EARLY CHICK EMBRYO. ((R. Sabovcik, J. Li, P. Kucera and B. Prod'homme)) Institut de physiologie, Université de Lausanne, CH-1005 Lausanne, Switzerland

The apical membrane of the ectoderm of the gastrulating chick embryo contains a monovalent cation channel blocked by low concentrations of extracellular calcium. In the presence of symmetrical sodium concentrations the current rectifies inwardly in both inside-out and outside-out patches. This channel selects poorly between the alkali cations with the following sequence:  $Li > Na > Cs > K$ . The minimal pore diameter, estimated from the reversal potential of ten organic cation currents, is 5.8 Å. Large organic cations (like TEA) behave as weak blockers with a block at an apparent electrical distance of 0.23. Organic cations containing hydroxyl groups (like NMDG or TRIS) block the sodium current at a higher apparent electrical distance (0.56) which decreases with hyperpolarization. These data suggest that the former bind inside the channel close to the extracellular entrance while the latter bind deeper inside the pore and can even cross the channel at hyperpolarized potentials. The apparent binding affinity of TEA increases with sodium concentration but deviates from a simple competition curve, which is inconsistent with a single binding site. Calcium binds with high affinity inside the channel ( $K_m = 1 \mu$ M at -30 mV) close to the extracellular entrance. The mean blocked time increases with decreasing sodium concentrations, which is also inconsistent with a single-ion channel.

The modulation of the organic cations and calcium block by the permeant ion strongly suggests that the calcium-blockable monovalent cation channel is a multi-ion channel.

## Tu-Pos46

NOISE ANALYSIS OF cAMP- and  $Ca^{2+}$ -GATED CHANNELS IN ISOLATED OLFACTORY CILIARY CABLES. ((S.J. Kleene, H.P. Larsson<sup>1</sup> and H. Lecar<sup>2</sup>)) <sup>1</sup>University of Cincinnati College of Medicine, Cincinnati, OH 45267-0521 and <sup>2</sup>University of California, Berkeley, CA 94720.

Olfactory cilia isolated from frog olfactory receptor neurons and sucked into patch pipettes allow recording from internally perfused ciliary cables. Ion-channel noise was observed as a fluctuation spectrum in the input admittance of the cilium and analyzed under the assumption that the channels are distributed uniformly along the ciliary membrane. Noise was recorded as a function of cytoplasmic cAMP concentration. Divalent cations, which block the cAMP-gated channels, were chelated to very low levels. The noise spectrum was fit to a single low-frequency Lorentzian with corner frequency approximately 2-5 Hz. From the analysis of variance-to-mean ratio corrected for cable decrement, we infer a unit conductance of 9 pS for the cAMP-gated channel. This is close to values determined by examining single cAMP-gated channels from frog olfactory receptor neurons. Increasing cytoplasmic  $Ca^{2+}$  concentration is known to activate a ciliary  $Cl^-$  current, but corresponding single channels have not yet been described. Noise analysis of this current indicated the presence of a  $Ca^{2+}$ -activated  $Cl^-$  channel with unit conductance of 0.6 pS, inferred from the cable variance-to-mean. In the absence of cAMP and  $Ca^{2+}$ , an order-of-magnitude smaller component of noise was observed, having a spectrum which could be fit by approximately two Lorentzians extending to frequencies of 50-200 Hz.

## Tu-Pos48

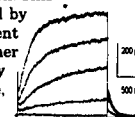
ATP-ACTIVATED CATION CURRENTS IN SINGLE GUINEA-PIG LIVER CELLS. ((T. Capiod)) INSERM U274 UPS, Bât.443, 91405 Orsay France (spon. by P. Champeil)

External ATP activates an inward cationic current in several types of cells and the role of purinergic receptors in the generation of a  $Ca^{2+}$  influx in guinea-pig liver cells was therefore investigated. The activation of an inward cationic current by external superfusion with ATP-Mg were studied in  $Cl^-$ -free and  $K^+$ -free external and internal solutions in whole-cell voltage clamped guinea-pig hepatocytes. External solutions contained (mM): NaOH, 75;  $Ca(OH)_2$ , 2; Hepes, 214 (pH 7.3). In  $Na^+$ -free experiments, NaOH was substituted by 75mM N-methyl-D-glucamine (NMDG). Internal solutions contained (mM): NMDG, 87; EGTA, 5; Hepes 199 (pH 7.3). In  $Na^+$ -containing solutions, fast applications of ATP (0.03 to 100  $\mu$ M) evoked an inward current at a holding potential of -40mV. Amplitudes of the inward current increased (range 1 to 10 pA/pF) and delays in the responses decreased (1-2s to 10-20ms) with increasing [ATP]. In  $Na^+$ -free solutions, ATP evoked a  $Ca^{2+}$  inward current of reduced amplitude (0.5 to 2 pA/pF). Cadmium (2mM) blocked the inward currents in both conditions. ADP (10-50  $\mu$ M) was less potent than ATP and AMP (50  $\mu$ M) had no effect on the activation of the current. The responses to prolonged application of ATP were not sustained and decreased to 50% of their peak values within 10s. These results demonstrate that the stimulation of  $P_2$ -purinergic receptors activates a large cationic inward current in guinea-pig liver cells.

## Tu-Pos50

EVIDENCE FOR THE SLOWLY-ACTIVATING COMPONENT OF THE DELAYED RECTIFIER  $K^+$  CURRENT ( $I_{Kd}$ ) IN RABBIT VENTRICULAR MYOCYTES. ((J.J. Salata, N.K. Jurkiewicz, B. Jow, P.J. Guinasso Jr., B. Fermini)) Merck Research Laboratories, West Point PA 19486.

In rabbit ventricle, the transient outward current ( $I_{to}$ ) and the rapidly activating component of delayed rectifier current ( $I_{Kr}$ ) are viewed as the major repolarizing  $K^+$  currents.  $I_{Kd}$ , the slowly-activating component of  $I_K$  is considered absent or too small to significantly affect action potential duration (APD). Therefore, detailed studies of  $I_{Kd}$  in rabbit are lacking. Using the patch clamp technique, we have investigated the electrophysiological properties of  $I_{Kd}$  in isolated myocytes from rabbit ventricle. Voltage ramps applied from -110 to +50 mV (32mV/sec) from a holding potential (HP) of -50 mV elicited an N-shaped I-V relationship showing outward rectification at potentials positive to 0 mV. Depolarizing voltage steps from a HP of -50 mV activated both  $I_{Kr}$  and  $I_{Kd}$ . After complete block of  $I_{Kr}$  by 3  $\mu$ M dofetilide, we observed slowly activating time- and voltage-dependent outward currents that did not inactivate during long pulses (>7.5 sec) and outward tail currents upon return to the HP (Figure). Both time-dependent and tail currents were increased by raising the bath temperature (from 25 to 35°C) or addition of isoproterenol (100 nM) to the superfusate. The threshold voltage for activation of the current was  $\approx -20$  mV and the I-V relationship displayed steep outward rectification. This dofetilide-insensitive current was nearly completely inhibited by 10  $\mu$ M NE-10064, a known inhibitor of  $I_{Kd}$ . In conclusion, a current component showing properties similar to  $I_{Kd}$  described in other cardiac preparations is present in rabbit ventricle and may play a yet unsuspected role in determining APD in this structure, especially during elevated sympathetic tone.



## Tu-Poe51

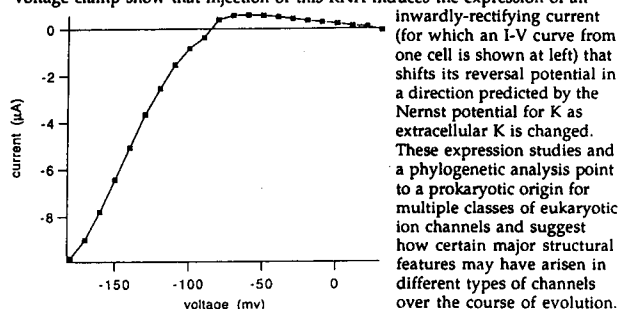
SINGLE CHANNEL CURRENTS OF CHANNELS THAT ARE PERMEABLE TO MONOVALENT AND DIVALENT CATIONS. ((Yoshio Oosawa)) International Institute for Advanced Research, Matsushita Electric Industrial Co., Ltd., 3-4 Hikaridai, Seika-cho, Kyoto-fu, 619-02, JAPAN.

A membrane potential of ciliate protozoa such as *Tetrahymena* and *Paramecium* is controlled by several ions, especially  $K^+$  and  $Ca^{2+}$ . Cation channels from *Tetrahymena* cilia were incorporated into planar lipid bilayers and were not voltage-dependent. In solutions of  $K^+$ , the channel conductance reached a maximum value as the  $K^+$  concentration was increased. The cation channel was permeable not only to monovalent cations but also to divalent cations. The single channel conductance in mixed solutions of  $K^+$  and  $Ca^{2+}$  could not be explained by a model assuming simple competitive inhibition between the cations. The single channel conductance was determined by the Donnan ratio of  $K^+$  and  $Ca^{2+}$  ( $[K^+]/[Ca^{2+}]$ ). For explaining this fact, the binding sites of the channel were considered to be always occupied by two potassium ions or by one calcium ion under the experimental conditions: 5-90 mM  $K^+$  and 0.5-35 mM  $Ca^{2+}$ . A two barrier model for the channel was introduced and the values of Michaelis-Menten constants and the maximum currents carried by  $K^+$  and  $Ca^{2+}$  were calculated using this model.

## Tu-Poe53

LCTB IS A K-SELECTIVE PROKARYOTIC RELATIVE OF EUKARYOTIC ION CHANNELS. ((W. Joiner<sup>1</sup>, Y. Yang<sup>1</sup>, F. Sigworth<sup>1</sup>, and L. Kaczmarek<sup>1,2</sup>)) Departments of Cellular and Molecular Physiology<sup>1</sup> and Pharmacology<sup>2</sup>, Yale University School of Medicine, New Haven, CT 06510. (Sponsored by G. Giebisch).

Based on the homology between two domains in the LctB proteins of *Bacillus stearothermophilus* and *Bacillus caldoteanax* and the corresponding P (or H5) and M2 (or S6) domains of eukaryotic K channels, RNA derived from a PCR product of one LctB gene was injected into *Xenopus* oocytes to test whether LctB might indeed be a primordial K channel. Recordings using a two-microelectrode voltage clamp show that injection of this RNA induces the expression of an



## Tu-Poe55

MODULAR DESIGN OF GLUTAMATE-GATED ION CHANNELS. ((Z.G. Wo and R.E. Oswald)) Dept. Pharmacology, Cornell University, Ithaca, NY 14853.

Ionotropic glutamate receptors (iGluRs) have been considered structurally homologous to other ligand-gated ion channels (e.g. nicotinic acetylcholine receptors). Recently, our work and that of others indicated that this assumption is incorrect. Analysis (1,2) of two cloned goldfish kainate receptors (GfKARa and GfKARb) indicated that these receptor subunits have three transmembrane segments (TMs) instead of four. TMII, which probably lines the channel pore, is not a true transmembrane segment, and the entire region between TMIII and TMIV is translocated (extracellular in mature receptors). This 3-TM model has important implications for the structure of the iGluR family. The recent convergence of several lines of evidence (1-4) has led us to propose that iGluRs are modular proteins consisting of four distinct domains: two (i & ii) related to bacterial periplasmic binding proteins, as has been suggested by O'Hara et al. (3); one related to the pore-forming region of  $K^+$  channels (iii); and one intracellular regulatory module of unknown origin (iv). We found that the sequence of the TMII and the surrounding region of iGluRs can be aligned with the pore-forming P-segment of voltage-gated  $K^+$  channels and the available mutagenesis data of the TMII region can be explained based on this alignment. Positioning of the  $K^+$  channel-like domain as an insertion in a crucial region of a bacterial periplasmic binding protein-like structure suggests a model for the transduction of binding energy to channel gating. This proposed modular design also suggests an evolutionary link between a ligand-gated ion channel family and voltage-gated ion channels, which emerged much earlier than ligand-gated ion channels in evolution.

1. Wo, Z.G. & R.E. Oswald. (1994) *PNAS* 91:7154-7158.
2. Wo, Z.G. & R.E. Oswald. *J. Biol. Chem.* in press.
3. O'Hara, P.J. et al. (1993) *Neuron* 11:41-52.
4. Kuryatov, A.B. et al. (1994) *Neuron* 12:1291-1300.

## Tu-Poe52

CATIONIC CHANNEL FROM THE MEMBRANES OF LARVAL *Echinococcus granulosus* STUDIED BY RECONSTITUTION ON PLANAR LIPID BILAYERS. ((Claudio Grosman & Ignacio L. Reisin)) Catedra de Química General e Inorgánica, Facultad de Farmacia y Bioquímica, Universidad de Buenos Aires, Junín 958, 1113, Buenos Aires, Argentina.

We have examined the properties of a cationic channel from the membranes of the cestode *Echinococcus granulosus* by using channel reconstitution techniques on planar lipid bilayers. The membrane vesicles from the larval stage of the parasite (protoscolices) were prepared following a procedure similar to that described by McManus D.P. & Barrett N.J. (*Parasitology*, 1985 90:111). Upon reconstitution on POPE/POPC planar bilayers the most frequent single channel we have observed was cationic (PC1/PK < 0.05) with a conductance of  $107 \pm 2$  pS ( $n=4$ ) in symmetrical 150 mM KCl. The selectivity for monovalent cations follows the sequence  $PCs : PK > PNa > PLi$  ( $Px/PK$ : 1.01:1.0:0.58:0.49) and the channel was not blocked either by TEA (10 mM) or by  $BaCl_2$  (4  $\mu$ M). The Popen of the channel -Ca insensitive- was usually observed to be higher than 0.9 and in this activation mode the channel was voltage independent. In 8 % of the same bilayers the Popen also exhibited periods of voltage dependence and its kinetics can be explained by a two state model. Multiple current levels of the 107 pS channel were also observed. In some cases these multiple levels are compatible with the activity of independent conductive units, while in others they are not. On occasions we observed both modes on the same bilayer, suggesting that the channels can reversibly fluctuate between those activation modes.

## Tu-Poe54

EPOCH-ORIENTED LIKELIHOOD MAXIMIZATION OF AN IDEALIZED ION CHANNEL RECORD.

((V. Pastushenko and H. Schindler)) Institute for Biophysics, J. Kepler University, A-4040 Linz, Austria

Recently we described a statistical method to find transitions and levels in ion channel records [1]. Starting from detected levels and noise variances we now have improved the procedure for optimum assignment of transitions. The optimization proceeds by deleting consecutively the least likely epochs and estimating the likelihood (L) of the entire trace at each stage. It is defined as the sum of products of dwell times and L's for each epoch. The L of an epoch is defined via the L densities of belonging to open or closed states. The L densities are expressed in terms of an efficient epoch dwell time which may not exceed the actual dwell time due to possible missed epochs. Deletion of the least likely epoch leads to a new epoch with an efficient dwell time calculated from efficient dwell times of participating epochs and their likelihoods of belonging to a certain level. This strategy allows to find the set of transitions at maximum likelihood. Accuracy and reliability of the method is demonstrated with simulated data. (Supported by the Austrian Research Funds, project S66/10).

[1]. V. Ph. Pastushenko, H. Schindler. Statistical filtering of the single ion channel records. *Acta Pharm.* (1993), 43, 7-13.

## Tu-Poe56

POLY-3-HYDROXYBUTYRATE/POLYPHOSPHATE COMPLEXES FORM VOLTAGE-GATED CALCIUM CHANNELS IN ESCHERICHIA COLI PLASMA MEMBRANES. ((L.L. Bramble and R.N. Reusch)) Dept. of Microbiology, Michigan State Univ, E. Lansing, MI 48824.

Two ubiquitous linear homopolymers - the salt-solvating amphiphile, poly-3-hydroxybutyrate (PHB), and the polyanion, inorganic polyphosphate (PPi), - associate to form complexes in bacterial plasma membranes that are highly selective for  $Ca^{2+}$  (Reusch and Sadoff, *PNAS*, 85, 4176, 1988). The composition, environment, and putative structure of the polymer salt complexes led Reusch and Sadoff to propose they function as  $Ca^{2+}$  channels. We extracted the complexes from *E. coli*, purified them by gel permeation chromatography, and incorporated them in planar bilayers of synthetic 1-palmitoyl, 2-oleoyl, phosphatidylcholine where we found them to exhibit many of the signal characteristics of proteinaceous  $Ca^{2+}$  channels: voltage-dependence, selectivity for divalent over monovalent cations, selectivity for  $Ca^{2+}$  over  $Mg^{2+}$ , permeance to  $Ca^{2+}$ ,  $Sr^{2+}$ , and  $Ba^{2+}$ , and concentration-dependent blocking by  $La^{3+}$ ,  $Co^{2+}$ , and  $Cd^{2+}$ . Voltage-dependent complexes were also reconstituted from purified recovered PHB and synthetic calcium polyphosphate. These ion-conducting polymer electrolyte complexes are the first reported non-proteinaceous calcium channels. We suggest that PHB/PPi complexes are primordial ion channels and evolutionary antecedents of protein channels. (Supported by NSF MCB 92 09364 and NIH GM13375)



## Tu-Pos57

**AN ARTIFICIAL CATION CHANNEL WITH A K<sup>+</sup>-SELECTIVE FILTER.**  
(M. Sokabe, Y. Tanaka\* and Y. Kobuke\*) Dept. Physiol. Nagoya Univ. Sch. Med. Nagoya 466, and \*Dept. Mater. Sci., Shizuoka Univ. Hamamatsu 432, Japan

We reported that amphiphilic molecules composed of oligoether carboxylate anions complexed with hydrophobic dialkyl ( $C_{18} \times 2$ ) ammonium cations could form cation channels in lipid bilayers (JACS, 116:7618, 1992). The channels exhibited a variety of conductances (10-1000 pS at 500mM KCl) with little selectivity among monovalent cations. Although the channel is supposed to be formed through molecular aggregation, we could not control the number of monomers, which may be the origin of the varied conductances. In the present study we prepared a resocinol-octadecanal cyclotetramer as a half-membrane spanning channel. As expected, this compound exhibited only one value of single channel conductance (6 pS at 500mM KCl). In addition this channel favored K<sup>+</sup> against Na<sup>+</sup> ( $P_K/P_{Na}=6$ ) as well as cation against anion ( $P_K/P_{Cl}=20$ ). Since the cyclic structure and the long alkyl tails were essential to this channel forming molecule, the cavity made up with four benzene rings and four consecutive alkyl tails seemed to provide an ion conducting pore in which the rigid sixteen-membered ring in the narrowest part may function as an ion selective filter to bring about such sharp ion selectivity. The data suggest that the transmembrane channel is produced by a tail-to-tail dimer.

## Tu-Pos59

**MOLECULAR DESIGN OF A AMPA/KA RECEPTOR HIGHLY PERMEABLE TO DIVALENT CATIONS.**

((A. V. Ferrer-Montiel, W. Sun and M. Montal))

Department of Biology, University of California San Diego, La Jolla CA 92093-0357

Glutamate receptors of the AMPA/KA subtype (GluR1) are weakly permeable to divalent cations. We converted GluR1 into a highly permeable channel to Ba<sup>2+</sup> and Ca<sup>2+</sup>. For this task, we used the M2 transmembrane segment of the N-methyl-D-aspartate receptor (NMDAR1) to identify the structural determinants that specify its remarkable permeability to Ca<sup>2+</sup>. The putative molecular determinants were implanted on M2 of the GluR1 by site-directed mutagenesis, and the mutant receptors were expressed and characterized in *Xenopus* oocytes. Notably, mutation of L577 to W produced a receptor mutant highly permeable to divalent cations (Table), with relative permeabilities to Ba<sup>2+</sup> and Ca<sup>2+</sup> similar to those characteristic of the NMDAR1. The L577W mutant displayed an inwardly rectifying I/V. In contrast, mutation of Q582 to N, a residue involved in the Mg<sup>2+</sup>-blockade of the NMDAR1, did not alter the ionic permeability of GluR1 but changed the I/V from inwardly rectifying to linear.

Hence, an aromatic residue at position 577 on the M2 of GluR1, or its equivalent at position 593 on the NMDAR1, is a key molecular determinant of the permeability to Ca<sup>2+</sup> in the family of ionotropic glutamate receptors.

	P <sub>K<sup>+</sup>/Na<sup>+</sup></sub>	P <sub>Ba<sup>2+</sup>/Na<sup>+</sup></sub>	P <sub>Ca<sup>2+</sup>/Na<sup>+</sup></sub>
GluR1	1.2	2.5	2.5
Q582N	1.1	3.0	2.2
A579V	1.0	1.7	2.9
L577W	1.3	11.0	7.7

Supported by NIH and ONR.

## GRAMICIDIN

## Tu-Pos60

**POLYPEPTIDE ION CHANNELS AS STUDIED BY SOLID STATE NMR.**  
(F. Tian, M. Cotten, F.A. Kovacs and T.A. Cross) National High Magnetic Field Laboratory, Institute of Molecular Biophysics and Department of Chemistry, Florida State University, Tallahassee, FL 32306-4005.

The <sup>15</sup>N-1H and <sup>13</sup>C-<sup>15</sup>N dipolar splittings show no significant change in the presence of Na<sup>+</sup>. These observations are in contrast to significant <sup>15</sup>N chemical shift differences in the presence of Na<sup>+</sup>. The results suggest that Na<sup>+</sup> binding does not induce any significant changes in structure or dynamics of the polypeptide backbone or sidechains.

Analog of gramicidin A containing tyrosine instead of tryptophan have been studied. Powder pattern spectra of hydrated samples of the analogs in DMPC lipid bilayers have been recorded at 5° C, and show the features of static pattern line shapes for positions Tyr11 and Tyr13. These results combined with spectra of oriented preparations constrain the structure of the tyrosine sidechains.

The peptide corresponding to the putative membrane spanning sequence of the M<sub>2</sub> protein of the Influenza virus (Udorn/72) has been synthesized. The M<sub>2</sub> protein is believed to function as a monovalent ion channel by tetrameric association forming a 4 helix bundle across the membrane. Solid state peptide synthesis utilizing Fmoc chemistry and HPLC purification for this highly hydrophobic peptide have been developed. The synthesized peptide has been oriented in planar lipid bilayers for the purpose of obtaining structural information using solid state NMR methods.

## Tu-Pos58

**CHANNELS OF POLY(2-ETHYLACRYLIC ACID) IN ARTIFICIAL PHOSPHOLIPID BILAYERS.** ((J. C. Chung, J. L. Thomas, L. R. Opsahl\*, D. J. Gross, and D. A. Tirrell)) Program in Molecular and Cellular Biology, University of Massachusetts, Amherst, MA 01003 and \*General Electric, Corporate Research and Development, Schenectady, NY 12301.

Synthetic poly(2-ethylacrylic acid) (PEAA) disrupts lipid vesicles in a pH-dependent manner.<sup>1</sup> Upon acidification from pH 7 to 6.5, PEAA binds to lipid membranes and reorganizes large vesicles into smaller structures. We explored the early stages of this disruption process by examining the effect of low [PEAA] on artificial bilayer conductance.

Channel events were recorded at various pHs with low [PEAA] (< 10 µg/ml) using bilayer patches formed on the tips of patch clamp pipettes.<sup>2</sup> Large current steps, rapid flickering, and noisy open channel activities were observed for symmetrical 200 mM NaCl solutions. At least three separate conductance levels were recorded.

<sup>1</sup> D. A. Tirrell, D. Y. Takigawa, and K. Seki, Ann. N. Y. Acad. Sci. 446: 237-248, 1985.

<sup>2</sup> R. Coronado and R. Latorre, Biophys. J. 43: 231-236, 1983.

Supported by NSF MCB93-04493 and NSF DMR90-23848.

## Tu-Pos61

**GLOBAL REFINEMENT OF THE GRAMICIDIN CHANNEL IMPROVED BY NEW SOLID-STATE NMR CONSTRAINTS.** ((R.R. Ketchum, M. Brennen, K.-C. Lee, W. Hu, S. Huo and T.A. Cross)) National High Magnetic Field Laboratory, Institute of Molecular Biophysics and Department of Chemistry, Florida State University, Tallahassee, FL 32306-4005.

A method for determining very high resolution membrane bound protein structures has been developed in our lab. The gramicidin channel structure has been experimentally determined and refined based on solid-state NMR derived orientational constraints for both the backbone and sidechains.

The backbone structure was determined based on experimental constraints using <sup>15</sup>N and <sup>13</sup>C chemical shifts, <sup>15</sup>N-1H and <sup>15</sup>N-<sup>13</sup>C dipolar splittings, and Cα-<sup>2</sup>H quadrupolar splittings. The Cα-<sup>2</sup>H data significantly improves the structural refinement. The sidechain structures and dynamics have been characterized through the observation of the C-<sup>2</sup>H quadrupole splittings and <sup>15</sup>N spectroscopy of the sidechains. Our technique for structural refinement is based on a simulated annealing protocol which takes advantage of the orientational constraints obtained from the solid-state NMR data. This protocol utilizes torsional changes to vary the protein structure and minimizes a penalty based on differences between calculated and observed NMR data. Backbone and sidechain dynamics are being included in the structural refinement.

## Tu-Pos62

MONTE CARLO ANALYSIS OF THE INFLUENCE OF A CHANNEL FORMING PEPTIDE ON ION FREE ENERGY BARRIERS IN SINGLE FILE ION CHANNELS ((V. Dorman<sup>1</sup>, M.B. Partenskii<sup>2</sup> and P.C. Jordan<sup>3</sup>)) <sup>1</sup>Dept. of Chemistry, Brandeis University, Waltham, MA 02254 and <sup>3</sup>Rampage Systems Inc., 411 Waverly Oaks Rd., Waltham, MA 02154.

The influence of a gramicidinlike channel former on ion free energy barriers and water polarization is studied using Monte Carlo simulation. Water in the channel is described by the "dipolar chain model" (M.B. Partenskii & P.C. Jordan, *Q. Rev. Biophys.* 25, 477, [1992]). Setting bulk water's  $\epsilon = \infty$  permits exact solution of this general type of statistical mechanical problem, including all long-range electrostatic interactions. The model treated is comprised of an ion, eight water dipoles, and gramicidin's thirty-two carbonyls. Ionic free energy profiles are computed via thermodynamic integration, using a charging process. In addition to cooperative effects, individual contributions of the waters and COs are determined separately. Possible effects due to uncertainty in positioning the water-channel boundary are considered. The ion's position is varied semi-continuously. We consider a wide range of possible CO partial charges ( $0.5 \leq q \leq 1.0$ ) and dielectric backgrounds (the high frequency  $\epsilon$ ,  $2 \leq \epsilon_{\text{background}} \leq 4$ ). We find that: if constrained to their original orientations, the COs substantially increase the permeation free energy; with or without water present, CO reorientation is crucial if ion-CO interaction is to lower the free energy barrier; only the three or four COs nearest the ion are notably perturbed due to interaction with the ion; unless the CO partial charge is large, the ion's permeation free energy barrier remains unphysically large.

## Tu-Pos64

A SEQUENCE OF MARKOV CHAINS CONVERGING TO LEVITT'S SINGLE-ION DIFFUSION THEORY. ((Pete McGill and Mark F. Schumaker)) Department of Pure and Applied Mathematics, Washington State University, Pullman, WA 99164-3113.

The Levitt theory (Ann. Rev. Biophys. Biophys. Chem. 1986, 15:29-57) combines a diffusive description of ion permeation through the pores of membrane channels with the single-ion restriction appropriate for modeling Na-permeation through Gramicidin A. We have constructed a sequence of Markov chain models of ion movement (models with first order transitions between discrete states) which converges to a diffusion process with ion currents that are identical to those of the Levitt theory. The diffusion process enables us to characterize the sample paths of particles as they enter and exit the channel. A surprising result is that particles enter and exit the channel "infinitely fast"; the channel never spends time intervals of finite duration in the empty state. This boundary behavior reflects a relationship between two time scales. The Levitt theory corresponds to a limiting case in which the typical time required for an ion to exit the channel, starting from a location close to an entrance, is very short compared with the time required for an ion to diffuse across the channel interior. The channel does spend finite time intervals in the empty state when the exit and translocation rates are treated as comparable.

## Tu-Pos66

BINDING SITES FOR SODIUM IN GRAMICIDIN A: COMPARISON OF MOLECULAR DYNAMICS CALCULATIONS AND SOLID-STATE NMR DATA ((T.B. Woolf & B. Roux)) Dept Physiol. Johns Hopkins Univ, Baltimore, MD 21205 & Dept of Chem, Univ of Montreal, Montreal, Canada H3C 3J7

The changes in solid state NMR chemical shifts when sodium is present in the gramicidin A channel were calculated using molecular dynamics methods. The largest shifts in backbone sites were observed at Leu-10 for 13-C and at Trp-11 for 15-N, in agreement with experimental data (Smith et al., *BBA* 1026:161-6). Based on experimental data and the present calculations, the dominant binding site is located at 9.0 Å from the center of the channel. The calculations were performed with the presence of a sodium ion within a GA:DMPC system at 1:8 concentration with 45 weight percent water (PNAS, in press). Twenty-four separate windows with a planar harmonic restraint on the ion from 8.0 to 13.0 Å were analyzed. The free energy profile for the ion was then used as an initial estimate for the probability of the ion being found at different local minima. The results provide insight into the dynamical averaging occurring in the measurement of NMR observables and into the nature of the changes induced in the channel structure by the presence of a sodium ion.

## Tu-Pos63

ION-WATER AND ION-CARBONYL CORRELATIONS IN A GRAMICIDINLIKE CHANNEL. ((Karen A. Duca<sup>1</sup> and Peter C. Jordan<sup>1,2</sup>)) <sup>1</sup>Biophysics Program and <sup>2</sup>Department of Chemistry, Brandeis University, Waltham, MA 02254

Previous work (Duca & Jordan, *Biophys. J.*, 64, A295 [1993]; 66, A220 [1994]) has indicated that cation-water and water-water correlations in a gramicidinlike channel (a configurationally constrained polyglycine analog) are noticeably dependent on ionic size and helix flexibility; they also depend significantly on explicit consideration of polarizability. This simplified model is thus well suited to studying the effect of a range of constraints on ion-channel interaction. We contrast behavior near local maxima and minima in the energy in two regions of the channel: the dimer junction and the mid-monomer domain. There are large ion specific differences in ion-carbonyl correlations when comparing maxima and minima. At the minima Na<sup>+</sup> coordinates more carbonyls; however, it is relatively less strongly bound to any of them. At the maxima, it is solvated by fewer carbonyls, is bound more strongly to those with which it associates, and the peak in the ion-carbonyl distribution function is sharper and has shifted to smaller separations. For K<sup>+</sup> the same behavior is evident, but less pronounced. For Cs<sup>+</sup> the pattern is less clear. Differences are muted; trends may even be reversed. The differences between the ion-water correlation functions at maxima and minima are distinct, but smaller; however, at the maxima, the peak in the ion-water correlation functions appears to be shifted to smaller separations. Again, the effect is least marked for Cs<sup>+</sup>. The influence of polarizability and helix flexibility on these correlations is studied. Possible implications for selectivity are discussed.

## Tu-Pos65

STRUCTURE AND DYNAMICS OF A PROTON WIRE: A THEORETICAL STUDY OF THE GRAMICIDIN CHANNEL. ((R. Pomès and B. Roux)) Department of Chemistry, University of Montreal, Montreal, Quebec, Canada H3C 3J7

The rapid transfer of protons along linear chains of hydrogen-bonded water molecules, or *proton wires*, governs their translocation through transmembrane channels. Quantum-classical and classical computer simulations were used to study the chain mechanism of proton translocation in the proton wire of the gramicidin A channel. The dissociation of the water molecules was accounted for by the "Polarization Model" of Stillinger and David, and in some simulations, all the water hydrogen nuclei were treated quantum mechanically using Feynmann path integrals.

The proton transfer mechanism was found to be largely delocalized and essentially determined by the geometry and the dynamics of the water chain. In turn, while the equilibrium structure of the hydrogen-bonded water chain reflects the quantization of hydrogen nuclei and the presence of an excess proton, the formation of transient hydrogen bonds between single-file water molecules and channel backbone carbonyl groups disrupts the connectivity of the chain, which ultimately limits the transfer.

## Tu-Pos67

DESIGNING GATES FOR GRAMICIDIN. ((G.A. Woolley, A.S.I. Jaikaran, Z. Zhang and S. Peng)) Department of Chemistry, University of Toronto, Toronto M5S 1A1, Canada

A key component in the design of artificial ion channels is the design of regulatory elements. As a first step in this direction, we have synthesized a derivative of the peptide ion channel, gramicidin, with an extension designed to act as a gate at the entrance (and exit) of the channel. A conformational change of the gate (cis-trans isomerization) moves a charged amino group relative to the mouth of the channel. This regulates cation flux. A *trans-to-cis* isomerization reduces cation flux by an amount which depends on voltage and bulk ion concentration. A series of derivatives with longer and shorter 'gates' has been synthesized to define exactly the effect of distance of the amino group from the channel mouth on channel current. The predictability of the system suggests that the design of more sophisticated types of channel regulation will be possible.



## Tu-Pos68

TRYPTOPHAN DEPENDENCE OF FORMAMIDINIUM EFFECTS ON GRAMICIDIN A CHANNELS. ((Sang Ah Seoh and David Busath)) Dept. of Physiology, Brown University, Providence, RI 02912.

Compared to alkali metal cations, permeating formamidinium ions stabilize the gramicidin A channel and N-acetyl gramicidin channels in monoolefin bilayers (Seoh and Busath, *Biophys. J.* 64:1017, 1993; Seoh and Busath, *Biophys. J.* 65:1817, 1993). We used electrophysiological measurements with W-to-F substituted gramicidin analogs and found that the formamidinium-induced stabilization was eliminated when the four gramicidin W's were replaced with F's (gramicidin M<sup>-</sup>), indicating that the stabilization is mediated by the tryptophan side chains. Replacement of Trp-9, 13, or 15 with Phe reduces but does not eliminate stabilization; stabilization in W11F is only slightly reduced. Additionally, with gramicidin M<sup>-</sup> formamidinium-induced I-V supralinearity and open channel noise are absent. When the lipid bilayer was formed with monoolefin ether (rather than the ester), the low voltage formamidinium-induced stabilization (relative to KCl) decreased by one half. The open channel noise was unaffected and the current-voltage relation was only modestly affected by the change of lipid. These results suggest that passing formamidinium ions affect the channel's Trp side chains which, in turn, affect channel lifetime, current-voltage supralinearity, and open channel noise. We propose that these effects are mediated by interactions between the Trp side chains and the lipid-water interface including the lipid ester carbonyl.

## Tu-Pos70

SEQUENCE DETERMINANTS OF GRAMICIDIN CHANNEL FOLDING ((G. Sabarwal\*, O. S. Andersen\*, D. V. Greathouse\*, R. E. Koeppe II\*)) Cornell Univ. Med. Coll., New York, NY, Univ. Arkansas, Fayetteville, AR.

Gramicidin A (gA) channels are head-to-head dimers of right-handed (RH), single stranded (SS)  $\beta^3$  helices. Changing the chirality of each residue causes the resulting gramicidin A<sup>-</sup> (gA<sup>-</sup>) to form left handed (LH) channels. The analogue (gLW, see below) forms channels that are double-stranded (DS) as well as SS. The following analogues were synthesized to identify sequence positions that determine channel handedness and strandedness:

L D L D L D L D L D L D L D	(residue chirality)
V G A L A V V V W L W L W	gA; SS, RH
V G A L A V V V W L W L W	gA <sup>-</sup> ; SS, LH
V G A L V V V A W L W L W	V <sup>3</sup> A <sup>8</sup> gA; SS, RH
V G A L A V V A W L W L W	A <sup>8</sup> gA; SS, RH
V G A L A V V V W L W L W	gLW; DS; SS, LH? & RH
V G A L A V V V W L W L W	V <sup>3</sup> gLW; DS; SS, LH & RH
V G A L V V V A W L W L W	V <sup>3</sup> A <sup>8</sup> gLW; SS, LH & RH
V G A L V V V V W L W L W	V <sup>3</sup> gLW; SS, LH & RH
V G A L A V V A W L W L W	A <sup>8</sup> gLW; DS; SS, LH? & RH

gLW and V<sup>3</sup>A<sup>8</sup>gLW have similarities with both gA and gA<sup>-</sup>; but, whereas gLW forms DS and SS channels, V<sup>3</sup>A<sup>8</sup>gLW forms only SS channels. In the context of gLW, the DS/SS bias is determined by position #5 because V<sup>3</sup>gLW forms only SS channels, while A<sup>8</sup>gLW forms DS and SS channels. V<sup>3</sup>A<sup>8</sup>gA, identical to V<sup>3</sup>A<sup>8</sup>gLW in the first 8 residues, forms only SS, RH channels. A<sup>8</sup>gA also forms only SS, RH channels. The handedness of gA can be changed by local sequence changes, which interact to produce non-additive effects on channel structure.

## Tu-Pos72

CONFORMATION OF THE ACYLATION SITE IN PALMITOYL-ETHANOLAMINE GRAMICIDIN ((Roger E. Koeppe II, T. C. Bas Vogt\*, Denise V. Greathouse, J. Antoinette Killian\*, and Ben de Kruijff\*)) Dept. Chem. Biochem., Univ. of Arkansas, Fayetteville, AR, USA 72701; \*Dept. of Biochem. of Membranes, Univ. of Utrecht, The Netherlands.

Gramicidin A (gA) can be palmitoylated by means of an ester linkage to the -OH group of the terminal ethanolamine that sits at the membrane-water interface in the functional gA channel. We have investigated palmitoyl-gA as a model transmembrane acyl-protein. D<sub>4</sub>-ethanolamine (NHCD<sub>2</sub>CD<sub>2</sub>OH) was incorporated into gA by total synthesis, and a portion of the labeled gA was palmitoylated. Solid-state <sup>2</sup>H NMR spectra of free and acyl gA in hydrated DMPC bilayers were compared. The spectra for both oriented and nonoriented samples at 4° and at 40° C suggest that the ethanolamine of free gA is mobile prior to acylation, but essentially immobile after palmitoylation. The <sup>2</sup>H quadrupolar splittings allow the conformation of the ethanolamine group in palmitoyl gA to be determined. Using the previously determined quadrupolar splittings for deuterium labels on the palmitoyl chain (T. C. B. Vogt, J. A. Killian, & B. De Kruijff [1994] *Biochemistry* 33, 2063-2070), we also propose a model for the C1-C5 portion of the acyl chain. The ethanolamine group rotates over Leu<sup>10</sup> and toward the outside of the gA channel's cylinder upon acylation, so that the acyl chain passes between the side chains of Trp<sup>9</sup> and Leu<sup>10</sup>.

## Tu-Pos69

FREE ENERGY PROFILE FOR SMALL ORGANIC CATIONS IN GRAMICIDIN A CHANNEL WITH UMBRELLA SAMPLING AND PERTURBATION DYNAMICS. ((Yili Hao and David Busath)) Dept. of Physiology, Brown University, Providence, RI 02912.

Umbrella sampling and dynamic perturbation techniques are explored to compute the free energy profiles and the mutation energy for formamidinium, guanidinium, methylammonium and ethylammonium in gramicidin model channel. Our system consists of the gramicidin polypeptide channel, the ion-water column which extends along the channel axis to well outside channel, and two water balls around the channel mouths modeling the solvent environment. We are taking the CHARMM parameters for all the atoms and using CHARMM dynamic simulations for the computer modeling. As a control, umbrella sampling was done with the center ion replaced by another water molecule. The shape of the free energy profiles for the four ions are similar. The barrier is located at 6-7 angstroms from the channel center on both sides, which is at the center of each monomer. There is a single well at the channel center. Without the correction for long range solvent effects, the barrier to formamidinium exit is 11-12 kcal/mol and the barrier to entry is higher. The entry barrier for guanidinium is about 6 kcal/mol higher than for formamidinium. Ethylammonium shows a much higher entry barrier than methylammonium. The differences in barriers are roughly consistent with the measured channel selectivity.

## Tu-Pos71

MODULATION OF GRAMICIDIN CHANNEL FUNCTION BY IONIC STRENGTH, [Ca<sup>++</sup>] AND [H<sup>+</sup>]-MANEUVERS THAT ALTER LIPID CURVATURE ((A. M. Maer, J. A. Lundbæk, L. L. Providence, and O. S. Andersen)) Cornell Univ. Med. Coll., New York, NY (Spon. by L. G. Palmer).

The linear gramicidins have no charged groups and have no high-affinity binding sites for Ca<sup>++</sup>, and the average duration of gramicidin channels usually varies only little as a function of [Ca<sup>++</sup>] or [H<sup>+</sup>]. But gramicidin channel function (average duration and equilibrium constant for channel formation) varies with maneuvers that alter the spontaneous curvature of the bilayer-forming lipids—a parameter that in negatively charged bilayers can be altered by changes in [H<sup>+</sup>], divalent cation concentration, and ionic strength. We therefore examined the effect of ionic strength, [H<sup>+</sup>], and [Ca<sup>++</sup>] on the conductance (g) and average duration (τ) of gramicidin channels in bilayers formed from dioleoylphosphatidylserine/n-decane. Increasing [NaCl] from 0.1 to 1.0 M (pH 7, 1 mM EDTA) has no effect on g but decreases τ two-fold. Increasing [Ca<sup>++</sup>] from 3 nM to 1 mM (0.1 M NaCl, pH 7) decreases g four-fold while τ is reduced seven-fold (with a two-fold reduction in τ at 10 μM Ca<sup>++</sup>). Decreasing pH from 8 to 3 (0.1 M NaCl, 1 mM EDTA) has no effect on g but reduces τ ten-fold. In parallel with the reductions in τ, the channel-forming potency is reduced (one must add ten-fold more gramicidin at pH 3 than at pH 8 to achieve comparable channel appearance rates). In summary, experimental maneuvers that reduce the electrostatic repulsion between the bilayer's polar headgroups reduce τ and the channel dissociation constant—most likely because a reduced headgroup repulsion will tend to increase the spontaneous curvature of the two lipid monolayers and thereby increase the membrane deformation energy associated with channel formation.

## Tu-Pos73

MULTIPLE CONFORMATIONS FOR GRAMICIDIN LW

((D. Greathouse, N. Le, R. Koeppe II, J. Hinton, G. Sabarwal\*, L. Providence\*, and O. Andersen\*)) Dept. Chem. Biochem., Univ. Arkansas, Fayetteville, AR 72701 & \*Dept. Phys. Biophys., Cornell Univ. Med. Coll., NY, NY 10021

An analogue of gramicidin A, L-Leu<sup>9,11,13,15</sup>, D-Trp<sup>10,12,14</sup> gramicidin (gLW), has previously been shown to form at least two types of channels in DPhPC membranes: normal, "Urry-type"  $\beta^3$  helical channels and long-lived, intertwined "Veatch-type" channels (25,000 ms average duration in 1 M NaCl, 100 mV). Circular dichroism spectra of gLW in DMPC or SDS suggest conformations very different from gA. 2-D NMR spectroscopy and size exclusion chromatography (SE-HPLC) now demonstrate that the conformation of gLW in lipid environments is primarily monomeric. The NOESY spectrum of gLW in SDS micelles shows no peaks due to secondary structure, suggesting the predominance of unstructured monomers. A comparison of the COSY fingerprint regions of gLW and gA in SDS reveals that the chemical shifts of residues 1-8 differ dramatically, even though they are identical in sequence. SE-HPLC shows that gLW exists predominantly as a monomer in both SDS micelles and DMPC vesicles. We propose that gLW is conformationally flexible and that the channels formed by gLW in DPhPC are relatively minor populations of double-stranded and single-stranded ( $\beta^3$  helical) dimers, both of which derive from unfolded monomers. These unfolded monomers may be the non- $\beta$ -helical monomers proposed by Cifu et al. (*Biophys. J.* 61, 189-203, 1992).

## Tu-Poe74

## STRUCTURAL STUDIES OF TYROSINE-1 GRAMICIDINS

((Kenneth F. Blount, Gwendolyn L. Mattice, Denise V. Greathouse, M. Jeffrey Taylor, Roger E. Koeppe II)) Dept. Chem. Biochem., University of Arkansas, Fayetteville, AR, 72701.

A substitution of L-tyrosine for L-valine at position one of gramicidin A (gA) gives rise to unusual channel properties. Specifically, the presence of L-Tyr<sup>1</sup> in only one monomer of the channel gives a lower single-channel conductance and a shorter mean channel lifetime than when L-Tyr<sup>1</sup> is present in both monomers of a symmetric dimer (J.-L. Mazet, R. E. Koeppe II, and O. S. Andersen 1984 *Biophys. J.* 45, 263-276.) We have investigated the structure of [L-Tyr<sup>1</sup>gA]/[L-Val<sup>1</sup>gA] mixtures in varying proportions in dimyristoylphosphatidylcholine (DMPC) vesicles using circular dichroism (CD) spectroscopy and size-exclusion liquid chromatography (SE-HPLC). The role of Gly<sup>2</sup> was monitored by comparing [L-Tyr<sup>1</sup>Gly<sup>2</sup>gA] with [L-Tyr<sup>1</sup>D-Ala<sup>2</sup>gA]. The dependence of the structural motif upon peptide length was checked using 16- and 17-residue analogues beginning with tyrosine. The results indicate that all of the Tyr<sup>1</sup> analogues exist as mixtures of double-helical and single-helical conformers in DMPC, regardless of the length or the second residue in the gramicidin. "Hybrid-specific" interactions are suggested by the SE-HPLC results but not by the CD spectra; the methods monitor different molecular properties. The double-helical conformers apparently are inert as channels, since no long-lived channels have been reported for Tyr<sup>1</sup> gramicidins. The unusual channel properties may relate to a conformational strain imposed by a single Tyr<sup>1</sup> residue that destabilizes the channel.

## Tu-Poe75

EFFECTS OF  $\beta$ -BRANCHED AMINO ACIDS AT POSITIONS 10, 12, AND 14 OF GRAMICIDIN CHANNELS

((Anthony R. Jude, Denise V. Greathouse, Roger E. Koeppe II, \*Subham Basu, \*Lyndon L. Providence, \*Olaf S. Anderson)) Dept. Chem. Biochem., Univ. of Arkansas, Fayetteville, AR, 72701; \*Dept. Physiol. Biophys., Cornell Univ. Medical College, New York, NY, 10021.

To investigate the influence of the "spacer" residues between the tryptophans of gramicidin A (gA), Leu-10, 12 and 14 of gA were replaced by Ala or Val or Ile. Circular dichroism spectra for Ala<sup>10,12,14</sup> gA, Val<sup>10,12,14</sup> gA, or Ile<sup>10,12,14</sup> gA in SDS or DMPC all show large differences from gA at 25°C and 68°C. All analogues show reduced positive ellipticity at 218 nm and 235 nm, with the Ala analogue giving the largest departure from the gA spectra. Size-exclusion chromatography does not give clear monomer or dimer peaks, but a broad intermediate peak in each case, suggesting the presence of interconverting conformations. All three analogues form membrane-spanning channels; but the channel-forming potency of the Ala analogue is much less than that of the other analogues or gA. In 1.0 M NaCl, the single-channel conductances (g) and durations ( $\tau$ ) are: Ala analogue, g = 7.5 pS,  $\tau$  = 210 ms; Ile analogue, g = 9.0 pS,  $\tau$  = 880 ms; Val analogue, g = 9.0 pS,  $\tau$  = 500 ms, compared to g = 15 pS,  $\tau$  = 600 ms for gA. The results demonstrate that both the size (bulk) and the branching (stereochemistry) of the aliphatic residues between the tryptophans of gA are important for channel properties.

## Na CHANNELS

## Tu-Poe76

## FUNCTIONAL EFFECTS OF DELETIONS THAT ELIMINATE POTENTIAL GLYCOSYLATION SITES IN THE rSKM1 SODIUM CHANNEL.

((E. Bennett, M.S. Urcan, C. Proenza, and S.R. Levinson)) Dept. Physiology & Program in Neurosciences, U. Colorado Health Sciences Center, Denver, CO 80262.

The rat skeletal muscle sodium channel 1 (rSKM1) and two deletion mutants of rSKM1 in which a portion of the heavily glycosylated part of the protein was deleted from each were stably expressed in Chinese Hamster Ovary cells (CHO) in an effort to describe the effects of specific glycosylation sites on channel function. Four (del2-5) or five (del1-5) consensus N-glycosylation sequences from the putative external loop between S5 and S6 of Domain I were removed in the mutant constructs. Although a potential  $\mu$ -conotoxin ( $\mu$ CTX) binding site is also within this loop, the sensitivity of the channel to  $\mu$ CTX is not altered by the deletions indicating that the deletions do not significantly alter channel structure in neighboring regions. The half activation voltages ( $V_{1/2}$ ) measured for del1-5 and del2-5 were 7 and 10 mV more depolarized than the  $V_{1/2}$  observed for the wild type channel, respectively, indicating an effect of these specific glycosylation sites on the voltage-dependence of channel activation. Furthermore, at equivalent potentials, the rates of activation and inactivation of these mutant channels were slower than the wild type, while the rate of deactivation was faster. Comparison of the voltage-dependence of these rates shows that gating kinetics of the mutant channels are also shifted along the voltage axis to the same degree as the steady-state parameters. Overall, such shifts are consistent with an electrostatic mechanism in which negatively-charged sugars influence the electric field detected by channel gating sensors.

## Tu-Poe77

FUNCTIONAL COMPARISON OF rSKM1 AND hH1 NA<sup>+</sup> CHANNELS STABLY EXPRESSED IN CHO CELLS.

((E. Bennett, R.G. Kallen, and S.R. Levinson)) Dept. Physiology, U.C.H.S.C., Denver, CO, 80262; Dept. Biochemistry/Biophysics, U. Penn. Sch. Med., Philadelphia, PA, 19104-6059.

The rat skeletal muscle sodium channel 1 (rSKM1) and the human heart sodium channel 1 (hH1) were stably expressed in Chinese Hamster Ovary (CHO) cells to compare the activity of the channel isoforms in a mammalian cell system. Both lines produced functional currents ranging from 500 pA to 10 nA in approximately 50-70% of the non-clonally selected transfected cells. rSKM1 activated and inactivated at more depolarized potentials than hH1. The half activation voltages were -22.34 mV and -33.78 mV for rSKM1 and hH1, respectively, while the respective half inactivation voltages were -58.07 mV and -66.43 mV. The time constants of activation at hyperpolarized potentials were faster for hH1 than for rSKM1 (30% faster at -50 mV). In addition, rSKM1 showed a faster rate of inactivation than hH1 at all membrane potentials (e.g., more than 2-fold faster at -20 mV) while the rate of recovery from inactivation for the two channels was virtually identical. These data indicate that a greater fraction of available hH1 will be activated at a given depolarization compared to the fraction of rSKM1 that is activated. However, previous studies expressing the two channels in *Xenopus* oocytes have shown quite different channel behavior. Thus, the inactivation rate of rSKM1 is much faster in CHO cells than in oocytes (18-fold faster at -10 mV). Also, rSKM1 activated at more hyperpolarized potentials than hH1 in *Xenopus* oocytes, while rSKM1 activated at more depolarized potentials than hH1 in CHO cells. The fact that the voltage dependence of channel activation varies between the two expression systems may indicate a role for other proteins or secondary modification in determining the activity of the channel. It is known that the posttranslational machinery of *Xenopus* oocytes is different than the machinery in mammalian cells, thereby producing channels that are likely to be modified differently, qualitatively or quantitatively. As a result, the discrepancy in channel activation voltages might be explained by the effect of different modifications on channel function.

## Tu-Poe78

DISTRIBUTION OF SQUID PUTATIVE SODIUM CHANNEL SQSCI mRNA IN THE TISSUES OF SQUID *Loligo bleekeri*

((C. Sato, O. Shouno, T. Kimura, K. Hirota and G. Matsumoto)) Electrotechnical Laboratory, Supermolecular Science Division, Tsukuba, Ibaraki 305, JAPAN

We previously reported the cloning of the cDNA, SQSCI, which encoded complete coding region of the putative sodium channel from squid optic lobe (Sato & Matsumoto, B.B.R.C. 186, 1158-1167, 1992). The cDNA clone was characteristic of its shortest amino acid sequence among other sodium channels so far cloned and sequenced, almost 3/4 of those of rat sodium channels. The transcriptional products were detected in all the nervous systems examined; optic lobes, cerebral ganglia and giant stellate ganglia. However, it was not detected in the muscle, suggesting the SQSCI gene is specific for sodium channels of squid nerve cells. SQSCI is more widely distributed in the nervous system than the GFLN1 which was known as specifically expressed in stellate ganglion of the squid (Rosenthal & Gilly, P.N.A.S. USA 90, 10026-10030, 1993).

## Tu-Poe79

## CHARACTERIZATION OF ANTI-PEPTIDE ANTIBODIES TO RAT BRAIN RII SODIUM CHANNEL. ((M. Jarnot and A.M. Corbett)) Dept. of Physiology &amp; Biophysics, Wright State University, Dayton, OH 45435

In this study, polyclonal antibodies to a peptide unique for the rat brain RII sodium channel were characterized, using both chickens and rabbits as immunological hosts. Three peptides (17 mer, 33% sequence homology) corresponding to sodium channel subtypes RI, RII and RIII were synthesized, and peptide RII coupled via a terminal cysteine to keyhole limpet hemocyanin. Peptide-carrier complexes were emulsified in Freund's adjuvant and 1.5 or 2 ml injected intramuscularly into three rabbits and two chickens, respectively. Serum IgG collected from rabbits 1 week after each boost was compared to IgY isolated from the yolks of eggs laid daily by immunized hens. IgG and IgY were quantitated by ELISA antibody sandwich assays. Specific IgY was first detected at day 40 and reached a peak at 138 days postinjection for one chicken; a second chicken showed almost no response, with specific antibody detected at 86 days postinjection. In rabbits, specific antibody was detected at 33 days and peaked at day 92 postinjection in two animals. A third rabbit maintained low levels of specific antibody production throughout the study. Maximal specific IgY for the chickens was approximately 0.5% of the peak total IgY or about 0.014 mg/ml; maximal specific IgG for rabbits ranged from 2-6% of peak total IgG or 0.05-0.7 mg/ml. No crossreactivity to peptides RI or RIII was observed with antibodies from either host at peptide concentrations less than 0.5 mM. Chicken and rabbit antibodies reached half-maximal block when preincubated with nanomolar and subnanomolar concentrations of peptide RII, respectively. Though the titer of chicken antibodies was lower than that found in rabbits, the total amount of specific antibody (in mg) produced monthly in chickens is approximately equal to rabbits. Supported by NIH Grant NS28377.

## Tu-Poe80

**IMMUNOLocalization of RII Sodium Channel in Rat Brain with High Affinity Antibodies.** (M. Jarnot, F. Alvarez, R.E.W. Fyffe and A.M. Corbett) Departments of Physiology and Anatomy, Wright State University, Dayton, OH 45435

In this study we have used high titer, high affinity polyclonal antibodies to a region in the carboxy tail of sodium channel RII to discretely localize RII channels in tissue sections of adult rat brain. Antibodies produced in rabbit were purified by  $(\text{NH}_4)_2\text{SO}_4$  fractionation and Protein A affinity chromatography. Purified antibodies were concentrated and assayed for specific IgG by ELISA. Rat brains fixed with 4% paraformaldehyde in phosphate-buffered saline (PBS) were cut in 40 micron sections on a freezing microtome and incubated overnight at 25°C with one of the following: preimmune serum, primary antiserum from either of 2 rabbits at 1:2500 or 1:10,000 dilution, or antiserum which had been preincubated with synthetic peptides from RII or RIII sodium channels. Staining of fine fibers and axon terminals was observed throughout the CNS, especially in the cortex, hippocampus, hypothalamus, and the dorsal horn of the spinal cord. Cell body staining was restricted to a small group of cells in the region of the zona incerta-subthalamic nucleus. No staining was observed in the cerebellum. Antibodies from two rabbits showed the same staining pattern in both rat and cat brain sections; preimmune controls showed no specific staining. Preabsorption of the antibody with 100 nM RII peptide resulted in nearly complete block of staining, while the same concentration of RIII peptide resulted in only a slight reduction of staining intensity. Incubation with  $(\text{NH}_4)_2\text{SO}_4$ -fractionated serum showed identical patterns of staining, at dilutions up to 1:50,000. The lack of staining in the cerebellum, reported to be rich in RII sodium channel, may reflect lability of the RII protein, or a processing variation of this subtype which cleaves the carboxy terminus region. Supported by NIH NS28377.

## Tu-Poe82

**DISCRETE OPEN- AND CLOSED-STATE AFFINITIES OF TWO SITE-3 NA CHANNEL TOXINS** ((G. R. Benzinger, C. L. Drum, P. K. Khara, K. M. Blumenthal, and D. A. Hanck) The University of Chicago, Chicago, IL 60637, and The University of Cincinnati, Cincinnati, OH 45267.

The sea anemone *Anthopleura xanthogrammica* produces two homologous peptide toxins, ApA and ApB, which bind to site 3 of the Na channel with isoform-specific affinities and selectively eliminate a major component of channel inactivation. We report here on the characterization, by whole-cell voltage clamp, of the on rates ( $k_{on}$ ) and off rates ( $k_{off}$ ) of both toxins for cardiac muscle (rat), brain (mouse), and skeletal muscle (human) isoforms. Apparent  $k_{on}$  values were relatively invariant between combinations of toxin and channel, ranging from  $0.27$ – $2.7 \times 10^6 \text{ s}^{-1} \text{ M}^{-1}$ .  $k_{off}$ , however, ranged from  $120 \times 10^3 \text{ s}^{-1}$  (ApA / skeletal) to  $0.13 \times 10^3 \text{ s}^{-1}$  (ApB / cardiac). Apparent  $K_D$  values, whose relative ordering was determined primarily by  $k_{off}$ , showed high affinity ( $<5 \text{ nM}$ ) for all combinations involving ApB and/or cardiac channels. Previous studies using  $^{22}\text{Na}$  flux have reported affinities significantly lower than those obtained here for all tested combinations of channel and toxin isoforms (see table). This discrepancy was particularly pronounced for the binding of ApB to cardiac channels, for which  $K_D$  estimates differed by a factor of 100, suggesting that these toxins possess a significantly higher affinity for the closed state, as measured by electrophysiology, than for the open conformation, as assayed by  $^{22}\text{Na}$  flux.

$K_D$ (nM)	cardiac	neuronal	skeletal
<b>V clamp</b>			
ApA	$2.6 \pm 0.85$	$120 \pm 30$	$45 \pm 19$
ApB	$0.090 \pm 0.026$	$5.1 \pm 0.67$	$3.4 \pm 0.87$
<b>flux</b>			
ApA	$14 \pm 3$	$400 \pm 83$	--
ApB	$9 \pm 3$	$22 \pm 3$	--

## Tu-Poe84

**THE EFFECTS OF INTRACELLULAR LYSOPHOSPHATIDYLCHOLINE ON CARDIAC  $I_{Na}$**  ((C.L. Watson and M.R. Gold) University of Maryland, Baltimore, MD 21201

Lysophosphatidylcholine (LPC) accumulates intracellularly during cardiac ischemia. Since ischemia is also marked by conduction abnormalities, it is possible that LPC affects  $I_{Na}$ . It has been reported that extracellular application of LPC causes a reduction in peak  $I_{Na}$  and slows both inactivation and reactivation kinetics. Since LPC first appears intracellularly, we chose to study neonatal rat cardiac cells internally perfused with 1 nM or 1  $\mu\text{M}$  LPC. We recorded  $I_{Na}$  in physiological extracellular  $\text{Na}^+$  using the whole cell voltage clamp method.

With LPC perfusion, steady-state one-half inactivation shifted in the depolarizing direction, from  $-81.8 \pm 1.4 \text{ mV}$  at control to  $-76.6 \pm 1.3 \text{ mV}$  during 1 nM LPC and  $-73.9 \pm 0.9 \text{ mV}$  during 1  $\mu\text{M}$  LPC perfusion. The fast (tf) and slow (ts) time constants of reactivation were accelerated in a similar graded manner with tf decreasing from  $43 \pm 13$  to  $23 \pm 9$  to  $12 \pm 3 \text{ ms}$  while ts decreased from  $247 \pm 84 \text{ ms}$  to  $169 \pm 110 \text{ ms}$  to  $57 \pm 22 \text{ ms}$ , respectively. Consistent with this finding, the frequency dependent decrease in  $I_{Na}$  over a train of 20 repetitive pulses was significantly less in LPC treated cells. There was no change in either maximal  $I_{Na}$  elicited from  $-140 \text{ mV}$  to a range of test potentials or in the time constant of current inactivation, measured from  $-100 \text{ mV}$  to a test potential of  $-30 \text{ mV}$ .

We suggest that the effects of intracellular LPC on  $I_{Na}$  are distinct from those previously reported for extracellular application of this lipid metabolite. Early accumulation of LPC intracellularly may have important implications for cardiac conduction during ischemia because of its effect on  $I_{Na}$ .

## Tu-Poe81

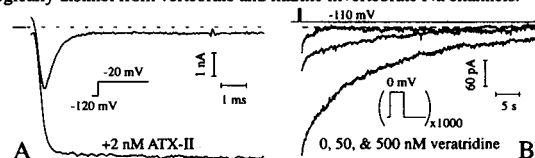
**SODIUM CHANNEL SUBTYPES IN RAT BRAIN DISPLAY DIFFERENTIAL SUSCEPTIBILITY TO PROTEOLYSIS.** ((M. Jarnot, T. Miller, A.M. Corbett) Dept. of Physiology & Biophysics, Wright State University, Dayton, OH 45435

In this study, polyclonal antibodies to sodium channel subtypes (RI, RII and RIII) and conserved regions in the sodium channels were used to probe differences in sodium channel proteolysis with development. Crude P3 membranes from embryonic, neonatal and adult regions of the brain were run on SDS-PAGE, transferred to nitrocellulose membranes, and incubated with antibody against conserved regions of the sodium channel: there was a progressive degradation of the alpha subunit band from 260 kD to smaller bands with development. This study seemed to indicate that RIII, the predominant sodium channel form in the embryo, was less susceptible to proteolysis than the adult forms of the sodium channel. In a separate study, sodium channel subtypes RII and RIII, purified by antibody-affinity columns, displayed differences in their alpha subunits. RIII subtypes displayed whole alpha subunits on Western Blots with no evidence of proteolysis, while RII subtypes displayed several bands characteristic of proteolytic fragments. Immunocytochemical studies with RII antibodies had not shown any specific interaction in the cerebellum, a location which two other investigators have shown to contain RII sodium channel and abundant mRNA for RII. When crude membranes from the cerebellum were compared with membranes from the rest of the brain, more proteolysis was observed in the cerebellum for RI and RII sodium channels. This suggests that the adult sodium channel subtypes, RI and RII, are more susceptible to proteolysis, as seen during the developmental switch in sodium channel subtype expression and in the adult cerebellum, than is observed for RIII sodium channel. This work is supported by NIH NS28377 and an NIH Research Supplement for Underrepresented Minority Undergraduate Students for Tahirah Miller.

## Tu-Poe83

**LOCUST NEURONAL Na CHANNELS ARE HIGHLY SENSITIVE TO NATURAL TOXINS.** ((Eric A. Ertel, Denise L. Wunderler and Charles J. Cohen) Merck Research Laboratories, Rahway, NJ 07065.

Voltage-gated Na channels have multiple binding sites for drugs that modify channel gating. We reported previously that locust channels differ from vertebrate channels at 2 of these sites: they are much more sensitive to the peptide spider toxin  $\mu\text{-Aga-IV}$  and to the pyrethroid deltamethrin. We now show that locust channels are also highly sensitive to 4 other types of ligands. (1) Toxin II from *Anemonea sulcata* (ATX-II) slows inactivation (Fig. A) and is >200-fold more potent than on vertebrate channels. ATX-II also increases  $g_{Na,max}$  as much as 3-fold and shifts the apparent activation curve to more negative potentials, suggesting that activation and inactivation occur at comparable rates. (2) At 50 nM, the alkaloid veratridine substantially slows the deactivation of locust channels (Fig. B), whereas effects on vertebrate channels require 1  $\mu\text{M}$ . As for vertebrate channels, modification is promoted by channel opening. (3&4) Mammalian Na channels are potently blocked by either TTX or transition metals; in contrast, locust channels are potently blocked by both (IC<sub>50</sub>: TTX,  $\approx 0.3 \text{ nM}$ ; Zn,  $\approx 100 \mu\text{M}$ ). Thus, locust Na channels are pharmacologically distinct from vertebrate and marine invertebrate Na channels.



## Tu-Poe85

**PROBING SODIUM CHANNEL DOMAIN STRUCTURE: EVIDENCE FOR BINDING BETWEEN AMINO- AND CARBOXY-TERMINI.** ((Weijiang Sun, Robert L. Barchi, and Sidney A. Cohen) University of Pennsylvania School of Medicine, Philadelphia, PA 19104

Competition between monoclonal and site-specific polyclonal antibodies was used to investigate the structure and spatial relationships among cytoplasmic segments of the rSKM1 sodium channel. Polyclonal antibodies against epitopes in the proximal amino- and carboxy-termini and each of the three interdomain regions did not interact with monoclonal antibodies directed against the proximal amino-terminus; however, each of these polyclonal antibodies did interfere with monoclonal antibody binding to epitopes in the interdomain 2-3 region. Polyclonal antibodies against the distal carboxy-terminus inhibited the binding of monoclonal antibodies to residues 1-6 and 19-24 in the amino-terminus with an unusually steep concentration dependence, suggesting that these two segments are in close proximity in the channel tertiary structure. A series of overlapping peptides covering the amino-terminus proximal to domain 1 was synthesized. One, encompassing residues 1-30, bound specifically to a fusion protein containing the rSKM1 carboxy-terminus but not to other proteins, including a fusion protein containing the rSKM2 carboxy-terminus. Our results suggest that: 1) the amino-terminus is a rigid structure with fixed orientation with respect to other channel cytoplasmic components; 2) interdomain 2-3 is centrally located on the channel cytoplasmic surface; and 3) the amino- and carboxy-termini directly interact. This interaction may help to stabilize protein conformation or may assist in intramembrane channel assembly.

## Tu-P086

**A NOVEL, ABUNDANT SODIUM CHANNEL EXPRESSED IN NEURONS AND GLIA.** ((J.H. Caldwell,\* Donna M. Krzemien,\* P.J. Yarowsky,\* B.K. Krueger\* and K.L. Schaller\*)) \*Departments of Cellular and Structural Biology and Physiology, University of Colorado Health Sciences Center, Denver, CO 80262; \*Department of Pharmacology and Experimental Therapeutics and \*Department of Physiology, University of Maryland School of Medicine, Baltimore, MD 21201

A novel, voltage-gated sodium channel cDNA, designated NaCh6, has been isolated from the rat central and peripheral nervous systems. RNase protection assays showed that NaCh6 is highly expressed in the brain, and NaCh6 mRNA is as abundant or more abundant than the mRNAs for previously identified rat brain sodium channels. *In situ* hybridization demonstrated that a wide variety of neurons express NaCh6, including motor neurons in the brainstem and spinal cord, cerebellar granule cells, and pyramidal and granule cells of the hippocampus. RT-PCR and/or *in situ* hybridization showed that astrocytes and Schwann cells express NaCh6. Thus, this sodium channel is broadly distributed throughout the nervous system and is shown to be expressed in both neurons and glial cells.

## Tu-P088

**REGULATION OF CARDIAC Na<sup>+</sup> CHANNEL EXPRESSION BY THE  $\beta$ 1 SUBUNIT IN *XENOPUS* OOCYTES.** ((Y. Qu, L.L. Isom, J.C. Rogers, T.N. Tanada, K.A. McCormick, T. Scheuer and W.A. Catterall)) Dept. of Pharmacology SJ-30, U. of Washington, Seattle, WA 98195. (Spon. by F.F. Vincenzi)

Currents due to brain and skeletal muscle Na channel  $\alpha$  subunits expressed alone by injection of mRNA in *Xenopus* oocytes are small and have abnormally slow kinetics. Coexpression with the  $\beta$ 1 subunit increases expression, speeds kinetics and causes a negative shift in the voltage-dependence of gating. To detect similar effects of  $\beta$ 1 subunits on currents due to expression of the cardiac Na channel  $\alpha$  subunit (rH1), mRNA encoding the rH1  $\alpha$  subunit was expressed in *Xenopus* oocytes alone or with the  $\beta$ 1-subunit. Current amplitudes measured with two-microelectrode voltage-clamp were increased up to 4-5 fold as a function of the amount of  $\beta$ 1 subunit mRNA coinjected and saturated at a  $\beta$ 1: $\alpha$  mRNA ratio of 10:1. Conversely, current amplitude was unaffected by coexpression of the  $\alpha$  subunit with a mutant  $\beta$ 1 subunit which is non-functional as indicated by its lack of effect on kinetics or expression of current due to rat brain type IIA Na channel  $\alpha$  subunits. Thus, the increases in Na current are due to association of the  $\alpha$  and  $\beta$ 1 subunits. In oocytes where increased currents with  $\beta$ 1 coexpression were confirmed, current kinetics without and with  $\beta$ 1 were compared in cell-attached macropatch experiments. Coinjection of  $\beta$ 1 subunits did not affect the voltage-dependence of Na current activation or inactivation (<5 mV shift), the time course of current during the pulse ( $\tau_{inac}$  at +20 mV:  $\alpha$  = 506  $\mu$ s,  $\alpha$ + $\beta$  = 510  $\mu$ s) or recovery from inactivation. Thus, whereas rat heart Na channel  $\alpha$  and  $\beta$ 1 subunits associate and increase expression, channel function appears unaffected.

## Tu-P090

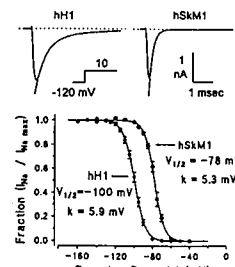
**INACTIVATION DEFECTS IN SODIUM CHANNEL III-IV LINKER MUTATIONS ASSOCIATED WITH MYOTONIA.** ((L. J. Hayward, R. H. Brown, Jr., and S. C. Cannon)) Dept. of Neurology, Mass. General Hospital, Boston, MA 02114.

Point mutations in the skeletal muscle Na channel  $\alpha$  subunit are associated with several myotonic disorders, including hyperkalemic periodic paralysis (HYPP), potassium-aggravated myotonia (PAM), and paramyotonia congenita (PC). These mutations interfere with normal channel inactivation. In order to clarify the biophysical mechanisms of defective Na channel inactivation, we introduced point mutations into the rat muscle Na channel cDNA (rSkM1) corresponding to the human PAM disease mutations G1306A, G1306E, and G1306V. cDNAs were cloned into pRC/CMV and expressed transiently in HEK293 cells. Whole cell Na currents were measured to characterize activation ( $G(v)$ ), steady-state inactivation ( $h_{\infty}$ ), macroscopic decay ( $\tau_h$ ), persistent current, and recovery from inactivation for the wild-type (WT) and each mutant channel. When compared to WT, the  $h_{\infty}$  curve was shifted by 10 mV to the right for the mutant G1306E and to a lesser degree for G1306V and G1306A. Macroscopic decay was 1.5-fold slower at 0 mV for the PAM mutants compared to WT. The ratio of steady-state (50ms) to peak current was ~0.3% for WT and ~0.4-1% for G1306E, G1306V, and G1306A. The persistent current was blocked by TTX. Activation and recovery from inactivation were not significantly affected by any of the mutations. Cotransfection of the  $\alpha$  subunit cDNA with an excess of human  $\beta$ 1 subunit cDNA dramatically increased current amplitudes, shifted the  $h_{\infty}$  curves by 5mV to the right, and speeded recovery ~2-fold in HEK293 cells.  $\tau_h$  was only slightly faster, and persistent current remained small. The defect of inactivation for Na channels containing the PAM mutations G1306E, G1306V, and G1306A differs from that of HYPP channels in that a large persistent current is not present. A slowed  $\tau_h$  plus an  $h_{\infty}$  shifted to the right is sufficient to cause the clinical features of PAM (myotonia without paralysis) in our mathematical model.

## Tu-P087

**CHARACTERIZATION OF CARDIAC AND SKELETAL MUSCLE Na<sup>+</sup> CHANNEL ISOFORMS FOLLOWING HETEROLOGOUS EXPRESSION IN TRANSFORMED EMBRYONIC KIDNEY CELLS.** ((D.W. Wang, A.L. George and P.B. Bennett)) Departments of Pharmacology & Medicine, Vanderbilt University School of Medicine, Nashville, TN 37232.

The human heart (hH1) skeletal muscle (hSkM1) sodium channel  $\alpha$ -subunits are encoded by distinct genes. Their primary amino acid sequences are similar but not identical. A first step in structure-function studies of voltage gated Na<sup>+</sup> channels is to compare the functional properties of heterologously expressed wild type Na<sup>+</sup> channels. hH1 and hSkM1 were transiently expressed in transformed human embryonic kidney cells (tsA201) and macroscopic Na<sup>+</sup> currents were recorded at 20–23°C. hSkM1 activated at more positive potentials than hH1. Both displayed fast activation and inactivation kinetics, similar to the native channels. The inactivation time course of hH1 was bi-exponential. The rate of inactivation was significantly ( $P<0.05$ ) faster in hSkM1 compared to hH1 (see figure) at membrane potential  $\geq -10$  mV ( $\tau_{fast, hH1} = 10$  ms, hH1:  $0.4 \pm 0.04$  ms; hSkM1:  $0.23 \pm 0.01$  ms;  $n=5$ ). The initial mid-point of steady-state inactivation ( $V_{1/2}$ ) of hH1 ( $-100 \pm 0.9$  mV  $n=10$ ) was more negative than that of hSkM1 ( $-78 \pm 1.0$  mV  $n=8$ ). These results demonstrate successful expression of the human cardiac channel and identify important functional distinctions in these channels.



## Tu-P089

**FAST INACTIVATION IN CHROMAFFIN CELL Na<sup>+</sup> CHANNELS MAY BE CONTROLLED BY DUAL 'H-GATES'.** ((Frank T. Horrigan and Richard J. Bookman)) Dept. of Molecular & Cellular Pharmacology, Box 016189, University of Miami School of Medicine, Miami, FL, 33101

$I_{Na}$  recorded from rat chromaffin cells rapidly inactivates with a time course that is well fit by a single exponential ( $\tau = 0.6$  ms @ +20 mV). Yet, recovery from fast inactivation is biphasic ( $\tau_1 = 8$  ms,  $\tau_2 = 130$  ms @ -80 mV). Such behavior could reflect: 2 distinct Na<sup>+</sup> channels, modal gating, or a single population with 2 inactivated states. The activation and inactivation kinetics of the fast recovering component are indistinguishable from that of total current. The fractions of current recovering via fast (30%) and slow (70%) paths and their time constants are essentially constant following single depolarizations of 0.3 to 50 ms duration. Thus, channels do not interconvert from one inactivated state to another during a pulse. However the fraction of current recovering rapidly is decreased 2-fold following repetitive depolarization. This ability of channels to shift from fast to slow recovery suggests that both phases of recovery are due to a single channel population. We present a model, consistent with the above results, in which channels can enter two distinct inactivated states ( $I_{slow}$ ,  $I_{fast}$ ) from the open state. The model is supported by the action of internal papain. After ~10 minutes,  $I_{Na}$  increases slightly and continues to inactivate completely, however the time constant of inactivation is slowed ~3-fold and recovery occurs exclusively via the fast route. The slowing of inactivation rate supports the idea that entry to  $I_{slow}$  normally occurs via the open state. Thus, papain appears to selectively abolish transitions to  $I_{slow}$  and allows all channels to enter  $I_{fast}$ , consistent with our model. This action of papain suggests that the two inactivated states are the result of dual h-gates in chromaffin cell Na<sup>+</sup> channels. (NSF & AHA/FL)

## Tu-P091

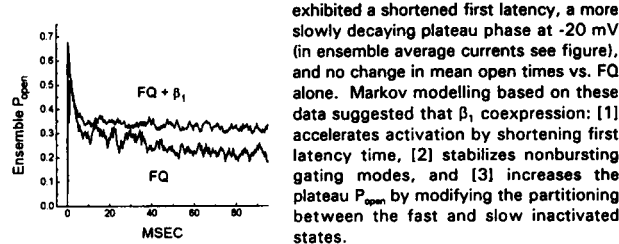
**VOLTAGE DEPENDENT S4 MOVEMENT SHOWN BY CYSTEINE REAGENTS.** ((N. Yang and R. Horn)) Department of Physiology, Jefferson Medical College, Philadelphia, PA 19107.

A naturally occurring pathogenic mutation in the adult human skeletal muscle Na channel (hSkM1)  $\alpha$ -subunit substitutes a cysteine for the outermost arginine in the S4 segment of domain 4. R1448C causes a dramatic slowing of inactivation and enhanced rate of recovery from inactivation (Chahine et al., '94, *Neuron* 12:281). We tested the accessibility of this residue to methanethiosulfonate reagents (Akabas et al., '92, *Science* 258:307) applied to the extracellular surface of cells transfected with this mutant. The three reagents tested attach small monovalently charged groups to cysteine by di-sulfide linkage. All reagents, at concentrations <50  $\mu$ M, dramatically increase the rate of inactivation and decrease the rate of recovery from inactivation of the R1448C mutant, effects not observed when the reagents were applied to wild-type hSkM1 channels. These modifications were obtained for both negatively and positively charged reagents. The mutation R1448C also decreases the voltage dependence of inactivation. This feature is not affected significantly by the cysteine reagents. The modification is prevented when the holding potential is more negative than -120 mV, and occurs within ~3 min when the holding potential is more positive than -100 mV. These data show that R1448 becomes exposed upon depolarization, as predicted by models of S4 as a voltage sensor.

## Tu-Poe92

MODULATION OF GATING IN AN INACTIVATION-DEFECTIVE SODIUM CHANNEL BY THE  $\beta_1$  SUBUNIT. (D.W. Orias, J.R. Balser and J.H. Lawrence) The Johns Hopkins University, Baltimore, MD 21205.

The  $\beta_1$  subunit of the voltage-gated sodium channel is found in muscle, nerve and heart in association with the pore-forming  $\alpha$  subunit. In whole-cell recordings of wild-type  $\alpha$  subunits, co-expression of  $\beta_1$  results in an acceleration of both activation and inactivation, and a reduction in cumulative inactivation with fast repetitive pulsing. To explore the mechanism of these effects, we examined single-channel currents from  $\mu_1$ -F1304Q (FQ), an inactivation-defective rat skeletal muscle  $\alpha$  subunit, with and without co-expression of  $\beta_1$  in *Xenopus* oocytes. Like the wild-type channel, FQ exhibits multiple gating modes. With  $\beta_1$  coexpression, a bursting mode was markedly less active. The predominant gating mode (high open probability, nonbursting)



exhibited a shortened first latency, a more slowly decaying plateau phase at -20 mV (in ensemble average currents see figure), and no change in mean open times vs. FQ alone. Markov modelling based on these data suggested that  $\beta_1$  coexpression: [1] accelerates activation by shortening first latency time, [2] stabilizes nonbursting gating modes, and [3] increases the plateau  $P_{open}$  by modifying the partitioning between the fast and slow inactivated states.

## Tu-Poe94

TWO CONFORMATIONAL STATES INVOLVED IN THE USE-DEPENDENT TTX BLOCKADE OF HUMAN CARDIAC  $Na^+$  CHANNELS. (R. Dumaine, H.A. Hartmann, G.E. Kirsch). Baylor College of Medicine Houston TX 77030

Mutations IFM-1QM and IFM-QQQ in the linker between domain III and IV of the sodium channels reduce the fast inactivation of the sodium current (Hartmann et al. 1994. *Circ. Res.* 75(1):114-122, West et al. 1992. *Proc. Natl. Acad. Sci. USA.* 89:10910-10914). We used a fast inactivation deficient mutant (QQQ) of the human heart sodium channels  $\alpha$ -subunit (hH1a) to assess the influence of the inactivation gate on tonic and phasic components of TTX blockade. The extra block developing during long depolarizing pulses (phasic block) followed the availability of the channels ( $VD_{50} = -83$  mV) on hH1a and the activation on QQQ ( $VD_{50} = -38$  mV). Its onset had a fast and slow component. The post-repolarization block (PRB) had similar time course of onset and offset for WT and QQQ. The time constant of onset for the phasic block and PRB were similar. These results suggest a common binding site for use dependent block (UB) and PRB in WT and QQQ. The onset of UB was 5 fold slower for QQQ and the steady state level of the block in 10  $\mu$ M TTX was 17% higher. These results cannot be solely explained by a slow recovery from an inactivated toxin bound state as proposed by Cohen et al. (Cohen et al., 1981. *J. Gen. Physiol.* 78:383-411.). They show that the higher affinity site proposed to explain the UB in TTX-sensitive sodium channels (Lonnendonker, 1989. *Biochim. Biophys. Acta.* 985:153-160. Makielaki et al. (1993) *Biophys. J.* 65:790-798.) is present in hH1a. We showed that at least two conformational states are involved in UB by TTX on heart sodium channels. We suggest that the later mechanism is responsible for UB during short depolarizations and that the accessibility of the toxin to this site is modulated by the fast inactivation of the channel. (Supported by a Department of Defense grant : DAMD 17-91-C-1093).

## Tu-Poe96

TEMPERATURE SHIFTS VOLTAGE DEPENDENCE AND VALENCE OF SLOW INACTIVATION. ((D. Featherstone, M. Henteleff, M. Hermosura, J. Starkus, M. Rayner, P. Ruben)) Békésy Lab, Pacific Biomedical Research Ctr., University of Hawaii, Honolulu, HI 96822

We, and others, have previously shown that voltage dependence of slow inactivation in RBIIa sodium channels expressed in *Xenopus* oocytes is shifted toward more hyperpolarized potentials when: a) channels are in 'fast' mode, as opposed to 'slow' mode, and b) prepulse durations are increased.

Here, we show that between 12-30 °C and with 200 ms prepulses, the voltage dependence of slow inactivation shifts by about 2.5 mV/°C for fast-mode channels and 0.5 mV/°C for slow-mode channels. In addition to being affected by channel mode, temperature dependence decreases with shorter prepulses. The interaction between temperature dependence, mode, and prepulse duration results in increased temperature-sensitivity when slow inactivation is more hyperpolarized. Extrapolation of linear fits to all data above suggest that at 38 °C, the midpoint voltage of slow inactivation remains at approximately -55 mV, despite varying modal content or prepulse duration. In addition to effects of temperature on voltage dependence, the apparent valence of slow inactivation increases by 0.2 to 0.4  $e^-$ /°C from about 2 $e^-$  at 15 °C.

Activation, in contrast to slow inactivation, showed no changes in voltage dependence or valence as a function of temperature.

(Supported by PHS grants #NS-21151, #NS-29204, NIH RCMI grant #RR-03061 and grants from American Heart Assoc. Hawaii Affiliate.)

## Tu-Poe93

MODELING GATING MUTATIONS OF THE SKELETAL MUSCLE  $Na^+$  ( $\mu_1$ ) CHANNEL. ((J. Balser, D. Orias, B. Nuss, J. Lawrence, E. Marban, G. Tomaselli)) The Johns Hopkins School of Medicine, Baltimore, MD 21287

Site-directed mutagenesis of single amino acids in voltage-gated ion channels assists in determining the structure-function relationships. For the skeletal muscle ( $\mu_1$ ) channel, single amino acid mutations modify specific gating functions. Examples include the F1304Q domain III-IV linker mutation, which removes fast inactivation, and the W402C P-loop mutation that accelerates channel activation and inactivation. Both mutations alter recovery from inactivation: F1304Q accelerates recovery from inactivation at negative potentials while W402C delays recovery from inactivation. As a paradigm for understanding this complex behavior, we implemented a model of  $Na^+$  channel gating similar to that recently validated by Kuo and Bean (1994). In this model, activation and deactivation are voltage-dependent  $m^4$  Hodgkin-Huxley sequences, while inactivation results from voltage-independent binding of a blocking particle to the channel. The affinity of the channel receptor for the inactivation particle changes as the channel activates. To faithfully reproduce the rapid and slow components of recovery from inactivation for the  $\mu_1$  channel, it was necessary to include two competing inactivation processes, which may represent alternate binding configurations for a single inactivation particle. Consistent with this view, modification of the receptor affinity for both inactivation processes was necessary to accurately reproduce the gating kinetics of F1304Q channels.

## Tu-Poe95

KINETIC ANALYSIS OF THE VOLTAGE-DEPENDENT SODIUM CHANNEL OF THE CATFISH HORIZONTAL CELL BASED ON ADMITTANCE MEASUREMENTS. ((E.C. Hymel, C.R. Murphey, L.E. Moore, and B.N. Christensen)) Dept. of Physiology & Biophysics, Univ. of Tx. Med. Br, Galveston, TX 77555-0641.

Catfish horizontal cells are known to possess a minimum of four active conductances, including the voltage-gated  $Na^+$  channel. In a continuing effort to develop a mathematical model of this cell, the sodium channel was investigated using admittance spectroscopy. Under voltage clamp conditions where all other active conductances were pharmacologically blocked, small voltage excursions (2-3 mV root mean square) around a given clamp potential in the steady state were used to elicit correspondingly small currents resulting from  $Na^+$  channel activation. The voltage stimulus was Fourier synthesized and has a spectrum of uniform magnitude and random phase. The constant magnitude spectrum drives the system uniformly at all frequencies of interest and a randomized phase spectrum is chosen to minimize the dynamic amplitude of the stimulus waveform. The ratio of the current response to the voltage stimulus, or admittance, was fitted in the complex plane to a kinetic model that allows for activation and inactivation of the  $Na^+$  current as well as the passive characteristics of the cell. The model used is general and equivalent to the linearized Hodgkin-Huxley formalism where the conductances are functions of the steady-state gating parameters. Because admittance data across a range of membrane potentials are simultaneously fitted, individual kinetic rate constants are not only optimized at each voltage, but their potential dependencies are also quantitatively determined. Voltage dependent relaxation time constants equivalent to the usual voltage-clamp exponential time constants were obtained. Supported by grant NEI-01897.

## Tu-Poe97

ON-CELL KINETIC VARIATION IN RAT BRAIN IIa  $Na^+$  CHANNELS. ((A. Hakeem, M. Henteleff, M.D. Rayner, J.G. Starkus, P. Ruben)) Békésy Lab, Pac. Biomed. Res. Ctr., Univ. Hawaii, Honolulu, HI 96822

On-cell recordings of RBIIa channels expressed in *Xenopus* oocytes show initial modal differences between patches from the same oocyte. Additionally, we have seen changes in time to peak and inactivation kinetics within the first 5-10 minutes of observation in single on-cell patches. The times to peak become shorter, and we observed a decrease in the amount of slow mode inactivation and/or an increase in the amount of fast mode inactivation as determined by four-exponential fits to the data. These observations suggest that sodium channels are differentially regulated by cytoplasmic constituents.

We also see a small component of channels that do not significantly inactivate during the duration of a 30 ms pulse at 20-24 °C. Although fast and slow mode channels have similar activation kinetics, this small component has a significantly slower activation rate than either fast or slow mode channels.

(Supported by PHS grants #NS-21151, #NS-29204, NIH RCMI grant #RR-03061 and grants from American Heart Assoc. Hawaii Affiliate.)

## Tu-Pos98

**SURFACE POTENTIAL DIFFERENCES BETWEEN HEART AND BRAIN SODIUM CHANNELS EXPRESSED IN *XENOPUS* OOCYTES** ((Thomas H. Hauser, Harry A. Fozzard, and Jonathan Satin\*)) Cardiac Electrophysiology Labs, The Univ. of Chicago, Chicago, IL 60637; \*Present address: Dept. of Physiology, Univ. of Kentucky, Lexington, KY 40536-0084

External divalent cations cause a depolarizing shift of the steady-state activation and inactivation curves for cloned sodium channels from heart (hH1a) and brain (rb2a) expressed in *Xenopus* oocytes. Steady-state activation and inactivation curves were measured with the two electrode voltage-clamp. Increasing  $Ca_{ext}$  or  $Ba_{ext}$  causes an equivalent shift of the midpoint ( $V_{1/2}$ ) of steady-state activation and inactivation curves of hH1a in the depolarizing direction. This is consistent with divalent cations screening negative surface charge. The same range of  $Ca_{ext}$  causes a greater shift for rb2a than for hH1a. Fitting the data to the Grahame equation predicts that there is approximately 2-fold more negative surface charge density affecting  $V_{1/2}$  for rb2a compared to hH1a. To assess the contribution by sialic acid residues we treated oocytes for 4 hours with neuraminidase and measured  $V_{1/2}$  as a function of external Ca. Neuraminidase treatment shifted the  $V_{1/2}$  of rb2a in the depolarized directions consistent with the cleavage of negatively charged sialic acid residues. Gouy-Chapman theory predicts an approximate 2-fold change in surface charge density after neuraminidase treatment of rb2a. Neuraminidase treatment of hH1a also shifted the  $V_{1/2}$ , but the shift was less than that for rb2a. Neuraminidase had no effect on  $V_{1/2}$  in the presence of high  $Ca_{ext}$  (10mM) for either isoform. These results are consistent with the presence of a greater density of negatively charged sialic acid residues on rb2a than on hH1a.

## Tu-Pos100

**UNIQUE ROLE FOR THE S4 SEGMENT OF DOMAIN 4 OF SODIUM CHANNELS.** ((L.-Q. Chen, V. Santarelli, P. Zhang, R. Horn, and R.G. Kallen)) Dept of Physiology, Jefferson Medical College, Philadelphia, PA 19107; Dept of Biochemistry & Biophysics, University of Pennsylvania, Philadelphia, PA 19104-6059. (Spon. by G. Panyi)

The Na channel is composed of four homologous domains each of which is thought to have 6 transmembrane spanning segments. The fourth transmembrane segment (S4) has a repeated sequence consisting of a positively charged amino acid (arginine or lysine) followed by two hydrophobic residues. There is evidence showing that the positive charges in the S4 segments of each domain are involved in the voltage sensing mechanism for activation of the channel (Stühmer et al, *Nature* 339:597, '89; Kontis et al, *Biophys J* 66:A135, '94). We examined the effects of these positive charges on the voltage dependence and rate of inactivation by making charge substitutions in the 1st (outermost) and the 3rd positive residue in the S4 segment of each domain of the human heart Na channel. We substituted the outermost positive residue with glutamine, and the 3rd with either glutamine or glutamate. Na channels were expressed in *Xenopus* oocytes and currents were recorded with either 2-microelectrode voltage clamp or the cut-open oocyte preparation. Some mutants cause shifts (<10 mV) in the voltage dependence of the peak current, as expected for an effect on activation. The rate and the voltage dependence of inactivation are strongly decreased by these mutations only in the S4 region of domain 4 (D4). The results are consistent with effects of mutations linked to paramyotonia congenita (Chahine et al, *Neuron* 12:281, '94) and indicate an important role for S4/D4 in the inactivation of the channel.

## Tu-Pos102

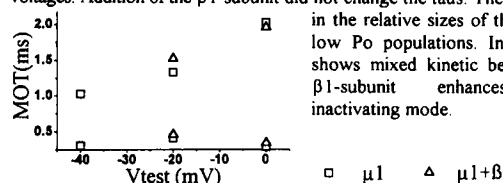
**EFFECT OF EXTERNAL pH ON EXPRESSED SODIUM CURRENT.** ((J.-P. Benitah, E. Marban and G. F. Tomaselli)) Johns Hopkins University, Baltimore, MD 21205.

The mechanisms proposed for external  $H^+$  inhibition of  $Na^+$  channels are binding to a site within the pore and/or reducing the local surface potential. We examined the effect of decreasing external pH on the current through the rat skeletal sodium channel ( $\mu 1$ ) expressed in oocytes. Increased  $[H^+]$  has two concentration-dependent effects on the whole-cell current. Reduction of pH from 7.6 to 7 decreased  $I_{Na}$  without any voltage shift in the current-voltage relationship (I-V). At lower pHs, the  $I_{Na}$  progressively decreased and was accompanied by a depolarizing shift of the I-V relationship. In comparison to pH 7.6 ( $[Na^+] = 96mM$ ), we observed a  $10.4 \pm 6.3\%$  ( $n=22$ ) reduction of the relative maximal conductance ( $G_{max}$ ) at pH 7 and a decrease of  $52.6 \pm 16.8\%$  and a shift for the I-V relationship of  $+14.8 \pm 8.8mV$  at pH 6 ( $n=22$ ), with an apparent  $pK_a$  of  $\sim 6.2$ . The steady-state inactivation curve ( $h_{\infty}$ ) was unchanged at pH 7 but was shifted  $+4.0 \pm 2.2mV$  ( $n=13$ ) at pH 6. If we assume that the shift of  $h_{\infty}$  is the result of a surface charge effect then the discrepancy could be accounted for by channel block. In order to distinguish between block and surface charge effects we measured  $I_{Na}$  in external solutions of different  $[Na^+]$ . At pH 7, there were no ionic strength-dependent changes in  $G_{max}$  and no shift of the I-V. At pH 6,  $G_{max}$  decreased more at  $[Na^+] = 56mM$  ( $63.0 \pm 13.6\%$ ,  $n=6$ ) than at  $[Na^+] = 140mM$  ( $47.5 \pm 10.8\%$ ,  $n=10$ ), with a similar depolarizing shift in the I-V. With  $Li^+$  as the permeant ion (96mM) we observed no reduction in  $G_{max}$  at pH 7 compared with pH 7.6 but at pH 6 the reduction of  $G_{max}$  and shift in the I-V was similar to that seen in  $Na^+$  ( $54.4 \pm 14.3\%$  and  $11.4 \pm 2.2mV$ ,  $n=6$ ). The unitary conductance progressively decreased with reduction in the pH (34pS at pH 7.6, 30pS at pH 7, 17pS at pH 6). Reduction of pH reduces  $I_{Na}$  by both proton block and surface charge titration, the latter effect occurs at lower pH.

## Tu-Pos99

**$\beta 1$ -SUBUNIT EXPRESSED WITH ADULT RAT SKELETAL MUSCLE Na CHANNEL  $\alpha$ -SUBUNIT RESTORES A NATIVE-LIKE FAST GATING MODE.** ((S.Chang, J.Satin, J.Kyle, and H.Fozzard)) The University of Chicago, Chicago, IL 60637.

Expression of the adult skeletal muscle Na channel  $\alpha$ -subunit ( $\mu 1$ ) in *Xenopus* oocytes results in a slowly decaying current, restored toward normal by coexpression of the  $\beta 1$ -subunit. Single channel recording of  $\mu 1$   $\alpha$ -subunits alone demonstrates stable kinetic behavior with alternating clusters of single openings (low Po) and bursts (high Po) indicative of modal behavior. Channels usually gate normally (low Po), but spend 20-30% of the time in high Po mode. Mean open times (MOT) show two kinetic populations of channel openings. Single channel analysis of  $\mu 1 + \beta 1$  also shows some high Po behavior and the same two populations of open times as  $\mu 1$  alone, but the longer open time fraction is greatly diminished. The figure shows taus for the two MOT populations at different voltages. Addition of the  $\beta 1$ -subunit did not change the taus. The differences are in the relative sizes of the high Po and low Po populations. In summary,  $\mu 1$  shows mixed kinetic behavior, and the  $\beta 1$ -subunit enhances the faster-inactivating mode.



## Tu-Pos101

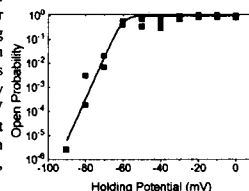
**ANALYSIS OF SODIUM CHANNEL D4-S3 AND D4-S4 MUTATIONS IN PARAMYOTONIA CONGENITA: IMPLICATIONS FOR CHANNEL FUNCTION.** ((S. Ji, A.L. George, R. Horn and R.L. Barchi)) Univ. of Pennsylvania School of Medicine, Phila., PA 19104; Vanderbilt Medical School, Nashville, TN 37232; Jefferson Medical College, Phila., PA 19107.

In order to explore possible molecular mechanisms underlying the effects of paramyotonia mutations L1433R and R1448C in S3 and S4 of D4, and to study the normal functional roles of these helices, we reconstructed these mutations in the hSkM1 sodium channel and also constructed 6 additional mutations at L1433. Double mutants containing both L1433R and R1448C were then created to probe the interaction between these two regions. Mutations were expressed in the mammalian tsA201 cell line and studied using patch clamp. R1448C and L1433R both slowed channel inactivation and accelerated recovery from inactivation without significantly affecting channel activation. However, R1448C shifted the  $h_{\infty}$  curve in the hyperpolarized direction and rendered  $\tau_1$  less voltage dependent while L1433R caused a shift of  $h_{\infty}$  in the opposite direction and did not alter the voltage-dependence of  $\tau_1$  significantly. Five of 6 new substitutions at 1433 produced effects qualitatively similar to L1433R while L1433A had no effect. Mutational activity at 1433 depended on sidechain size and polarity rather than charge, while effects at 1448 reflected the loss of positive charge at that site. The R1448C-L1433R double mutant resembled R1448C in its effects on  $\tau_1$ , but L1433R in regard to its effects on  $h_{\infty}$  and recovery from inactivation. These data suggest that kinetic rather than steady-state factors determine channel phenotype in PC, and that S3 and S4 in D4 play separate dominant roles in inactivation and recovery from inactivation.

## Tu-Pos103

**A MOVEMENT OF 10-11 ELECTRONIC CHARGES IS SUGGESTED BY THE VOLTAGE DEPENDENCE OF THE STEADY-STATE OPEN PROBABILITY IN NON-INACTIVATING SODIUM CHANNELS.** ((J. Patlak, A. Rovner, M. Lieberman, and B. Hirschberg)) Dept. of Molecular Physiology, Univ. of Vermont, Burlington, VT 05405.

At the most hyperpolarized potentials, plots of the Na channel's open probability versus voltage reach a limiting slope. Hodgkin and Huxley originally suggested that this limiting slope should be a measure of the total charge that has to be moved during channel opening. For *Shaker B* potassium channels, values as high as 12-16 electronic charges have recently been found (Zagotta et al, 1994, *J.Gen.Physiol.* 103:279). This value agrees well with the hypothesis that each of the four homologous subunits of the functional channel contribute 3.5 electronic charges to activation gating. In contrast, limiting slope analysis of sodium channels has generally yielded total charge estimates of 4-7 electronic charges (e.g. Oxford, 1981, *J.Gen.Physiol.* 71:227 using pronase-treated Na channels of squid axon). These studies have relied on the measurement of macroscopic current from inactivating or enzyme-modified channels. In order to improve these measurements, we constructed a mutated Na channel that lacks fast inactivation (IFM1303QQQ), and studied it in *Xenopus* oocytes with inhibition of Protein Kinase C-modulation. This mutation, together with the use of mean-variance analysis to analyze long on-cell recordings, allowed us to determine open probabilities for holding potentials as negative as -90mV. At the most negative potentials, open probability increases approximately 100-fold with each 10mV change in membrane potential suggesting that movement of at least 10-11 electronic charges is required to open the channel. Our results imply that up to four gates, each with 2.5 charges, are needed for gating.

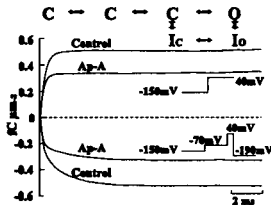




## Tu-Pos104

**SITE-3 TOXINS MODIFY CARDIAC NA CHANNEL INACTIVATION BY ELIMINATING A MOLECULAR CONFORMATIONAL STATE ASSOCIATED WITH INACTIVATION** (M. F. Sheets and D. A. Hanck) Northwestern University Medical School and the University of Chicago, Chicago, IL

Site-3 toxins slow inactivation of voltage-gated Na channels by modifying inactivation from the open state. We tested whether site-3 toxins eliminated an inactivated state ( $I_o$ ) or whether they only delayed entry of channels into  $I_o$ . To determine this we compared ON- and OFF-gating charge in cardiac Na channels in control and after modification by the site 3 toxin, *Anthopleurin-A* (Ap-A). If toxin only slowed entry to  $I_o$  from the open state (intact  $I_c \rightarrow I_o$ ), then OFF-charge after a long inactivating pulse should exceed the ON-charge measured during a short depolarization. Na channels were inactivated by stepping to -70 mV for 500 ms, and OFF-gating charge was measured following repolarization to -190 mV (bottom). In the same cell ON-gating charge was measured during a short step depolarization to +40 mV from a  $V_{hp}$  of -150 mV (top). In control, the magnitude of the OFF-charge at -190 mV equalled the maximum ON-charge obtained from a step depolarization to 40 mV. After Ap-A toxin the ON-charge at 40 mV was reduced by 33%, but OFF-charge remained equal to ON-charge ( $n=3$ ), consistent with toxin eliminating rather than slowing entry to a distal inactivated state ( $I_o$ ).



## Tu-Pos106

**TTX BUT NOT STX DETECTABLY ALTERS NA CHANNEL GATING CURRENT.** (C.M. Armstrong and K. Khodakhah) University of Pennsylvania, Department of Physiology, Philadelphia, Pa.

If Ca binds in sodium channels, it might be expected to interact with TTX. Such an interaction was sought by recording gating current ( $I_g$ ) of Na channels in squid axons, with NMG inside and out. With improved resolution, we find that TTX has an effect on  $I_g$ , small enough that it previously escaped detection. Up to -40 mV, adding TTX to 100 Ca increases  $I_g$  amplitude (~1.25X) with little kinetic effect. At higher V, amplitudes are similar, but  $I_g$  in TTX peaks earlier and decays faster. Tail kinetics are little affected by TTX. Changing from 100 to 10 Ca when TTX is present affects  $I_g$  ON much less than in the absence of the toxin.  $I_g$  OFF is smaller and slower in 10 than in 100 Ca, with or without TTX. Surprisingly, STX is quite different: it has no detectable effect on  $I_g$ . Further, changing from 10 to 100 Ca has, as best we can tell, exactly the same effect as in the absence of STX. The results with TTX show that the Ca site involved in the gating effects on  $I_g$  is sufficiently close to the permeation path that TTX alters Ca action. The STX experiments, on the other hand, suggest that Ca binds in the pore at a point external to the presumably common site where TTX and STX block permeation. TTX but not STX interferes with this external Ca binding site.

## Tu-Pos108

**NA CHANNEL  $\beta_1$  ASSOCIATION WITH CARDIAC NA CHANNEL  $\alpha$  SUBUNITS DEMONSTRATED BY LIDOCAINE BLOCK.**

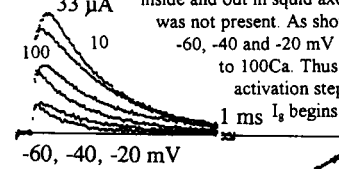
(Jonathan C. Makielski, James T. Limberis, Steven Y. Chang, Zheng Fan, and John W. Kyle) Cardiac Electrophysiology Labs, University of Chicago, Chicago IL, 60637.

The  $\beta_1$  subunit accelerates decay and shifts steady-state availability ( $h_{\infty}$ ) when co-expressed with  $\alpha$ -subunits of non-cardiac Na channels. The cardiac  $\alpha$ -subunit decays rapidly without  $\beta_1$  and  $\beta_1$  effects on  $h_{\infty}$  are reported to be negligible. Does  $\beta_1$  associate with and affect the function of the cardiac isoform? We expressed human heart Na channels alone and with rat brain  $\beta_1$  in oocytes and studied Na current using a two micro-electrode voltage clamp (holding potential -120 mV, test potential -10 mV). For  $h_{\infty}$  type protocols with 500 ms conditioning steps  $\beta_1$  caused a small but significant positive shift (-75.7 $\pm$ 1.9 to -71.3 $\pm$ 4.7 n=10 p=0.03) in the midpoint. The  $K_d$  for tonic lidocaine block was increased from 280  $\mu$ M to 1135  $\mu$ M.  $\beta_1$  also reduced phasic block in response to pulse trains (10 Hz).  $\beta_1$  increased the  $K_d$  for the inactivated state from 4.5  $\mu$ M to 8.1  $\mu$ M (after a 1s depolarization to -10 mV).  $\beta_1$  also accelerated recovery (1s conditioning step) from lidocaine block ( $\tau=689\pm176$  ms to  $\tau=314\pm158$  ms n=8) but had no effect on recovery in control. We conclude that  $\beta_1$  can associate with the cardiac isoform and that this association decreases tonic and phasic lidocaine block. Because the effects on gating are minimal,  $\beta_1$  may act at the lidocaine binding site either directly or via allosteric effects.

## Tu-Pos105

**CALCIUM DOES NOT AFFECT NA CHANNEL GATING STEPS UNIFORMLY.** ((K. Khodakhah and C.M. Armstrong.)) University of Pennsylvania, Department of Physiology, Philadelphia, Pa.

We examined gating current ( $I_g$ ) to see how [Ca] affects different steps in the opening and closing of Na channels. Permeant ions were replaced by NMG inside and out in squid axons. TTX, which interacts with Ca, was not present. As shown, the initial amplitude of  $I_g$  at -60, -40 and -20 mV is unaffected by changing from 10 to 100Ca. Thus the forward rate of the first activation step is unaffected. At -60 and -40mV,  $I_g$  begins to decay almost immediately in 100



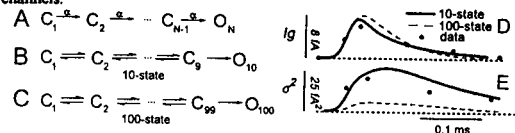
-60, -40, -20 mV  
Ca, but shows a rise in suggesting that steps or their reverse rates mV (sufficient to open value of  $I_g$ , as the 100Ca: Ca speeds the probably subsequent steps

amplitude in 10 Ca, after the first one are accelerated, made smaller. After the step to -20 some of the channels) the initial channels close, is larger in first step in closing (and as well).

## Tu-Pos107

**LARGE-SCALE SIMULATION OF GATING CURRENT NOISE FOR VOLTAGE-GATED ION CHANNELS: EVIDENCE FOR ~10 CHARGE-MOVING TRANSITIONS** (W. Guo and D.T. Yue) Johns Hopkins Sch. Med., Baltimore, MD 21205 (Spon. by S.C.Kuo)

How many charge-moving transitions underlie the activation of voltage-dependent ionic channels? Classical models explain gating as voltage-dependent transitions among several states (e.g., Armstrong and Gilly, 1979), whereas recent proposals envision gating as a diffusion-like process with charge movement distributed among transitions linking hundreds of states (Langer, 1988; Oswald et al, 1991). Distinguishing between these proposals is critical, but customary experimental measures, e.g., mean gating current ( $I_g$ ), fail to provide compelling distinctions. The theoretical work here argues that recent measurements of statistical fluctuations in  $I_g$  (e.g., Conti and Stuhmer, 1989; Sigg et al, 1994) may be inconsistent with diffusion-like gating. For an idealized activation scheme (A), we prove that if charge movement is shared equally among all transitions, then  $\sigma^2 \propto 1/N$ , where  $\sigma^2$  is the variance of  $I_g$ . Hence,  $\sigma^2$  will be too small relative to data if  $N$  is larger than 10-20 states. By numerical simulation, we verify that  $\sigma^2 \propto 1/N$  for generalized activation schemes of the form shown in B and C. Panel D shows that while both 10-state (B) and 100-state (C) models can account for experimentally measured  $I_g$  (e.g., Conti and Stuhmer, 1989), the 100-state prediction for  $\sigma^2$  is too small (E). Gating models with a "small" number of dominant charge-movement transitions may be appropriate for understanding voltage-dependent gating of ionic channels.



## Tu-Pos109

**PHOTOAFFINITY LABELING OF SODIUM CHANNEL IN MAMMALIAN BRAIN SYNAPTOSOMES WITH A MODEL LOCAL ANESTHETIC.** (W.M. Mok, J. McHugh, G.K. Wang and G.R. Strichartz) Department of Anesthesia Research Laboratories, BWH, Harvard Medical School, Boston, MA 02115.

N-(2-di-N-butylaminoethyl)-4-azidobenzamide (DNB-AB) has previously been identified as a model local anesthetic which, upon UV irradiation, caused irreversible inhibition of sodium currents in mammalian GH<sub>1</sub> cells and of batrachotoxin binding in mammalian brain synaptosomes. In this study, the corresponding tritiated, photoactivatable compound, [<sup>3</sup>H]-DNB-AB, has been synthesized from tritiated N-hydroxysuccinimide-4-azidobenzamide and has been photoaffinity labeled to brain synaptosomes. Brain synaptosomes (50  $\mu$ g protein) were incubated for 30 min at 37°C in a total volume of 60  $\mu$ l buffer solution (pH 7.4) containing 2  $\mu$ M [<sup>3</sup>H]-DNB-AB. The preincubated synaptosomes were then irradiated for 5 min at room temperature under N<sub>2</sub> with a 254 nm UV lamp at a distance of 5 cm. The membranes were solubilized in 2% SDS-PAGE buffer and were resolved by electrophoresis using 7.5% gel and the buffer system of Laemmli. SDS-PAGE revealed labeling of a ~230,000 Da protein which is suspected to be the sodium channel. Photoaffinity labeling of [<sup>3</sup>H]-DNB-AB to this protein was reduced in the presence of local anesthetics including unlabeled DNB-AB, tetracaine, bupivacaine, benzocaine and tricaine. This protein at ~230,000 Da was specifically recognized in Western blots on nylon membrane with an affinity purified polyclonal antibody (courtesy of S.R. Levinson, Univ. Colo.) directed against the intracellular III-IV loop of cel sodium channel. Our results strongly suggest that the voltage sensitive sodium channel is a target site for DNB-AB. (Supported by USPHS grant GM 15904 to GS).

## Tu-Pos110

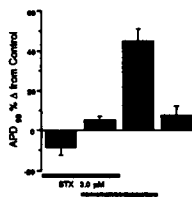
INHIBITION OF CARDIAC SODIUM CHANNELS BY THE NEURO-PROTECTIVE AGENT BW1003C87. ((M.T. Slawsky, N.A. Castle). Boston University Medical Center and Harvard Medical School. Boston, MA 02215.

BW1003C87 [5-(2,3,5-trichlorophenyl)-2,4-diaminopyrimidine] is a neuroprotective agent which has been proposed to exert its antischemic effects by inhibiting glutamate release from presynaptic neurons through inhibition of sodium ( $\text{Na}^+$ ) channels. To date, there has been no direct electrophysiological examination of the effect of this agent on  $\text{Na}^+$  channels nor has the neural selectivity of this agent been tested. Therefore the present study used whole-cell patch clamp recording from isolated adult rat ventricular myocytes to investigate the effects of BW1003C87 on cardiac  $\text{Na}^+$  channels. BW1003C87 inhibited cardiac  $\text{Na}^+$  channels in a voltage-dependent manner with an  $\text{IC}_{50}$  of  $>10 \mu\text{M}$  at  $-140 \text{ mV}$  and  $0.2 \mu\text{M}$  at  $-80 \text{ mV}$ .  $3 \mu\text{M}$  BW1003C87 produced a  $20 \text{ mV}$  hyperpolarizing shift in voltage-dependence of steady-state  $\text{Na}^+$  channel inactivation ( $-90 \text{ mV}$  to  $-111 \text{ mV}$ ,  $n=5$ ). Magnitude and time course of  $\text{Na}^+$  current inhibition by BW1003C87 was dependent on the duration of depolarization and drug concentration. Time constants for block ranged from  $8 \text{ s}$  at  $0.1 \mu\text{M}$  to  $560 \text{ ms}$  at  $3 \mu\text{M}$ . The  $K_D$  derived from the plot of  $1/\tau_{\text{BLOCK}}$  versus drug concentration was  $0.28 \mu\text{M}$  (similar to  $\text{IC}_{50}$ ). In the presence of BW1003C87 there was an additional slow phase of recovery from inactivation ( $\tau_{\text{RECOV}} = 1.1 \text{ s}$ ). Increasing drug concentration resulted in an increase in the fraction of current which recovered with slow kinetics; however,  $\tau_{\text{RECOV}}$  was independent of drug concentration. In summary, BW1003C87 is a potent inhibitor of cardiac  $\text{Na}^+$  channels. The shift in voltage-dependence of steady-state inactivation produced by BW1003C87 together with the slow kinetics of  $\text{Na}^+$  channel block by this agent suggest a preferential interaction of this agent with the inactivated state of the cardiac  $\text{Na}^+$  channel.

## Tu-Pos112

EFFECTS OF RWJ-24517 (CARSATRIN) ON ACTION POTENTIALS, LATE SODIUM CURRENT, AND POTASSIUM CURRENTS IN GUINEA PIG VENTRICULAR MYOCYTES ((N.K. Jurkiewicz, B. Jow, R.G. Tsushima\*, J.A. Wasserstrom\*, J.J. Salata) Merck Research Laboratories, West Point, PA 19486 and \*Northwestern University, Chicago, IL 60611

RWJ-24517 (RWJ) is a new positive inotropic agent that is structurally similar to the cardiotonic agent DPI 201-106. We studied the effects of RWJ in guinea pig isolated ventricular myocytes to understand better its mechanism of action. RWJ ( $0.1 \mu\text{M}$ ) increased action potential duration (APD) during stimulation at  $0.2 \text{ Hz}$  by  $45 \pm 6\%$  ( $n=5$ ). This prolongation of APD was prevented by pretreatment with  $3 \mu\text{M}$  saxitoxin (STX) and was reversible upon washout of RWJ (Figure). During  $600 \text{ ms}$  long voltage clamp steps from a  $V_h$  of  $-80$  to a  $V_t$  of  $-10 \text{ mV}$  at  $24^\circ\text{C}$ ,  $0.1 \mu\text{M}$  RWJ increased net inward current by  $1036, 979, 820, 594 \text{ pA}$  at  $50, 100, 250, 500 \text{ ms}$ , respectively, and this effect was blocked by  $3 \mu\text{M}$  STX. Outward  $\text{K}^+$  currents were studied in the presence of  $10 \mu\text{M}$  tetrodotoxin (TTX) and  $0.4 \mu\text{M}$  nifedipine with  $[\text{Ca}^{2+}]_0 = 0$ , to block  $I_{\text{Na}}$  and  $I_{\text{Ca}}$ , respectively. RWJ blocked the rapidly activating component of the delayed rectifier,  $I_{\text{Kr}}$ , measured as tail current by  $23 \pm 9$  and  $62 \pm 7\%$  at  $0.1$  and  $1 \mu\text{M}$  ( $n=5$ ), respectively. RWJ ( $10 \mu\text{M}$ ) did not block the inward rectifier  $\text{K}^+$  current ( $I_{\text{K1}}$ ). We conclude that 1) the dominant effect of RWJ is an enhancement of  $I_{\text{Na}}$  due to slowing of inactivation; 2) RWJ also inhibits  $I_{\text{Kr}}$  at higher concentrations; 3) these actions explain its positive inotropic and APD prolonging effects.



## Tu-Pos114

A LOW-THRESHOLD NON-INACTIVATING SODIUM CURRENT IN HUMAN ANTERIOR PITUITARY TUMOR CELLS. ((Y.A. Kuryshv, G.V. Childs, S.A. Lieberman, W.W. Maggio, A.K. Ritchie)) Depts. of Physiology and Biophysics, Anatomy and Neurosciences, Internal Medicine, and Surgery, University of Texas Medical Branch, Galveston, TX 77555.

A voltage-dependent non-inactivating inward current was studied in human adrenocorticotropin hormone-secreting tumor cells. The tumor cells, obtained by surgical excision from a female patient with Nelson's syndrome, were maintained in culture and identified as corticotropes by immunocytochemistry. Currents were recorded at room temperature using the giga-seal, whole cell recording technique. The compositions of the recording solutions were (in mM): pipette -  $10 \text{ NaCl}$ ,  $140 \text{ N-methyl-D-glucamine}$  (NMDG),  $80 \text{ L-aspartic acid}$ ,  $1 \text{ MgCl}_2$ ,  $10 \text{ HEPES}$ ,  $15 \text{ EGTA}$ ,  $5 \text{ BAPTA}$ ,  $\text{pH } 7.2$ ; bath -  $160 \text{ NaCl}$ ,  $0.05 \text{ CaCl}_2$ ,  $1 \text{ MgCl}_2$ ,  $10 \text{ HEPES}$ ,  $\text{pH } 7.4$ . The current was non-inactivating (2 s test pulse), exhibited slow activation kinetics and was low-threshold, activating at potentials more positive than  $-70 \text{ mV}$ . The activation curve (averaged from 5 cells) was well fit by the Boltzmann relation with a potential of half-maximal conductance at  $-30.1 \text{ mV}$  and a slope factor of  $9.6 \text{ mV}$ . Deactivation of the current at  $-90 \text{ mV}$  was described by a single exponential with  $\tau = 55 \pm 10 \text{ ms}$  ( $X \pm \text{SEM}$ ,  $N=6$ ). The current was carried by  $\text{Na}^+$  since it reversed close to  $E_{\text{Na}}$  and was absent when external  $\text{Na}^+$  was replaced with NMDG, tetraethylammonium (TEA) or  $10 \text{ mM Ca}^{2+}$  plus TEA. Unlike the conventional tetrodotoxin-sensitive, rapidly inactivating  $\text{Na}^+$  current that was also present in these cells, the non-inactivating current was resistant to  $1 \mu\text{M}$  tetrodotoxin. The non-inactivating current was blocked by external  $\text{Cs}^+$  and  $\text{La}^{3+}$ , with half-maximal inhibition occurring at  $3.7 \text{ mM}$  and  $150 \mu\text{M}$ , respectively. The non-inactivating current could contribute to resting membrane potential or play an important role in action potential generation. Supported by NIH grants DK 44363 and DK 39553.

## Tu-Pos111

EFFECTS OF MEXILETINE ENANTIOMERS ON  $\text{Na}^+$  CURRENTS OF ADULT SKELETAL MUSCLE FIBERS. ((A. De Luca, F. Natuzzi, G. Lentini\*, C. Franchini\*, V. Tortorella\* and D. Conte Camerino\*)) Unit of Pharmacology, Dept. of Pharmacobiology and \*Dept. of Medicinal Chemistry, Faculty of Pharmacy, University of Bari, Italy. (Spons. by J.A. Heiny).

Mexiletine, a blocker of voltage-dependent sodium channels, effectively suppress myotonic hyperexcitability. To search for safer antimyotonic agents, we tested the stereoselective effectiveness of mexiletine. The R-(-) and S-(+) enantiomers were synthesized and tested on  $\text{Na}^+$  currents of frog semitendinosus muscle fibers voltage clamped by means of three vaseline gap technique (holding potential, h.p. =  $-100 \text{ mV}$ ). The tonic block by each isomer was evaluated as percent reduction of the maximum peak  $\text{Na}^+$  current, elicited with single test pulses from the h.p. to  $-20 \text{ mV}$  for  $15 \text{ ms}$ . The half-maximal concentrations ( $\text{IC}_{50}$ ) for tonic block were  $44 \pm 1 \mu\text{M}$  and  $104 \pm 2 \mu\text{M}$  for R-(-) and S-(+) enantiomers, respectively. When the above test pulse was applied repetitively at the frequency of  $2 \text{ Hz}$ , both the enantiomers produced a further cumulative reduction of peak sodium current. The  $\text{IC}_{50}$  values for such phasic block were twofold lower with respect to those for tonic block, without change of the eudismic ratio. The mexiletine enantiomers also produced a left-shift of the steady-state inactivation ( $h_{\infty}$ ) curve, constructed with a pulse protocol by which the membrane potential, held for  $500 \text{ ms}$ , was cyclically varied from  $-140$  to  $-40 \text{ mV}$  and followed by a test pulse at  $-20 \text{ mV}$ . The observed shift of the  $h_{\infty}$  curves was dependent upon the optical configuration, being  $6.7 \text{ mV}$  and  $3.5 \text{ mV}$  with  $5 \mu\text{M}$  of R-(-) and S-(+) mexiletine, respectively. The present data support the presence of a stereospecific site on sodium channels of adult skeletal muscle. The constant eudismic ratios during tonic and use-dependent block suggest that the receptor does not assume conformations that may enhance stereoselectivity during repetitive stimulation. However, the very low concentrations of R-(-) mexiletine effective in these conditions may be useful for a more safe treatment of myotonic syndromes (Support of Telethon-Italy to Conte Camerino's project # 579, 1994 is acknowledged).

## Tu-Pos113

BACKGROUND SODIUM CURRENT AND ELECTRICAL INSTABILITIES IN CARDIAC CELLS.

((Y.I. Zilberter, C.F. Starmer, J. Starobin, and A.O. Grant)) Duke University, Durham, NC 27710 (Spon. by C.F. Chignell)

An imbalance of hyper and depolarizing currents during rest and the action potential (AP) plateau can shift these potentials resulting in slowed conduction and abnormal impulse generation that may initiate cardiac arrhythmias. Computer simulations revealed that small tissue regions of reduced excitability can promote spiral wave reentry that may lead to cardiac tachyarrhythmias. Recently we identified with single channel measurements, channels that permit a background  $\text{Na}$  current ( $\text{bNa}$ ) that can significantly modulate both diastolic and plateau potentials and thus is a potentially important determinant of conditions leading to membrane electrical instabilities. When  $I_{\text{K1}}$  in atrial

cells was partially reduced (simulating diseased atrial cells) by  $30 \mu\text{M Ba}^{2+}$ , the rest potential was depolarized by  $15.3 \pm 4.7 \text{ mV}$  ( $n=9$ ),  $dV/dt(\text{max})$  decreased from  $130 \pm 55 \text{ V/s}$  to  $24 \pm 13 \text{ V/s}$ , and spontaneous activity was often initiated. Blockade of  $\text{bNa}$  with  $5 \mu\text{g/ml}$  lidocaine partially restored membrane parameters: the rest potential was hyperpolarized by  $11.5 \pm 7.9 \text{ mV}$ ,  $dV/dt(\text{max})$  increased to  $58 \pm 13 \text{ V/s}$ , and spontaneous activity terminated.

The negative resistance region of the membrane steady-state  $i/v$  and its proximity to  $i=0$  determine the possibility of abnormal impulse generation (e.g. EAD). In atrial and Purkinje cells, both these factors were critically dependent on  $\text{bNa}$ . Measurements performed with the action potential clamp revealed that  $I_{\text{Na}}$  persists throughout the action potential repolarization and its magnitude is comparable or greater than that of  $\text{Ca}$  current.

## Tu-Pos115

SODIUM-CHANNEL MYOTONIA: BIOPHYSICAL AND CLINICAL IMPLICATIONS OF THREE G1306 MUTATIONS OF THE HUMAN MUSCLE SODIUM CHANNEL. ((N. Mitrovic, A.L. George, S. Wagner, U. Hartlaub, H. Lerche, F. Lehmann-Horn)) Department of Applied Physiology, University of Ulm, Germany. (Spon. by P. Iuzzo)

Three mutations (G1306A/V/E) at the same nucleotide position of the gene encoding the  $\alpha$ -subunit of the human adult muscle sodium channel, produce three clinically different phenotypes of the  $\text{Na}^+$ -channel myotonia disease. Two of the mutations (G1306V/E), expressed in HEK293 cells, significantly disturbed sodium channel inactivation. In whole cell mode, the sodium current decay was best fitted with double exponential function. The time constants of inactivation ( $\tau_{1,2}$ ) and steady-state to peak current ratio ( $I_{\text{ss}}/I_{\text{peak}}$ ) were significantly increased with G1306E/V mutations compared to WT (e.g. G1306E vs. WT;  $\tau_{1,2}$ ,  $1.29 \pm 0.10 \text{ ms}$  vs.  $0.52 \pm 0.01 \text{ ms}$ ,  $I_{\text{ss}}/I_{\text{peak}}$ ,  $2.90 \pm 0.40\%$  vs.  $0.93 \pm 0.19\%$  at  $0 \text{ mV}$ ). The steady-state inactivation curve with G1306E/V was shifted by  $15 \text{ mV}$  to depolarizing potentials. The recordings with G1306A mutation showed an increase in  $\tau_{1,2}$  ( $0.74 \pm 0.07$  vs.  $0.52 \pm 0.01$ ) but no significant change of the  $I_{\text{ss}}/I_{\text{peak}}$  was observed. Analysis of single-channel data with G1306E/V mutant channels showed prolonged openings and increased frequency of reopenings. The intracellular loop between domains III and IV of the sodium channel is proposed to serve as the inactivation gate. The pair of glycines G1306/7 is a part of the III-IV interlinker. Due to their high flexibility (no side chains), two glycines are proposed to act as a hinge of the lid occluding the sodium channel pore. The side chain properties for the substitutes for G1306 are in good correlation with the observed  $\text{Na}^+$  channel dysfunction *in vitro* and the severity of the myotonia *in vivo*. Alanine with the short side chain is the most benign mutation whereas the glutamic acid with a long side chain shows a major steric effect. (Supported by DFG Le 481/3-1 and MDA).

## Tu-P05116

A ONE-MINUTE PULSE OF NGF INDUCES LONG-TERM MEMBRANE EXCITABILITY IN PC12 CELLS THROUGH THE EXPRESSION OF A PERIPHERAL NERVE TYPE SODIUM CHANNEL GENE. ((J. J. Toledo-Aral, P. Brehm, S. Halegoua and G. Mandell)) Dept. Neurobiology and Behavior, SUNY, Stony Brook, NY 11794-5230.

The continual presence of Nerve Growth Factor (NGF) is thought to be required for the differentiation of rat pheochromocytoma (PC12) cells into sympathetic-like neurons. Surprisingly, we find that long-term membrane excitability is established in PC12 cells following only a one-minute exposure to NGF. The acquisition of excitability is due to the induction of the peripheral nerve type sodium channel (PN1) gene, through a transcriptional program requiring expression of immediate-early genes. Although continuous treatment with NGF induces a family of voltage-gated sodium channels (brain type II/IIA and PN1), brief treatment selectively induces the PN1 sodium channel. Northern-blot analysis indicated that levels of PN1 transcripts began to increase by three hours after removal of NGF, peaked between 4 and 5 hours (11-fold induction), and declined slowly to near basal levels by 24 hours. Whole cell patch clamp showed that the production of functional voltage-gated sodium channels was associated with the increase in mRNA levels. The voltage activated sodium current was induced approximately 6-fold, as soon as 8 hours after the brief exposure to NGF, and persisted for at least 24 hours (10-fold induction). The molecular basis for PN1 gene induction is unknown but, unlike the case for brain type II/IIA sodium channels, the signaling pathway is not dependent upon cAMP. PN1 induction is also independent of extracellular calcium, and is not stimulated by depolarization with high potassium or by treatment with phorbol esters. As with NGF, brief exposure of PC12 cells to Epidermal Growth Factor, Fibroblast Growth Factor and the cytokine interferon- $\gamma$  also stimulated PN1 gene induction. Our data provide the first demonstration that a brief pulse of NGF can trigger a long-term change in neuronal phenotype, by initiating a program of gene induction events leading to the acquisition of membrane excitability. This new triggered pathway may be important during nervous system development, allowing neurons to acquire membrane excitability in response to a wide variety of growth factor molecules which may be present only transiently.

## Tu-P05118

KINETIC ANALYSIS OF TIME-DEPENDENT OPEN CHANNEL BLOCK BY AN INACTIVATION GATE PEPTIDE OF NON-INACTIVATING TYPE IIA SODIUM CHANNELS. ((Galen Eaholtz, William N. Zagotta, and William A. Catterall)) Graduate Program in Neurobiology, Dept. of Physiology and Biophysics, and Dept. of Pharmacology, University of Washington, Seattle, WA 98195

The synthetic peptide acetyl-KIFMK-amide (KIFMK) was found to block wild-type Type IIA sodium channels and restore inactivation to non-inactivating mutant channels (Eaholtz *et al.*, 1994, *Neuron*, 12:1041). We analyzed the kinetics of the open channel block by KIFMK in Type IIA sodium channels where inactivation has been disrupted by the mutation F1489Q. The channels were expressed by transient transfections of tsA-201 human embryonic kidney cells and RNA injections into *Xenopus* oocytes. In both expression systems, KIFMK exhibited a time-dependent block of the F1489Q type IIA channels. From the time course of KIFMK block, the on-rate constant was found to be voltage-dependent while the off-rate constant was not appreciably voltage-dependent. The concentration dependence of the rate constants was examined in macropatches of *Xenopus* oocytes where the KIFMK concentration could be varied. Here the on-rate constant was found to depend linearly on concentration while the off-rate was independent of concentration. These experiments suggest that KIFMK binds to open sodium channels and blocks them in a time-dependent manner that is voltage- and concentration-dependent.

## MYOSIN II

## Tu-P05119

BIOCHEMICAL CHARACTERIZATION OF THE ACANTHAMOEBA MYOSIN-I ATPase. ((E. M. Ostap and T. D. Pollard)) Department of Cell Biology and Anatomy, Johns Hopkins University School of Medicine, Baltimore, MD 21205.

*Acanthamoeba* myosin-IA (MIA) and myosin-IB (MIB) are single-headed molecular motors that may play an important role in the movement of organelles and membranes along actin filaments. To better define the types of motility that myosin-I can support, we have determined the rate constants for key steps on the myosin-I ATPase pathway using transient kinetic techniques. The rate of ATP binding to MIA and MIB was determined by (a) monitoring the fluorescence change that accompanies the binding of the ATP analog, mant-ATP, to MI in the absence of actin, and (b) monitoring the fluorescence of pyrene-actin during the actomyosin dissociation reaction. The rate of ATP binding to MIA is  $0.65 \mu\text{M}^{-1} \text{s}^{-1}$ , and rate of ATP binding to MIB is  $1.7 \mu\text{M}^{-1} \text{s}^{-1}$ . These rates were independent of the method used. The dissociation rate of MIA-ATP and MIB-ATP from actin is  $> 600 \text{ s}^{-1}$ . Phosphorylation of the MI heavy chain did not change these rate constants. The dissociation constant of ADP was obtained from the inhibition of the rate of ATP binding to pyrene-actin-myosin-I for a range of ADP concentrations. The data was best fit assuming that ADP was in rapid equilibrium with the actomyosin-I complex. The dissociation constant ( $K_d$ ) of ADP from the actin-MIA complex is  $95 \mu\text{M}$ , and the  $K_d$  for MIB is  $53 \mu\text{M}$ . The rate and percent of ATP hydrolysis by MIB was determined using rapid-quench. MIB hydrolyzes ATP at a rate  $\geq 50 \text{ s}^{-1}$ . Measurement of the  $P_i$  burst in the absence of actin indicated that MIB hydrolyzed 0.22  $P_i$ /myosin head. This low value was confirmed with single turn over experiments. The results suggest that although the rate constants that define the MIA and MIB ATPase differ significantly from skeletal myosin, the overall ATPase mechanism is more like that of skeletal myosin than the cytoplasmic motor kinesin.

## Tu-P05117

SEA ANEMONE TOXIN MODULATES HUMAN HEART SODIUM CHANNELS EXPRESSED IN A HUMAN CELL LINE. ((M. Chahine, E. Plante and R. G. Kallen)) Québec Heart Institute, Laval Hospital, Laval University, St-Foy, Québec, G1V 4G5 and Dept. of Biochem. & Bioph. Sch. of Med. Univ. of Pennsylvania, Philadelphia, PA 19104-6059. (Spon. P. Daleau)

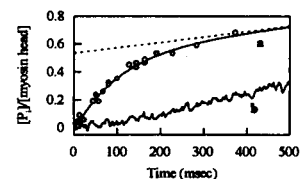
Sea anemone toxin (ATX II) is a 47 amino acid polypeptide that slows the inactivation of voltage-gated sodium channels. Previous studies showed that this toxin selectively acts on heart sodium channels. The  $\alpha$  subunit of cloned voltage gated sodium channels contains sites for drugs and toxins known to interact with voltage-gated sodium channels from native tissue. In this study we have expressed hH1 (human heart subtype1) and rSkM1 (rat skeletal muscle subtype1) sodium channels expressed in tsA201 (HEK293) cells, a human kidney cell line, and we compared the effect of ATX II on both isoforms. On hH1, ATX II dramatically slows the inactivation phase with little effect on activation. For example at  $-20 \text{ mV}$   $\tau_h$  is increased by a factor of approximately 27. The inactivation phase is multiexponential in presence of the toxin. The voltage-dependence of inactivation is reversed suggesting that ATX II may reduce the rate of inactivation from open state. The steady-state inactivation-voltage relationship is shifted to more depolarized voltages. The recovery from inactivation is faster in presence of the toxin ( $\tau_{\text{control}}=79.6 \text{ ms}$ ,  $\tau_{\text{ATX II}}=62.9 \text{ ms}$ ) suggesting that the inactivated state is destabilized. ATX II has only a small effect on rSkM1. We are using rSkM1-hH1 chimeric sodium channels to identify the ATX II binding site of hH1.

## Tu-P05120

TIME RESOLVED MEASUREMENTS OF PHOSPHATE RELEASE IN MYOFIBRILLAR ATPases SHOW THAT  $P_i$  RELEASE IS RATE LIMITING ((C. Lionne<sup>1</sup>, M. Brune<sup>2</sup>, M. Webb<sup>2</sup>, F. Travers<sup>1</sup> and T. Barman<sup>1</sup>)) <sup>1</sup>U128 INSERM, CNRS, BP5051, 34033 Montpellier, France. <sup>2</sup>National Institut for Medical Research, Mill Hill, London NW7 1AA, UK.

We are testing rabbit psoas myofibrillar ATPases at  $4^\circ\text{C}$  as a model for muscle fibre ATPase with the Scheme:  $\text{M} + \text{ATP} \rightleftharpoons \text{M} \cdot \text{ATP} \rightleftharpoons \text{M} \cdot \text{ADP} \cdot \text{P}_i \rightleftharpoons \text{M} \cdot \text{ADP} + \text{P}_i \rightleftharpoons \text{M} + \text{ADP}$ . We first used the flow quench method in which reaction mixtures are quenched in acid and  $P_i$  determined. With Ca-activated myofibrils there was a  $P_i$  burst (figure, curve a) showing that  $\text{M} \cdot \text{ADP} \cdot \text{P}_i$  (which decomposes in acid) and/or  $P_i$  accumulate, i.e. that either  $P_i$  or ADP release is rate limiting (Houadjeto *et al.*, 1992, *Biochemistry* 31, 1564). To decide, we now studied the ATPase by a method specific for free  $P_i$ . These are based on the *E. coli* phosphate binding protein (PBP) labeled with a fluorophore with which stopped-flow measurements are possible (Brune *et al.*, 1994, *Biochemistry* 33, 8261). With the PBP method, there was a transient lag phase of  $P_i$  (curve b). With relaxed myofibrils too there was a large  $P_i$  burst by flow quench but not by the PBP method. Therefore, with the myofibrillar ATPases at  $4^\circ\text{C}$  complexes of the type  $\text{M} \cdot \text{ADP} \cdot \text{P}_i$  accumulate, the  $P_i$  release step is rate limiting and the ADP release step is rapid.

Supported by the EU.



## Tu-Pos121

GLYCATION OF RABBIT SKELETAL MYOSIN ((G. Avigad, A. Kniep and G. Bailin)) UMDNJ-RWJ Med. School, Piscataway, NJ 08854 and Sch. Osteopathic Med., Stratford, NJ 08084

Treatment of rabbit skeletal myosin with 3 mM D-glucose-6-phosphate inhibited its  $K^+$  and actin activated-ATPase activities as a function of time while fructose- or glucose-6-phosphate and ribose-5-phosphate had little or no effect. Substrate ATP protected the ATPase activity of myosin against glycosylation when its effect was studied over a modification interval that ranged between 1 and 15 hours. Less than one mole of glucose 6-phosphate was incorporated per  $4.7 \times 10^5$  g of myosin up to the 28 hour reaction interval. In contrast to the extensive protection of the ATPase activity by ATP, there was only a 20% reduction in the labeling of the modified myosin in the presence of ATP. The labeling was limited to the heavy chain region of myosin as judged by gel electrophoresis which resolved the heavy and light chain components. In vitro glycosylation of a long lived protein such as myosin may be a suitable model system for the study of hyperglycemic effects seen in diabetics. (Supported by Grants-in-Aid From AHA, NJ Affiliate to G.A. and G.B.)

## Tu-Pos123

CHEMICAL MODIFICATION AND SMALL-ANGLE X-RAY SCATTERING OF MYOSIN-ADP-FLUOROMETAL COMPLEXES.

((S. Maruta, T. Kanbara, Y. Sugimoto\*, Y. Takezawa\*, M. Ikebe\* & K. Wakabayashi\*) Dept. of Bioengineering, Soka University, Hachioji, Tokyo 192, Japan. \*Dept. of Biophysical Engineering, Osaka University, Osaka 560 Japan. #Dept. of Physiology & Biophysics, School of Medicine, Case Western Reserve University, Cleveland, Ohio 44106.

Myosin forms stable ternary complexes which mimic transition state of the ATP hydrolysis with phosphate analogues of aluminium fluoride ( $AlF_4^-$ ), beryllium fluoride ( $BeF_3^-$ ) and vanadate ( $Vi$ ) in the presence of  $Mg^{2+}$ -ADP. Our previous experiments on interaction between the ternary complexes and actin showed that each complex may mimic different steps along ATPase kinetic pathway [Maruta et al. J. Biol. Chem. 268, 7093-7100 (1993)]. To show how different conformations the complexes have at the local flexible region, reactivity of the cysteine residues SH1 (707), SH2 (697) and reactive lysine residue, RLR (83) were studied. And global shapes of the complexes were studied using small angle X-ray scattering. SH1, SH2 and RLR reactivities of Myosin (S-1)-ADP- $BeF_3^-$  complexes were similar to the reactivities of S-1 in the presence of ATP. Interestingly, SH1, SH2 and RLR reactivities of S-1-ADP- $AlF_4^-$  were the same as reactivities of myosin in the absence of ATP. Small angle X-ray scattering of the complexes showed that as same as Rg of ATP/S-1, Rg of S-1-ADP- $Vi$  complex was about 2 Å less than that of nucleotide-free S-1, showing that the shape of S-1-ADP- $Vi$  is more compact. On the other hand, the Rg value of the S-1-ADP- $AlF_4^-$  and S-1-ADP- $BeF_3^-$  were almost the same as that of nucleotide-free S-1. It is suggested that the conformational changes at the local SH1-SH2 and RLR region are not accompanied with global shape change of myosin head, and these three kinds of ternary complexes differ in conformation of myosin head.

## Tu-Pos125

TIME-RESOLVED FLUORESCENCE SPECTROSCOPY OF ACETAMIDOTETRAMETHYL RHODAMINE FREE IN SOLUTION AND BOUND TO MYOSIN REGULATORY LIGHT CHAIN. (T. St. Allen and A. Arner) Dept of Physiology and Biophysics, Lund University, Lund, Sweden.

Fluorescence polarization of acetamidotetramethylrhodamine (ATR) covalently bound to chicken gizzard myosin regulatory light chains (cgRLC) and exchanged for native RLC in demembrated rabbit psoas fibers has been used to study the relationship between angular motions of cross-bridges and the elementary force generating process (Allen, Irving, and Goldman, *Biophys. J.* 66:A234, 1994). Analysis of changes in polarization in terms of angular motions of cross-bridges requires knowledge of mobility of ATR on RLC. To gain this knowledge, we have begun time-resolved fluorescence spectroscopy of ATR free in solution and bound to Cys-108 of cgRLC. 5- and 6-Iodo-ATR were reacted with 2-mercaptoethanesulfonate and then excited by pulsed synchrotron light at 540 nm. Fluorescence (>570 nm; pH 7.0; ionic strength 0.2 M; 20°C) detected with emission polarizer at 54.7° with respect to polarization of excitation decayed exponentially; the lifetime of excited state was  $2.55 \pm 0.04$  ns (s.d., n=3) for the 5 isomer and  $2.59 \pm 0.03$  ns (n=3) for the 6 isomer. Cys-108 of cgRLC was modified with 6-Iodo-ATR, and labelled RLC was exchanged into rabbit psoas fibers. With the long axis of fibers aligned parallel to polarization of excitation, fluorescence emission at 54.7° decayed biexponentially. Time constants were  $0.42 \pm 0.15$  ns and  $3.41 \pm 0.04$  ns (n=4) in relaxed fibers and were  $0.37 \pm 0.11$  ns and  $3.40 \pm 0.05$  ns (n=3) in fibers in rigor. In both cases, the amplitude of the fast component was approximately 10% of total. These time constants obtained with fibers should not be equated with excited state lifetimes: fibers are ordered assemblies, and consequently 6-ATR-cgRLC is not isotropically distributed. To obtain a better measure of total fluorescence and anisotropy decay for probes in fibers, we now are pursuing measurements with excitation and emission polarizers varied between 0° and 90° with respect to fiber axis. We thank J.E.T. Corrie and J.S. Craik for providing 5- and 6-Iodo-ATR and thank J. Kendrick-Jones, C. Sabido-David, and M. Irving for the 6-ATR-cgRLC. Supported by a grant from the American-Scandinavian Foundation.

## Tu-Pos122

THE RADII-OF-GYRATION OF MYOSIN SUBFRAGMENT 1 FROM NEUTRON SCATTERING. ((R. A. Mendelson, D. B. Stone and D. K. Schneider\*)) C.V.R.I. and Dept. Biochem. & Biophys., Univ. Calif. San Francisco, CA 94143; \*Biology Dept., Brookhaven National Laboratory, Upton, NY 11973.

Small-angle neutron scattering has been used to investigate the  $R_g$  of chicken skeletal muscle myosin subfragment 1 in solution. Reductive methylation, employed as an aid in the recent crystallization of myosin subfragment 1 (Rayment et al., *Science* 261: 50, 1993), causes no large scale changes in the structure of S1 in solution. We find that the measured  $R_g$  and its concentration dependence in the absence of nucleotide is in better agreement with some X-ray scattering results than with others. The S1 crystal structure predicts an  $R_g$  close to that measured by neutron scattering. These results suggest that the overall shape found by crystallography resembles that found in solution. The addition of ADP plus vanadate, which is thought to produce an analog of the S1-ADP-P<sub>i</sub> state, decreases the  $R_g$  significantly. Calculations using the complete crystal structure show that a simple closure of the nucleotide cleft by a rigid-body torsional rotation of residues (172-180 to 670) around an axis running along the base of the cleft does not produce changes as large as seen here and in X-ray scattering results (Wakabayashi et al., *Science* 258: 443, 1992). On the other hand, a rigid body rotation of either the light chain binding domain (767 to 843) or of a portion of 20 kD peptide plus this domain (706 to 843) is more readily capable of producing such changes. We speculate that in myosin-linked regulation in molluscs such a rotation might allow the 105-114 α-helix in ELC to interact with the 21-29 α-helix in the heavy chain. (Supported by NIH AR39710 & AR42895)

## Tu-Pos124

CHARGE MEASUREMENTS OF METHYLATED HEAVY MEROMYOSIN.

((E. Wilińska, G.F.Elliott)) Oxford Research Unit, The Open University, Boars Hill, Oxford, OX1 5HR, UK

Rabbit heavy meromyosin (HMM) was methylated following the procedure given for the s1 subfragment of myosin by I.Rayment et al (*Science*, 261, 50: 1993). The extent of modification was checked by amino acid analysis and SDS gel electrophoresis. Charge measurements were carried out using a Donnan potential method in 10 mM KCl and 1 mM Bistris buffer at pH 6.7. The results are summarized in the table.

Table. Mean charge per molecule ± standard deviation (n=6 in both cases).

HMM	meth HMM
-40.3 ± 4.8	-46.4 ± 5.9

The methylated protein has a larger negative charge than the native one by about 15%. However more measurements need to be done to see whether the observed difference is significant.

The proteins were also extensively dialysed against 0.1 M KCl and titrated with KOH in 0.1M KCl. The curves for the methylated HMM are slightly shifted to lower pH values but by not more than half a pH unit.

The direction of the change in the charge and the shift in the titration curves are as would be expected from the pK values of lysine (10.8) and di-N<sup>ε</sup>-methyllysine (10.2), measured by NMR (J.E.Jentoft et al, *J. Biol. Chem.*, 254, 4366:1979).

## Tu-Pos126

A DIFFERENTIAL SCANNING CALORIMETRIC STUDY OF STABLE MYOSIN-NUCLEOTIDE COMPLEXES ((D.I.Levitsky\*, N.L.Golitsina\*, A.A.Bobkov\*, O.P.Nikolaeva\*, I.V.Dedova\* and D.A.Pavlov\*)) \* A.N.Bakh Institute of Biochemistry, Russian Academy of Science, Moscow 117071 and \*A.N.Belozersky Institute of Physico-Chemical Biology, Moscow State University, Moscow 119899, Russia.

It has been recently shown by differential scanning calorimetry (DSC) that the formation of stable ternary complexes of myosin subfragment 1 (S1) with MgADP and phosphate analogues, orthovanadate ( $Vi$ ) or beryllium fluoride ( $BeF_3^-$ ), causes the global conformational change of S1 reflected in a pronounced increase of S1 thermal stability and a significant change of S1 domain structure [Levitsky et al. (1992) *Eur. J. Biochem.* 209, 829-835; Bobkov et al. (1993) *FEBS Lett.* 332, 64-66]. A similar effect was observed in the case of the stable complex of S1 with MgADP and  $AlF_3^-$ . In continuation of these works we now report a DSC study of complexes of S1 with various nucleoside diphosphates (NDP) and of complexes with specifically modified S1. The effectiveness in inducing conformational changes of S1 in the S1-NDP- $Vi$  and S1-NDP- $BeF_3^-$  complexes decreased in the following order: ADP > CDP > UDP > IDP > GDP. Specific modification of the SH1-group of Cys-707, trinitrophenylation of Lys-83, and reductive methylation of lysine residues decreased significantly the S1 thermal stability in the S1-MgADP- $Vi$  complex. However, the effects of these modifications were much less for S1-MgADP- $BeF_3^-$  complexes. In the case of SH1 modification the effect depended on the reagent employed; NEM was the most effective. It is concluded that DSC is a very convenient method for probing the conformational changes in the myosin head caused by the formation of its stable ternary complexes with nucleotide and phosphate analogues. (Supported by NIH Grant 1 R03 TW00270-01 and ISF Grant MEI000).

## Tu-Pos127

**PHOSPHATE ANALOG PROBES OF THE NUCLEOTIDE SITE ON S1.** ((B. C. Phan, P. Cheung and E. Reisler)) Dept. of Chemistry and Biochemistry, UCLA, Los Angeles, CA 90024.

Previous work has revealed phosphate-dependent differences in the complexes formed from S1.ADP with aluminum fluoride ( $\text{AlF}_4^-$ ) and beryllium fluoride ( $\text{BeF}_3^-$ ) (Phan & Reisler, *Biophysical J.* 66, A78, 1994), with the former resembling more the  $\text{S1}^{\text{ADP}}\cdot\text{P}_i$  state while the latter is closer to the  $\text{S1}^{\text{ADP}}$  state. In this work, the conformation of the  $\text{S1}\cdot\text{ADP}\cdot\text{AlF}_4^-$  and  $\text{S1}\cdot\text{ADP}\cdot\text{BeF}_3^-$  complexes was examined by nucleotide chase and collisional quenching experiments.  $\epsilon\text{ADP}$  release from  $\text{S1}\cdot\text{ADP}\cdot\text{AlF}_4^-$  was slower than from  $\text{S1}\cdot\text{ADP}\cdot\text{BeF}_3^-$ . Furthermore, acrylamide titrations of the two complexes showed greater nucleotide protection in  $\text{S1}\cdot\text{ADP}\cdot\text{AlF}_4^-$  than  $\text{S1}\cdot\text{ADP}\cdot\text{BeF}_3^-$ . These results are consistent with a greater closure of the active site in the  $\text{S1}\cdot\text{ADP}\cdot\text{AlF}_4^-$  complex. The hydrodynamic properties of  $\text{S1}\cdot\text{ADP}\cdot\text{BeF}_3^-$  and  $\text{S1}\cdot\text{ADP}\cdot\text{AlF}_4^-$  are investigated in difference sedimentation velocity experiments.

## Tu-Pos129

**MYOSIN CATALYTIC DOMAIN FLEXIBILITY IN  $\text{MgADP}$** 

Drazen Raucher<sup>1</sup>, Cecilia P. Sar<sup>2</sup>, Kalman Hideg<sup>2</sup>, and Piotr G. Fajer<sup>1</sup>  
<sup>1</sup> Institute of Molecular Biophysics and Department of Biological Science, Florida State University, Tallahassee, FL 32306-3015;

<sup>2</sup> Central Research Laboratory, Chemistry, University of Pecs, Pecs, Hungary, H-7643  
 Conventional EPR studies of muscle fibers labeled at cys-707 of myosin head with a novel  $\alpha$ -iodoketo spin label revealed substantial internal domain reorganization the labeled domain on the addition of ADP to rigor fibers. The spin probes which are well ordered in the rigor state, become disordered and form two distinct populations. These orientational changes do not correspond to rotation of the myosin catalytic domain as a whole, because other probes (maleimide and iodoacetamide nitroxides attached to the same cys-707 of myosin head) report only a small,  $5\cdot 10^\circ$ , torsional rotation and little or no change in the tilt angle (Ajtai *et al.*, 1992; Fajer, 1994). In the presence of ADP the labeled domain becomes more flexible and executes large-amplitude microsecond motions as measured by saturation-transfer EPR with rates ( $t_r = 150$  ms) intermediate between the rotations of detached ( $t_r = 7$  ms) and rigor heads ( $t_r = 2,500$  ms). This finding contrasts with an absence of global motion of the myosin head in ADP ( $t_r = 2,200$  ms) as reported by maleimide spin label. These results imply that the myosin head in a single chemical state ( $\text{AM}\cdot\text{ADP}$ ) is capable of attaining many internal configurations, some of which are dynamic. The presence of slow structural fluctuations might be related to the slow release of the hydrolysis products of actomyosin ATPase.

Ajtai K, Riegler A & Burghardt TP, (1992) *Biochemistry* 31, 207-17.  
 Fajer P.G., (1994) *Biophys. J.* 66, 1-12.

## Tu-Pos131

**MODELING ATP INTO THE ACTIVE SITE OF MYOSIN** ((David Lawson\*, Ralph G. Yount\*, and Ivan Rayment\*)) \*Department of Biochemistry and Biophysics, Washington State University, Pullman, WA 99164. †Department of Biochemistry and Institute for Enzyme Research, University of Wisconsin, Madison, WI, 53705.

We have used molecular modeling techniques to place ATP in the active site of myosin subfragment 1 (Rayment *et al. Science* 261, 50-58, 1993). The crystal structure of the adenylate kinase- $\text{AP}_3\text{A}$  complex was used as a reference to dock ATP into the active site of the S1 crystal structure based on the virtually identical P-loop structures of the two enzymes. The docked S1-ATP model was then energy minimized using Biosym's Discover program. The location of ATP in this model is proximal to Trp-131, Ser-181, Val-187, Ser-243, and Ser-324, five residue positions which have been previously photolabeled by ATP analogs and thus help confirm the accuracy of the docking.

The docked S1-ATP structure has also given new insight into how substrates and products may enter and leave the active site. Because the  $\gamma$ -phosphate of ATP is buried at the bottom of the active site in the model, it cannot be seen from above the nucleotide binding pocket. It is visible, however, from a large cleft in the 50 kD region through a small opening that is partially blocked by residues Ser-181 and Arg-245. The model indicates that  $\text{P}_i$  is sterically blocked from leaving by the  $\alpha$ - and  $\beta$ -phosphates of ADP. Thus,  $\text{P}_i$  cannot leave through myosin's "front door" unless ADP first dissociates. For this reason, it is postulated that a conformational change moves Ser-181 or Arg-245 from its position blocking the "back door" allowing  $\text{P}_i$  to exit while ADP remains bound.

## Tu-Pos128

**PREPARATION OF AFFINITY COLUMN PURIFIED MYOSIN SUBFRAGMENT-1 TO BE USED FOR CRYSTALLOGRAPHIC STUDIES.** ((Louis Riccelli, Tamara Gallagher-Stobb, and Ralph Yount)) Department of Biochemistry & Biophysics, Washington State University, Pullman, WA 99164.

Additional methods of purifying myosin subfragment-1 (S1) and its crosslinked derivatives using an IBPA-ATP(ADP) Affi-Gel 10 affinity column (Gallagher-Stobb, Riccelli, Rayment, & Yount, (1994) *Biophys. J.* 66, 78a) have been developed. Specifically, techniques of reversibly and irreversibly trapping S1 to the affinity column have been used for the purification of native and cross-linked S1. It is believed that cross-linking the two most reactive sulfhydryls in S1 (Cys697 and Cys707) yield a conformational state of S1 that mimics the weak binding state of S1 for actin. We have developed a method of using the affinity column to purify S1 both before and after crosslinking with *N,N'*-p-phenylenedimaleimide (pPDM) using substoichiometric amounts of reagent (0.9 mol/mol S1). Uncross-linked S1 is then removed by purification over the IBPA-ATP(ADP) Affi-Gel 10 affinity column in the presence of vanadate. Preliminary results indicate that pPDM-S1 with nucleotide can be crystallized (Ivan Rayment, U. Wisconsin, unpublished results). This method of cross-linking and purifying S1 with nucleotide at the active site should allow the preparation of S1 cross-linked with differing length bifunctional thiol reagents. The goal is to define how the  $\alpha$ -helical region connecting Cys697 and Cys707 can move from 18Å down to 2Å and how this movement affects the actin-binding region of S1. Supported by NIH (DK 05195) and by a Howard Hughes Undergraduate Research Fellowship (L.R.).

## Tu-Pos130

**STUDIES OF THE SOLVENT ACCESSIBILITY OF MANT-NUCLEOTIDES BOUND TO MYOSIN AND TO ACTOMYOSIN.** ((Kathleen Franks-Skiba and Roger Cooke)) Dept. of Biochem/Biophysics, and CVRI, UCSF.

We measured the accessibility of mant-nucleotides bound to myosin and to actomyosin by measuring the quenching of their fluorescence using the solvent phase quencher acrylamide, 25-400mM. Previous investigations have shown that ethenoADP is partially buried both in myosin and actomyosin. As found by Cremo *et al* (JBC, 1989), mantADP is highly protected from the solvent when bound to myosin. The degree of protection changed very little during steady state hydrolysis by S1. It also did not change when S1-mantADP bound to actin, or when mantADP bound to myosin in myofibrils. Thus the mant-nucleotides give the same result as found for the etheno nucleotides, the solvent accessibility changes little upon formation of the actomyosin bond. Fluorescent probes reacted with lysine residues on myosin were not highly protected from the solvent, showing that simple attachment of the probe to a protein surface does not provide the degree of protection found for either the mant or etheno nucleotides. Supported by AR30868.

## Tu-Pos132

**ANALYSIS OF CONFORMATIONAL CHANGE ON SMOOTH MUSCLE MYOSIN ASSOCIATED WITH PHOSPHORYLATION USING  $^{19}\text{F}$ -NMR** (Misato Yamada, Stéphane M. Gagné\*, Brian D. Sykes\*, Mitsuo Ikebe# and Shinsaku Maruta) Dept. of Bioengineering, Soka University, Hachioji, Tokyo 192 Japan. \*Dept. of Biochemistry, Alberta University, Edmonton, Alberta T6G 2H7 CANADA #Dept. of Physiology & Biophysics, Case Western Reserve University, Cleveland, Ohio 44106. (Spon. by T. Mitsu)

To study how phosphorylation signal transduce from regulatory light chain (LC20) to actin binding site on smooth muscle myosin heavy chain, we have been trying to label the specific site of myosin head and analyze the conformational change at the labelled site using  $^{19}\text{F}$ -NMR. As the preliminary experiments, in the present study, Phe 22 which close to phosphorylation site Ser19 in LC20 was substituted to 5-fluoro-Trp using site directed mutation. The cDNA clone encoding the open reading frame of the mutant LC20 (Phe 22→Trp) was subcloned into the polylinker of pT7-7 vector, giving the mutant LC20 expression vector and it was transformed into E.coli BL21 tryptophan auxotroph strain. The recombinant mutant LC20 (Phe 22→Trp) were expressed in the presence of 5-fluoro-Trp. The recombinant LC20 (Phe 22→5-F-Trp) was purified by the column chromatography of DEAE-Sephacel and Sephacryl S-200. Quantitative analysis of Trp fluorescence of LC20 (Phe 22→5-F-Trp) showed that one Trp residue was incorporated in the molecule as natural LC20 has no Trp in the molecule. Actin-activated ATPase activity of smooth muscle myosin HMM exchanged with the mutant LC20 (Phe 22→5-F-Trp) was regulated by phosphorylation as well as native HMM.  $^{19}\text{F}$  signal of the mutant LC20 (Phe 22→5-F-Trp) has different chemical shift from free 5-fluoro-Trp. Phosphorylated LC20 (Phe 22→5-F-Trp), phosphorylated HMM and dephosphorylated HMM exchanged with the mutant LC20 (Phe 22→5-F-Trp) were also analyzed by  $^{19}\text{F}$ -NMR.

## Tu-Pos133

N-TERMINAL CLEAVAGE IN MYOSIN HEAVY CHAIN AFFECTS THE PROPERTIES OF MYOSIN HEAD. ((A.A. Bobkov, T. Chen, O.P. Nikolaeva, D.I. Levitsky and E. Reisler)) Dept. of Chem. & Biochem., UCLA, LA, CA 90024. (Spon. by E. Reisler)

In the absence of nucleotides trypsin splits the heavy chain of the myosin head into three fragments. In the presence of ADP, ATP, ADP and orthovanadate ( $V_i$ ) or ADP and beryllium fluoride ( $BeF_4$ ) trypsin (or subtilisin) also produces an additional cleavage between Arg-23 and Ile-24 (or Gln-27 and Asn-28). The effect of this cleavage on the structure and function of isolated myosin head (S1) was studied.

It was found that this cleavage dramatically decreased the stability of S1. The cleaved S1, after removing ADP, lost between 60 and 80% of its  $K^+$ -EDTA-,  $Ca^{2+}$ - and  $Mg^{2+}$ -ATPase activities; had a decreased thermostability (a shift by about 8°C); its ATP-induced tryptophan fluorescence enhancement was decreased by about ten fold, and S1 binding to F-actin became ATP insensitive. Incubation of such S1 with ADP slowly and partially restored its original properties. When nucleotides were not removed from the cleaved S1 it showed ATPase activities, tryptophan fluorescence enhancement, and actin binding similar to that of uncleaved S1. This results show nucleotide related changes in the vicinity of myosin N-terminus and implicate this region in structural stability of S1.

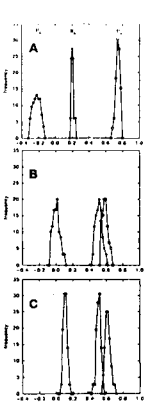
## Tu-Pos135

CARDIAC MYOSIN HEAD CAN MAKE ACTIN FILAMENT BUNDLES. ((T. Miyashita, T. Hayashibara & T. Maita)) Biochemistry, Nagasaki Univ. Schl. of Med., Nagasaki 85200, JAPAN.

Myosin head (Subfragment-1, S-1) hydrolyzes ATP to stroke and move on actin filament and that S-1 binds actin molecule via actin binding sites on the heavy chain. Skeletal S-1 has two kinds of essential light chains (A1 and A2 types) while cardiac S-1 has the larger one of them (A1 type). We found cardiac S-1 with A1 can make bundles of actin filaments more rapidly and stably than skeletal S-1 with A1. Bundle formation was monitored by light scattering measurement and electron microscopic observation. Bundle formed by cardiac S-1 was resistant to mechanical shaking and the rate of formation by cardiac S-1 was much faster than that by skeletal S-1. In bundles, polarity of two adjacent actin filaments was anti-parallel. Distance of the two filaments was about 20 nm and connections between the filaments were observed at about 36 nm intervals. Raising KCl concentration from 0 to 0.15 did not suppress bundle formation significantly, and over 0.2 M KCl there was very little bundles. Adding ATP dissociated bundles to single actin filaments. Water soluble carbodiimide (EDC) crosslinking made bundles resistant to increasing KCl or to ATP addition. SDS-PAGE analysis of the cross-linked bundles showed that A1-actin and A1-S-1 heavy chain were evidently cross-linked in the bundles. This work was supported in part by the Ministry of Science, Culture and Education of Japan.

## Tu-Pos137

RIGOR CROSS-BRIDGES BIND TO TWO ACTIN MONOMERS IN THIN FILAMENTS OF RABBIT PSOAS MUSCLE. ((M. Xiao, O. Andreev & J. Borejdo)) Baylor Research Institute, Baylor Univ Med Cntr, 3812 Elm St., Dallas, TX 75226.



We compared conformation of heads in muscle with conformation of low [S1] added to fibers (in solution low [S1] forms 1:2 complex with actin; Andreev & Borejdo, *J. Muscle Res. Cell Motil.*, 13, 523-533, 1992). Conformation was assessed by accessibility to trypsin and by orientation of rhodamine label. Figure shows histograms of polarizations (P) and of linear dichroism (R) of rigor muscle irrigated with 2 μM S1 (A), 0.1 μM S1 (B) and of muscle in which myosin was labeled (C). 20/50 KDa junction of S1 added to muscle at 2.0 μM was readily digested by trypsin and label orientation was approximately perpendicular to muscle axis. 20/50 KDa junction of S1 added to muscle at 0.1 μM was protected from trypsinolysis and label orientation was more parallel to axis. 20/50 KDa junction of myosin heads in muscle was protected from trypsinolysis and label orientation was similar to low [S1]. We conclude that in rigor rabbit psoas muscle each head binds to two actin monomers in a thin filament, and that rigor head in muscle has different conformation than S1 bound to equimolar concentration of actin in solution. Supported by AHA.

## Tu-Pos134

FORMATION OF STABLE INHIBITORY COMPLEXES OF MYOSIN SUBFRAGMENT 1 USING FLUOROSCANDIUM ANIONS ((D. Gopal and M. Burke)) Department of Biology, Case Western Reserve University, Cleveland, OH 44106.

Incubations of myosin subfragment 1 in the presence of MgADP and  $ScCl_3$  in the presence of NaF results in the loss of the ATPase properties of the protein with concomitant trapping of the nucleotide. The rate of inhibition in the presence of  $MgCl_2$  at 25 °C is  $8.7 M^{-1} s^{-1}$  which is too slow for a simple collisional mechanism and this low rate suggests that a subsequent slow isomerization step is responsible for the formation of a stable ternary complex,  $S1.MgADP.ScF_4^-$  in a manner analogous to that reported for the  $V_i$  stabilized protein (Goodno, *Proc. Natl. Acad. Sci. USA* 76, 2620-2624 (1979)). Loss of ATPase function with concomitant trapping of ADP is also observed in the absence of  $MgCl_2$  indicating formation of  $S1.ADP.ScF_4^-$ . The rate of nucleotide loss at 4 °C from both these inhibitory complexes was biphasic indicating that each exists in two distinct states as previously proposed for the ternary complexes formed with  $V_i$  (Mihashi et al., *J. Biochem. (Tokyo)* 107, 464-469 (1990)) and  $BeF_4^-$  (Phan and Reisler, *Biochemistry* 31, 4787-4793 (1992)). Formation of these complexes resulted in a marked enhancement of the tryptophan fluorescence indicating that conformationally they may be similar to the steady-state intermediate formed during hydrolysis of MgATP. Irradiation of these complexes in the presence of excess  $V_i$  by near UV light resulted in protection at  $V_i$  dependent photolysis sites associated with the ATP consensus sequence. This observation indicates that  $V_i$  cannot bind to the inhibitory complex at this region presumably because it is occupied by the  $ScF_4^-$  anion. (Supported by NIH NS 15319)

## Tu-Pos136

TWO STATES OF BINDING OF MYOSIN SUBFRAGMENT 1 TO F-ACTIN. ((O.A. Andreev, V.S. Markin & J. Borejdo)) Baylor Research Institute, Dallas, TX 75226 and UT Southwestern Medical Center, Dallas, TX 75235.

We have previously showed that myosin subfragment 1 (S1) can bind to one or two monomers in F-actin (Andreev & Borejdo, 1992, *J. Muscle Res. Cell Motil.* 13:523; Andreev et al., 1993, *Biochem.*, 32:12046). The binding of S1 to F-actin can be described by two equations: (i)  $M+A \rightleftharpoons MA$ ; (ii)  $MA+A \rightleftharpoons AMA$ , where M and A stand for S1 and actin, respectively. The rate of the first reaction ( $\lambda_1$ ) is proportional to concentrations of S1 and actin. The rate of the second reaction ( $\lambda_2$ ) depends on the probability that the second actin is free. The model predicts that when molar ratio  $M/A \ll 1$ , the kinetics of binding of S1 is biphasic for  $\lambda_1 \gg k_{-1}$  and is monophasic for  $\lambda_1 < k_{-1}$  (the second reaction is too fast to be distinguished from the first reaction). When  $M/A \gg 1$  the kinetics is monophasic for  $\lambda_1 \gg k_{-1}$  (the transition from state 1 to state 2 does not occur) and deviates slightly from monophasic for  $\lambda_1 < k_{-1}$ . When molar ratio is  $0.5 < M/A < 2$ , the significant deviation from monophasic kinetics is expected for  $\lambda_1 \gg k_{-1}$  or  $\lambda_1 < k_{-1}$ . The experimental data confirmed all these predictions. The kinetics of binding of S1 to F-actin was monitored by measuring fluorescence signal originating from pyrene covalently attached to Cys374 of actin or from 5-IAF attached to Cys707 of S1. Qualitatively the kinetics of binding were similar when actin or S1 were labeled. The S1 isomers carrying alkali light chains LC1 or LC3 showed similar kinetics. Supported by AHA and NIH.

## Tu-Pos138

FLUORESCENCE ENERGY TRANSFER DISTANCES IN ACTOSUBFRAGMENT-1. ((J. Xing and H.C. Cheung)) Department of Biochemistry & Molecular Genetics, University of Alabama at Birmingham, Birmingham, AL 35294-2041.

Two distances in actosubfragment-1 were determined by FRET between (1) Cys374 of actin and Cys707 ( $SH_1$ ) of myosin subfragment-1 (S1) and (2) Cys374 of actin and Cys697 ( $SH_2$ ) of S1. Two donors (IAEDANS and MIANS) were used to label S1, and DABMI was the acceptor attached to the actin site. The distances were determined at 20 °C in 60 mM KCl, and 30 mM TES at pH 7.5 for (a) actoS1, (b) actoS1 in the presence of MgADP, and (c) actoS1 in the presence of MgADP and vanadate ( $V_i$ ). Because of the dissociating effect of ADP on actoS1, it was necessary to choose protein concentrations to minimize the concentrations of species containing donor probe not participating in energy transfer and to correct for contribution of donor signal from these species. The donor IAEDANS yielded a distance (based on  $\kappa^2 = 2/3$ ) of 51 Å for the Cys374- $SH_1$  distance. MgADP had a negligible effect on the distance, but (MgADP +  $V_i$ ) reduced the distance by 8 Å. When MIANS was the donor attached to  $SH_1$ , the calculated distances were somewhat smaller, but (MgADP +  $V_i$ ) reduced the distance by 7 Å. The distance between actin Cys374 and  $SH_2$  in actoS1 was 47 Å with IAEDANS as donor and 44 Å with MIANS as donor. This second distance was reduced by less than 1 Å in the presence of MgADP +  $V_i$ . These results suggest that the region of actin Cys374 and the region of  $SH_1$  in S1 move toward each other in an intermediate state of actomyosin ATPase hydrolysis. However, the regions of actin Cys374 and S1  $SH_2$  do not appear to undergo relative movement in the intermediate state. If it is assumed that the actin subunit is rigid, the present results suggest that the known relative movement between  $SH_1$  and  $SH_2$  may be due to mobility of  $SH_1$  toward  $SH_2$ . (Supported by NIH AR31239).



## Tu-Pos139

STRUCTURE OF CO-CRYSTALS OF TROPOMYOSIN AND CALDESMON ((E.J. Hnath and G.N. Phillips Jr.)) Department of Biochemistry and Cell Biology, Rice University, Houston, Texas 77251.

Caldesmon is a protein found in both smooth-muscle and non-muscle cells that has been implicated in the regulation of smooth muscle contraction. Smooth-muscle caldesmon is an 87kDa elongated (75x11.9nm) molecule that can be divided into four domains. Here we report the X-ray structure determination at 17Å resolution of tropomyosin crystals containing bound whole caldesmon and fragments of caldesmon. Our preliminary results show that caldesmon appears to bind strongly to skeletal  $\alpha$ -tropomyosin in three places along the length of the tropomyosin molecule. We also show that several caldesmon domains interact with tropomyosin. This work supports the idea that caldesmon lies in an extended configuration in parallel with tropomyosin in the thin filaments of smooth-muscle.

This work supported by NIH grants AR32764 and AR41637.

## Tu-Pos141

CALDESMON (CAD) INHIBITS FORCE AT LOW BUT NOT AT HIGH LEVELS OF ACTIVATION IN TRITON SKINNED CHICKEN GIZZARD FIBERS. ((G. Pfister, C. Zeugner, M. Troschka, U.S. Schmidt, J.M. Chalovich)) University of Heidelberg, Humboldt University of Berlin, and East Carolina University, Greenville, NC, 27858-4354

CaD inhibits force at low but not at high levels of myosin light chain (MLC) phosphorylation (Pfister et al. 1993 PNAS 90:5904-5908). However, it was not clear whether the lack of inhibition was due to high MLC or CaD phosphorylation. To clarify this question we investigated the effect of CaD and the 20 kDa actin binding fragment on triton skinned gizzard fibers activated by thiophosphorylation. Following incubation with ATP $\gamma$ S at different pCa for 10 min, CaD or the actin binding fragment were allowed to diffuse into the fibers for 30 min in rigor solution. Tension was elicited by addition of ATP at pCa >8. Force was normalized in respect to activation with 30  $\mu$ M Ca<sup>2+</sup> and 1  $\mu$ M calmodulin (F<sub>max</sub>). Submaximal force (40  $\pm$  3 of F<sub>max</sub>, n=12) was inhibited by CaD and was 17  $\pm$  5 (n=5) and 11  $\pm$  3 (n=3) of F<sub>max</sub> in the presence of 0.4 and 1 mg/ml CaD. At high levels of activation (95% of F<sub>max</sub>) neither CaD nor the actin binding fragment inhibited tension. We also attempted to extract CaD. Incubation with 50 mM MgCl<sub>2</sub> and 15-30 mM BDM for 6-15 hours resulted in about 80% extraction of CaD, calponin, and SM22. In extracted fibers, the force-pCa relation was shifted to the left; this was most pronounced at low pCa values. There was a small contraction at pCa >8 (about 20% of F<sub>max</sub>), even at 10 mM EGTA. There was no increase in Ca-insensitive MLCK activity. Both the increase in Ca-activated and Ca-independent force were reversed in fibers reconstituted with CaD (1 mg/ml) for 2.5 hrs. In conclusion, our data suggest, that CaD decreases force in triton skinned gizzard fibers at low but not at high levels of activation.

## Tu-Pos143

DEPHOSPHORYLATION OF CALPONIN BY TYPE 2B PROTEIN PHOSPHATASE (CALCINEURIN). ((E.D. Fraser and M.P. Walsh)) Dept. of Medical Biochemistry, University of Calgary, Alberta, Canada T2N 4N1. (Spon. by G.J. Kargacin)

Calponin is a smooth muscle-specific, thin filament-associated protein implicated in the regulation of contraction via its interaction with actin and inhibition of cross-bridge cycling rate. Calponin is phosphorylated by protein kinase C (PKC) and Ca<sup>2+</sup>/calmodulin-dependent protein kinase II (CaM kinase II) primarily at S175 with loss of actin binding and actomyosin ATPase inhibition. We previously isolated calponin phosphatase from chicken gizzard smooth muscle and identified it as a type 2A protein phosphatase (Pato et al. (1993) Biochem. J. 293:35). Our assay procedures would have detected type 1 and 2C phosphatases, but not type 2B (Ca<sup>2+</sup>/CaM-dependent phosphatase or calcineurin). We have therefore examined the expression of type 2B phosphatase in smooth muscle and its ability to dephosphorylate calponin. Western blotting with polyclonal antibodies to the brain enzyme revealed the expression of type 2B phosphatase in chicken gizzard. The purified brain phosphatase dephosphorylated calponin (phosphorylated by PKC or CaM kinase II) in a Ca<sup>2+</sup>/CaM-dependent manner. We conclude that calponin dephosphorylation may be catalyzed not only by type 2A phosphatase but also by type 2B phosphatase raising the possibility that both phosphorylation and dephosphorylation of calponin could be regulated by Ca<sup>2+</sup>/CaM.

## Tu-Pos140

AN EVALUATION OF THE COMPETITION OF BINDING OF CALDESMON AND S1 TO ACTIN. ((A. Sen and J.M. Chalovich)) ECU School of Medicine, Greenville, NC 27858-4354

We have shown earlier that caldesmon and S1 are competitive for binding to actin in both the presence and absence of tropomyosin. We have undertaken two additional approaches to verify this competition. First, we measured the rate of association of fluorescein-labeled S1 to actin-tropomyosin at varying caldesmon concentrations. Caldesmon reduced both the amplitude of the change and the apparent rate of association. Second, we measured the effect of caldesmon on the binding of pPDM-S1 to actin. pPDM-S1 was used so that high concentrations of S1 could be used without depletion of ATP. Binding and ATPase activities were measured at 25°C with 4  $\mu$ M actin-tropomyosin, 6  $\mu$ M pPDM-S1 and variable concentrations of caldesmon in 2 mM MgATP, 2 mM MgCl<sub>2</sub>, 10 mM imidazole pH 7.0, 10 mM potassium propionate and 0.5 mM EGTA. Under these conditions, the ATPase activity and fraction of bound S1 decreased with increasing caldesmon concentrations. However, the concentration of caldesmon required for 50% inhibition of binding was approximately twice that required to reach 50% inhibition of the maximum ATPase activity. This experiment suggests that part of the inhibition could be due to modulation of a rate process. Additional experiments are being conducted to determine if that is the case.

## Tu-Pos142

CALPONIN BINDS SLOWLY TO ACTIN. ((F.W.M. Lu, H. Luo and J.M. Chalovich)) East Carolina Univ. Med. Sch. Greenville, NC 27858

Calponin is an actin binding protein that inhibits actomyosin ATPase activity. Calponin labeled with IANBD underwent a 35 % increase in fluorescence upon binding to actin. At high protein concentrations, the rate of this process was biphasic. The first phase was thought to represent the actual association reaction while the second phase could be due to bundling of the actin filaments. The half-time for the first phase of the reaction, at high protein concentrations and 15°C, was approximately 0.8 sec. By comparison, caldesmon binds about 400 times faster under similar conditions. This result was confirmed in a "race" between caldesmon and calponin. When actin was mixed rapidly with a solution of IANBD labeled caldesmon and unmodified calponin there was a rapid increase in fluorescence resulting from caldesmon binding. This was followed by a very slow partial reversal of the fluorescence change as the calponin displaced the caldesmon. We also measured the rate of dissociation of calponin from actin in the presence of Ca<sup>2+</sup>-calmodulin. This reaction was very slow and had a half-time of 140 sec. It is possible that the reversal of calponin function occurs prior to the actual slow dissociation reaction. The function of calponin must be considered in terms of these slow kinetics.

## Tu-Pos144

STRUCTURE-FUNCTION RELATIONS OF CALPONIN. ((D.-C. Tang, H.-M. Kang, J.-P. Jin and M.P. Walsh)) Dept. of Medical Biochemistry, University of Calgary, Alberta, Canada T2N 4N1.

Calponin is a thin filament-associated protein implicated in the regulation of smooth muscle contraction. Calponin binds to F-actin/tropomyosin with high affinity (K<sub>d</sub> = 50 nM) and inhibits the actin-activated MgATPase activity of phosphorylated smooth muscle myosin. Both properties are lost upon phosphorylation of calponin by protein kinase C (PKC) or Ca<sup>2+</sup>/calmodulin-dependent protein kinase II (CaM kinase II) and restored following dephosphorylation by type 2A protein phosphatase. The principal site of phosphorylation is S175. To assess further the importance of S175, the T7 promoter-based expression vector pAED4 was used to express wild-type calponin (WT) and 3 site-specific mutants (S175A, S175D and S175T) in *E. coli* strain BL21(DE3)pLysS. Chicken gizzard calponin (CG) was compared with WT and the 3 mutant proteins in terms of actin binding, ATPase inhibition and phosphorylation. The affinity of actin for WT and S175T was similar to that for CG whereas the affinity for S175A and S175D was very low. Consistent with these observations, CG, WT and S175T displayed similar inhibition of actin-activated myosin MgATPase activity whereas S175A and S175D were much less effective. Phosphorylation by PKC and CaM kinase II supported the conclusion that S175 is the principal site of phosphorylation. We conclude that S175 plays an important role in the interaction of calponin with actin.

## Tu-Pos145

**EFFECTS OF THE INOTROPIC THIADIAZINONE, EMD57033, ON CARDIAC ACTOMYOSIN ATPASE AND SKINNED FIBERS** ((B.-S. Pan, S.M. Krause, R.G. Johnson, Jr. and R.J. Barsotti.\*\*) Merck Res. Labs, West Point, PA, Bockus Res. Inst., Graduate Hospital, Phila., PA\*

We studied the effects of EMD57033 (EMD) on cardiac actomyosin ATPase and skinned rabbit ventricular trabeculae contraction. Bovine cardiac myosin S-1 MgATPase was measured at low ionic strength ( $\approx 15$  mM) as a function of [actin]. EMD stimulated actoS-1 MgATPase over the entire range of [actin] studied. The estimated  $V_{max}$  increased from  $5.3 \text{ sec}^{-1}$  to  $5.9 \text{ sec}^{-1}$  in the presence of  $12 \mu\text{M}$  EMD. The data suggest that EMD accelerated the rate-limiting step of the ATPase cycle. Suprapharmacological concentrations of EMD induced isometric tension production in skinned trabeculae in a relaxing solution (pCa 9.0, 5 mM MgATP) at  $21^\circ\text{C}$ . At  $10 \mu\text{M}$ , the drug induced measurable tension production that increased in a dose-dependent manner. At  $75 \mu\text{M}$  EMD, tension reached  $36 \pm 4\%$  ( $n=4$ ) of that measured at pCa 4.4 in the same trabecula in the absence of EMD. The tension-stiffness ratio in the drug-induced contractions was similar to that measured during  $\text{Ca}^{2+}$  activation in the absence of the drug. This suggests that EMD induced tension was not caused by rigor-like cross-bridges. The data from skinned fibers are consistent with previous report that EMD stimulates myofibrillar ATPase in the absence of  $\text{Ca}^{2+}$  (Solaro *et al.* Circ. Res. 73:981-990, 1993). The  $\text{Ca}^{2+}$ -independent tension observed at high, non-pharmacological [EMD57033] is most likely mediated by a direct effect of the drug on myosin or the myosin-actin interaction and not by a change in the  $\text{Ca}^{2+}$  affinity of troponin C. (Supported in part by HL40953 to RJB).

## Tu-Pos147

**DECREASE IN SMOOTH MUSCLE MYOSIN LIGHT CHAIN PHOSPHATASE ACTIVITY FOLLOWING TREATMENT WITH ATP $\gamma$ S.** ((L. Trinkle-Mulcahy, M.J. Siegman and T.M. Butler)) Dept. of Physiology, Thomas Jefferson University, Philadelphia, PA 19107.

In experiments originally designed to test the effect of varying degrees of myosin light chain thiophosphorylation on calcium sensitivity of force output in smooth muscle, we found a large increase in calcium sensitivity after treatment with ATP $\gamma$ S even when there was no detectable thiophosphorylation of the myosin light chain. Specifically,  $\alpha$ -toxin permeabilized rabbit portal veins were exposed to  $1 \text{ mM}$  ATP $\gamma$ S for 10 min at  $20^\circ\text{C}$ , pCa  $> 8$  with  $300 \mu\text{M}$  ML-9, an inhibitor of myosin light chain kinase (MLCK). There was no detectable thiophosphorylation of the light chains, and no force with  $1 \text{ mM}$  ATP, pCa  $> 8$ . Subsequent treatment with pCa 6 resulted in  $70 \pm 9\%$  of maximum force and  $70 \pm 4\%$  light chain phosphorylation (MLCP) in the presence of ML-9. Without ATP $\gamma$ S pretreatment, force in pCa 6 was much lower, both with ML-9 (0%) and without ML-9 ( $39 \pm 11\%$ ), as was MLCP ( $4 \pm 2\%$  and  $34 \pm 5\%$ , with and without ML-9 respectively). Phosphatase activity was estimated from the time course of dephosphorylation of the light chain following removal of ATP. In pCa 6 with ML-9 following the ATP $\gamma$ S treatment, the phosphatase rate constant ( $0.003 \text{ s}^{-1}$ ) was much lower than in pCa 4.5 ( $0.016 \text{ s}^{-1}$ ), and even lower than in pCa 6 with  $10 \mu\text{M}$  GTP $\gamma$ S ( $0.011 \text{ s}^{-1}$ ). The increased calcium sensitivity of force and MLCP seen with ATP $\gamma$ S pretreatment seems at least, in part, due to the five-fold decrease in myosin light chain phosphatase activity. This might result from the thiophosphorylation of a protein involved in regulation of the phosphatase. (Supported by HL 50586)

## Tu-Pos149

**MECHANISMS BY WHICH AMPHIPATHIC PEPTIDES INCREASE CA AFFINITY AT CALMODULIN'S N AND C-TERMINAL CA BINDING SITES.** ((C.H. Snyder, J.D. Johnson and Z. Grabarek\*\*)) Dept. Medical Biochemistry, The Ohio State Univ., Columbus, OH 43210 and \*Muscle Research Group, Boston Biomedical Research Inst., Boston, MA, 02114.

CaM41/75 and CaM85/112 are two mutant calmodulins with cysteine residues at positions 41 & 75 or 85 & 112. Upon oxidation, a disulfide bridge is formed which inhibits the Ca dependent opening of a hydrophobic cleft in either the N or C-terminal domain of these mutants. The Ca dependent binding of ANS to CaM, CaM85/112 and CaM41/75 produce a 2.7, 2.4, and 1.2-fold increase in ANS fluorescence, respectively. Thus, Ca binding to the N-terminal domain of CaM produces an much greater exposure of a hydrophobic region than Ca binding to the C-terminal domain. Ca dissociates from the N and C-terminal domains of CaM at  $\sim 400/\text{s}$  and  $\sim 2.4/\text{s}$ , respectively at  $10^\circ\text{C}$ . Binding of an amphipathic peptide decreases Ca dissociation from the N-terminal domain of CaM by  $\sim 150$ -fold and decreases Ca dissociation from the C-terminal domain of CaM and CaM41/75 by  $\sim 8$ -fold. We propose that the N-terminal domain of CaM has lower Ca affinity because it exposes a larger hydrophobic surface to solvent upon Ca binding. Amphipathic peptides which shield this hydrophobic surface from solvent produce dramatic increases in N-terminal Ca affinity.

## Tu-Pos146

**THE ATP COST OF COVALENT REGULATION IN SWINE CAROTID MEDIAL RINGS.** ((C. J. Wingard, A. K. Browne, R. J. Paul\* and R. A. Murphy)) Department of Molecular Physiology and Biological Physics, University of Virginia, Charlottesville, VA. 22908; \*Department of Molecular and Cellular Physiology, University of Cincinnati, Cincinnati, OH. 45267-0676.

Increases in ATP consumption during contraction in smooth muscle are attributable to activation processes and crossbridge cycling. Our objective was to partition the increased ATP consumption between activation and crossbridge cycling. We altered actin-myosin interactions by varying ring length from the optimal length for force generation ( $L_0$ ) to  $1.8 L_0$ . At  $1.8 L_0$  the active stress was reduced to 20% of the force at  $L_0$ . Steady-state oxygen consumption, MRLC phosphorylation and active stress were determined at lengths of 1.0, 1.4, 1.6 and  $1.8 L_0$  at rest and with  $\text{K}^+$ -depolarization. Resting phosphorylation levels were 5.4, 5.4, 4.7 and 1.7% respectively. Total steady-state phosphorylation in KCl-activated tissues also showed no significant changes (24.4, 24.4, 22.5 and 25.1%). Both suprabasal oxygen consumption and active stress fell linearly between 1.0 and  $1.8 L_0$ . Suprabasal ATP consumption attributable to activation processes (i.e., length-independent) was 15-25% of the total at  $L_0$ . If there were no length dependence of MRLC-kinase and phosphatase activities leading to decreased phosphate turnover on Ser<sup>19</sup> of MRLC, and no changes in ATP utilization by reactions other than length-dependent changes in actin-myosin interaction, our results suggest that the metabolic cost of covalent regulation is moderate. Supported by NIH grants PO1 HL19242 (RAM), HL 23240 (RJP) and AHA VA Fellowship (CJW).

## Tu-Pos148

**AN OPTICAL BIOSENSOR OF SMOOTH MUSCLE REGULATORY LIGHT CHAIN PHOSPHORYLATION IN SKINNED SMOOTH MUSCLE FIBERS** ((W. Glenn L. Kerrick, Kathleen M. Trybus\*, Young Soo Hann, Jung Ren Chen and Pei-Ren Wang)) Department of Physiology and Biophysics, Univ. of Miami, Miami, FL 33101 and \*Rosenstiel Basic Medical Sciences Research Center, Brandeis Univ., Waltham, Mass.

A genetically engineered monocysteine derivative of the chicken gizzard regulatory light-chain (Cys18/RLC) when labeled with acrylodan (AC) acts as an optical biosensor of light-chain phosphorylation in purified myosin (Post, P.L., Trybus K. M., and Taylor, D.L., J.B.C. v.269, 12880-7, 1994). In the present study approximately 30 percent of the endogenous RLC was substituted with AC-Cys18/RLC in skinned chicken gizzard fibers in order to determine the feasibility of measuring RLC phosphorylation simultaneously with force. Activation of the skinned fibers by  $\text{Ca}^{2+}$  caused an increase in acrylodan fluorescence which preceded the activation of force. Removal of  $\text{Ca}^{2+}$  from the fibers resulted in a rapid decrease in acrylodan fluorescence which also preceded a slower decline in force. When the skinned fibers were transferred to a rigor solution, only a small calcium sensitive increase in fluorescence was observed, less than 10% of maximal change. These results in rigor solutions suggest that only a small fraction of the  $\text{Ca}^{2+}$ -activated fluorescence change in the presence of  $\text{Mg} \cdot \text{ATP}^2$  can be due to cross-bridge attachment, or associated directly with  $\text{Ca}^{2+}$ . The fluorescence changes observed in skinned chicken gizzard fibers are consistent with the AC-Cys18/RLC acting as a temporal optical biosensor of RLC phosphorylation.

## Tu-Pos150

**STRUCTURAL ANALYSIS OF THE C-TERMINAL DOMAIN OF CALMODULIN. MUTANTS WITH ALTERED  $\text{Ca}^{2+}$ -INDUCED CONFORMATIONAL TRANSITION.** ((D.F. Meyer & Z. Grabarek\*\*)) Muscle Research Group, Boston Biomedical Research Institute, Boston, MA. 02114.

We are searching for structural elements responsible for the  $\text{Ca}^{2+}$  dependent regulatory function of calmodulin (CaM). The purpose of the current studies was to mutate the C-terminal domain of CaM to cause uncoupling of  $\text{Ca}^{2+}$  binding from the resulting conformational transition. Four mutant peptides of the C-terminal domain of CaM (residues 77-148) were obtained: 1) Wild type (C-W); 2) Ala substituted for Phe92 - the position immediately preceding the first  $\text{Ca}^{2+}$  ligand in site III (C-FA); 3) Cysteine residues introduced at position 85 and 112 to lock the domain with a disulfide bond in the closed ( $\text{Ca}^{2+}$  free) conformation (C-SS); 4) Mutations #2 and #3 combined (C-FASS). Both C-SS and C-FASS readily form intramolecular disulfides as indicated by a large increase in electrophoretic mobility. Although only the C-W peptide exhibits  $\text{Ca}^{2+}$ -dependent binding to phenyl-sepharose, all peptides show some  $\text{Ca}^{2+}$ -dependence in the enhancement of bisANS fluorescence. The enhancement decreases in the order: C-FA  $>$  C-W  $>$  C-FASS  $>$  C-SS. The two types of mutations counteract in their effect on  $\text{Ca}^{2+}$ -binding. The substitution of Ala for Phe causes a 1.7 fold increase in  $\text{Ca}^{2+}$ -affinity. The C85-C112 disulfide bond causes an 8.5 fold decrease or 5 fold decrease in  $\text{Ca}^{2+}$ -affinity depending whether Phe or Ala is present at position 92 respectively. These results indicate that Phe92 plays an important (but not exclusive) role in the structural coupling mechanism in the C-terminal domain of CaM. (Supported by NIH, AR-41156)

## Tu-Pos151

VICINAL METHIONINES DEFINE THE OXIDATIVELY SENSITIVE SITES ON CALMODULIN. Dan Yin\*, Andreas Hühmer†, Christian Schöneich†, and Thomas Squier\*. Departments of Biochemistry\* and Pharmaceutical Chemistry†, University of Kansas, Lawrence, KS 66045.

Using reversed-phase HPLC and FAB mass spectrometry, we have identified the tryptic fragments associated with both native and oxidatively modified calmodulin from wheat germ and bovine sources. We find that the vicinal methionines found near the carboxyl-terminal domain (i.e., Met<sub>146,147</sub>) of wheat germ calmodulin (CaM) are selectively oxidized by H<sub>2</sub>O<sub>2</sub>, resulting in a modified CaM that acts as a noncompetitive inhibitor to the plasma membrane Ca-ATPase. We find that the other six methionines (including Met<sub>72</sub>) are not oxidatively modified to any significant extent under these experimental conditions. In order to assess the role of neighboring group effects with respect to the sensitivity of these vicinal methionines to oxidative modification, we have compared the sensitivity of bovine CaM, which contains two pairs of vicinal methionines located at Met<sub>144,145</sub> and Met<sub>171,172</sub>, to oxidative modification by H<sub>2</sub>O<sub>2</sub>. We find that both pairs of vicinal methionines are oxidized to a similar extent, suggesting that the proximity of these neighboring methionines defines their sensitivity to oxidative modification.

## Tu-Pos153

RESONANCE ENERGY TRANSFER AND PHOTOCROSSLINKING STUDIES OF THE INTERACTION BETWEEN TROPONIN C AND THE INHIBITORY REGION OF A MONOCYSTEINE MUTANT OF TROPONIN I. ((Z. Li, J. Gergely and T. Tao)) Muscle Research Group, Boston Biomedical Research Institute, 20 Staniford St., Boston, MA 02114.

We have obtained by *in vitro* mutagenesis a mutant rabbit skeletal troponin-I (TnI<sup>117</sup>) with a single cysteine at position 117 at the C-terminal end of the so-called inhibitory region. All three endogenous Cys's were replaced with Ser's, and Ser117 was converted to Cys. The distance between Cys-98 of rabbit skeletal troponin C (TnC) and Cys-117 of TnI<sup>117</sup> in reconstituted binary and ternary troponin complexes was measured by resonance energy transfer with 1,5-IAEDANS and DDP-Mal as the donor and the acceptor, respectively. We found that the distance between the two residues is dependent on the Ca<sup>2+</sup>-binding state of the complexes, being 40Å when the low-affinity sites are empty and 28Å when Ca<sup>2+</sup> is bound at these sites. Since these sites have been implicated as the physiological triggering sites, our results show that Ca<sup>2+</sup> activation is accompanied by a considerable (12Å) decrease in the distance between the Cys-98 region of TnC and the inhibitory region of TnI. When TnI<sup>117</sup> labeled with the heterobifunctional photocrosslinker benzophenone-4-maleimide (BP-Mal) was complexed with TnC or TnC plus TnT only one photocrosslinked product was obtained in the absence of Ca<sup>2+</sup> for both the binary and the ternary complexes, while two photocrosslinked products were obtained in the presence of Ca<sup>2+</sup>. These results are consistent with the picture that the inhibitory region of TnI undergoes considerable conformational rearrangement with respect to TnC in response to Ca<sup>2+</sup> activation. (Supported by NIH HL5949 and AR21673.)

## Tu-Pos155

EFFECT OF MUTATIONS IN THE INHIBITORY REGION OF SKELETAL MUSCLE TROPONIN I ON ITS BIOLOGICAL ACTIVITY. ((R. Zhang, Z. Sheng, M. Jones, B. Parsons, J.D. Potter)), Dept. of Mol. & Cell. Pharm., Univ. of Miami School of Med., Miami, FL 33136

Residues from 96-116 in skeletal muscle troponin I (TnI) are thought to represent the functional domain which inhibits actomyosin ATPase, while the NH<sub>2</sub>-terminal region of TnI plays a structural role in maintaining the functional troponin complex (Sheng *et al.*, 1992, *J. Biol. Chem.* 267:25407-25413). The inhibitory region may also contain two potential troponin C (TnC) binding sites, which interact with either the NH<sub>2</sub>- or COOH-terminus of TnC in a Ca<sup>2+</sup>-dependent manner (Farah, *et al.*, 1994, *J. Biol. Chem.* 269:5230-5240). To investigate the biological properties of the inhibitory region in TnI and to locate the possible TnC and actin binding sites in this inhibitory region, we have created three mutants, TnI<sub>14</sub> (deletion of residues 96-107), TnI<sub>24</sub> (deletion of residues 96-116) and TnI<sub>34</sub> (deletion of residues 105-115). Both TnI<sub>14</sub> and TnI<sub>34</sub> could still partially inhibit actomyosin ATPase, while deletion of residues 96-116 totally abolished the ability of TnI to inhibit actomyosin ATPase. A solution containing 6 M urea and 2 mM Ca<sup>2+</sup> could not elute wildtype TnI from a TnC affinity column, but could elute TnI<sub>24</sub> from the column. In contrast, TnI<sub>14</sub> and TnI<sub>34</sub> were partially bound under these conditions. These results indicate that further work will be required to precisely locate the TnC and actin binding sites on TnI. Supported by NIH HL42325, AR37701 & AR40727.

## Tu-Pos152

FURTHER IMMUNOCYTOCHEMICAL CHARACTERIZATION OF CYTOSKELETON IN CHICKEN GIZZARD SMOOTH MUSCLES. ((Katsuhide Mabuchi)) Muscle Research Group, Boston Biomedical Research Institute, Boston Ma 02114

We reported that the cytoskeleton of chicken gizzard smooth muscles contain calponin (CaN), desmin, filamin,  $\beta$ -actin,  $\alpha$ -actinin and tubulin, and that the majority of CaN molecules most likely exist on  $\beta$ -actin filaments (Mabuchi, *J. Biophys.* 66, a197, 1994). While the preliminary study suggested that the degree of overlaps between anti-CaN and anti- $\beta$ -actin was significant but not extremely high, we had not determined the degree of cross-reaction of the 2nd antibodies (e.g. anti-rabbit IgG to mouse IgG) or the leakage in our optical system (cross-talk). The methods have been refined to reduce the cross-talks and we examined more details. It appears that the degree of overlaps between anti-CaN vs anti-desmin was clearly better than those between anti-actin vs anti- $\beta$ -actin. This is puzzling because if the  $\beta$ -actin filaments are saturated with CaN molecules, the relative intensity of anti-CaN to anti- $\beta$ -actin at various points should be the same. One possibility is that CaN may bridge two or more different proteins. An another interesting observation was that the degree of overlaps between anti-Tm (immunized with gizzard isoforms) vs anti- $\beta$ -actin was poor, suggesting that the gizzard isoforms are not on  $\beta$ -actin filaments. (Supported by grants from NIH).

## Tu-Pos154

Ca<sup>2+</sup>-INDUCED MOVEMENT OF THE N-TERMINAL REGION OF TROPONIN-I RELATIVE TO TROPONIN-C AND ACTIN ((J. Jiang, J.-L. Wu, J. Gergely and T. Tao)) Muscle Research Group, Boston Biomedical Research Institute, 20 Staniford St., Boston, MA 02114.

Using site-directed mutagenesis we changed Cys's at positions 64 and 133 of rabbit skeletal troponin I (TnI) to Ser to obtain a TnI that contains a single Cys at residue 48. The distance between Cys-48 of TnI and Cys-98 of rabbit skeletal troponin C (TnC) in the ternary complex was measured by resonance energy transfer, with 1,5-IAEDANS and DAB-Mal as the donor and the acceptor, respectively. Measurements were made in 2 mM EGTA plus 8 mM MgCl<sub>2</sub> and 0.1 mM CaCl<sub>2</sub> to simulate the relaxed and active state, and the distances obtained were 49 and 40 Å, respectively, a decrease of ~9 Å. The distance between Cys-48 of TnI and Cys-374 of F-actin in regulated reconstituted thin filaments was 53Å in the absence of Ca<sup>2+</sup>, and 58 Å in its presence, an increase of ~5 Å. These results show that, like the C-terminal region containing Cys-133 (Tao *et al.*, *Science* 247, 1339-1341, 1990), the N-terminal region of TnI containing Cys-48 moves away from actin towards TnC upon activation. However, the movement with respect to Cys-374 of actin is considerably less for Cys-48 (5 Å) than for Cys-133 (14 Å), suggesting that the C-terminal region of TnI undergoes more extensive Ca<sup>2+</sup>-induced movement than the N-terminal region. This may be relevant to the hypothesis (Farah *et al.*, *J. Biol. Chem.* 269, 5230-5240, 1994) that the C-terminal domain of TnI in association with the N-terminal domain of TnC plays a key role in the regulation of muscle contraction. (Supported by NIH HL5949 and AR21673)

## Tu-Pos156

EPR STUDIES OF MSL-TROPONIN I RECONSTITUTED IN RABBIT SKELETAL MUSCLE ((H.-C. Li and P.G. Fajer)) Dept. of Biol. Sci. Florida State University, Tallahassee, FL 32306

In vertebrate skeletal muscle, contraction is initiated by elevation of intracellular Ca<sup>2+</sup> concentration. The current hypothesis about thin filament activation considers that binding of Ca<sup>2+</sup> to TnC induces a series conformational changes which relieves the inhibition of acto-myosin ATPase by TnI. We have previously labeled rabbit skeletal troponin C and reconstituted back into fiber system to study its orientational change during Ca<sup>2+</sup> and/or myosin head binding activation using electron paramagnetic resonance (Biophys. J. 66: A189, 1994). Now we extend our study to TnI.

The orientation and dynamics of rabbit skeletal Troponin I (TnI) labeled with a maleimide spin label (MSL) at Cys-133 was investigated with electron paramagnetic resonance. The labeled TnI was reconstituted into oriented ghost fiber system, and the fiber was placed parallel to the external magnetic field. On addition of Ca<sup>2+</sup>, there was a clear change in the label's orientational distribution, while binding of S1 induced less significant effect.

It seems that both TnC and TnI undergo conformational changes manifested in the change of orientation during Ca<sup>2+</sup> activation (TnC and TnI) or myosin head binding (TnC).

## Tu-Pos157

FLUORESCENCE LIFETIME, ACRYLAMIDE QUENCHING AND PHOTOCROSSLINKING STUDIES OF THE INTERACTIONS BETWEEN TROPONIN I AND TROPONIN-T AND MONOCYSTEINE MUTANTS OF TROPONIN-C ((T. Tao, Y. Qian, I. Boldogh and J. Gergely)) Muscle Research Group, Boston Biomedical Research Institute, 20 Staniford St., Boston, MA 02114.

We have used *in vitro* site-directed mutagenesis to express in *E. coli* rabbit skeletal troponin C (TnC) with single Cys's at residue number 5 (in the N-helix), 12 and 21 (A-helix), 41 (B-helix), 49 (B-C linker), 89 (central D/E helix), 122 (F-helix), 125 (F-G linker), 133 (G-helix), and 153 and 158 (H-helix). All the chosen mutation sites are substantially solvent-exposed in the crystal structure of chicken skeletal TnC (Herzberg & James, Nature, 313, 653-659, 1985), so that the mutations are unlikely to compromise the structural and functional integrity of the protein. Each mutant was labeled with the fluorescent probe 1,5-IAEDANS, and the effect of troponin-I (TnI) and TnI-troponin-T (TnT) on the fluorescence lifetime ( $\tau$ ), and acrylamide quenching rate constant ( $k_q$ ) was measured. The results show that all the mutants exhibit an increase in  $\tau$  and decrease in  $k_q$  upon binding to TnI. The additional binding of TnT caused a further small change. In another set of experiments each mutant was labeled with the photocrosslinker benzophenone-4-maleimide. All the mutants formed photocrosslinks with TnI in both the binary TnC:TnI and the ternary TnC:TnI:TnT complexes. Taken together, our results indicate that all parts of TnC are in the vicinity of some part of TnI, and support a model for the TnC:TnI complex wherein TnI wraps around both domains of the dumbbell-shaped TnC molecule (Olah & Trewella, Biophys. J. 66, A311, 1994). (Supported by NIH HL5949 and AR21673).

## Tu-Pos159

Expression of regulated cardiac troponin I in *E. coli*.

Anthony J. Stracski, Antonio S. Nakouzi and Ashwani Malhotra. Department of Medicine and Cardiology, Montefiore Medical Center and Albert Einstein College of Medicine, Bronx, N.Y.

To assess the role of troponin isoforms in regulating myofibrillar ATPase activity in different pathologic and physiologic models, we have expressed rat cardiac troponin I (cTnI) in *E. coli* and purified the protein to near homogeneity. We utilized the inducible expression vector pGEX-KG to create a glutathione-S-transferase fusion protein which could be cleaved with thrombin. Approximately 8 mg of cTnI could be purified from 1 liter of culture.  $\text{Ca}^{2+}\text{Mg}^{2+}$  ATPase activity was measured using the bacterially synthesized cTnI and the other components of the regulated actomyosin complex (troponin T, troponin C, tropomyosin, actin, and myosin) isolated and purified to homogeneity from mammalian hearts. In the presence of free  $\text{Ca}^{2+}$  ranging from  $10^{-5}$  to  $10^{-6}$  M, bacterially synthesized cTnI exhibits specific activity similar to that observed for control cTnI isolated from rat hearts. The bacterially synthesized protein is capable of stoichiometric phosphorylation and demonstrates appropriately regulated specific activity. These results establish the feasibility of using bacterial expression to study functional consequences of changes in expression of troponin isoforms. Studies are currently underway to characterize the contribution of the other Tn subunits in the regulation of the actomyosin complex.

## Tu-Pos161

Competitive binding of calponin, troponin-I and myosin subfragment-1 to actin. (P. T. Szymanski & T. Tao). Muscle Research Group, Boston Biomedical Research Institute, 20 Staniford St., Boston, MA 02114.

Calponin (CaP) is a thin filament-associated protein that has been proposed to be involved in the regulation of smooth muscle contractility. *In vitro* studies revealed that like skeletal muscle troponin-I (Tn-I), CaP can bind to actin and inhibit actomyosin ATPase activity. The amino acid sequence of CaP contains a region (residues 146-171) that bears a considerable similarity to the inhibitory region (residues 96-114) of TnI, the region that is thought to be involved in actin binding and inhibition of ATPase activity. To investigate whether CaP interacts with actin in a manner similar to TnI, we examined how CaP competes with TnI and with myosin subfragment-1 (S1) for binding to actin. Using a high speed cosedimentation assay, we found that the amount of TnI bound to actin decreased with the addition of increasing amounts of CaP, and *vice versa*. Both CaP and TnI were capable of displacing S1 from actin in the presence of AMPPNP and ADP. In the absence of nucleotides, S1 was capable of displacing both CaP and TnI from actin. Our results suggest firstly that CaP, TnI and S1 share a common binding site on actin. Secondly, the mode of interaction between CaP and actin must be very similar to that between TnI and actin, so that the mechanisms whereby these two proteins inhibit actomyosin ATPase activity are also likely to be similar. Our results further implicate the involvement of CaP in the regulation of smooth muscle contractility. (Supported by NIH PO1-AR41673, AHA 92012390 & AHA 13-523-934)

## Tu-Pos158

THE ROLE OF TROPONIN I AND TROPONIN T IN THE CALCIUM-DEPENDENT REGULATION OF RECONSTITUTED THIN FILAMENTS. ((L. Thomas, J.E. Van Eyk, C.S. Farah\*, F.C. Reinach\*, R.S. Hodges, and L.B. Smillie\*)) Dept. of Biochemistry, Univ. of Alberta, Edmonton, Canada and \*Dept. de Bioquímica, Univ. de São Paulo, Brazil.

The colorimetric ATPase assay at pH 7.8 has been applied to reconstituted rabbit skeletal muscle thin filament at tropomyosin (TM):actin:myosin S1 ratios of 2.7:1.16. Under these conditions in the presence of native troponin (TnI, TnT, TnC), the pCa vs ATPase curve shows high cooperativity ( $n_H > 3$ ) with a pCa<sub>50</sub> value of 6.06. In the presence of  $\text{Ca}^{2+}$ , the ATPase activity is potentiated to >160% (TM-actin S1 ATPase=100%). In order to determine the pCa vs ATPase relationship of TnI fragments with different binding affinities for TnT-TnC or actin-TM, manipulation of the ratios of TnI fragments with respect to these proteins is required. Therefore, the concentration of a TnI fragment required for maximum inhibition of the actin-S1-TM ATPase activity is initially determined. At this concentration of TnI fragment, increasing quantities of TnC or a TnT-TnC complex (1:1 mole ratio) are added until maximum  $\text{Ca}^{2+}$ -activation of the actin-S1-TM ATPase activity is achieved. Finally, the pCa vs ATPase curve is obtained using the concentrations of TnI fragment and TnC or TnT-TnC that induces the maximum  $\text{Ca}^{2+}$ -dependent change in ATPase activity. The deletion of TnT from the reconstituted system (TnI-TnC-TM-actin-S1) has minimal effect on cooperativity and the pCa<sub>50</sub> value of the ATPase vs pCa curves; however, there is no potentiation ( $+\text{Ca}^{2+}$ ) of the ATPase activity. A fully functional system is achieved when the TnT-TnC complex is renatured from urea/KCl. The effects of substituting intact TnI<sub>1-182</sub> by TnI<sub>104-115</sub> or TnI<sub>1-116</sub> in the reconstituted system increased the  $\text{Ca}^{2+}$  sensitivity (pCa<sub>50</sub>), while the cooperativity is significantly reduced. Potentiation ( $+\text{Ca}^{2+}$ ) is dependent on the presence of both TnT and TnI<sub>1-116</sub> and is not seen with TnT and TnI<sub>104-115</sub>. (Supported by MRC of Canada, Alberta Heritage Foundation for Medical Research, and the Alberta Heart and Stroke Foundation).

## Tu-Pos160

$\text{Ca}^{2+}$ -SPECIFIC FLUORESCENCE CHANGES UPON INTERACTION OF TROPONIN-I INHIBITORY PEPTIDES WITH THE N AND C DOMAINS OF TROPONIN-C TRYPTOPHAN MUTANTS. ((J.R. Pearlstone and L.B. Smillie\*)) Medical Research Council Group in Protein Structure and Function, Department of Biochemistry, University of Alberta, Edmonton, Alberta, Canada T6G 2H7.

Three troponin-I (TnI) peptides (Ip1, residues 96-116; I(117-148); I(96-148)) around the inhibitory region were used to study interactions with the N and C domain fragments of chicken skeletal troponin-C (TnC) in which the Phe (F) at positions 29 and 105 in the respective domains were replaced by Trp (W) for use as an intrinsic spectral probe. Perturbations in the fluorescence emission spectra induced by addition of Ip1 to the N and C domains of TnC in both the intact molecules (F29W and F105W) and the isolated fragments (F29W N domain, residues 1-90 and F105W C domain, residues 88-162) were  $\text{Ca}^{2+}$ -dependent. Both F105W mutants displayed unique spectra when the  $\text{Ca}^{2+}/\text{Mg}^{2+}$  sites were occupied by  $\text{Ca}^{2+}$  versus  $\text{Mg}^{2+}$ . Titrations of  $\text{Ca}^{2+}$ -saturated TnC mutants with the TnI peptides showed tighter binding in the order I(96-148) > I(117-148) ≥ Ip1(96-116). C domain mutants bound 7 to 8-fold stronger to Ip1 than did the N domain mutants. (Supported by the Medical Research Council of Canada.)

## Tu-Pos162

MOLECULAR BASIS OF HUMAN CARDIAC TROPONIN T ISOFORMS EXPRESSED IN THE DEVELOPING, ADULT, AND FAILING HEART. ((A. Greig, T.M. Mark, N.N. Malouf, A.E. Oakeley, R.M. Ungerleider, P.D. Allen, B.K. Kay, and P.A.W. Anderson)) University of North Carolina, Chapel Hill, NC; Brigham and Women's Hospital, Boston, MA, and Duke University, Durham, NC.

Cardiac troponin T (cTnT), a protein essential for calcium-regulated myofibrillar ATPase activity, is expressed in the human heart as four isoforms. Their expression at the protein level differs among the fetal and the normal and failing adult human heart. We have cloned and sequenced four full-length human cDNAs corresponding to the four native cTnT protein isoforms and have expressed these cDNAs *in vitro*. The cDNAs differ by the variable inclusion of a 15- and a 30-nt sequence in the 5' coding region. These cDNAs yielded proteins that comigrated with the native isoforms cTnT<sub>1</sub>-cTnT<sub>4</sub>. Polyclonal antisera, raised against a synthetic peptide corresponding to the 10-residue peptide encoded by the 30-nt sequence, reacted with the two largest human isoforms, cTnT<sub>1</sub> and cTnT<sub>2</sub>, which are expressed in the fetal human heart and that contain either both peptides encoded by the 30- and 15-nt sequences or the 30-nt alone. cTnT<sub>4</sub>, lacking both of these sequences, is expressed in the fetus and is re-expressed in the failing adult heart. cTnT<sub>3</sub> that contains the 5-residue peptide is the dominant isoform in the adult heart. The identification and acquisition of these full length clones that encode the four human cTnT isoforms should prove valuable in identifying human cTnT mutations and studying the functional role of these isoforms in the normal and the diseased human heart.

## Tu-Pos163

A NOVEL EXON COMPLEX, USE OF A CRYPTIC SPLICE SITE, AND A DEVELOPMENTALLY-REGULATED EXON CONTRIBUTE TO THE HETEROGENEITY OF CHICKEN NEONATAL TROPONIN T MESSENGER RNAs ((F. Schachar, J. Schmidt, M. Maready, B. Almond and M. Briggs)) Department of Cell Biology, Duke University Medical School, Durham, NC 27710.

During early neonatal development, chicken skeletal muscles transiently express a novel set of troponin T (TnT) isoforms. Derived from the fast TnT gene, they exhibit higher  $M_r$ s and more acidic pIs than their adult counterparts. Their heterogeneity is thought to reflect combinatorial splicing of a group of 5'-cassette exons as proposed for the rat TnT gene. An alternative explanation was raised by the discovery of an additional developmentally-regulated 5'-cassette exon in mammalian fast troponin T genes, which is incorporated into mammalian fetal and early neonatal TnT mRNAs. To distinguish between these explanations, we amplified the 5'-alternatively spliced region of TnT mRNAs and sequenced the cDNAs generated. Our results indicate that neither explanation is correct. No homologue of the fetal exon was found. But neither was combinatorial splicing. Instead three RNA processing events characteristic of fetal and neonatal chick TnT mRNA processing were observed. One, includes the incorporation of sequences from a three exon complex that encodes the x-sequence identified by Wilkinson, another involves the use of a cryptic splice site in exon 5, and the last is the expression of a developmentally-regulated exon that exhibits no homology with the mammalian fetal exon.

## Tu-Pos165

OPPOSITE EFFECTS OF MYOSIN SUBFRAGMENT 1 ON BINDING OF TROPONIN AND TROPOMYOSIN TO ACTIN. ((M. Cassell and L. S. Tobacman)) Depts. of Int. Medicine and Biochemistry, University of Iowa, Iowa City, IA 52242

The binding of myosin subfragment 1 (S-1) to actin is profoundly influenced by tropomyosin and troponin, especially under conditions of rigor crossbridge formation. Less is known, however, about the effects of myosin S-1 on the interactions of troponin and tropomyosin with actin. We have investigated the effects of myosin S-1 on the binding of tropomyosin or troponin-tropomyosin to actin, as well as the effect of myosin S-1 on the binding of troponin to tropomyosin-actin. Tropomyosin was labelled on cyst-190 with  $^3\text{H}$ -iodoacetate. Similarly, cardiac muscle troponin was labelled at cyst-39 of TnT. Binding to actin in the presence of 300 mM KCl, no nucleotide, and no  $\text{Ca}^{2+}$  was assessed by ultracentrifugation and liquid scintillation counting. As previously, the data were analyzed as a linear lattice binding problem, permitting the determination of both the affinity of the ligand (tropomyosin or troponin-tropomyosin) for an isolated site on the thin filament and the strength of the cooperative interactions between ligands. Troponin binding to actin-tropomyosin was assessed by calculation from equilibrium linkage relationships and by direct measurement of  $^{14}\text{C}$ -cardiac troponin cosedimentation with actin-tropomyosin-S-1. Myosin S-1 increased the affinity of tropomyosin for actin approximately 700-fold, from  $600 \text{ M}^{-1}$  to  $4 \times 10^5 \text{ M}^{-1}$ . However, it increased the affinity of troponin-tropomyosin for actin only 4-fold, from  $5 \times 10^5 \text{ M}^{-1}$  to  $2 \times 10^6 \text{ M}^{-1}$ . The affinity of troponin for myosin S-1-actin-tropomyosin was between  $0.3$  and  $2 \times 10^7 \text{ M}^{-1}$ , depending upon the method of measurement. This is much weaker binding than occurs in the absence of myosin S-1 ( $5 \times 10^8 \text{ M}^{-1}$ ), and suggests that thin filament activation by myosin (in contrast to  $\text{Ca}^{2+}$ ) requires substantial weakening of troponin's interaction with the thin filament.

## Tu-Pos167

IN VITRO MOTILITY ANALYSIS OF THIN FILAMENT REGULATION BY TROPONIN AND CALCIUM. ((I.D.C. Fraser and S.B. Marston)) Dept. of Cardiac Medicine, NHLI, Dovehouse St., LONDON SW3 6LY, UK

We have used an *in vitro* motility assay to examine troponin regulation of individual actin-tropomyosin filaments moving over immobilised skeletal muscle heavy meromyosin (HMM). Thin filament proteins were pre-mixed at 10x assay concentrations and diluted immediately prior to infusion into the assay flow cell. At  $28^\circ\text{C}$ , in 0.08M ionic strength buffer containing 0.5% methyl cellulose, 10nM actin filaments showed >85% motility at an average velocity of  $3.7 \mu\text{m/s} \pm 0.05$  over  $100 \mu\text{g/ml}$  HMM. Inclusion of 10nM tropomyosin had little effect on either %motility or filament velocity. Actin-tropomyosin binding was confirmed by SDS-PAGE. At pCa 9.0, addition of up to 4 nM troponin caused the %motility to decrease from >85% to 20% with no dissociation of the filaments from the HMM surface or change in velocity. At fixed actin, tropomyosin and troponin concentrations of 10, 10 and 5nM respectively, the  $\text{Ca}^{2+}$  concentration was increased from pCa 9.0 to 4.5. The %motility increased from <20% to >85% with half maximal increase at pCa 5.8-6.0. There was a modest increase in filament velocity but no alteration in the number of filaments attached to the HMM. In the absence of tropomyosin, increasing troponin to 20nM had no effect on %motility or velocity. At concentrations of 10nM and above however, filament density was reduced by up to 50%. Our results demonstrate that, in the reconstituted thin filament, troponin mediates its control through a tropomyosin dependant switch. Rather than undergoing subtle changes in velocity, filaments are switched "on" or "off" as a unit. Thus the effect of  $\text{Ca}^{2+}$  upon the thin filament is to recruit motile filaments.

## Tu-Pos164

PHENOTYPIC AND MOLECULAR ANALYSES OF TROPONIN T MUTATIONS IN *C. ELEGANS*. ((T.S.C. Allen, C. Myers, P.-Y. Goh\*, T. Bogaert\*, and E.A. Bucher\*)) Dept of Cell and Developmental Biology, U. of Pennsylvania, Philadelphia, PA 19104-6058; \*MRC-LMB, Cambridge, U.K.; \*U. of Gent, Gent, Belgium.

To elaborate the mechanisms by which troponin T (TnT) functions in the assembly and contraction of developing and mature muscle, we are studying a TnT homolog in *Caenorhabditis elegans*. The genetic locus, *mup-2*, encoding the homolog was first defined by a heat sensitive allele, designated *e2346ts*, arising from a screen for worms with mutant muscle attachment positioning (called Mup). A subsequent non-complementation screen with *mup-2* (*e2346 ts*) has yielded a second allele, designated *up1*, believed null. Phenotypically, both alleles cause muscle positioning defects during embryogenesis and result in kinked, dead larvae. Because mutants for these alleles can show muscular contraction prior to death, the phenotype is distinct from the severe paralysis of worms with mutations tentatively identified in troponin C and tropomyosin (Williams and Waterston. *J. Cell Biol.* 124:475, 1994). When hermaphroditic worms homozygous for *mup-2* (*e2346 ts*) are shifted from  $15^\circ\text{C}$  to  $25^\circ\text{C}$  after embryogenesis, paralysis does not occur, but the worms show subtly compromised function of the striated body wall musculature and are sterile, the latter believed caused by impaired function of the non-striated oviductal musculature. The predicted gene product comprises 405 amino acids and shows high sequence similarity to other invertebrate and vertebrate homologs in regions of TnT believed to interact with tropomyosin and the other troponin subunits. Like other invertebrate isoforms, TnT encoded by *mup-2* is predicted to have a carboxyl terminal extension not found in vertebrate isoforms. The *e2346 ts* mutation creates a premature stop codon, truncating expression to a product of 341 amino acids. The *up1* mutation creates a premature stop at codon 94, preventing expression of the regions homologous to the functional domains of vertebrate TnT. Genetic interaction studies and site-directed mutagenesis of *mup-2* will contribute towards defining the *in vivo* structure-function relationship for TnT. Supported by the American Heart Association and the American Philosophical Society.

## Tu-Pos166

INTERACTION OF CARDIOTONIC THIADIAZINONE DERIVATIVES WITH CARDIAC TROPONIN C ((B.-S. Pan and R.G. Johnson, Jr.)) Merck Research Labs, West Point, PA 19486

The positive inotropic effects of thiadiazinone derivative EMD 57033 are thought to be mediated by its direct, stereospecific effects on myofilaments. We investigated if EMD 57033 interacts with cardiac troponin C. EMD 57033 ((+)) enantiomer and its (-) enantiomer, EMD 57439, caused quenching of the fluorescence of recombinant human cardiac troponin C (hcTnC) covalently labeled with IAANS. Both drugs altered  $\text{Ca}^{2+}$ -dependent interaction of hydrophobic probe bis-ANS with hcTnC, inducing decreases of bis-ANS fluorescence in the presence of  $\text{Ca}^{2+}$ -saturated hcTnC. The relationships of bis-ANS fluorescence and drug concentration for the two drugs differed in a manner hinting that EMD 57033 bound cTnC more strongly than did EMD 57439. EMD 57033 and EMD 57439 caused quenching of intrinsic tyrosine fluorescence of hcTnC at  $100 \mu\text{M}$   $\text{Ca}^{2+}$ , and had little or no effect on the fluorescence in the presence of  $1.8 \text{ mM}$   $\text{Mg}^{2+}$  and no  $\text{Ca}^{2+}$ , indicating that the binding of the drugs is  $\text{Ca}^{2+}$ -dependent. Titration of tyrosine fluorescence of hcTnC at pCa 4 allowed estimates of  $K_d$  for hcTnC/drug complexes, which was approximately  $40 \mu\text{M}$  for EMD 57033 and  $160 \mu\text{M}$  for EMD 57439. The stereo-selectivity and  $\text{Ca}^{2+}$ -dependence of the drug/hcTnC interaction were confirmed by an equilibrium dialysis-based binding assay. EMD 57033/hcTnC interaction seems unlikely to be a primary mediator of the pharmacological effects of EMD 57033 because of the relative low affinity of the interaction.

## Tu-Pos168

TROPONIN I AND TROPONIN I-C BINDING TO ACTIN-TROPOMYOSIN AND DISSOCIATION BY MYOSIN S1. ((X. Zhou\*, E.P. Morris\* & S.S. Lehrer\*)) \*Boston Biomedical Research Institute, Boston, MA and \*Imperial College, London, England.

Previous studies have indicated that the binding to actin of troponin I (TnI) and the troponin I-C complex (TnIC) in the absence of  $\text{Ca}^{2+}$ , is enhanced by tropomyosin (Tm) (Perry et al, 1973; Hitchcock, 1975). To learn more about the influence of Tm, the monomer fluorescence of pyrene-labeled Tm (Tm\*), which increased 35% on binding both TnI and TnIC to actin.Tm\*, was monitored during binding and S1 titrations. The S1-induced dissociation of TnIC from actin.Tm was also studied by ultracentrifugation and PAGE. TnIC bound to actin.Tm\* with a stoichiometry,  $n = 1$  TnIC/7 actin subunits and  $K = 7 \times 10^6 \text{ M}^{-1}$ , at  $25^\circ$  in  $0.05 \text{ M}$  NaCl + buffer ( $5 \text{ mM}$   $\text{Mg}^{2+}$ ,  $2 \text{ mM}$  EGTA,  $10 \text{ mM}$  Hepes pH 7.5). In contrast, for TnI binding to actin.Tm\* in  $0.1 \text{ M}$  NaCl + buffer, 2 classes of binding sites fit the binding profile. For site 1,  $n_1 = 1$  TnI/7 actin subunits,  $K_1 = 7 \times 10^6 \text{ M}^{-1}$ ; for the remaining 6 actin sites,  $K_2 = 5 \times 10^5 \text{ M}^{-1}$ . Addition of S1 to the TnI- and TnIC- actin.Tm complexes caused dissociation of TnI and TnIC at S1/actin < 0.5. These studies indicate that: (1) TnIC and, to a somewhat smaller extent, TnI, interacts with a specific region of Tm on actin near the pyrene label (1/3 from the carboxyl end), facilitating binding; (2) the dissociation of TnIC and TnI from actin.Tm by S1 appears to be related to the S1-induced "off-on" change in state of Tm.actin which, in the "on-state", weakens the interaction of TnIC and TnI with Tm. (Supported by NIH HL22461).

## Tu-Pos169

**CYCLIC NUCLEOTIDES DIFFERENTIALLY REGULATE MYOSIN LIGHT CHAIN PHOSPHORYLATIONS INDUCED BY PHORBOL ESTER IN RAT AORTA.** ((Hee Yul Ahn, Hyun Moon, Young Chul Ahn, Jin Young Jung, Ki Chul Chang\*, Myung Hee Chung<sup>+</sup> and Myung Suk Kim<sup>+</sup>)) Dept. of Pharmacol. College of Med. Chungbuk Nat'l Univ. Cheongju 360-763 S. Korea, \*Dept. of Pharmacol. College of Med. Gyeongsang Nat'l Univ. Chinju and <sup>+</sup>Dept. of Pharmacol. College of Med. Seoul Nat'l Univ. Seoul. (Spon. by P. D. Ryu)

In rat aorta, the vasodilating mechanism of 8-Br-cAMP and 8-Br-cGMP were investigated on the contraction induced by 0.1  $\mu$ M phorbol dibutyrate (PDBu) respectively. In 1.5 mM extracellular  $\text{Ca}^{2+}$ -PSS (normal PSS), 8-Br-cAMP and 8-Br-cGMP dose-dependently inhibited the sustained contraction by PDBu respectively. 8-Br-cGMP was more effective than 8-Br-cAMP in relaxing PDBu-induced contractions. 0.1  $\mu$ M PDBu increased 20-kDa myosin light chain (MLC) phosphorylations time-dependently. 8-Br-cGMP inhibited the MLC phosphorylations by PDBu. However, 8-Br-cAMP did not inhibit the MLC phosphorylations by PDBu. In  $\text{Ca}^{2+}$ -free 2mM EGTA solution, 0.1  $\mu$ M PDBu still induced sustained contraction. The relaxing effects of 8-Br-GMP on the contractions by PDBu in  $\text{Ca}^{2+}$ -free 2 mM EGTA solution were not different from those on the contractions by PDBu in normal PSS. However, the relaxing effects of 8-Br-cAMP on the contractions by PDBu were attenuated in  $\text{Ca}^{2+}$ -free 2 mM EGTA solution compared with those in normal PSS. From these results, it seems that phorbol ester, activator of protein kinase C, induces contraction resulting from increase of MLC phosphorylations in normal physiological conditions. cGMP inhibits MLC phosphorylations by PDBu resulting in vasodilation in normal physiological conditions. However, cAMP has other  $\text{Ca}^{2+}$ -dependent vasodilating mechanism, which is not related with modifications of MLC phosphorylations.

## Tu-Pos171

**ALTERED KINETICS OF CONTRACTION IN SKELETAL MUSCLE FIBERS CONTAINING A MUTANT REGULATORY LIGHT CHAIN WITH REDUCED DIVALENT CATION BINDING** ((GM Diffie, FC Reinach<sup>+</sup>, ML Greaser, and RL Moss)) Dept of Physiology and Muscle Biology lab, University of Wisconsin, Madison, WI 53706 and <sup>+</sup>Institute of Chemistry, University of Sao Paulo, Brazil.

We have previously shown (Diffie, *et al.*, *Biophys J.*, 66:A192, 1994) that, when a mutant myosin regulatory light chain (D47A) with significantly reduced ability to bind divalent cations is exchanged into skinned skeletal muscle fibers, the isometric tension generating ability of the fibers is severely reduced. In this study we have examined the effect of D47A incorporation on the kinetic properties of skinned fibers. Up to 80% of the endogenous myosin regulatory light chain (RLC) can be replaced by exogenous RLC with minimal effect on fiber integrity. When the endogenous RLC in rabbit psoas skinned fibers was replaced with the D47A mutant, the maximal shortening velocity ( $V_o$ ) of the fibers, as measured by the slack test, was reduced to an average of 51% of the  $V_o$  of the fibers prior to exchange. This effect is not an artifact of the exchange procedure because exchange of a native mammalian RLC into fibers had no effect on either maximum isometric tension or on  $V_o$ . These results provide further evidence that the divalent cation binding site on myosin regulatory light chain plays an important role in modulating contractile properties in vertebrate striated muscle.

Supported by NIH AR08226 and HL25861

## Tu-Pos173

**EFFECTS OF MYOSIN LIGHT CHAIN KINASE INHIBITION ON CONTRACTILE FORCE IN CANINE GASTRIC ANTRAL MUSCLE.** ((E.P. Burke, K.M. Sanders & N.G. Publicover)) Department of Physiology, University of Nevada School of Medicine, Reno, NV 89557-0046

The role of myosin light chain kinase (MLCK) in regulating phasic contractions was investigated using wortmannin, a specific inhibitor of the kinase. Experiments were performed on strips of canine gastric antral muscle with the long axis cut parallel to circular muscle fibers, allowing the simultaneous recording of electrical slow waves using intracellular microelectrodes and tension using a force transducer. Wortmannin (10 to 30 mM) abolished slow wave-induced contractions within 10-15 min. The block was not due to an effect on electrical activity since slow wave amplitude, duration and frequency as well as resting membrane potential were not significantly altered ( $n=9$ ). The effects of wortmannin were irreversible since contractions did not return following 2 hours of washout. Wortmannin also inhibited contractions (<3%) induced by elevated  $[\text{K}^+]_o$  (50 mM). However, in the same preparations, a significant contractile response to micropressure ejection of acetylcholine (ACh) remained after wortmannin perfusion (>20%). In muscle strips pre-contracted with 100 mM  $[\text{K}^+]_o$ , wortmannin perfusion evoked relaxation. In strips pre-contracted with ACh ( $10^{-6}$ M) wortmannin caused only partial relaxation. Results suggest that spontaneous slow wave-evoked contractions are MLCK-dependent. During cholinergic stimulation there may be a MLCK-independent component or sensitization of contraction. (Supported by NIH grant DK32176.)

## Tu-Pos170

**MECHANISM OF VANADATE ACTIVATION OF SMOOTH MUSCLE CONTRACTION IN THE ABSENCE OF MYOSIN LIGHT-CHAIN PHOSPHORYLATION.** ((Jung-Ren Chen, Young-Soo Han and W. Glenn L. Kerrick)) Department of Physiology and Biophysics, University of Miami School of Medicine, Miami, FL 33101. (Spon. by Lu Song).

It has been reported that pre-treatment of skinned smooth muscle fibers with sodium orthovanadate ( $\text{VO}_4$ ) caused them to contract in the absence of  $\text{Ca}^{2+}$ , with little phosphorylation of the regulatory myosin light-chain, LC<sub>20</sub> (Biophys. J. 66:A410, 1994). Since Strauss *et al* (FEBS Letters 310, 229-234, 1992) reported that  $\text{VO}_4$  extracted TnC and TnI from skinned cardiac muscle fibers, we examined the possibility that  $\text{VO}_4$  activates smooth muscle contraction by extracting regulatory proteins from skinned chicken gizzard fibers (smooth muscle). We pre-treated skinned chicken gizzard fibers with 10 mM  $\text{VO}_4$ , which caused the fibers to contract in the absence of  $\text{Ca}^{2+}$  as previously reported. SDS-PAGE analysis showed that myosin light-chains as well as other proteins were extracted. The extracts, after removal of  $\text{VO}_4$ , when added back to the  $\text{VO}_4$  activated skinned gizzard fibers, inhibited the activation and partially recovered  $\text{Ca}^{2+}$ -activated contractions. In conclusion, the activation of force in smooth muscle by  $\text{VO}_4$  is in part due to the removal of endogenous regulatory proteins.

## Tu-Pos172

**EFFECTS OF EXTRACTION AND RECONSTITUTION OF THE REGULATORY LIGHT CHAINS OF MYOSIN ON THE RATE OF FORCE DEVELOPMENT IN SKELETAL MUSCLE FIBERS** ((Danuta Szczesna, Jiaju Zhao and James D. Potter)) Dept. of Mol. & Cell. Pharm., Univ. of Miami Sch. of Med., Miami FL 33136

We investigated the kinetics of the  $\text{Ca}^{2+}$  triggered skeletal muscle activation elicited by the photolysis of caged  $\text{Ca}^{2+}$ . Previously we showed that partial extraction of the 18-kDa regulatory light chain (RLC) of myosin decreased the rate of force development which was subsequently increased by 20% following reconstitution with RLC. We extended here, the RLC-extraction study to complete removal of the light chains, achieved by incubation of the skinned fibers in a solution of 10 mM DTNB, 20 mM KCl, pH 8 for 15 min at RT. Extraction of RLC was completed in a solution of 20 mM KCl, 10 mM EDTA, 10 mM imidazole buffer, pH 7 and 2 mM DTT for 30 min and for 1 hr in the same solution containing 30 mM DTT to restore the blocked SH groups within the fiber. Under these conditions the total extraction of RLC was accompanied by 80-90% extraction of the TnC. The steady state isometric force was restored fully after TnC was replenished into the fiber. The rate of force development generated with the UV-flash of DM-nitrophen photo-liberating the bound  $\text{Ca}^{2+}$ , decreased from  $t_{1/2}=46 \pm 5$  ms to  $t_{1/2}=80 \pm 9$  ms,  $n=4$ , as a result of the RLC extraction. Subsequently, full reconstitution of the fiber with RLC was performed by incubation of the TnC replenished fibers in a solution of 30  $\mu$ M RLC for 2 hrs. The time course of isometric tension developed by the RLC-reconstituted fiber showed the same exponential characteristic, with a half time of  $53 \pm 6$  ms, as the native skinned fiber. Comparable results were obtained with the nitrophenyl-EGTA, a photosensitive specific chelator of  $\text{Ca}^{2+}$ . These results support our earlier findings that the regulatory light chains of myosin play an important role in the kinetics of crossbridge cycling.

## Tu-Pos174

**MYOSIN LIGHT CHAIN-ACTIN INTERACTION REGULATES CARDIAC CONTRACTILITY** (I. Morano, O. Ritter, A. Bonz, T. Timek C. F. Vahl, and G. Michel) Max-Delbrück-Center for Molecular Medicine, Robert-Rössle-Straße 10, 13122 Berlin, Germany,

The amino-terminal domain of the essential myosin light chain (MLC-1) binds to the most carboxy-terminus of the actin molecule. We studied the functional role of this interaction using two approaches: 1st incubation of intact and chemically skinned human heart fibres with synthetic peptide corresponding to the sequences 5-14 (P5-14), 5-8 (P5-8), and 5-10 (P5-10) of the human ventricular MLC-1 (VLC-1) in order to saturate actin binding sites, and 2nd incubation of skinned human heart fibres with a monoclonal antibody (mabVLC-1) raised against the actin-interacting N-terminal domain of human VLC-1 using P5-14 as antigen in order to deteriorate VLC-1 binding to actin. P5-14 increased isometric tension generation of skinned human heart fibres at both submaximal and maximal  $\text{Ca}^{2+}$  activation the maximal effective peptide dosage being in the nanomolar range. A scrambled peptide of P5-14 had no effects up to  $10^{-8}$ M, i.e. where P5-14 was maximally effective. P5-8 and P5-10 increased isometric force to the same extent as P5-14 but micromolar concentrations were required. Amplitude of isometric twitch contraction, rate of tension development, rate of relaxation, and shortening velocity at near-zero load of electrically driven intact human atrial fibers increased significantly upon incubation with P5-14. These alterations were not associated with modulation of intracellular  $\text{Ca}^{2+}$  transients as monitored by Fura-2 fluorescence measurements. Incubation of skinned human heart fibres with mabVLC-1 increased isometric tension at both submaximal and maximal  $\text{Ca}^{2+}$  activation levels having a maximal effective concentration in the femtomolar range. Thus, VLC-1-actin interaction modulates cardiac contractility and may be a target for new inotropic intervention.



## Tu-Pos175

MYOSIN LIGHT CHAIN (MLC) PHOSPHORYLATION DURING  $\text{Ca}^{2+}$ -INDEPENDENT SMOOTH MUSCLE CONTRACTION. ((C. Bergh Menice, C.A. Lajoie and K.G. Morgan)) Program In Smooth Muscle Research, Harvard Medical School, Beth Israel Hospital, Boston, MA 02215

A phenylephrine(PE)-induced contraction that occurs in single vascular smooth muscle cells at constant  $[\text{Ca}^{2+}]_i$  has been reported to result from activation of protein kinase C (PKC) (Collins et al. 1992). In the present study we characterized a  $[\text{Ca}^{2+}]_e$ -independent contraction observed in ferret aorta preparations in response to stimulation with PE in order to determine if the mechanism involves an effect of PKC on MLC phosphatase or a pathway distinct from MLC phosphorylation. In this study the temporal pattern of MLC phosphorylation during  $[\text{Ca}^{2+}]_e$ -independent contraction was determined. In contrast to observations made in normal  $\text{Ca}^{2+}$ -containing solutions, a transient increase in LC 20 phosphorylation during initiation of the contractile response was not observed, furthermore, there was no significant elevation at any time point measured throughout the initial 10 min of  $[\text{Ca}^{2+}]_e$ -independent contraction. Results obtained using aequorin luminescence to measure  $[\text{Ca}^{2+}]_i$  during  $[\text{Ca}^{2+}]_e$ -independent contraction showed that no  $\text{Ca}^{2+}$  transient occurred during initiation of contraction, indicating that neither  $\text{Ca}^{2+}$  release from the sarcoplasmic reticulum nor traditional latch bridge phenomena can explain the initiation of contraction. These results suggest that the mechanism of  $[\text{Ca}^{2+}]_e$ -independent contraction involves a pathway distinct from myosin phosphorylation. Support: NIH HL31704, HL 42293

## Tu-Pos177

CONTROL OF THE TURNOVER OF MYOSIN-BOUND ADP BY LIGHT CHAIN PHOSPHORYLATION IN SMOOTH MUSCLE. ((L. Trinkle-Mulcahy, S.U. Moers, S.R. Narayan, M.J. Siegman and T.M. Butler)) Dept. of Physiology, Thomas Jefferson University, Philadelphia, PA 19107.

Single turnover experiments were performed on the ADP bound to myosin in an effort to determine how myosin light chain phosphorylation (MLCP) controls both the number of activated crossbridges and possible distribution of activated crossbridges between slow and fast kinetic cycles under isometric conditions. Previous results showed that thiophosphorylation of the light chain appeared to mediate the distribution of the myosin between two activated pools: phosphorylated crossbridges (fast cycling) and cooperatively activated unphosphorylated crossbridges (slow cycling). In a calcium-mediated contraction, the myosin light chain kinase and phosphatase may equilibrate the myosin between the two pools, and this would be reflected in the time course of ADP turnover. Freeze glycerinated, triton X-100 treated portal veins were incubated in  $[\text{C}^{14}]$ ATP and high specific activity caged  $[\text{H}^+]$ ATP. Following photolysis the time course of appearance of  $^3\text{H}$  in myosin-bound ADP was determined. In pCa 4.5 (~60% MLCP) the maximum number of crossbridges increase their rate of ADP exchange, and the overall time course is slower ( $t_{1/2} \approx 10$  sec) than that seen with 80% thiophosphorylation ( $t_{1/2} \approx 5$  sec). In pCa 6.1 (~20% MLCP), the ADP exchange is quite slow ( $t_{1/2} \approx 35$  sec), but still 5-fold higher than the resting rate. The ADP exchange in pCa 4.5 contains a fast component which is not seen in pCa 6.1. There may be a more uniform pool of cycling crossbridges at low than at high MLCP during calcium-mediated isometric contractions. (Supported by HL 50586)

## Tu-Pos179

EARLY DETECTION OF CARDIAC  $\alpha$ -ACTIN GENE EXPRESSION DURING THE IN VITRO DIFFERENTIATION OF MOUSE EMBRYONIC STEM CELLS. ((Wan-In Lin, Linda C. Samuelson and Joseph M. Metzger)) Department of Physiology, University of Michigan, Ann Arbor, MI 48109 (Sponsored by David C. Dawson)

Mouse embryonic stem (ES) cells differentiate *in vitro* into a variety of cell types including spontaneously contracting cardiac myocytes. Previous studies have shown that differentiating ES cells express cardiac-specific contractile genes indicating that this system represents a new model to determine the mechanisms of cardiac gene expression and function *in vitro*. We have established a transformed ES cell line using the human cardiac  $\alpha$ -actin promoter/enhancer (-440 to +6) to direct expression of the E. coli reporter gene, lacZ (ActlacZ), into ES cell-derived cardiac myocytes during cardiogenesis *in vitro*. Undifferentiated ES cells were electroporated with ActlacZ together with a plasmid containing the neomycin gene under direction of the PGK promoter. Results showed that the ActlacZ reporter construct was expressed very early during the ES cell differentiation program, at time points prior to the appearance of spontaneous contractile activity of the ES cell cardiac myocytes. For example, at day 6 of differentiation ActlacZ expression was detected in about 25% of the differentiation cultures and increased to about 70% at day 9. Expression of the lacZ gene was also detected in the contracting ES cell cardiac myocytes. Expression was evident in cardiac myocytes that had been contracting for 1 to 40 days *in vitro*, indicating stable expression of the reporter gene. Indirect immunofluorescence assays demonstrated that expression was restricted to the contracting myocytes in culture. In addition, it was also possible to detect transgene expression in living contracting myocytes by using lipophilic, fluorogenic  $\beta$ -galactopyranoside substrates. This permitted real-time detection of the reporter gene during contraction of the ES cell myocytes *in vitro*. These studies demonstrate that this actin promoter fragment is sufficient to direct cardiac specific gene expression into ES cell contracting myocytes.

## Tu-Pos176

STRAIN DEPENDENCE OF CROSSBRIDGE KINETICS IN SMOOTH MUSCLE. ((T.M. Butler, S.R. Narayan, S.U. Moers, and M.J. Siegman)) Dept. of Physiology, Thomas Jefferson University, Philadelphia, PA 19107

The strain dependence of a limited number of the kinetic steps in the crossbridge cycle was determined from changes in the time course of the single turnover of myosin-bound ADP in the transition from isometric to shortening or stretching conditions. Permeabilized portal veins of the rabbit, in which the myosin light chains were about 80% thiophosphorylated were incubated in  $^{14}\text{C}$ -ATP and high specific activity caged  $^3\text{H}$ -ATP at 20°C. Initially, the myosin-bound ADP has the  $^{14}\text{C}$  label alone, but following the photolytic release of  $^3\text{H}$ -ATP from caged  $^3\text{H}$ -ATP, it acquires a tritium label with a time course which reflects the rate at which the ADP is released from myosin and replaced by new ADP derived from ATP splitting. Since the ADP release step is likely to be one of the strain dependent steps in the cycle, there should be a change in the time course of ADP turnover with mechanical perturbation of the muscle. Compared to isometric conditions, there is up to a 10-fold increase in the rate constant for turnover of myosin-bound ADP when the muscle shortens ( $k=0.12$   $\text{s}^{-1}$  for isometric,  $k=0.34$   $\text{s}^{-1}$  for shortening at 0.017  $\text{L}/\text{s}$ , and  $k=1.1$   $\text{s}^{-1}$  for shortening at  $V_{\text{max}}$ , 0.032  $\text{L}/\text{s}$ ). In contrast, stretch has little effect ( $k=0.12$  and 0.10  $\text{s}^{-1}$  for stretches of 0.005  $\text{L}/\text{s}$  and 0.017  $\text{L}/\text{s}$ , respectively). The data suggest that the process controlling ADP release from AMADP is very sensitive to axial displacement of the crossbridge in the shortening direction, but much less so in the stretching direction. (Supported by HL50586)

## Tu-Pos178

THE INFLUENCE OF PHYSIOLOGICAL LEVELS OF L(+) LACTATE ON THE CONTRACTILITY OF FAST- AND SLOW-TWITCH SKELETAL AND CARDIAC MUSCLE FROM RABBIT. ((M.A. Andrews, R.E. Godt<sup>2</sup>, and T.M. Nosek<sup>3</sup>)) Div. of Physiol., NY Coll. Osteopath. Med., Old Westbury, NY 11568 and <sup>2</sup>Dept. of Physiol. and Endocrinol., Med. Coll. Georgia, Augusta, GA 30912-3000

Hypoxic conditions prevail during strenuous physical activity, and, as a result, there is a build-up of L(+) lactate in both active and surrounding muscle. Here we report the effects of physiological levels of L(+) lactate on contractility of Triton X-100 skinned rabbit psoas, soleus, and cardiac papillary muscle fibers at a constant pH of 7, and 22°C. Solutions were formulated according to programs which solve the set of simultaneous equations describing the multiple equilibria of ions in the solutions. All solutions contained (mM): 5 EGTA, 20 imidazole, 2  $\text{Mg}^{2+}$ , 5  $\text{MgATP}$ , 15 phosphocreatine, with 100 u/ml CPK and K salts of L(+) or D-lactate or propionate, as needed. Solutions had an ionic strength of 200 mM (KMeSO<sub>3</sub> added). L(+) lactate, in and of itself, exerted a biphasic influence on the maximal calcium activated force ( $F_{\text{max}}$ ) of all muscles: the greatest inhibitory effects on  $F_{\text{max}}$  occurred at moderate physiological levels (10 - 20 mM), psoas muscle being most inhibited (9.25%), soleus less so (4.4%), with papillary muscle being least inhibited (3.4%). In all cases,  $F_{\text{max}}$  returned to near control levels as L(+) lactate was increased to its maximal physiological level (30 mM), and was not significantly different from control at 50 mM. The L(+) lactate effect was specific, as substitution of D-lactate or propionate resulted in no significant effects. At 25 mM L(+) lactate, the slope (Hill coefficient) of the force vs. pCa relationship of the contractile apparatus of psoas fibers is decreased with no change in the  $\text{Ca}_{50}$ . L(+) lactate had no effect on the force vs. pCa relationship of either soleus or cardiac muscle.

## Tu-Pos180

EFFECTS ON UNLOADED SHORTENING VELOCITY DUE TO ADDED ADP IN CALCIUM-ACTIVATED SINGLE PSOAS SKELETAL MUSCLE FIBERS ((Joseph M. Metzger)) Department of Physiology, University of Michigan, Ann Arbor, MI 48109.

The influence of increased concentration of ADP upon unloaded velocity of shortening was examined in rabbit psoas skinned single skeletal muscle fibers. Maximum velocity of unloaded shortening was determined by the slack-test method. In psoas fibers activated at maximal  $\text{Ca}^{2+}$  (solutions: in mmol  $\text{l}^{-1}$ , EGTA, 7; free  $\text{Mg}^{2+}$ , 1;  $\text{MgATP}$ , 4; creatine phosphate, 14.5; imidazole, 20; ionic strength of 180 mmol  $\text{l}^{-1}$ , pH 7.00, experimental temperature 15°C, ADP zero or 5 mM added + 100  $\mu\text{M}$  AP5A) plots of slack length versus duration of unloaded shortening were well fit a single straight line. However, in the presence of 5 mM added ADP slack-test plots were biphasic consisting of an initial high velocity phase of shortening followed by a low velocity phase of shortening which was typically initiated after 70 nm/half sarcomere of high velocity shortening. In psoas fibers activated at submaximal concentrations of  $\text{Ca}^{2+}$  in the absence of added ADP, biphasic slack-test plots were apparent as reported previously. Interestingly, at submaximal  $\text{Ca}^{2+}$  in the presence of 5 mM added ADP, both the high and low velocity phases of shortening were reduced with respect to control velocities despite the fact that relative tension values were greater with ADP due to the effect of ADP to shift the tension-pCa relationship to the left. The length dependent decrease in velocity could result from an increase in internal load due to cross-bridges which bear a compressive or negative load that would hinder rates of filament sliding. These results are consistent with the hypothesis that added ADP may increase the population of cross-bridges which bear a compressive load thus reducing rates of shortening.

## Tu-Pos181

TROPONIN I ISOFORM SWITCHING IN EMBRYONIC STEM CELL-DERIVED CARDIOMYOCYTES FOLLOWS THE MAMMALIAN CARDIAC DEVELOPMENTAL PROGRAM. ((M.V. Westfall, L.C. Samuelson and J.M. Metzger)) Dept. of Physiology, University of Michigan, Ann Arbor, MI 48108.

We examined whether embryonic stem (ES) cell-derived cardiomyocytes display the developmentally regulated transition in troponin I (TnI) isoform switching observed in mammalian cardiac development. Pluripotent ES cells derived from preimplantation mouse blastocysts were differentiated *in vitro*. Aggregates of differentiating ES cells were plated onto gelatin-coated coverslips and then cultured for up to 30 days. Distinct foci of contracting myocytes were monitored regularly during the culture period. In these contracting areas, TnI isoform expression was examined using indirect immunocytochemistry. In our initial experiments, we compared cardiac specific (Tl-1) anti-TnI antibody (Ab) immunostaining to the immunoreactivity of an Ab which recognized all muscle related TnI isoforms (Tl-4) in ES cultures of comparable age. A second, polyclonal Ab to myosin light chain-2 was used to confirm that TnI-stained cells were of muscle origin. The Tl-4 Ab stained ES-derived cardiomyocytes at the onset of contraction while cardiac TnI (cTnI)-specific staining was only detectable several days after the onset of contraction. We then used indirect immunofluorescence with dual monoclonal Abs and confirmed that cardiac-specific Tl-1 immunostaining lagged behind Tl-4 staining in the contracting myocytes. In addition, the area and intensity of Tl-4 staining was greater than Tl-1 staining within each contracting focus. Use of the dual monoclonal Ab approach on fetal (13-17 day p.c.) and adult mice confirmed that Tl-4 staining, which represents slow skeletal TnI (ssTnI) expression in fetal myocardium, preceded cardiac specific Tl-1 staining during murine cardiac development. These results indicate differentiation cultures of ES cells are a good model system to study the significance of developmental changes in myocardial contractile gene expression and function *in vitro*.

## Tu-Pos183

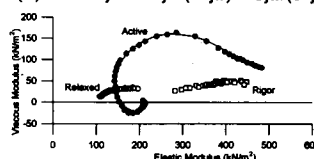
MICROTUBULE DEPOLYMERIZATION DOES NOT AFFECT THE INCREASED PASSIVE STIFFNESS OF SINGLE CARDIAC MYOCYTES FROM THE SPONTANEOUSLY HYPERTENSIVE RAT. ((R.E. Palmer and K.P. Roos)) Cardiovascular Research Lab., UCLA School of Medicine, Los Angeles, CA 90024-1760

Microtubules have been shown to alter the contractile function of cells from pressure overload feline myocardium (Tsutsui et al. *Science* 260:682, 1993), and may also play a role in the passive characteristics of the hypertrophied heart in which diastolic stiffness is increased. We determined the passive stiffness modulus-length relationships of single chemically skinned cells isolated from the left ventricle of Spontaneously Hypertensive Rats (SHR), a model of cardiac hypertrophy. Single cells were attached at each end using double-barreled micropipettes and the passive oscillatory stiffness determined (100 Hz). SHR (4-6 months old) cells demonstrated a greater passive stiffness modulus (range of s.l.  $1.9\mu\text{m}$  to  $>2.5\mu\text{m}$ ) than controls (Wistar-Kyoto). Thus, the increased diastolic stiffness of the SHR cells is in part due to an increased cellular passive stiffness independent of extracellular changes (e.g. collagen). This increased stiffness in the SHR was unaltered following the depolymerization of microtubules ( $10^{-6}$  M colchicine, 60 min). This indicates that in the SHR, the increased steady-state passive stiffness is not due to microtubular remodeling. Repeated stretch protocols indicated that at sarcomere lengths in the range of  $2.5\mu\text{m}$ - $2.8\mu\text{m}$  and beyond, irreversible damage occurs to the intracellular structures which produce passive force/stiffness. *Spdt. by HL-47065 (KPR) and AHA-GLAA (REP).*

## Tu-Pos185

CROSSBRIDGE REACTION SCHEME FOR HUMAN NON-FAILING LEFT VENTRICULAR MYOCARDIUM. ((D. Maughan<sup>1</sup>, L.A. Muller<sup>1</sup>, C. Hyatt<sup>1</sup>, G. Sleeper<sup>1</sup>, B.J. Leavitt<sup>2</sup>, P. Vaitkus<sup>3</sup>, M. Watkins<sup>3</sup>, N.R. Alpert<sup>1</sup> and M. LeWinter<sup>3</sup>))<sup>1</sup>Dept. of Molecular Physiology and Biophysics; Div. Surgery<sup>2</sup>; Div. Cardiology<sup>3</sup>, Univ. of Vermont, Burlington, VT 05405.

We investigated the effect of varying MgATP (0-10mM), MgADP (0-20mM) and Pi (0-30mM) concentrations on  $Y(\omega)$ , the complex stiffness of saponin-skinned muscle strips (BDM method) at 27°C (where  $\Delta L = 0.25\% L_0 \sin \omega$ ;  $\omega/2\pi = 0.5$ -100 Hz). In active strips (pCa 4.5)  $Y(\omega)$  was fitted by a frequency dependent viscous element A and two exponential processes B and C, where  $Y(\omega) = H + A/\omega^k + B/\omega/(b+\omega) + C/\omega/(c+\omega)$ . As a first approximation (with H=0) for the example shown, A, B and C were 209, -353 and 412 kNm<sup>-2</sup>; k was 0.11; b and c were 2.2 and 5.7 s<sup>-1</sup>. The Q<sub>10</sub>'s of k, b, and c were 1.04, 2.76, and 2.31, respectively. In relaxed (pCa 8) and rigor (no MgATP) states, A was 86 and 302 kNm<sup>-2</sup>; k was 0.13 and 0.06 (B and C absent); A may not be crossbridge related. At pCa 4.5, b and c increased with [MgATP] and [Pi] but decreased with [MgADP], consistent with a crossbridge reaction sequence in which MgADP competes with MgATP for the nucleotide binding site and Pi release follows force production (Saeki et al., *Circ. Res.* 68, 772-781, 1991). Supported by NIH AR40234 and PHS-P01-28001.



## Tu-Pos182

ADENOVIRUS MEDIATED GENE TRANSFER INTO CARDIAC MYOCYTES *IN VITRO* ((E.M. Rust, W.I. Lin, M.V. Westfall, L.C. Samuelson and J.M. Metzger)) Dept. of Physiology, Univ. of Mich., Ann Arbor, MI 48109 (spon. by J. Jacquetz)

We are using replication-deficient recombinant adenovirus as a vehicle for gene transfer into cardiac myocytes *in vitro*. In the first study, cardiac myocytes were derived from differentiating mouse embryonic stem (ES) cells *in vitro*. These myocytes spontaneously contract in culture and express cardiac specific markers. The differentiating ES cells were plated onto gelatin-coated coverslips and infected with an adenovirus construct containing the bacterial lacZ gene under the control of the CMV promoter (AdCMVlacZ). After 48 hours, expression of the lacZ reporter gene was determined by histochemical staining for  $\beta$ -galactosidase activity in the cultured cells. Troponin T expression was determined by indirect immunofluorescence using a monoclonal antibody against troponin T, thus permitting the identification of lacZ positive cells as myocytes. Results showed that adenovirus is an effective vehicle for gene delivery into the multiple cell lineages present in differentiating ES cell cultures, including the cardiac lineage. In a second study, primary cultures of ventricular myocytes (VMs) were established by isolation and collagenase digestion of the hearts of female Sprague-Dawley rats and plating of the cells on laminin coated plates. After 24hr in culture, the VMs were infected with AdCMVlacZ and stained for  $\beta$ -galactosidase activity 24-48 hr later. The plates were scored for total number of viable myocytes expressing lacZ. In this analysis, the viable ventricular myocytes showed increasing expression of lacZ with increasing dose of AdCMVlacZ, with approximately 90% of cells expressing at  $10^8$  PFU/ml. This indicates that efficient gene transfer and expression is obtained using recombinant adenovirus to infect isolated ventricular myocytes. A recombinant adenovirus is being constructed which will use the human cardiac  $\alpha$  actin promoter to direct expression of lacZ specifically to cardiac myocytes. This adenovirus vector will be useful for analysis of cardiac-specific gene expression in heterogeneous cell systems, including ES cell differentiation cultures.

## Tu-Pos184

DEPRESSED MYOCARDIAL CONTRACTION ASSOCIATED WITH A HEART DEFECT: POSSIBLE INVOLVEMENT OF MICROTUBULES. ((R.E. Godt, R.T.H. Fogaça, S.V. Zhelamsky, J.C. Chu, M.L. Kirby & T.M. Nosek.)) Dept. of Physiology & Endo.; Medical College of Georgia; Augusta, GA 30912

Ablation of cardiac neural crest cells at stage 9 produces structural heart defects in chick embryos (Kirby & Waldo, *Circ.* 82:332, 1990). We found that twitch force of isolated trabeculae from left ventricles of chicks at embryonic days (ED) 7 and 15 was reduced by about 50% in preparations from experimental hearts relative to that of trabeculae from sham-operated control chicks. When the membranes are removed with Triton X-100 detergent, we saw a similar two-fold difference in the maximum  $\text{Ca}^{2+}$ -activated force of trabeculae from experimental and control hearts. We have considered three possible mechanisms for the depression in isometric force: 1) Less contractile material: At ED 7 and 15 the content of myosin, actin and tropomyosin was similar in experimental and control hearts. 2) Disorganization of the myofibrils: Electron micrographs showed that sarcomere organization was normal in experimental hearts from ED 5 to 19. 3) Increased cytoskeletal content: Tsutsui et al. (*Science* 260:682, 1993) showed an association between elevated levels of microtubules and reduced isotonic shortening of myocytes from pressure-overloaded cat ventricle. We found that desmin and  $\alpha$ -actinin content are not different in experimental and control chick ventricle at ED 7, 11, or 15. At ED 7 and 11, total  $\beta$ -tubulin content is not different, whereas, at ED 15, total  $\beta$ -tubulin in experimental ventricles is twice that of control. When trabeculae are treated with Triton, microtubules depolymerize slowly (half-time ca. 1hr). This rate can be accelerated by treatment with colchicine or nocodazole. Using Triton-treated trabeculae, we are currently testing whether manipulation of the microtubular content affects isometric force. (Support: NIH HL36059).

## Tu-Pos186

KINETICS OF TENSION PRODUCTION OF SKINNED CARDIAC FIBERS OF NORMAL AND DISEASED HUMAN HEARTS (U. Zacharzowsky, P.E. Lange, M. Maier, R. Schwinger, H. Haase, and I. Morano) Max-Delbrück-Center for Molecular Medicine, Robert-Rössle-Straße 10, 13122 Berlin, Germany.

We investigated the half-times of tension development ( $t_{1/2}$ ) of Triton X-100-skinned fibers of normal and diseased human hearts from rigor after photochemical release of ATP from caged ATP at maximal  $\text{Ca}^{2+}$ -activation (pCa 4.5), 21°C, and pH 7. To avoid deterioration of fibers, contractions were initiated from low tension rigor (100mM BDM). Values are expressed as mean $\pm$ SEM with number of patients/fibers per patient in parenthesis. Tension produced upon photolysis of caged-ATP at pCa 4.5 was 98% of that obtained in activating solution (10mM ATP, pCa 4.5). Fibers of normal hearts (NH), dilated cardiomyopathy (DCM), ischaemic cardiomyopathy (ICM), Tetralogy of Fallot (TF), and hypertrophic obstructive cardiomyopathy (HOCM) revealed  $t_{1/2}$  of  $0.171\pm 0.020$ s (4/5),  $0.530\pm 0.048$ s (4/5),  $291\pm 0.048$ s (1/5),  $136\pm 0.016$ s (1/5), and  $0.286\pm 0.02$ s (1/5), respectively. Compared to NH,  $t_{1/2}$  of DCM ( $p<0.001$ ), ICM ( $p<0.05$ ), and HOCM ( $p<0.01$ ) were significantly elevated (student's T-test). Depletion of ADP by incubation with apyrase (30U/ml) had no influence on  $t_{1/2}$ .

## Tu-Pos187

**$\beta$ -ADRENERGIC AGONIST-INDUCED CHANGES IN CALCIUM SENSITIVITY OF TENSION AND MAXIMUM SHORTENING VELOCITY OF SKINNED CARDIAC MUSCLE INVOLVES PHOSPHORYLATION OF TNI BUT NOT C-PROTEIN.** ((K.T. Strang, K.S. McDonald and R.L. Moss)) Department of Physiology, University of Wisconsin, Madison, WI 53706

Isoproterenol treatment prior to skinning reduced the  $\text{Ca}^{2+}$  sensitivity of tension, increased maximum velocity of shortening ( $V_o$ ), and increased the phosphate content of both troponin I (TnI) and C-protein of skinned cardiac myocytes (Strang et al. *Circ Res* 1994;74:542), and these effects were mimicked by treatment with PKA. We used skinned slow-twitch skeletal muscle fibers from rat as a model system to test whether C-protein phosphorylation has an important role in mediating these changes. PKA treatment (45 min) of soleus fibers significantly increased C-protein phosphorylation while TnI phosphorylation was unaffected, allowing a test of the role of C-protein phosphorylation on functional properties of skinned fibers. PKA treatment significantly increased maximum tension generating capability (Control =  $91 \pm 20 \text{ kN/m}^2$ ; PKA =  $102 \pm 26 \text{ kN/m}^2$ , (n=6)  $p < 0.05$ ).  $\text{Ca}^{2+}$  sensitivity of tension, on the other hand, was unaltered by PKA treatment. Cumulative  $\text{pCa}_{50}$  (i.e., pCa for half-maximal tension) was 5.62 both before and after PKA treatment. Similarly,  $V_o$  was unaltered following 45 min PKA treatment.  $V_o$  was  $0.33 \pm 0.05$  and  $0.34 \pm 0.05$  fiber lengths/sec before and after treatment, respectively. These results suggest  $\beta$ -adrenergic-induced alterations in calcium sensitivity of tension and maximum shortening velocity of cardiac muscle are both mediated by TnI phosphorylation.

## Tu-Pos189

**HIGH DOSE D-PROPRANOLOL (D-PRO) ATTENUATES CONTRACTION OF EQUINE TRACHEALIS MUSCLE *IN VITRO*.** ((R.L. Wardle, Y. Jiang, J.D. Johnson and L.E. Olson)) The Ohio State University, Columbus, OH 43210. (Spon. by J.D. Strauss)

Isometric tension was measured in muscle strips at optimal length, 37 °C. Muscle strips were contracted with either  $10^{-5} \text{ M}$  acetylcholine (ACh),  $10^{-4} \text{ M}$  histamine (HIST), or 30 mM KCl, then treated with cumulative additions of D-PRO ( $10^{-5}$  to  $10^{-3} \text{ M}$ ). D-PRO completely relaxed ACh-, HIST-, and KCl-induced contractions with mean  $\pm$  SD  $\text{IC}_{50}$ 's  $121.2 \pm 26.4$ ,  $131.5 \pm 26.5$ , and  $138.7 \pm 28.2 \mu\text{M}$ , respectively. In other experiments, the Fura-2 fluorescence ratio ( $F_{340}/F_{380}$ ; index of myoplasmic free calcium ion concentration) and isometric tension were measured simultaneously in muscle strips at 37 °C. ACh ( $10^{-6} \text{ M}$ ) induced sustained increases in  $F_{340}/F_{380}$  and tension. Administration of D-PRO ( $\geq 10^{-4} \text{ M}$ ) to ACh-contracted muscles induced decreases in  $F_{340}/F_{380}$  (half-time for decrement,  $t_{1/2}$  15-30 sec) and tension ( $t_{1/2} > 60$  sec). Pretreatment with D-PRO attenuated ACh-induced increases in  $F_{340}/F_{380}$  and tension. We conclude that the membrane stabilizing effects of D-PRO attenuate calcium ion flux across the plasmalemma. These effects of D-PRO are not related to competitive antagonism of  $\beta$ -adrenergic receptor-mediated events.

## Tu-Pos191

**PHENYLEPHRINE INCREASES  $\text{Mn}^{2+}$  INFLUX AND  $[\text{Ca}^{2+}]_i$  BEYOND THAT EXPECTED BY DEPOLARIZATION IN RAT TAIL ARTERY.** ((Xiao-Liang Chen & Christopher M. Rembold)) Cardiovascular Div., Internal Medicine, University of Virginia, Charlottesville, VA 22908 USA

In patch clamped arterial smooth muscle cells,  $\alpha_1$  adrenergic stimulation increased a dihydropyridine sensitive  $\text{Ca}^{2+}$  current at a constant holding potential (Nelson et al. *Nature* 336:382). This finding led to the hypothesis that  $\alpha_1$  receptors cause arterial smooth muscle contraction by directly activating L-type  $\text{Ca}^{2+}$  channels independent of changes in membrane potential ( $E_m$ ). The goal of this study was to determine whether this mechanism occurred in intact arterial smooth muscle. We stimulated deendothelialized rat tail artery with phenylephrine or high  $[\text{K}^+]_o$ . We then measured  $E_m$  with microelectrodes,  $\text{Ca}^{2+}$  influx (estimated from the rate of Fura 2 quenching after addition of extracellular  $\text{Mn}^{2+}$ ),  $[\text{Ca}^{2+}]_i$  with Fura 2, and isometric force. In the presence of 2  $\mu\text{M}$  propranolol, 0.3  $\mu\text{M}$  phenylephrine (PE) and 30 mM  $[\text{K}^+]_o$  depolarized rat tail artery to a similar extent. PE (0.3  $\mu\text{M}$ ) increased  $\text{Mn}^{2+}$  influx,  $[\text{Ca}^{2+}]_i$ , and force to significantly higher levels than that observed with 30 mM  $[\text{K}^+]_o$ . This effect was not observed in the absence of propranolol. These data suggest that  $\alpha_1$  adrenergic stimulation activates  $\text{Ca}^{2+}$  entry into rat tail artery independent of  $E_m$  and this effect is inhibited by activation of  $\beta$  adrenergic receptors. We propose that  $\alpha_1$  adrenergic stimulation of rat tail artery activates  $\text{Ca}^{2+}$  channels, probably L type, which enhances contractility.

## Tu-Pos188

**REDUCTION OF MAXIMUM CALCIUM-ACTIVATED FORCE ( $F_{\text{max}}$ ) BY HYPOCHLOROUS ACID IN SKINNED DIAPHRAGM MUSCLE FIBERS.** ((L.A. Callahan, Z.W. She, W.B. Davis, R.C. Kolbeck, and T.M. Nosek)) Biophysics Research Group, Medical College of Georgia, Augusta, GA 30912.

Neutrophils are recruited to multiple capillary beds in sepsis and other inflammatory states. Once recruited, they undergo respiratory burst activity and produce reactive oxygen species, including the potent oxidant hypochlorous acid (HOCl). Does HOCl contribute to diaphragmatic fatigue characteristic of these states? We have investigated the effect of HOCl on  $F_{\text{max}}$  of single, Triton-skinned, rat diaphragm muscle fibers. Experimental procedures were similar to those published previously (Nosek et al., *Am.J.Physiol.* 259:C933, 1990). After determining control  $F_{\text{max}}$ , we performed three sequential exposures (each averaging 25 sec.) of the fibers to 10-100  $\mu\text{M}$  HOCl in a calcium-containing (pCa 5.2) solution that produced  $F_{\text{max}}$ . In another series of experiments, we performed three sequential exposures (25 sec.) of the fibers to 100  $\mu\text{M}$  HOCl when the fibers were relaxed (pCa 8.5). After each exposure, the fibers were contracted in pCa 5.2. When compared to control fibers,  $F_{\text{max}}$  was progressively reduced by the three exposures to 100  $\mu\text{M}$  HOCl.  $F_{\text{max}}$  was also reduced to a lesser extent by 20-50  $\mu\text{M}$  HOCl, but the inhibitory effect did not reach statistical significance until after the second or third exposures. Reduction in  $F_{\text{max}}$  was more pronounced if the fibers were exposed to HOCl in pCa 8.5, suggesting that the contractile proteins are more susceptible to injury from this oxidant in the resting state. We conclude that neutrophil production of HOCl may contribute to diaphragm fatigue by directly affecting the contractile apparatus. (Support: NIH AR 40598, American Lung Association)

## Tu-Pos190

**POSITIVE INOTROPIC AGENT EMD 53998 DECREASES CROSS-BRIDGE'S NUCLEOTIDE AND PHOSPHATE ASSOCIATION CONSTANTS IN SKINNED PORCINE MYOCARDIUM.** ((Yan Zhao and Masataka Kawai)) Dept. of Anatomy, University of Iowa, Iowa City, IA 52242, U.S.A.

Several studies have shown that inotropic agent EMD 53998 enhances contractility of myocardium by increasing the myofilament responsiveness to  $\text{Ca}^{2+}$  and by inhibiting the phosphodiesterase III activity. To further understand the mechanism of force enhancement by this inotropic agent, we studied the effect of EMD on elementary steps of the cross-bridge cycle. Since we used a skinned preparation and muscle fibers were activated at the maximal  $\text{Ca}^{2+}$  concentration (pCa 4.4), the effect of EMD on Ca load and PDE III inhibitory activity can be ignored. We studied the effect of MgATP on exponential process (C) and the effect of Pi on exponential process (B) with sinusoidal analysis in the presence of 50  $\mu\text{M}$  EMD 53998 and in its absence. Our results show that the isometric tension increases by 1.5 fold with 50  $\mu\text{M}$  EMD and saturates with a further increase in EMD. The rate constants and the equilibrium constants of cross-bridge detachment and attachment steps are not significantly affected by EMD, whereas the association constants of MgATP and Pi decrease 2 and 2.5 times, respectively. These results are consistent with tension enhancement with EMD, because the Pi release step is accelerated by EMD. The effect of EMD on the MgATP association constant does not affect isometric tension much, because the MgATP effect is already saturated under our activating condition (5 mM). We conclude that EMD increases the resistance to phosphate accumulation in myocardium.

## Tu-Pos192

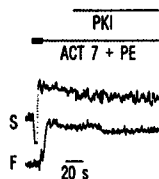
**THE EFFECTS OF ADRENALINE ON POTASSIUM CONTRACTURES IN SLOW SKELETAL MUSCLE FIBERS OF THE CHICKEN.** ((X. Trujillo\*, M. Huerta, L. Hernández\* and C. Vázquez\*)) Centro Universitario de Investigaciones Biomédicas, Universidad de Colima, Apdo. Postal 199, Colima, Colima, 28000 México.

The effects of adrenaline on  $\text{K}^+$  contractures of slow skeletal fibers of the chicken were investigated. Isometric tension was recorded from slow bundles of the anterior latissimus dorsi muscle of the chicken up to 3 weeks old. Normal solution was (mM): NaCl, 167; KCl, 5;  $\text{CaCl}_2$ , 5;  $\text{MgCl}_2$ , 2 and glucose 2 g/l. pH was adjusted to 7.4 with imidazole-hydrochloride. In all experiments, the muscles were curarized with 50  $\mu\text{M}$  d-tubocurarine. Adrenaline and isoprenaline were used. Experiments were performed at room temperature (20-22°C). The  $\text{K}^+$  contractures of slow fibers have a peak tension followed by a sustained tension. The peak tension of the  $\text{K}^+$  contracture (60 mM) was reduced by adrenaline and isoprenaline (10  $\mu\text{M}$ ),  $23 \pm 7\%$  (n=5) and  $21 \pm 8\%$  (n=3) respectively. This effect was reversible. The present results suggest that adrenaline modulates the tension in slow muscle fibers of the chicken.

## Tu-Pos193

**Mechanism for Agonist Induced Force Enhancement in Vascular Smooth Muscle Cells** ((Frank V. Brozovich)) *Depts. of Medicine (Cardiology) and Physiol. & Biophys., CWRU, Cleveland, OH, 44106.*

To determine if protein kinase C (PKC) is involved in the molecular mechanism of agonist induced force enhancement in smooth muscle, force and stiffness were measured in both  $\text{Ca}^{2+}$  and phenylephrine (PE) induced contractions of single  $\alpha$ -toxin permeabilized smooth muscle cells. Protein kinase C function was inhibited with the pseudosubstrate inhibitor (PKI) of PKC (residues 19-31). For  $\text{Ca}^{2+}$  activation ( $n=17$ ), PKI did not change ( $p>0.05$ ) steady state force or stiffness. For PE activation at  $p\text{Ca } 7$  ( $n=13$ ), PKI depressed force by  $28.7 \pm 4.5\%$  ( $p<0.05$ ) and stiffness by  $35.4 \pm 4.0\%$  ( $p<0.05$ ), and for PE activation at  $p\text{Ca } 4$  ( $n=7$ ), PKI depressed force by  $25.8 \pm 2.9\%$  ( $p<0.05$ ) and stiffness by  $35.6 \pm 5.6\%$  ( $p<0.05$ ). PKI's depression of force and stiffness were similar ( $p>0.05$ ), suggesting PKI decreased the number of attached cross-bridges.



These results suggest that agonist induced force enhancement in  $\alpha$ -toxin permeabilized smooth muscle is due to an activation of protein kinase C which results in an increase in the number of attached cross-bridges. Supported by the NIH, HL44181, and an AHA EI.

## Tu-Pos194

**METABOLISM OF INOSITOL (1,4,5)TRISPHOSPHATE DURING DEVELOPMENT OF RAT SKELETAL MUSCLE IN PRIMARY CULTURE.** ((M.A. Carrasco, P. Maramba and M. Fonseca)) *Dept. Fisiol. Biofis., Fac. Med., U. de Chile, Casilla 70005, Santiago, and C.E.C.S. (Spon. C. Hidalgo)*

We have studied the ontogenesis of the metabolic routes responsible for the formation and removal of  $\text{IP}_3$ , as well as the mass of  $\text{IP}_3$ , in rat skeletal muscle in primary culture. The biochemical assays were performed in homogenates obtained from both myoblasts and mature myotubes.

Phospholipase C activity determined with  $100 \mu\text{M}$  [ $^3\text{H}$ ]-PIP<sub>2</sub>, was already present in myoblasts with values comparable to those determined in myotubes (27 nmol/mg protein).  $\text{IP}_3$  5-phosphatase and  $\text{IP}_3$  3-kinase activities, determined with  $50 \text{ nM}$  [ $^3\text{H}$ ]- $\text{IP}_3$ , were 13 and  $1.9 \text{ pmol/mg protein}$  respectively in myoblasts, increasing to 45 and  $5.4 \text{ pmol/mg protein}$  in myotubes. Measurements of  $\text{IP}_3$  mass using a radioreceptor assay, gave similar values for both cells (50 to  $80 \text{ pmol/mg protein}$ ).

We found that  $0.1 \mu\text{M}$  calcitonin gene-related peptide (CGRP), which is present in the nerve terminal of the rodent neuromuscular junction, produced a 50 % decrease in the mass of  $\text{IP}_3$  in less than 1 min, returning to control values within 5 min. The study of the ontogenesis of  $\text{IP}_3$  metabolic machinery might constitute an approach to the study of the role of this messenger in skeletal muscle.

Supported by FONDECYT 1940538.

## Tu-Pos195

**INTRODUCTION OF ANTISENSE OLIGODEOXYNUCLEOTIDES INTO REVERSIBLY PERMEABILIZED SMOOTH MUSCLE.** ((R.E. Lesh, A.P. Somlyo, G.K. Owens, and A.V. Somlyo)) *Department of Molecular Physiology and Biological Physics, University of Virginia Health Sciences Center, Charlottesville, VA 22908.*

Antisense oligodeoxynucleotides (ODNs) are promising agents for experimental and therapeutic gene expression. However, the limited transmembrane permeability of antisense ODNs presents a major limitation to their utility. Reversible permeabilization, previously used to load smooth and cardiac muscle with the low molecular weight compounds aequorin and heparin (1,2), is an efficient method for introducing fluorescent ODNs into cells of the outer, longitudinal ileum smooth muscle. A 3'-FITC-labeled, antisense ODN (5'-AAGGGCCATTTTGT-FITC-3') was introduced into small ( $\sim 12 \text{ mm} \times 6 \text{ mm}$ ) sheets of the outer, longitudinal smooth muscle of rat ileum and maintained in organ culture for seven days. Confocal micrographs of these sheets revealed intense nuclear and less intense cytosolic fluorescence in most cells. Ileum sheets loaded with FITC-labeled antisense ODNs can be maintained in organ culture for seven days, with no discernible change in tension (produced by either membrane depolarization or agonist binding). Electron micrographs of organ cultured ileum (loaded with antisense ODNs by reversible permeabilization) showed a normal array of thin, thick and intermediate filaments and occasional electron-dense lysosomes. The cells retained predominantly nuclear fluorescence from introduced antisense ODNs over seven days. We conclude that reversible permeabilization is an efficient technique for introducing antisense ODNs into thin sheets of ileum smooth muscle, and that this tissue can be maintained in organ culture for seven days without apparent changes in structural or functional properties. However, while nuclear fluorescence due to labeled fluorescent ODNs persists through seven days in organ culture, the intracellular stability of the ODNs and the duration of their antisense effect remain to be determined and are currently under investigation. References: 1.) Morgan and Morgan, *J. Physiol. (London)* 351, pp. 155-167, 1984; 2.) Kobayashi, et al., *J. Biol. Chem.* 264(30), pp. 17997-18004, 1989.

## Tu-Pos196

**DIFFERENTIAL EXPRESSION OF MYOTONIN KINASE IN MUSCLE AND NON MUSCLE CELLS.** ((Salvatori, S., Biral, D., Furlan, S. and Marin, O.)) *CNR Unit for Biology and Physiopathology of Muscle and (\*) CRIBI Biotechnology Center, 35100- Padova, Italy. (Spon. by R. Sabbadini)*

Myotonic dystrophy (DM) is a disease affecting many organs and tissues. The molecular defect of this dominant inherited disease lies in the presence of multiple CTG repeat on the DNA of affected people. The gene product (myotonin) is assumed to be a protein kinase, based on the cDNA-deduced sequence. Among relevant symptoms, cardiomyopathy and myotonia have received particular attention, but Northern analysis has revealed that mRNA is produced at different level depending on the tissue. We raised antibodies against synthetic peptides chosen on the basis of a computer-aided analysis of the putative primary structure of myotonin. We used anti-myotonin antibodies to compare the protein expression in rabbit and rat tissues and to preliminarily characterize the skeletal and cardiac muscle isoforms, on a biochemical basis. Results showed that myotonin was revealed in kidney, cerebellum and testis, other than muscles, but not in liver and brain, and that, among skeletal muscles, type I fibers had 2-3 times more myotonin than type II fibers. Myotonin was mainly present in a membrane-bound form, but it was easily removed by  $\text{NH}_2\text{OH}$ -treatment at neutral pH, suggesting that myotonin is a peripheral, possibly acylated, protein. Work supported by "Telethon-Italy" (grant # 361 to S.S.).

SKELETAL SR  $\text{Ca}^{2+}$  RELEASE AND E-C COUPLING

## Tu-Pos197

**EFFECTS OF PROPOFOL ON  $\text{Ca}^{2+}$  REGULATION BY MALIGNANT HYPERTHERMIA-SUSCEPTIBLE MUSCLE MEMBRANES.** ((B.R. Fruen, J.R. Mickelson, and C.F. Louis)) *Department of Veterinary Pathobiology, University of Minnesota, St. Paul, MN 55108.*

The effects of the general anesthetic propofol on skeletal muscle  $\text{Ca}^{2+}$  regulation were investigated using terminal cisternae-derived membrane vesicles isolated from malignant hyperthermia-susceptible (MHS) and normal pigs. Propofol ( $10\text{-}500 \mu\text{M}$ ) had no effect on ryanodine receptor-mediated  $\text{Ca}^{2+}$  efflux from MHS or normal muscle membrane vesicles. Similarly, propofol ( $1\text{-}100 \mu\text{M}$ ) had no effect on membrane vesicle [ $^3\text{H}$ ]ryanodine binding, whereas higher concentrations ( $200\text{-}300 \mu\text{M}$ ) slightly inhibited [ $^3\text{H}$ ]ryanodine binding. Binding of the dihydropyridine receptor  $\text{Ca}^{2+}$  channel blocker [ $^3\text{H}$ ]PN200-110 to these preparations was significantly inhibited by propofol ( $10\text{-}300 \mu\text{M}$ ).  $\text{Ca}^{2+}$ -ATPase activity was stimulated by  $10\text{-}100 \mu\text{M}$  propofol and inhibited by higher concentrations. Together these results demonstrate effects of propofol on skeletal muscle  $\text{Ca}^{2+}$  regulation which are consistent with this agent's properties as a nontriggering anesthetic in the treatment of the MHS patient. In particular, the absence of a stimulatory effect of propofol on ryanodine receptor-mediated  $\text{Ca}^{2+}$  efflux and ryanodine binding contrasts with the stimulatory effects of MH-triggering inhalation anesthetics on ryanodine receptor channel activity described previously. The effects of propofol on dihydropyridine receptor and  $\text{Ca}^{2+}$ -ATPase function, however, are similar to the previously described effects of inhalation anesthetics on these membrane proteins. These results thus underscore the critical role of anesthetic interactions with ryanodine receptor  $\text{Ca}^{2+}$  channels in the pathogenesis of MH. Supported by NIH grant GM31382.

## Tu-Pos198

**INHIBITION OF SARCOPLASMIC RETICULUM (SR)  $\text{Ca}^{2+}$ -ATPase AFFECTS TWITCH FUSION SIMILARLY IN MALIGNANT HYPERTHERMIC (MH) AND NORMAL PORCINE SKELETAL MUSCLES.** ((N. Enzmann, E.M. Balog and E. M. Gallant.)) *Department of Veterinary Pathobiology, University of Minnesota, St. Paul, MN 55108.*

MH SR  $\text{Ca}^{2+}$  channels inactivate abnormally and MH resting [ $\text{Ca}^{2+}$ ], may be elevated, both of which might contribute to development of contractures. To determine whether the SR  $\text{Ca}^{2+}$ -ATPase can adequately reduce [ $\text{Ca}^{2+}$ ], in MH muscles or might contribute to contracture development, we compared twitch fusion frequencies of small bundles of intact MH and normal muscle cells. At  $36^\circ\text{C}$ , peak force of MH muscles was significantly elevated compared to normal muscles at stimulation frequencies of 5, 10 and 25 Hz, but not at higher frequencies (50 to 200 Hz). There was no significant difference in fusion frequency between MH and normal muscles. Slowing the SR  $\text{Ca}^{2+}$ -ATPase by cooling to  $26^\circ\text{C}$ , significantly increased the degree of fusion in both MH and normal muscles (e.g., at 5 Hz: MH =  $41 \pm 7\%$ , normal =  $21 \pm 8\%$  vs. 0% for both at  $36^\circ\text{C}$ ). Exposure of muscles to cyclopiazonic acid (CPA), which specifically blocks the SR  $\text{Ca}^{2+}$ -ATPase, also resulted in a significant enhancement of fusion in both muscle types at both 26 and  $36^\circ\text{C}$  (e.g., at 5 Hz,  $36^\circ\text{C}$ : MH =  $66 \pm 7\%$ , normal =  $42 \pm 9\%$ ). Thus, since treatments that slow the SR  $\text{Ca}^{2+}$ -ATPase activity affect both MH and normal muscles similarly, it is unlikely that the inability of the SR  $\text{Ca}^{2+}$ -ATPase to rapidly re-sequester  $\text{Ca}^{2+}$  contributes to the development of contractures in MH muscles. Our data are consistent with the defective SR  $\text{Ca}^{2+}$  release channel being primarily responsible for elevated [ $\text{Ca}^{2+}$ ], and contractures in MH muscles. Supported by NIH RO1AR41270.

## Tu-Pos199

**$\text{Mg}^{2+}$  REGULATION OF THE MALIGNANT HYPERTHERMIA-SUSCEPTIBLE (MHS)  $\text{Ca}^{2+}$  RELEASE CHANNEL.** (N. H. Shomer, B. Fruen, J. R. Mickelson, and C. F. Louis). University of MN, St. Paul, MN 55108.

We have demonstrated previously that the  $\text{Ca}^{2+}$  concentration that inhibits the sarcoplasmic reticulum (SR)  $\text{Ca}^{2+}$  release channel (CRC) single channel percent open time ( $P_o$ ) 50 % is significantly increased in MHS pigs, suggesting that the mutation affects the low-affinity inhibitory  $\text{Ca}^{2+}$  binding site. The sensitivity of MHS and normal CRCs to the inhibitory effects of the divalent cation  $\text{Mg}^{2+}$  has now been examined, as  $\text{Mg}^{2+}$  has been proposed to inhibit the channel by binding at the low-affinity  $\text{Ca}^{2+}$  inhibitory site. Single channel recordings of purified MHS ( $n=5$ ) and normal ( $n=5$ )  $\text{Ca}^{2+}$  release channels revealed that the addition of  $\text{Mg}^{2+}$  to the cis (cytoplasmic) side of the bilayer decreased the single channel percent open time of both MHS and normal channels, but that the half-inhibitory concentration (approx. 200  $\mu\text{M}$ ) was not significantly different for MHS and normal channels.  $\text{Mg}^{2+}$  inhibited  $^3\text{H}$ ryanodine binding to both MHS and normal SR; the half-inhibitory concentrations ( $292 \pm 95 \mu\text{M}$  and  $217 \pm 113 \mu\text{M}$ , for MHS and normal, respectively) were not significantly different. Thus, as the MH mutation affects the low affinity  $\text{Ca}^{2+}$  inhibitory site but not the  $\text{Mg}^{2+}$  inhibitory site, these two sites are likely different. Furthermore, in single channel studies the addition of millimolar cis  $\text{Ca}^{2+}$  partially reversed the channel inhibition by millimolar cis  $\text{Mg}^{2+}$ . In the presence of 5 mM  $\text{Mg}^{2+}$ , the optimal  $\text{Ca}^{2+}$  concentration for channel activation was approximately 4 mM, versus 10  $\mu\text{M}$  in the absence of  $\text{Mg}^{2+}$ . This suggests that  $\text{Mg}^{2+}$  was competing with  $\text{Ca}^{2+}$  for the CRC high-affinity  $\text{Ca}^{2+}$  activation site rather than acting in an additive fashion at the low-affinity inhibitory  $\text{Ca}^{2+}$  binding site. Supported by NIH grant GM-31382.

## Tu-Pos201

**SEPARATION OF THE AFFINITY EFFECTS FROM FUNCTIONAL EFFECTS AMONG SUBSTITUENT MODIFICATIONS ON RYANODINE.** (K.R. Bidaee, H.R. Besch, Jr. T. Wisler, M. Su, T. Vanvoort, S. Kwon and L. Ruest). Dept. of Pharmacol. and Toxicol., Indiana Univ. Sch. of Med., Indianapolis, IN 46202 and \*Department de Chemie, Université de Sherbrooke, Québec J1K 2R1. (Spon. by G. Nicol).

Our previous attempts to define a minimal pharmacophore that retains ryanodine (Ry) high affinity for the sarcoplasmic reticulum calcium release channel (SR-CRC) from rabbit skeletal muscles as well as its biphasic, channel modulating characteristics have focused primarily on derivatizing the  $\text{C}_{10}$  secondary hydroxyl of Ry and dehydroryanodine (DehyRy). The present study examines the effects of such  $\text{C}_{10}$ - $\text{O}_{\text{eq}}$  modifications on other natural and semi-synthetic ryanoids in attempts to identify whether those substituent groups on Ry crucial for the high affinity binding to the SR-CRC are responsible as well for channel activation and deactivation. Expansion of the five-membered pyrrole ring on the  $\text{C}_3$  substituent of Ry to a six-membered pyridine moiety as in 3-O-(pyridyl-3-carbonyl) ryanodol (RPC), significantly reduces this ryanoid's affinity for the SR-CRC ( $\text{IC}_{50} = 900\text{nM}$  for RPC as compared to 6.2nM for Ry). Interestingly, in calcium efflux assays, RPC activated the SR-CRC at concentration ranges similar to those of Ry ( $\text{EC}_{50\text{act}} = 3\mu\text{M}$ ), with an unexpected 6-fold rightward shift in the deactivation curve ( $\text{EC}_{50\text{deact}} = 1500\mu\text{M}$  for RPC as compared to 280 $\mu\text{M}$  for Ry). Esterification of the secondary hydroxyl at the  $\text{C}_{10}$  position of RPC with carbobenzyloxy- $\beta$ -alanine,  $\beta$ -alanine and guanidino-propionate, significantly enhances the affinity of these ryanoids for the SR-CRC ( $\text{IC}_{50} = 200\text{nM}$ , 25nM and 20nM, respectively), but produces little change in their ability to activate the SR-CRC. Like the same  $\text{C}_{10}$  derivatives of Ry and DehyRy, these compounds do not deactivate the SR-CRC. These data provide direct evidence that although the pyrrole-3-carbonyl substituent on the  $\text{C}_3$  carbon of Ry is very important for its high affinity binding to the SR-CRC, it plays a much lesser role in the channel modulating characteristics of ryanoids. Supported in part by the Showalter Trust.

## Tu-Pos203

**CALMODULIN ACTIVATION AND INHIBITION OF SKELETAL MUSCLE  $\text{Ca}^{2+}$  RELEASE CHANNEL.** (G. Meissner, A. Tripathy, L. Xu and G. Mann). Department of Biochemistry & Biophysics, University of North Carolina, Chapel Hill, NC 27599-7260.

The calmodulin binding properties and regulation by calmodulin of the rabbit skeletal muscle  $\text{Ca}^{2+}$  release channel were determined. [ $^{125}\text{I}$ ]Calmodulin and [ $^3\text{H}$ ]ryanodine binding to sarcoplasmic reticulum vesicles and purified  $\text{Ca}^{2+}$  release channel preparations indicated that the tetrameric  $\text{Ca}^{2+}$  release channel complex binds with high affinity (5 - 25 nM) maximally 4 calmodulins at  $\mu\text{M}$  [ $\text{Ca}^{2+}$ ] and 16 calmodulins at nM [ $\text{Ca}^{2+}$ ]. Calmodulin binding affinity to the channel was highest at pH 6.8 and 0.15 M KCl at both nM and  $\mu\text{M}$  [ $\text{Ca}^{2+}$ ]. SR vesicle -  $^{45}\text{Ca}^{2+}$  flux, single channel and [ $^3\text{H}$ ]ryanodine binding measurements showed that at nM [ $\text{Ca}^{2+}$ ] calmodulin activated the  $\text{Ca}^{2+}$  release channel 2 - 3-fold, whereas at  $\mu\text{M}$  [ $\text{Ca}^{2+}$ ] calmodulin inhibited the channel 3 - 5-fold. Hill coefficients of 1.0 - 1.3 suggested no or only weak cooperative inhibition of  $\text{Ca}^{2+}$  release channel activity by calmodulin. These results show that calmodulin both activates and inhibits the skeletal muscle  $\text{Ca}^{2+}$  release channel depending on  $\text{Ca}^{2+}$  concentration.

## Tu-Pos200

**CALCIUM-INFLUX METHOD FOR ASSESSING FUNCTIONAL EFFECTS OF RYANODINE IN THE LOW NANOMOLAR RANGE.** (H.R. Besch, Jr., K.R. Bidaee, and S. Kwon) Dept. of Pharmacol. and Toxicol., Indiana Univ. Sch. of Med., Indianapolis, IN 46202-5120.

In passive  $\text{Ca}^{2+}$  efflux assays, the sarcoplasmic reticulum calcium-release channels (SR-CRC) of rabbit skeletal muscle microsomes demonstrate dual responses to ryanodine (Ry) treatment (activation followed by deactivation). The concentrations of Ry necessary to effect activation and deactivation of the SR-CRC in this assay ( $\text{EC}_{50\text{a}} > \mu\text{M}$ ) are substantially higher than the  $\text{K}_d$  (low nM) revealed in displacement binding affinity assays. A major cause of this concentration disparity likely is that the apparent association rate of ryanodine is slowed in the high  $\text{Ca}^{2+}$  medium necessitated in  $\text{Ca}^{2+}$  efflux assays. An alternate means to assess the SR-CRC patency in SR vesicles was used herein. Junctional SR membrane vesicles (3.5mg/ml) were preincubated with 0.1-1000nM Ry in a 25 $\mu\text{M}$   $\text{Ca}^{2+}$  buffer for various times up to 180 min. The Ry-bound vesicles were then diluted 100-fold into a buffer containing 500 $\mu\text{M}$   $^{45}\text{Ca}^{2+}$ . Influx was stopped after 5 sec by diluting the vesicles 6-fold with a ice-cold stop solution (5mM  $\text{MgCl}_2$ , 580 $\mu\text{M}$   $\text{LaCl}_3$  and 10 $\mu\text{M}$  ruthenium red) and rapid filtration. The time course of the activation and deactivation effects was concentration-dependent. Ry at 0.1nM did not alter  $\text{Ca}^{2+}$  influx rate, even after a 3 hr preincubation. Ry at 1nM activated (opened) the SR-CRC maximally within 10 min. Thereafter apparent channel patency declined, returning to control value following a 3 hr preincubation. The onset of activation at higher Ry concentrations (5 to 25 nM) was similar to that at the lower concentration but the maximal opening achieved was diminished, and the duration of the increased patency was foreshortened by intervention of the deactivation effect. Concentrations of Ry greater than 25nM produced only deactivation of the SR-CRC, the extent of which showed time and concentration dependence. Thus, with this assay protocol the center of the ryanodine concentration-effect curve at steady state was super-imposable on that of the displacement binding affinity isotherm. These results show a good kinetic concordance between fractional ryanodine receptor occupancy and the functional modulation of the CRC in junctional SR vesicles. Supported in part by the Showalter Trust.

## Tu-Pos202

**NANOMOLAR DANTROLENE ACTIVATES SINGLE RYR1 CHANNELS AND POTENTIATES HALOTHANE AND CAFFEINE CONTRACTURE IN MAMMALIAN SKELETAL MUSCLE.** (T. Nelson, M. Lin and \*G. Suarez-Kurtz) Dept of Anesthesiology, Bowman Gray School of Medicine of Wake Forest University, Winston-Salem, NC and \*Dept of Biochemistry, Universidade Federal Do Rio De Janeiro

Dantrolene is a direct acting skeletal muscle relaxant and is efficacious for treatment of anesthetic-drug induced malignant hyperthermia (MH). We previously reported that dantrolene activates and then inactivates RYR1 calcium release channels (1). We now characterize the dantrolene concentration dependency for activation and inactivation of single RYR1 channels and demonstrate that nanomolar (nM) dantrolene can potentiate caffeine and halothane contractures in skeletal muscle. Single RYR1 channels incorporated from SR membrane vesicles into a planar lipid membrane were activated at nM concentrations of dantrolene. This activation is associated with 3 to 5-fold increases in  $P_o$  and in open state dwelltime. Increasing dantrolene concentration to the  $\mu\text{M}$  range reversed the activation and diminished channel activity to levels below control. In muscle biopsied from MH dogs, 20 nM dantrolene produced a contracture above that caused by halothane and in biopsied MH human muscle (1 subject) 20 nM dantrolene alone produced contracture. In single, skinned rat EDL muscle, 1-10 nM dantrolene potentiated and prolonged caffeine induced tensions and these effects were reversed by  $\mu\text{M}$  dantrolene. Together, these findings support two dantrolene binding sites for the RYR1. A high affinity binding site (nM) increases open state probability and dwell times and a low affinity ( $\mu\text{M}$ ) site inactivates the channel. Under pharmacologic and pathophysiologic conditions, dantrolene binding to the high affinity site can produce increased contracture, suggesting that [ $\text{Ca}^{2+}$ ] regulation is altered at the cellular level. The low affinity dantrolene binding site could represent the previously known muscle relaxant effects of dantrolene.

(1) Biophysical J 64:A380, 1993.

## Tu-Pos204

**FORMATION AND MATURATION OF PERIPHERAL COUPLINGS IN CHICK MYOCARDIUM.** (Feliciano Protasi, Xin-Hui Sun and Clara Franzini-Armstrong) Dept. Cell Dev. Biol., Un. PA. Philadelphia, PA 19104 (Spon. by Dr. J. W. Weisel)

Ryanodine receptors (RyRs), or SR calcium release channels, and dihydropyridine receptors (DHPRs), or surface membrane (SM) calcium channels, are co-clustered at junctions between SR and SM of cardiac muscle (peripheral couplings, PCs). We have studied the formation and maturation of PCs in chick myocardium in ovo (E2.5-E21) and after hatching (D1-D14), using electron microscopy to detect feet of the junctional SR (RyRs) and large particles (presumably DHPRs) of SM's junctional domains. PCs are present at E2.5, and their frequency along the fiber profiles increases 2.5 fold between E2.5 and E18. At E2.5 PCs are not fully formed, since arrays of feet are incomplete in 72% of the junctions. The arrays become gradually more complete and at E11 practically all SR vesicles are fully zippered to the surface membrane. Areas of feet arrays and of junctional domains increase in size by 1.7 fold between E4 and E14 and then remain constant to D1. The ratio between the two areas is approximately 1 throughout. The density of large particles in the junctional domains (1100-1400/ $\mu\text{m}^2$ ) does not significantly change through development. PCs are disposed fairly randomly at early stages, but acquire a preferred location at the Z line and immediately flanking it after hatching. This process of gradual alignment of junctional membranes with the striations is similar to that observed in skeletal muscle. We conclude that there are three stages in the formation and maturation of cardiac PCs. Stage 1: coupling of SR to the surface; stage 2: formation of arrays of feet and correspondent grouping of surface membrane particles; stage 3: acquisition of an ordered location of PCs relative to the striation.

## Tu-Pos205

**REGULATION AND MAPPING OF THE SKELETAL MUSCLE RYANODINE RECEPTOR BY A 2', 3'-DIALDEHYDE ATP ANALOGUE** (M. Hohenegger\*, A. Herrmann-Frank\*, and F. Lehmann-Horn\*)\* Inst. of Pharmacology, University Vienna, A-1090 Wien, Austria, and \*Inst. of Applied Physiology, University Ulm, D-89069 Ulm, Germany (Spon. by M. Hohenegger)

The contraction of skeletal muscle is triggered by the rapid release of calcium from sarcoplasmic reticulum (SR) via the ryanodine receptor calcium release channel. ATP is known to regulate the ryanodine receptor by direct binding. In order to further investigate the adenine nucleotide binding site the oxidized ATP analog, 2', 3'-dialdehyde adenosine triphosphate (oATP) was synthesized. oATP is found to induce calcium release from passively loaded heavy SR from skeletal muscle in a biphasic manner. The half-times of the first phase is in the range of 100-200 ms, whereas the second phase is much slower ( $t_{1/2}$  2-10 sec). The  $\text{EC}_{50}$  for oATP calculated from rates of the first calcium release phase is about 160-200  $\mu\text{M}$ . The initial phase of the oATP-induced calcium release was specifically inhibited by  $\text{Mg}^{2+}$  and ruthenium red. Therefore oATP can be directed to interact specifically with the ryanodine receptor. This hypothesis was confirmed by single channel recordings of the purified ryanodine receptor. Addition of oATP to the *cis*-compartment activated a calcium current with an affinity ( $\text{EC}_{50}$  76  $\mu\text{M}$ ) roughly 30-fold higher than for ATP. A Hill coefficient of about 2, obtained from calcium release experiments and single channel recordings, indicates a positive cooperativity between the adenine nucleotide binding site(s) of the subunits of the tetrameric protein. The oATP-preactivated ryanodine receptor is able to display a typical subconductance state following the addition of ryanodine. Increasing concentrations of ryanodine and millimolar concentrations of magnesium inhibit oATP-stimulated channel activity. The ribosyl aldehyde groups of oATP form a Schiff's base with the  $\epsilon$ -amino group of lysine sidechains within the binding pocket. The specificity of the  $[\alpha\text{-}^{32}\text{P}]\text{oATP}$  binding confirms the incorporation of the ligand into the ATP-binding pocket of the purified ryanodine receptor of skeletal muscle and introduces this nucleotide analogue as a useful tool for functional and structural investigations.

## Tu-Pos207

**INHIBITION OF THAPSIGARGIN EVOKED  $\text{Ca}^{2+}$  TRANSIENTS IN BC3H1 CELLS AND SKELETAL SARCOPLASMIC RETICULUM.** (Matthew M. Mack, Tadeusz F. Molinski\*, Treva D. Mcloy and Isaac N. Pessah) Department of Molecular Biosciences, School of Veterinary Medicine and \*Department of Chemistry University of California Davis, CA 95616.

The sesquiterpene lactone, thapsigargin, induces rapid  $\text{Ca}^{2+}$  mobilization in BC3H1 cells and rabbit skeletal sarcoplasmic reticulum. Bestadins, isolated from the marine sponge *Ianthella basta*, interact with the RyR associated protein, FKBP12, to stabilize the high affinity ryanodine conformation. Under myoplasmic ionic conditions, bestadin 5 enhances high affinity ( $K_D$  1-4nM) [ $^3\text{H}$ ]ryanodine binding to SR membranes (1.6 and 14pmole/mg for control and 10 $\mu\text{M}$  bestadin 5, respectively). The effects of bestadins on thapsigargin-induced  $\text{Ca}^{2+}$  release in differentiated BC3H1 cells were assessed using Fura-2,AM and fluorescence ratio photometry. Rapid mobilization of SR  $\text{Ca}^{2+}$  stores is induced by 200 $\mu\text{M}$  ryanodine (Ry), 20mM caffeine and 200nM thapsigargin. The response to ryanodine, but not thapsigargin, is prevented by prior treatment of cells with 500 $\mu\text{M}$  ryanodine. The thapsigargin effect is blocked by addition of a combination of bestadins and 200 $\mu\text{M}$  ryanodine. Thapsigargin induced  $\text{Ca}^{2+}$  release from SR microsomes is insensitive to ryanodine (500 $\mu\text{M}$ ), bestadin 5 (10 $\mu\text{M}$ ) or ruthenium red (1 $\mu\text{M}$ ) alone. However, the combination of bestadin 5 (2-10  $\mu\text{M}$ ) and ryanodine (200 $\mu\text{M}$ ) or ruthenium red (RR) (1 $\mu\text{M}$ ) inhibits the effects of thapsigargin. RyR-1 blockers (200 $\mu\text{M}$  Ry or 1 $\mu\text{M}$  RR) or bestadin 5 alone do not alter the  $\text{Ca}^{2+}$  capacity of SR vesicles. However, bestadin 5 (10 $\mu\text{M}$ ) in the presence of RR (1 $\mu\text{M}$ ) or Ry (500 $\mu\text{M}$ ) significantly enhances the capacity of SR vesicles. This is the first report regarding the modulation of passive sarcoplasmic  $\text{Ca}^{2+}$  efflux pathways in cells and suggests that a conformation of the FKBP12/RyR-1 channel complex may be responsible for the SR  $\text{Ca}^{2+}$  leak unmasked by ATPase inhibition.

## Tu-Pos209

**A COMPONENT OF  $\text{Ca}^{2+}$ -INDUCED  $\text{Ca}^{2+}$  RELEASE NOT MEDIATED BY RYANODINE RECEPTORS IN RABBIT SKELETAL MUSCLE SARCOPLASMIC RETICULUM.** (M. Sukhareva and R. Coronado) Dept. of Physiology, Univ. of Wisconsin, Madison, WI 53706.

We previously showed that rabbit skeletal muscle junctional SR equilibrated in Choline-Cl is effectively devoid of ryanodine receptor mediated  $\text{Ca}^{2+}$  fluxes. (BJ 67:751, 94). Here we investigated whether  $\text{Ca}^{2+}$ -induced  $\text{Ca}^{2+}$  release (CICR) was detectable in SR loaded with Choline-Cl. SR was passively equilibrated with 5 mM  $^{45}\text{Ca}^{2+}$  plus 150 mM K-Gluconate and separately with 150 mM Choline-Cl. After dilution of the extravesicular  $\text{Ca}^{2+}$ , the SR was exposed to a  $\text{Ca}^{2+}$ -releasing solution delivered by rapid filtration. We performed jumps of extravesicular free  $\text{Ca}^{2+}$  to 1) pCa 8, 5 mM total ATP, 0.8 mM free  $\text{Mg}^{2+}$  and to 2) pCa 6, 5 mM total ATP, 0.8 mM free  $\text{Mg}^{2+}$ . CICR was defined as the excess of release in solution 2) relative to 1). CICR of approximately the same magnitude was observed in the  $\text{Cl}^-$ -free and  $\text{Cl}^-$ -containing SR. However, procaine (10 mM) blocked ~60% of the CICR in SR equilibrated in K-Gluconate but no more than ~30% of the CICR in SR equilibrated in Choline-Cl. The presence of a large procaine-insensitive component of CICR in SR loaded with Choline-Cl suggested that this flux was probably not mediated by ryanodine receptors but presumably, by the SR channel permeable to  $\text{Ca}^{2+}$  and  $\text{Cl}^-$  described recently (ref. above). Thus, two separate CICR pathways may be present in skeletal muscle SR, ryanodine receptors and  $\text{Cl}^-/\text{Ca}^{2+}$  channels (Supported by NIH, MDA and AHA).

## Tu-Pos206

**MODULATION OF  $\text{Ca}^{2+}$  FLUX OF SARCOPLASMIC RETICULUM (SR) BY PROTEIN KINASES (PK) / PHOSPHATASES (PPT)** ((M. Mayreiter\*, R.E. Chandler\*, H. Schindler\* and Sidney Fleischer\*)) Dept. of Mol. Biol., Vanderbilt University, Nashville, TN; \*Institute for Biophysics, University of Linz, Austria

We previously found that ryanodine receptor (RyR) channel activity can be made insensitive to block by  $\text{Mg}^{2+}$  when treated with PKA or  $\text{Ca}^{2+}$ /calmodulin dependent protein kinase type II (CamPK II) and again made sensitive by treatment with PPT (Biophys. J. 67: Nov. 1994, in press). The effect of PK and PPT on net  $\text{Ca}^{2+}$  loading rate (CLR) by SR is now presented. Phosphorylation of terminal cisternae (TC) SR vesicles with PKA, CamPK II, or PKC reduced the CLR 3-fold, 2.1-fold and 1.7-fold, resp. There is no effect when AMP-PNP is substituted for ATP. Phosphorylation of the RyR was also measured by incorporation of  $^{32}\text{P}$ . A ( $^{32}\text{P}$ /RyR) stoichiometry of  $1.94 \pm 0.1$  for PKA,  $0.89 \pm 0.08$  for CamPK II and  $0.95 \pm 0.16$  for PKC was obtained under these conditions. The effect on CLR was blocked in the presence of PK inhibitors, using a mixture of H7, H89 and PKI as PKA inhibitor, the CamPK II peptide (281-309) as CamPK II inhibitor, and Calphostin C as PKC inhibitor. PPT1 enhances the CLR again after it is reduced by PKA. Even at higher [ $\text{Mg}^{2+}$ ] (6mM), PKA phosphorylated TC vesicles have a 2.3-fold reduced CLR indicating insensitivity to block by  $\text{Mg}^{2+}$ . PK's have no effect on  $\text{Ca}^{2+}$  ATPase activity in TC, or on CLR in longitudinal tubules of SR which are devoid of RyR. We interpret the decreased net CLR as being due to enhanced  $\text{Ca}^{2+}$  leakage via the RyR. These studies show at a macroscopic level that the RyR is modulated by PK / PPT. (NIH HL32711 and FWF S45/03 and 07).

## Tu-Pos208

**CHLORIDE-INDUCED  $\text{Ca}^{2+}$  RELEASE FROM SARCOPLASMIC RETICULUM IN GLYCERINATED PSOAS FIBERS.** (J.R. Patel, M. Sukhareva, R. Coronado, and R.L. Moss) Department of Physiology, Univ. of Wisconsin, Madison, WI 53706.

In mechanically skinned skeletal fibers, chloride ( $\text{Cl}^-$ ) elicited tension transients are thought to be exclusively due to T-Tubule depolarization mediated  $\text{Ca}^{2+}$  release from the sarcoplasmic reticulum (SR). We have examined the ability of  $\text{Cl}^-$  to directly induce  $\text{Ca}^{2+}$  release from the SR using glycerinated psos fibers and isolated heavy SR vesicles, preparations which are believed to have fewer functional T-tubule-SR junctions.  $\text{Ca}^{2+}$  release from SR in glycerinated fibers and SR vesicles was evaluated by amplitude and integrated area of tension transients and by fast filtration of  $^{45}\text{Ca}^{2+}$ , respectively. In both preparations, saponin had no significant effect on  $\text{Ca}^{2+}$  efflux from SR. This suggests that the  $\text{Cl}^-$  elicited tension transients and  $\text{Cl}^-$ -induced  $\text{Ca}^{2+}$  efflux from isolated SR vesicles were due to a direct activation of a  $\text{Ca}^{2+}$  release pathway in the SR membrane. In both preparations,  $\text{Ca}^{2+}$  release from the SR was initiated by 75 mM  $\text{Cl}^-$  and was maximum at 191 mM. The integrated area of the tension transient elicited by (caffeine +  $\text{Cl}^-$ ) was twice that elicited by (caffeine + propionate). Procaine totally blocked (caffeine + propionate) elicited tension transients and blocked only the caffeine component of the (caffeine +  $\text{Cl}^-$ ) elicited tension transients. These results suggest that  $\text{Cl}^-$  directly increases the  $\text{Ca}^{2+}$  permeability of the SR, probably by activating SR channels other than ryanodine sensitive  $\text{Ca}^{2+}$  release channels.

## Tu-Pos210

**MEASUREMENT OF SARCOPLASMIC RETICULUM CALCIUM- AND VOLTAGE-GATED CALCIUM RELEASE IN SLOW TWITCH RAT MUSCLE FIBERS.** (Osvaldo Delbono and Gerhard Meissner\*). Bowman Gray School of Medicine, Wake Forest University, Dept. of Physiology and Internal Medicine, NC. 27157. \*Dept. of Biochemistry & Biophysics, University of North Carolina, Chapel Hill, NC. 27599.

The same isoform of RYR (type-1) is expressed in both fast and slow mammalian skeletal muscles. However, differences in contractile activation and calcium release kinetics in skinned fibers have been reported (Salviati *et al.*, Am. J. Physiol. 254: C459, 1988). In this work, intracellular calcium transients were measured in soleus and extensor digitorum longus (EDL) single muscle fibers using mag-fura-2 ( $K_D = 49 \mu\text{M}$ ) as calcium fluorescent indicator. Fibers were voltage-clamped at  $V_h = -90 \text{ mV}$ , as described previously (Delbono *et al.*, J. Physiol. 463: 689, 1993). Sarcoplasmic reticulum calcium release was measured at the peak (a) and at 100 ms in 200 ms pulses (b) at +10 mV. Values at a and b corresponded to calcium-gated and voltage-gated calcium release, respectively (Jaquemond *et al.*, 1991). Ratios (b/a) in soleus fibers were  $0.29 \pm 0.03$  ( $n=12$ ). This result suggested that the proportion of dihydropyridine receptor (DHPR)-linked and -unlinked ryanodine receptors (RYR) is different in soleus and EDL muscle. The number of DHPR and RYR were determined by measuring high-affinity [ $^3\text{H}$ ]PN200-110 and [ $^3\text{H}$ ]ryanodine binding in soleus and EDL rat muscle homogenates (Anderson *et al.* Am. J. Physiol. 266:C462, 1994). The  $B_{\text{max}}$  values corresponded to a PN200-110/ryanodine binding ratio of  $0.33 \pm 0.13$  ( $n=6$ ) and  $0.84 \pm 0.26$  ( $n=6$ ) for soleus and EDL muscles, respectively. Thus, soleus muscle has a larger calcium-gated calcium release component and a larger proportion of unlinked RYR.



## Tu-Pos211

**A CALCIUM SYNAPSE MODEL OF CONTROL OF  $\text{Ca}$  RELEASE IN SKELETAL MUSCLE.** ((E. Ríos & G. Pizarro\*)) Rush Univ., Chicago, IL 60612, and \*Univ. de la República, Montevideo, Uruguay.

Some evidence, both anatomical (Block et al, J.C.B. 1988) and functional (Jacquemon et al., Biophys.J. 1991; Ríos and Pizarro, Biophys.J. 1994; Anderson and Meissner, Biophys.J. 1993), suggests a role for  $\text{Ca}^{2+}$ -induced  $\text{Ca}^{2+}$  release (CICR) in excitation-contraction coupling (ECC) of skeletal muscle. CICR, however, is intrinsically self-reinforcing, while release is graded with voltage, and can be stopped by repolarization at all times. Stern (Biophys.J. 1993) proposed local control by  $\text{Ca}^{2+}$  in the vicinity of the pore mouth as a way to circumvent this problem in heart. We have compared with experimental results a model of ECC in skeletal muscle that uses the same idea. Two types of release channels, one gated by the voltage (V) sensors and the other  $\text{Ca}^{2+}$ -gated (Ríos and Pizarro, NIPS, 1988), are arranged in pairs (Stern's calcium synapse). The V-gated channel contributes a steady release (does not inactivate), the  $\text{Ca}^{2+}$ -gated channel is activated and inactivated by  $\text{Ca}^{2+}$ , binding on two sites. These sites face a local  $[\text{Ca}^{2+}]$  resulting from additive contributions of the V-gated and  $\text{Ca}^{2+}$ -gated channels in the presence of diffusion and removal. The model robustly generated: 1) release flux finely graded with clamp pulse voltage; 2) realistic kinetics of release activation and inactivation at all voltages; 3) large ratio of peak to steady levels of release, which corresponds to the model's "gain" (ratio of CICR to V-gated release); 4) fast termination of release at the break of the clamp pulse, at all times. Supported by NIH and CONICYT (Uruguay).

## Tu-Pos213

**HALOTHANE-INDUCED  $\text{Ca}^{2+}$  RELEASE FROM THE SR IN SAPONIN-SKINNED ARTERIAL RINGS.** ((J. Y. Su, and L. J. Tang)) Dept. of Anesthesiology, Univ. of Wash., Seattle, WA 98195.

Halothane has been shown to enhance caffeine-induced tension transients in saponin-treated arterial strips as a function of halothane concentration. This study was performed to test the hypothesis that halothane directly releases  $\text{Ca}^{2+}$  from the SR resulting in increases in caffeine-induced tension transients. Muscle rings (approx. 200  $\mu\text{m}$  thick, 1 mm wide) from adult rabbit femoral arteries (FA) were mounted on two hooks and skinned with saponin. The skinned rings were cycled through solutions to load  $\text{Ca}^{2+}$  into and release  $\text{Ca}^{2+}$  from the SR using 10 mM caffeine, various concentrations of halothane, or combined caffeine and halothane. Steady-state levels of  $\text{Ca}^{2+}$  released by these activators were measured with the fluorescent  $\text{Ca}^{2+}$  indicator fura-2 and calculated from the calcium standard curve (Calcium Calibration Buffer, Molecular Probes). The results [mean $\pm$ SEM (n) in nM  $\text{Ca}^{2+}$ ] showed that caffeine released 101.6 $\pm$ 8.4(20), and halothane (0.5%, 1% & 2%) directly released 83.4 $\pm$ 7.7(17), 71.8 $\pm$ 4.8(20), 65.6 $\pm$ 6.0(19), respectively. However, the amount of  $\text{Ca}^{2+}$  released was not increased by the combination of caffeine and halothane; in contrast, it was decreased at 2% halothane [103.3 $\pm$ 8.3(12), 95.0 $\pm$ 9.1(12), 66.2 $\pm$ 9.6(12) for 0.5%, 1%, and 2% halothane, respectively]. In conclusion, halothane causes  $\text{Ca}^{2+}$  release from the SR which reaches a maximum at 0.5%. However, the absence of enhancement of this halothane-induced  $\text{Ca}^{2+}$  release by caffeine, in contrast to that of tension measurements, suggests a direct activation of the contractile proteins by halothane. (Supported by NIH GM48243)

## Tu-Pos215

**ELECTRICAL AND MECHANICAL EFFECTS OF TETRACAIN ON INTACT CRUSTACEAN SKELETAL MUSCLE FIBERS.** ((J. Monterrubio, L. Lizardi and C. Zuazaga)) Inst. of Neurobiology, U. of Puerto Rico Med. Sci. Campus, San Juan, PR 00901

We examined the effects of tetracaine (0.3 mM) on muscle fibers of the crustacean *Atya lanipes*. Mechanical activation in these tonic fibers is dependent on  $[\text{Ca}^{2+}]$ , even though they do not generate action potentials (Lizardi et al. J. Membr. Biol. 129: 167, 1992; Bonilla et al. Tissue & Cell 24: 525, 1992). Tetracaine initially (1-5 min) suppressed the tension generated by directly injected current pulses. Action potentials whose amplitude increased with time of exposure, stabilizing in 20-40 min, then appeared; tension increased and was directly correlated to  $\dot{V}_{max}$  during this time. Three-microelectrode voltage clamp measurements showed that the current induced by tetracaine exposure is carried by  $\text{Ca}^{2+}$ . Tetracaine blocked caffeine (4mM)-induced contractures, indicating that it suppresses SR  $\text{Ca}^{2+}$  release. The effect of tetracaine on electrical excitation was mimicked by intracellular injections of BAPTA. We conclude that: a) under control conditions, most of the  $\text{Ca}^{2+}$  channels are inactivated at rest and a small influx of  $\text{Ca}^{2+}$  triggers the release of  $\text{Ca}^{2+}$  from the SR, the latter providing a very large amplification mechanism for the increase in  $[\text{Ca}^{2+}]$  required for contraction; b) suppression of SR  $\text{Ca}^{2+}$  release by tetracaine results in the reduction of  $[\text{Ca}^{2+}]$  to levels low enough for electrical excitation to occur and  $\text{Ca}^{2+}$  entry directly triggers contraction. (Supported by NIH grants NS07464 and RR03051).

## Tu-Pos212

**SPHINGOSYLPHOSPHORYLCHOLINE MODULATES CALCIUM RELEASE FROM CARDIAC SARCOPLASMIC RETICULUM RYANODINE RECEPTOR.** ((R. Betto, G. Salvati, R. Sabbadini, P. McDonough, C. Giemotaki, C. Dettbarn, K. Yasui, P. Palade)) C.N.R. Unit for Muscle Biology and Physiopathology, Italy. Dept. Biology, San Diego State University, San Diego. Dept. Physiology & Biophysics, Univ. Texas Medical Branch at Galveston, Galveston, TX. (Spon. by G. Salvati)

Sphingosylphosphorylcholine (SPC) modulates calcium release from cardiac sarcoplasmic reticulum membranes. 20  $\mu\text{M}$  SPC induces the release of 50% of total calcium accumulated. SPC releases calcium from cardiac sarcoplasmic reticulum through the ryanodine receptor since the release is inhibited by 4  $\mu\text{M}$  ruthenium red and 20  $\mu\text{M}$  sphingosine, two ryanodine receptor blockers. Furthermore, the release is not blocked by flunarizine and cinnarizine, inhibitors of inositol 1,4,5-trisphosphate and arachidonic acid induced calcium releases. SPC-induced calcium release is observed both in isolated microsomes and in intact cardiac myocytes. Whole cell patch clamping demonstrates that the effect on cardiac myocytes does not involve the L-channel conductance. SPC action on the ryanodine receptor is calcium dependent. SPC shifts to the left the bell-shaped curve of the calcium dependent  $[\text{PH}]\text{ryanodine}$  binding, but only at high pCa values, suggesting that SPC might increase the sensitivity to calcium of the calcium-induced calcium release mechanism. We conclude that SPC releases calcium from cardiac sarcoplasmic reticulum membranes by activating the ryanodine receptor. Supported by the Telethon Italy (grant #469), CNR, MDA, AHA, NIH, FATMA, and Ministero Pubblica Istruzione.

## Tu-Pos214

**DIFFERENTIAL MODULATION OF  $[\text{Ca}^{2+}]$  IN NORMAL AND MUTANT MYOTUBES BY CAFFEINE.** ((D.S. Lake, L.S. Cheng, L.J. Zoclein, E.M. Gallant, and S.R. Taylor)) Department of Pharmacology, Mayo Foundation, Rochester, MN, 55905 and Department of Veterinary Pathobiology, University of Minnesota, St. Paul, MN, 55108.

Mutant porcine  $\text{Ca}^{2+}$ -release channels/ryanodine-receptors (Ry-Rs) fused with planar lipid bilayers are less sensitive than normal to  $\text{Ca}^{2+}$ -induced inhibition. We measured  $[\text{Ca}^{2+}]$  in myotubes cultured from neonatal piglets homozygous for normal and mutant malignant hyperthermia susceptible (MHS) Ry-Rs to test the idea that Ry-Rs *in situ* are also differentially modulated. We used digital imaging microscopy and fluorescent dyes to monitor  $[\text{Ca}^{2+}]$ . Caffeine (10-20 mM; 22-26°C) raised myoplasmic  $[\text{Ca}^{2+}]_{myo}$  in three ways: (i) a sustained progressive rise in either normal or MHS with delays of several minutes; (ii)  $\text{Ca}^{2+}$  transients in normal only with little delay; (iii) spontaneous transients and waves in normal only. Raising  $[\text{K}^{+}]_{ext}$  (2.6 to 26 mM) had no effect on  $[\text{Ca}^{2+}]_{myo}$ . A fraction of the intracellular stores (presumably SR) dominated the resting 340/380 nm fluorescence from myotubes self-loaded with Fura-2 AM. The opposite pattern appeared with ester-loaded Fluo-3. Bulk  $[\text{Ca}^{2+}]_{myo}$  was less than the  $[\text{Ca}^{2+}]$  near SR. Normal myotubes (n=20) had a lower resting  $[\text{Ca}^{2+}]_{myo}$  (0.798 $\pm$ ; P = 0.004) than MHS myotubes (n=15) when cultured and loaded identically with Fluo-3. Insensitivity of MHS Ry-Rs to  $\text{Ca}^{2+}$ -induced inhibition may sustain the elevated resting  $[\text{Ca}^{2+}]_{myo}$  in MHS myotubes and fill myoplasmic buffers. In contrast,  $\text{Ca}^{2+}$  transients and waves in normal myotubes may be fostered by unsaturated myoplasmic buffers. (Supported by NSF IBM 92-13160, NIH CA 15083 and NIH AR-41270.)

## Tu-Pos216

**TRIADIC  $\text{Ca}^{2+}$  MODULATES CHARGE MOVEMENT IN FROG SKELETAL MUSCLE.** ((K. Stroffekova-Polakova\* and J.A. Heiny)) Dept. of Molecular and Cellular Physiology, University of Cincinnati College of Medicine, Cincinnati, OH 45267, and \*Institute of Molecular Physiology and Genetics, Bratislava, Slovak Republic

We previously reported that the amount of charge that can move upon depolarization is sensitive to the triadic  $\text{Ca}$  concentration and proposed the existence of a  $\text{Ca}^{2+}$  binding site which could modulate the distribution of voltage sensors between available and unavailable states. The putative site(s) would be partially bound at rest and become further saturated under conditions when triadic  $\text{Ca}$  rises (Polakova & Heiny, *Biophys J* 66:A86, 1994). The present experiments tested whether these effects were mediated by a fast,  $\text{Ca}$ -dependent modulation mechanism. We recorded charge movement from single voltage-clamped frog fibers and applied agents to promote or block known ion channel phosphorylation pathways. 20  $\mu\text{M}$  PKI, a specific blocker of cAMP dependent phosphorylation, or 10-20  $\mu\text{M}$  Calmodulin Inhibitor, a specific blocker of  $\text{Ca}$ -calmodulin dependent phosphorylation did not alter resting  $Q_{max}$  or prevent the stimulation-dependent increase in charge. Likewise, these were not changed by 10  $\mu\text{M}$  Okadaic Acid in combination with 4 mM ATPs and 1 mM ATP, suggesting that phosphorylation via PKA or PKC pathways was not involved. The stimulation-dependent enhancement disappeared when the SR was depleted of  $\text{Ca}^{2+}$  confirming that  $\text{Ca}$  ions released from the SR are required for this effect. These results suggest that the  $\text{Ca}$ -dependent modulation is probably not mediated by phosphorylation, but may occur via direct binding of  $\text{Ca}$  ions to a site on or near the voltage sensor. (Supported by NIH RO1 AR40243).

## Tu-Pos217

STATE-DEPENDENT EFFECTS OF PERCHLORATE ANION ( $\text{ClO}_4^-$ ) ON  $\text{Ca}$  RELEASE IN FROG SKELETAL MUSCLE FIBERS. ((Elizabeth W. Stephenson)), Department of Physiology, UMD-New Jersey Medical School, Newark, NJ 07103.

The mechanism of  $\text{ClO}_4^-$  potentiation of E-C coupling is not completely understood. In our previous studies, 8 mM  $\text{ClO}_4^-$  increased the stimulation of  $\text{Ca}$  release by submaximal depolarization in skinned fibers without changing unstimulated  $^{45}\text{Ca}$  efflux (J. Gen. Physiol. 92:173, 1989). The present study assessed effects of 12 mM  $\text{ClO}_4^-$  per se in polarized, depolarized, and reprimed semitendinosus fibers skinned by microdissection. Methods were as described previously (choline Cl replacement of K methanesulfonate at constant  $[\text{K}^+][\text{Cl}^-]$ , 800  $\mu\text{M}$  free  $[\text{Mg}^{2+}]$ ), but initial SR  $\text{Ca}$  was set with 50 nM free  $[\text{Ca}^{2+}]$ , 3 mM EGTA.  $\text{Ca}$  release was assayed from normalized isometric force responses. In polarized segments, 12 mM  $\text{ClO}_4^-$  stimulated maximal responses in  $<1$  s; depolarized segments from the same fibers gave no response ( $>25$  s exposure), but were altered. After repolarization without  $\text{ClO}_4^-$ , segments reprimed for 63-135 s did not respond to  $\text{ClO}_4^-$ , but then gave normal responses to depolarization. Segments repolarized briefly (24-32 s) often gave prompt large  $\text{ClO}_4^-$  responses. These results suggest that 1) sufficient  $\text{ClO}_4^-$  activates a stimulatory site in the polarized coupling pathway that is inaccessible or inoperative during inactivation, but may function transiently during repriming; 2) binding to a site in inactivated fibers inhibits stimulation, after repriming, by  $\text{ClO}_4^-$ , but not by depolarization; 3)  $\text{ClO}_4^-$  binding probes conformational changes in coupling controlled by the state of the TT voltage sensor.

## Tu-Pos219

ELECTROTONIC PROPERTIES OF HYPERTROPHIED MAMMALIAN SKELETAL MUSCLE. ((Y. Chen, F.W. Banks, and M.S. Brodwick\*)) ((Chicago State University, Chicago, IL 60643, \*UTMB, Galveston, TX. 77550))

Muscles exposed to increased load respond by enlarging. The enlargement process includes muscle fiber hypertrophy. The focus of our investigation is to describe the compensatory electrical membrane property changes accompanying muscle fiber hypertrophy. We have developed a hypertrophied muscle preparation utilizing the rat soleus muscle. We are able to enlarge the soleus muscle by surgically removing the medial head of the gastrocnemius and denervating the lateral head that covers the soleus muscle. Since the smaller soleus and the plantaris now pronate the foot without the much larger gastrocnemius muscle, these muscles enlarge in order to develop more tension. Fiber hypertrophication in the soleus was accomplished four weeks post surgical. Electrophysiological investigation revealed a 73% increase in the input impedance in enlarged soleus muscle fibers when compared to control soleus muscle fibers. This unexpected result coupled with a 33% increase in the space constant of hypertrophied muscle fibers suggests membrane changes are made in hypertrophied muscle that maintain the safety factor for excitation. Changes in neurotransmitter release will also be discussed. (NIGMS GM08043)

## Tu-Pos218

RAISED INTRACELLULAR  $[\text{Ca}^{2+}]$  ABOLISHES EXCITATION-CONTRACTION COUPLING IN SKELETAL MUSCLE FIBRES. ((G.D. Lamb, P.R. Junankar and D.G. Stephenson)) School of Zoology, La Trobe University, Bundoora, Vic., 3083, Australia.

Raising the intracellular  $[\text{Ca}^{2+}]$  for 10s at 23°C irreversibly abolished depolarization-induced force responses in mechanically skinned muscle fibres of toad and rat (half-maximal effect at 10  $\mu\text{M}$  and 23  $\mu\text{M}$ , respectively), without affecting the  $\text{Ca}^{2+}$ -dependence or maximum force of the contractile apparatus or the ability of caffeine or low  $[\text{Mg}^{2+}]$  to open the ryanodine receptor (RyR)/ $\text{Ca}^{2+}$  release channels. This uncoupling had a  $Q_{10} > 3.5$ , and was not noticeably affected by removal of ATP or application of kinase or phosphatase inhibitors. The protease inhibitor, leupeptin (1mM), did not prevent uncoupling unless it was induced at a relatively slow rate (eg. over 60s with 2.5  $\mu\text{M}$   $\text{Ca}^{2+}$ ). Immunostaining showed no evidence of proteolysis of the RyR, the  $\alpha_1$  subunit of dihydropyridine receptor (DHPR) or triadin in uncoupled fibres. The transverse tubular system was not perforated in uncoupled fibres, but electron microscopy revealed Z-line aberrations and distorted or severed triad junctions. This  $\text{Ca}^{2+}$ -dependent uncoupling of depolarization-induced  $\text{Ca}^{2+}$  release may have an important regulatory function in normal muscle and may be responsible for long-last muscle fatigue after severe exercise and contribute to muscle weakness in various dystrophies.

## Tu-Pos220 (Presented at Tu-PM-A9)

A SLOW CALCIUM-DEPENDENT COMPONENT OF CHARGE MOVEMENT IN FROG SKELETAL MUSCLE FIBERS. ((Chiu Shuen HUI)) Dept. of Physiol. and Biophys., Indiana Univ. Med. Ctr., Indianapolis, IN 46202, USA.

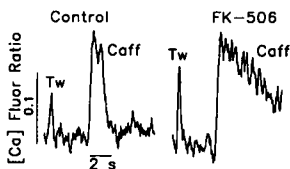
Charge movement and  $\text{Ca}$  transient were measured in stretched cut frog twitch fibers with the double Vaseline-gap voltage clamp technique. When the nominal free  $[\text{Ca}^{2+}]$  in the end-pool solutions was raised from 1 to 50 nM and the  $\text{Cl}^-$  in the center-pool solution was replaced by an impermeant anion, a slowly decaying OFF current appeared following the usual OFF charge movement. The magnitude of the slow current follows the order: in  $\text{CH}_3\text{SO}_3^- > \text{in } \text{SO}_4^{2-} > \text{in gluconate}$ . Since the current is absent in  $\text{Cl}^-$  it cannot be carried by anions. Also, it cannot be carried by  $\text{Ca}^{2+}$  as it still exists in a  $\text{Ca}$ -free center-pool solution. To test the possibility that it is a capacitive current, experiments were performed by using TEST pulses of a fixed amplitude but with varying durations. After correcting for the ON baseline in the trace elicited by a 2-s pulse, the ON transient also showed a slow component and the running integral of the ON transient matched the integrals of the OFF transients elicited by pulses of different durations. Thus, the slow ON and OFF currents could represent the movements of some intramembranous charge, but whether the charge belongs to the  $Q_R/Q$ , pool or not remains unknown. However, the slow OFF charge has a steeper temperature dependence than the fast OFF charge ( $Q_R$  and  $Q$ , combined). More importantly, the slow ON charge movement decays with a time course parallel to that of the  $\text{Ca}$  release waveform computed from the ApIII absorbance signal monitored simultaneously. (Supported by NIH NS-21955 and a grant from MDA).

E-C COUPLING AND  $[\text{Ca}^{2+}]_i$ -TRANSIENTS

## Tu-Pos221

THE EFFECTS OF FK-506 ON CARDIAC  $\text{Ca}$  TRANSIENTS AND CONTRACTION. ((E. McCall, L. Li and D.M. Bers)), Department of Physiology, Loyola Univ., Maywood, IL 60153.

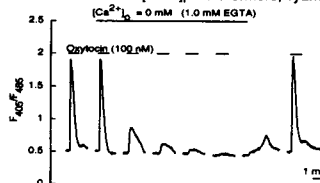
FK-506 binding protein (FKBP) has been reported to be closely associated with the ryanodine receptor and may modulate SR  $\text{Ca}$  release channel gating (Brillantes *et al.*, Cell 77:513-523, 1994). FK-506 can inhibit FKBP's activity, reversing its channel stabilizing effects. However, little is known about FKBP's function during normal contraction in intact myocytes. Using Indo-1 AM-loaded rat and rabbit cardiac myocytes we investigated the effect of 5  $\mu\text{M}$  FK-506 on steady-state (SS) contraction (0.5 Hz), SR  $\text{Ca}$  load (using caffeine contractions, CaC) and rest decay of SR  $\text{Ca}$ . In rat myocytes FK-506 enhanced SS contraction and  $\text{Ca}$  transient by 58  $\pm$  15% and 62  $\pm$  7% respectively. FK-506 did not alter SS SR  $\text{Ca}$  content since the  $\text{Ca}$  transient induced by caffeine was not altered by FK-506 (105  $\pm$  4%). This suggests that FK-506 increases the SR  $\text{Ca}$  released during E-C coupling. The SS CaC was increased by FK-506 however (by 32  $\pm$  12%), raising the possibility of increased myofilament  $\text{Ca}$  sensitivity. We saw no evidence of increased resting SR  $\text{Ca}$  leak with FK-506 based on  $\Delta[\text{Ca}]_i$  during CaC after differing rest intervals. Surprisingly, FK-506 had no effects on any of these parameters in rabbit ventricular myocytes. Thus FKBP may be more critically involved in E-C coupling in rat than in rabbit cardiac muscle.



## Tu-Pos222

MECHANISMS OF OXYTOCIN INDUCED CALCIUM TRANSIENTS IN SINGLE HUMAN MYOMETRIUM SMOOTH MUSCLE CELLS ((J. R. Holda, C. Oberti, E. Perez-Reyes, L. A. Blatter)) Department of Physiology, Loyola University Chicago, Maywood, IL 60153

Oxytocin is a peptide hormone known to increase intracellular calcium ( $[\text{Ca}^{2+}]_i$ ) in uterine smooth muscle and to cause contraction. We investigated the mechanisms of oxytocin-induced rise of  $[\text{Ca}^{2+}]_i$  in a smooth muscle cell line derived from non-pregnant, human myometrium, using the fluorescent  $\text{Ca}^{2+}$  indicator Indo-1. Oxytocin (100 nM) induced a rapid and transient increase of  $[\text{Ca}^{2+}]_i$ . Removal of extracellular  $\text{Ca}^{2+}$  did not affect the oxytocin-induced  $[\text{Ca}^{2+}]_i$ -transients initially, suggesting that  $[\text{Ca}^{2+}]_i$  increased primarily through  $\text{Ca}^{2+}$  release from intracellular stores. When the cells were repeatedly stimulated with oxytocin in a  $\text{Ca}^{2+}$ -free environment the  $[\text{Ca}^{2+}]_i$ -transients decreased and eventually were abolished due to depletion of the stores (see Figure; time gaps between exposures to oxytocin = 30 min.). Restoration of extracellular  $\text{Ca}^{2+}$  (2.0 mM) led to refilling of the stores and subsequent stimulation with oxytocin caused a typical  $[\text{Ca}^{2+}]_i$ -transient. In these experiments  $\text{Ca}^{2+}$  entry through voltage-operated  $\text{Ca}^{2+}$  channels did not contribute to the oxytocin-induced rise of  $[\text{Ca}^{2+}]_i$  since nifedipine (10  $\mu\text{M}$ ) did not affect the action of oxytocin. Thapsigargin, a blocker of  $\text{Ca}^{2+}$  uptake into the stores, caused a transient increase of  $[\text{Ca}^{2+}]_i$ , and subsequent stimulation with oxytocin failed to trigger an increase of  $[\text{Ca}^{2+}]_i$ . Caffeine (10 mM) diminished or abolished the oxytocin stimulated  $[\text{Ca}^{2+}]_i$ -transient, however by itself it failed to increase  $[\text{Ca}^{2+}]_i$ . Furthermore, ryanodine (10  $\mu\text{M}$ ) did not inhibit the oxytocin-induced increase of  $[\text{Ca}^{2+}]_i$ , suggesting that calcium-induced calcium release did not contribute significantly to the increase in  $[\text{Ca}^{2+}]_i$ . The effect of caffeine, however, was consistent with the known inhibition of  $\text{IP}_3$ -induced  $\text{Ca}^{2+}$  release by caffeine. It was concluded that oxytocin caused a transient increase of  $[\text{Ca}^{2+}]_i$  through release of  $\text{Ca}^{2+}$  from a thapsigargin-sensitive store, presumably by activating the  $\text{IP}_3$  pathway.



## Tu-Pos223

CALCIUM TRANSIENTS IN RAT INTACT FAST- AND SLOW-TWITCH SKELETAL MUSCLE FIBERS. ((S. Carroll, M.G. Klein, M.F. Schneider)) Dept. Biochem., UMAB, Baltimore, MD 21201

Fibers were enzymatically dissociated from fast- (FDB) or slow- (Soleus) twitch muscles, loaded with fura-2-AM, embedded in agarose in 2.5 mM  $Ca^{2+}$  Ringer's and stimulated via external electrodes (30 °C). Calcium transients  $\Delta[Ca^{2+}]_i$  in response to action potentials were calculated from fluorescence ratios for 380 and 358 nm excitation considering non-instantaneous equilibration of  $Ca^{2+}$  with fura-2. For a single action potential  $\Delta[Ca^{2+}]_i$  was larger in FDB than in Sol (0.54  $\pm$  0.12 vs 0.35  $\pm$  0.15  $\mu$ M; mean  $\pm$  SEM; N  $\geq$  8 fibers for all means) and had a shorter  $t_{1/2}$  of decay from peak to pseudo-steady level (5.0  $\pm$  0.4 vs 11.0  $\pm$  0.8 ms). Resting  $[Ca^{2+}]_i$  was 51  $\pm$  5 and 59  $\pm$  4 nM in FDB and Sol. For a train of 10-30 action potentials at 4-10 ms intervals the pseudo-steady  $\Delta[Ca^{2+}]_i$  at 0.5 to 1 s after the end of the train in FDB fibers was 8.8  $\pm$  1.3 nM but was not significantly different from 0 in Sol. The pseudo-steady  $\Delta[Ca^{2+}]_i$  after the train and the decay  $t_{1/2}$  both increased with increasing train duration in FDB but not in Sol. These differences are consistent with the presence of parvalbumin in FDB but not in Sol. Parv becomes increasingly saturated with  $Ca^{2+}$  with increasing duration of  $\Delta[Ca^{2+}]_i$ , decreasing its contribution to lowering  $[Ca^{2+}]_i$  immediately after the train but increasing the pseudo-steady  $\Delta[Ca^{2+}]_i$  later on due to dissociation of the increased Ca-Parv. Sol lacks Parv and consequently cannot exhibit these effects. Supported by NIH and MDA.

## Tu-Pos225

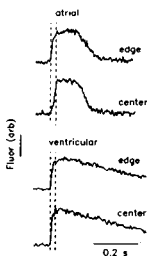
EFFECTS OF SARCOPLASMIC RETICULUM  $Ca^{2+}$  LOADING ON TWO COMPONENTS OF CONTRACTION IN CARDIAC MYOCYTES. ((S.E. Howlett and G.R. Ferrier)) Dalhousie University, Halifax, Canada, B3H 4H7.

We have reported that excitation-contraction coupling in guinea pig myocytes can be separated into two components: contractions triggered by L-type  $Ca^{2+}$  current ( $I_{Ca}$ ) at membrane potentials positive to -30 mV, and a voltage sensitive sarcoplasmic reticulum (SR) release mechanism (VSRM) which becomes fully activated at membrane potentials negative to -30 mV. This study examines the effects of loading and unloading SR  $Ca^{2+}$  stores on these two components of contraction. Experiments were conducted with whole cell voltage clamp and video monitoring of unloaded cell shortening at 37°C in the presence of 250  $\mu$ M lidocaine. Voltage steps to activate contraction were preceded by trains of 10 conditioning pulses to 0 mV to load SR stores, or to -40 mV to unload SR stores. Contractions triggered by the VSRM were abolished by SR unloading, whereas contractions triggered by  $I_{Ca}$  were unaffected by loading or unloading. Contraction-voltage (CV) relations determined with voltage steps from -40 mV to inactivate VSRM were bell-shaped and proportional to the magnitude of  $I_{Ca}$ . In contrast, CV relations elicited by voltage steps from -65 mV to activate both mechanisms were sigmoidal and plateaued at positive potentials, when SR stores were loaded. When SR stores were unloaded, the CV relation from -65 mV became bell-shaped and identical to that when VSRM was inactivated. Ryanodine (30 nM) mimicked the effects of unloading on CV relations. Results suggest that the SR release component of contraction is attributable to the VSRM.

## Tu-Pos227

SPATIO-TEMPORAL CHANGES IN  $[Ca^{2+}]_i$  DURING ELECTRICALLY-EVOKED CONTRACTIONS IN CARDIAC ATRIAL AND VENTRICULAR MYOCYTES. ((J.R. Berlin)) Bockus Research Inst., Philadelphia, PA 19146

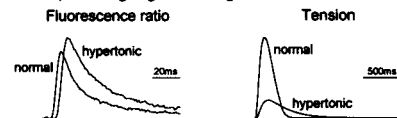
Morphometric studies have shown that mammalian ventricular muscle cells contain an extensive t-tubular network that is absent in many atrial myocytes. To understand how t-tubules affect spatio-temporal changes in  $[Ca^{2+}]_i$  during cell contraction, the pattern of fluorescence transients in fluo-3 AM loaded myocytes was measured with a laser scanning confocal microscope during field-stimulation. In rat ventricular myocytes, which contain t-tubules,  $[Ca^{2+}]_i$  increased throughout the cell at the same time (26 ms/image) during a transient. Increased temporal resolution obtained by scanning along a single z-line every 2 ms (line scan image) showed that the rise of  $[Ca^{2+}]_i$  occurred synchronously at the edge and center of the cell (see figure). In guinea-pig atrial myocytes, which lack t-tubules,  $[Ca^{2+}]_i$  first increased in focal areas at the cell periphery prior to a generalized increase in  $[Ca^{2+}]_i$  during the transient. Line scan images of atrial cells showed the rise in  $[Ca^{2+}]_i$  occurred more rapidly at the cell periphery (see figure), with the half-maximal increase in fluorescence at the cell edge leading that in the center by 34  $\pm$  4 ms (n=3). The rapid rise of  $[Ca^{2+}]_i$  during transients in ventricular myocytes could be made to occur in a focal manner by blocking sarcolemmal Ca channels with nifedipine. Thus, t-tubules ensure E-C coupling occurs synchronously in the myocyte; however, without t-tubules or with limited activation of sarcolemmal Ca channels, E-C coupling can be observed in focal areas of the myocyte. (Supported by NIH and a MBL Lakian Fellowship)



## Tu-Pos224

THE INTRACELLULAR  $Ca^{2+}$  TRANSIENT IN FROG SKELETAL MUSCLE FIBERS UNDER HYPERTONIC CONDITIONS. ((DR Claffin, P Garzella, DG Stephenson\* & FJ Julian)) Dept. of Anesthesia, Brigham & Women's Hospital, Boston, MA 02115; \*School of Zoology, La Trobe University, Melbourne, Australia.

The twitch tension generated by a skeletal muscle fiber is reduced markedly during exposure to hypertonic media. The aim of the experiments described here was to determine the effect of increased tonicity on the intracellular calcium transient (ICT) in intact single frog muscle fibers at low temperature, where most mechanical experiments are done. Fibers from the tibialis anterior muscles of *R. temporaria* were used. Mean sarcomere length was 2.2-2.3  $\mu$ m and experimental temperature was 3°C. The fluorescent dye Mag-Fura-2 (MF2), loaded as MF2-AM (30min at 20°C) was used as the  $Ca^{2+}$ -reporter because of its ability to follow the large, rapid ICT found in skeletal muscle with high temporal fidelity and without saturating. Twitch tension and MF2 fluorescence responses to excitation at both 344nm (isosbestic) and 380nm were recorded in normal Ringer's solution and in the same solution made hypertonic by adding 98mM sucrose (1.44R). The hypertonic Ringer's caused a reduction in twitch tension to 53.3 $\pm$ 16.3% (mean $\pm$ SEM, n=3) of the value in normal Ringer's and caused both a delay of 5.5 $\pm$ 1.6ms and an increase of 15.4 $\pm$ 3.5% (n=4) in the peak of the MF2 signal. MF2 fluorescence responses (Fig., left) and tension responses (Fig., right) from one fiber are shown below. The MF2 records were obtained by dividing the 344nm response by the 380nm response (after background subtraction) and aligning the resting levels. We conclude that reduced availability of activator  $Ca^{2+}$  is not a factor contributing to the reduced twitch tension observed under hypertonic conditions. Supported by NIH HL35032 and ARC (DGS).



## Tu-Pos226

FREQUENCY-DEPENDENT EFFECTS ON  $Ca^{2+}$  CURRENTS,  $Ca^{2+}$  TRANSIENTS AND CONTRACTION IN MYOCYTES DISPERSED FROM THE EPICARDIAL BORDER ZONE OF THE ARRHYTHMIC 5 DAY INFARCTED HEART. ((A.Licata, R.Agarwal, R.Robinson, P. Boyden)) Dept of Pharmacology, Columbia University, New York NY 10032.

Previous studies from our laboratory showed that the density of  $I_{Ca}$  is reduced by 40% in myocytes dispersed from the epicardial border zone of the 5 day infarcted heart (IZs). Further studies now show that while there is little or no decrease in these reduced  $I_{Ca}$  at slow voltage clamp steps (0.125Hz), there is a further reduction in peak  $I_{Ca}$  in IZs at fast clamp rates (1Hz). This differs from findings using epicardial myocytes from normal noninfarcted hearts (NZs). Since  $I_{Ca}$  is one of the many factors that can influence  $Ca_i$ , we sought to determine how  $Ca_i$  was handled in response to rate in IZs and compared these responses to those observed for NZs. We determined changes in cytoplasmic free calcium in myocytes after loading with fura2/AM and in response to extracellular stimulation. All changes are described in terms of 340/380 ratio. At a slow pacing rate (0.2Hz), diastolic  $Ca_i$  ratio and duration of  $Ca_i$  transients differed in two groups yet the average peak  $Ca_i$  ratios (NZs 3.27, n=15; IZs 2.95, n=20) and the average change in  $Ca_i$  per stimulated beat did not. In NZs, increasing drive rate from 0.2 to 0.5 to 1Hz increased both peak  $Ca_i$  (17%) and the average change in  $Ca_i$  per beat (21%) while reducing the duration of the  $Ca_i$  transient (45%). In contrast, in IZs, an increase in pacing rate decreased both peak  $Ca_i$  ratio (4%) and the average change in  $Ca_i$  per beat (15%). This was accompanied by a modest shortening in the time course of the  $Ca_i$  transient (27%). In a subset of cells, (NZs n=12, IZs n=6) contractile function was assessed by the cell shortening response at the different pacing rates. Increase in pacing rate produced a positive inotropic effect in NZs while diminished shortening in IZs. Thus, at rapid rates, cells that survive in the infarcted heart show impaired myocyte contraction, reduced levels of peak  $Ca_i$  as well as a further reduction in  $I_{Ca}$ .

## Tu-Pos228

CROSS-SIGNALING BETWEEN  $Ca^{2+}$  CHANNELS AND RYANODINE RECEPTORS IN VENTRICULAR MYOCYTES: VOLTAGE-DEPENDENCE OF  $Ca^{2+}$ -RELEASE-INDUCED INACTIVATION OF  $Ca^{2+}$  CHANNELS ((James S.K. Sham)) Department of Medicine, The Johns Hopkins School of Medicine, Baltimore, MD 21205.

In rat ventricular myocytes,  $Ca^{2+}$  current ( $I_{Ca}$ ) can trigger  $Ca^{2+}$  release from sarcoplasmic reticulum (SR), and  $Ca^{2+}$  release from the SR can inactivate  $Ca^{2+}$  current ( $I_{Ca}$ ), when the global cytoplasmic  $[Ca^{2+}]_i$  was buffered at 150 nM with 10 mM EGTA and 5 mM  $Ca^{2+}$  (Sham and Morad, 1994), suggesting local cross-signaling between  $Ca^{2+}$  channels and ryanodine receptors at a submicroscopic level. Such local cross-signaling should depend on the magnitude of the unitary  $Ca^{2+}$  current (the local stimuli), rather than the macroscopic  $I_{Ca}$ . This notion was tested by examining the voltage-dependence of the inactivation of  $I_{Ca}$  induced by  $Ca^{2+}$  release in ventricular myocytes dialysed with different concentrations of EGTA and BAPTA.  $[Ca^{2+}]_i$  was buffered at 150 nM with  $Ca^{2+}$  to provide adequate  $Ca^{2+}$  loading for the SR. The kinetics of  $I_{Ca}$  inactivation were compared before and after SR was disabled by caffeine (5 mM) or ryanodine (20  $\mu$ M). In control myocytes, inactivation of  $I_{Ca}$  was observed at test potentials ranging from -30 to +40 mV, with the greatest inactivation at -20 mV and less inactivation at positive potentials, in contrast to the bell-shaped voltage-dependence of macroscopic  $I_{Ca}$  and  $Ca^{2+}$  transient. Intracellular dialysis with EGTA (10 mM), did not alter significantly the voltage-dependence of  $Ca^{2+}$ -release-induced inactivation of  $I_{Ca}$ , whereas BAPTA (3-15 mM) completely abolished the inactivation of  $I_{Ca}$  caused by  $Ca^{2+}$  release at positive potentials and attenuated significantly those at negative potentials. The inhibitory effect of BAPTA was concentration-dependent. The voltage-dependence of the  $Ca^{2+}$ -release-induced inactivation of  $I_{Ca}$  therefore, resembled that of the unitary  $Ca^{2+}$  current, and was affected only when the local  $Ca^{2+}$  domains were effectively restricted by BAPTA. These results provide further support to the local cross-signaling between  $Ca^{2+}$  channels and ryanodine receptors. (Supported by a grant-in-aid from AHA)

## Tu-Pos229

CHARACTERISTICS OF THE  $Ca_i$  TRANSIENT IN VENTRICULAR MYOCYTES FROM THE RAT HEART. ((J. C. Hancox, S.J. Evans and A.J. Levi.)) Department of Physiology, University of Bristol, Bristol BS8 1TD, UK.

We have investigated characteristics of the  $Ca_i$  transient in rat ventricular myocytes at 37 °C. Cells were loaded with Fura-2 AM and internally dialysed with a K-based, 10mM Na-containing pipette solution; holding potential was set at -40mV. The  $Ca_i$  transient at all potentials was abolished by 5  $\mu$ M ryanodine, showing it was due to Ca release from the sarcoplasmic reticulum (SR). In all cells, L-type  $Ca$  current ( $I_{CaL}$ ) had a bell-shaped voltage-dependence, with a maximum at +10mV. The voltage-dependence of the  $Ca_i$  transient fell broadly into two groups. Some cells showed a bell-shaped  $Ca_i$  transient relation, in others a large  $Ca_i$  transient remained at positive potentials where there is little  $I_{CaL}$ . Many cells displayed a distinct slowing of the  $Ca_i$  transient upstroke and time-to-peak with depolarisations more positive than +80mV. Switching to 20  $\mu$ M nifedipine between beats abolished the  $Ca_i$  transient elicited at +100mV, indicating it might be due to SR release triggered by Ca entry via  $I_{CaL}$ . However, in other cells a depolarisation to +140mV still elicited a phasic  $Ca_i$  transient. Since this potential is close to (or more positive than)  $E_{Ca}$ , it seems unlikely this  $Ca_i$  transient might be triggered by  $I_{CaL}$ . In further experiments we reduced external Ca to 0.1mM to make  $E_{Ca}$  less positive (+90mV) and depolarisation to levels more positive than  $E_{Ca}$  still elicited phasic  $Ca_i$  transients. These latter results suggest that  $I_{CaL}$  might not be the only trigger for SR release. Supported by the British Heart Foundation and Wellcome Trust.

## Tu-Pos231

L-TYPE CA CURRENT AND INWARD RECTIFIER K CURRENTS IN ADULT RABBIT VENTRICULAR MYOCYTES MAINTAINED IN CULTURE. ((J. S. Mitcheson, J.C. Hancox and A.J. Levi.)) Dept. of Physiology, School of Medical Sciences, University Walk, Bristol BS81TD, UK.

Maintaining adult cardiac myocytes in short term culture may offer advantages, but little is known about how membrane currents become altered. Rabbit ventricular myocytes were placed in a basic medium (Medium 199, Sigma) for up to 8 days and the L-type Ca current ( $I_{CaL}$ ) and inward rectifier current ( $I_{K1}$ ) was monitored using whole cell patch clamp. Over 50% of the cells remained rod shaped and striated, although the ends tended to round up slightly. Cell capacitance declined significantly from  $127 \pm 9.5$  pF at day 0 to  $59 \pm 2.2$  pF at day 6.

For measuring  $I_{CaL}$  a Na-free external solution was used and Ba replaced Ca as the charge carrier. With a pulse from -80 to +10mV the amplitude of  $I_{CaL}$  decreased markedly during culture. However when normalised to cell capacitance the decrease in  $I_{CaL}$  was not significant ( $18.5 \pm 2$  pA/pF at day 0,  $n=8$  and  $13.0 \pm 2.7$  pA/pF at day 6,  $n=7$ ). There were no changes in the current-voltage relation and kinetics of  $I_{CaL}$ .

There was a very dramatic fall in the amplitude of  $I_{K1}$  during culture, from  $5.3 \pm 0.5$  nA at day 0 (current measured with a pulse from -80 to -130mV) to  $1.9 \pm 0.1$  nA at day 1 and  $0.5 \pm 0.1$  nA at day 6.

These results show that the density of ion channels appear to decline to different degrees during culture. There is only a slight fall in  $I_{CaL}$  channel density, but a much larger fall in  $I_{K1}$  channel density.

This work was supported by the MRC and Wellcome Trust.

## Tu-Pos233

REMOVAL OF EXTERNAL Mg LEADS TO THE APPEARANCE OF AN INWARD CA CHANNEL CURRENT WITH FAST KINETICS IN RAT VENTRICULAR MYOCYTES - IS IT T-TYPE CA CURRENT? ((S.J. Evans, A.J. Levi, J.P. Issberner, & J.V. Jones. Department of Physiology, School of Medical Sciences, University Walk, Bristol BS8 1TD, UK.))

In rat myocytes held at -80mV, we have found that switching to Mg-free external solution causes the appearance of an extremely rapid and large inward Ca channel current. Experiments were carried out at 37 °C, and myocytes were internally dialysed with a Cs- and BAPTA-containing pipette solution to eliminate outward K currents and buffer intracellular Ca. The external solution was Na-free to eliminate inward Na current, it contained Cs to block K conductance, 1mM Mg was present and 2mM Ba replaced external Ca. In 60% of the cells, removal of external Mg caused the appearance of a large and fast inward current carried by Ba. This could be clearly separated from L-type Ca channel current since it activated over a more negative voltage range (-50 to -30mV). This current also had faster kinetics than the L-type Ca current. Both the fast and the L-type Ca current were blocked by 20  $\mu$ M nifedipine. However, 1  $\mu$ M nickel fully blocked the fast current and had no effect on the L-type current. Our results indicate that removal of external Mg causes the appearance of a large "T-type-like" Ca channel current. This may play a role in causing arrhythmias, since hypomagnesaemia is associated with ventricular arrhythmia. Supported by the Wellcome Trust and Bristol Healthcare Trust.

## Tu-Pos230

EFFECTS OF BAPTA ON FORCE AND INTRACELLULAR  $Ca^{2+}$  TRANSIENT DURING TWITCH AND TETANUS OF FROG MUSCLE FIBERS ((K.A.P. Edman, Y.-B. Sun, C. Caputo and F. Lou.)) Dept. of Pharmacology, University of Lund, S-223 62 Lund, Sweden.

BAPTA is a calcium chelating agent that can be transported into intact muscle fibers by diffusion in its acetoxymethyl (AM) form. We here report experiments suggesting that BAPTA, in low concentrations, inhibits calcium binding to troponin without reducing the intracellular  $Ca^{2+}$  transient. Single fibers from the anterior tibialis muscle of *Rana temporaria* were immersed in a Ringer solution containing 50  $\mu$ M BAPTA, AM for approx. 30 min followed by immersion in ordinary Ringer (10-11 °C). The peak twitch force and the duration of the twitch were both progressively reduced by BAPTA, the peak twitch force being depressed to less than 5 % of the control value within 30-60 min after exposure to BAPTA. The rate of rise of force during tetanus was also markedly reduced, but the final tension reached during tetanic stimulation was 85-90 % of the control. The amplitude of the intracellular  $Ca^{2+}$  transient (recorded by Fluo-3) during a single twitch remained quite constant while the twitch force declined. However, the mean intracellular  $Ca^{2+}$  concentration during tetanus was nearly doubled after treatment with BAPTA. There was no contribution to the measured fluorescence from BAPTA. Instantaneous stiffness was recorded by applying a 4 kHz (low amplitude) sinusoidal length oscillation to the fiber. The decrease in active force during twitch and tetanus produced by BAPTA was matched by a drop in stiffness such that the force/stiffness ratio was maintained constant. The decrease in contractile force was thus attributable to a decrease in the number of active cross-bridges with no change in average force per bridge. The results suggest that BAPTA reduces the affinity of the troponin binding sites for calcium.

## Tu-Pos232

SLOW CALCIUM CURRENT ACTIVATION IN TWITCH SKELETAL MUSCLE FIBERS OF THE FROG. ((F. Francini, C. Bencini and R. Squecco.)) Dpt. di Scienze Fisiologiche, Università di Firenze, 50134 Firenze, Italy.

In previous works on L-type calcium current ( $I_{Ca}$ ) activation several possible kinetic models have been proposed. This work was planned to determine the minimal kinetic scheme that will account for calcium channel activity in skeletal muscle. Single cut twitch muscle fibers of *Rana esculenta* were voltage clamped in a double Vaseline-gap chamber. Solutions were without  $Na^+$ ,  $K^+$  and  $Cl^-$ , and blockers of  $Na^+$ ,  $K^+$  and  $Cl^-$  channels were used to minimize ionic currents and have  $Ca^{2+}$  as the only permeant ion. The holding potential (HP) was -100 mV throughout. Voltage test pulses from the HP were applied in 10 mV increments. Hyperpolarizing control pulses of 20 mV were superimposed on a pre-pulse to -140 mV. Current traces during voltage pulses are the sum of intramembrane charge movement (ICM) and  $I_{Ca}$  (voltage threshold for  $I_{Ca}$  was at  $-57 \pm 2$  mV).  $I_{Ca}$  activation time course during long (3-5 s) depolarizing voltage pulses was evaluated after removal of  $I_{Ca}$  inactivation from the original current records. The kinetic of  $I_{Ca}$  activation time course was determined by multiexponential fitting. Fitting procedure was performed 50-100 ms after the pulse onset to avoid ICM contamination. Two or three exponential curves could be resolved depending on the voltage pulse. However, the best fit on the time constants vs. voltage plots was obtained assuming four transitions. The time integral of ICM ( $Q_{\infty}$ ) during voltage pulses was calculated after subtraction of  $I_{Ca}$  from the original current. Steady-state activation curve was obtained by subtracting the  $Q_{\infty}$  from the time integral of tail currents evoked by short (150 ms) pulses. The best fit on the activation curve was obtained by using a four-states cyclic model. Supported by grant n° 239 from Telethon-Italy.

## Tu-Pos234

RECURRENCE OF CALCIUM TRANSIENTS IN RAT CARDIOMYOCYTES INDUCED BY ELECTRICAL STIMULATION IN CALCIUM-FREE TYRODE'S SOLUTION. ((K.-X. Li, D. Williford, T. Gunter and S.-S. Sheu.)) Dept. of Pharmacology and Biophysics, Univ. of Rochester, Rochester, NY 14642

It is well known that entry of extracellular calcium is a trigger of contraction by inducing calcium release from sarcoplasmic reticulum (SR) in cardiac myocytes. Whether or not calcium from another source can induce calcium release from SR has not been widely investigated. Using the fluorescence microscopy and the  $Ca^{2+}$  indicator Fura-2, we investigated calcium transients in rat ventricle cardiomyocytes in warm ( $37 \pm 1^\circ$  C)  $Ca^{2+}$ - and  $Mg^{2+}$ -free ( $Ca^{2+}$ -free) Tyrode's solution. We found that (1) Calcium transient induced by 0.5 Hz electrical stimulation (ES) disappeared very quickly after the application of  $Ca^{2+}$ -free Tyrode's solution. Without continuous ES applied only sparse spontaneous spikes of calcium transients were seen in 1 of 7 cells in the  $Ca^{2+}$ -free Tyrode's solution. If ES was continuously applied calcium transients reappeared in 7 of 9 cells observed: 4 cells showed a spike pattern and 3 cells showed a train pattern. The frequency of the recurring calcium transient train seems higher than that produced by ES in the normal Tyrode's solution showing that ES increases frequency of the recurring calcium transients in the  $Ca^{2+}$ -free Tyrode's solution. (2) Pretreatment with ryanodine (1  $\mu$ M) for 3 minutes completely abolished the recurrence of the calcium transients in all cells tested ( $n=5$ ) with ES in the  $Ca^{2+}$ -free Tyrode's solution indicating the SR involvement in this recurrence. A further study is being carried out to locate sources of the calcium triggering the calcium release from SR in the  $Ca^{2+}$ -free Tyrode's solution.

## Tu-P0235

**A VOLTAGE-SENSITIVE TRIGGER FOR CONTRACTION IN RAT CARDIAC MYOCYTES IN THE ABSENCE OF  $Na^+$  AND L-TYPE  $Ca^{2+}$  CURRENTS.** ((J.-Q. Zhu and G.R. Ferrier)) Dalhousie University, Halifax, Canada, B3H 4H7.

Currents and contraction were studied in rat ventricular myocytes at 37°C using whole cell voltage clamp and video monitoring of cell shortening.  $I_{Na}$  was eliminated with 250 mM lidocaine. Contraction-voltage (CV) relations were determined with voltage steps from a conditioning potential (CP) of -65 or -40 mV. The CV relationship from -40 mV was bell-shaped and proportional to  $L$ -current ( $I_{Ca}$ ). Contractions approached zero near +80 mV. Verapamil abolished  $I_{Ca}$  and contractions initiated by steps from -40 mV. When the CP was -65 mV, threshold for contraction was -55 mV, at which no or only a small slowly developing inward current was observed. The CV relation from -65 mV was sigmoidal and resembled that of skeletal muscle; contractions remained large even at +80 mV and were not proportional to  $I_{Ca}$ . When CP was -65 mV contractions could be elicited in the presence of 10 mM verapamil, although  $I_{Ca}$  was abolished. However, contractions in the presence of verapamil were abolished by 2 mM ryanodine. Thus, despite known differences between contraction in rat and guinea pig, rat exhibits both components of contraction previously demonstrated in guinea pig: a voltage sensitive sarcoplasmic reticulum release component, which is independent of  $I_{Ca}$  and  $I_{Na}$ , and a second component dependent on and proportional to  $I_{Ca}$ .

## Tu-P0237

**MECHANISMS ASSOCIATED WITH A STRETCH-INDUCED INCREASE IN  $[Ca^{2+}]_i$  IN GUINEA-PIG VENTRICULAR MYOCYTES.** ((J.-Y. Le Guennec, E. White\*, F. Gannier, D. Garnier.)) Laboratoire de Physiologie Animale, CNRS EP21, Fac. des Sciences, Tours (France) and \*Dept. of Physiology, University of Leeds, Leeds (UK). (spon. I. Duchatelle-Gourdon).

Stretching single guinea pig ventricular myocytes can provoke; a profound depolarization of the membrane potential, a large increase in diastolic calcium ( $[Ca^{2+}]_i$ ) and a loss of excitability (White et al, 1993, *Exp. Physiol.*, 78, 65-78). In addition, the stretch-induced increase in  $[Ca^{2+}]_i$  is abolished by incubation of cells with the stretch-activated channel (SAC) blocker streptomycin or reversed by acute application of this agent (Gannier et al, 1994, *Cardiovasc. Res.*, 28, 1193-1198).

We now report that the stretch-induced increase in  $[Ca^{2+}]_i$  is rapidly reversed by removing extracellular calcium (1.8 mM) from the superfusate ( $n=10$  cells). Acute application of 1  $\mu$ M verapamil also reversed the phenomenon ( $n=6$ ). In contrast, when cells were stored in the presence of ryanodine, sufficient to abolish contractions (1  $\mu$ M for 1 hour), the stretch-induced increase in  $[Ca^{2+}]_i$  was not affected ( $n=4$ ). These observations suggest that extracellular rather than intracellular sources of  $Ca^{2+}$  are important in maintaining the stretch-activated increase in  $[Ca^{2+}]_i$ . Our hypothesis; that activation of SAC depolarizes the cells to a new membrane potential, where a  $Ca^{2+}$  window current can maintain the increase in  $[Ca^{2+}]_i$ , is supported by studies with the OXSOFT HEART model.

## Tu-P0239

**THE EFFECTS OF REST INTERVAL ON THE RELEASE OF CALCIUM FROM THE SARCOPLASMIC RETICULUM IN ISOLATED GUINEA-PIG VENTRICULAR MYOCYTES.** ((C.M.N. Terracciano, R.U. Naqvi and K.T. MacLeod)) Dept. Cardiac Medicine, Nat. Heart & Lung Inst., Univ. London, Dovehouse St., London, SW3 6LY, U.K.

Ca was released from the sarcoplasmic reticulum (SR) of guinea-pig cardiac myocytes by rapidly cooling the cells or by rapid application of 10mM caffeine. The amount of releasable SR Ca after different rest intervals (RIs) was estimated by measuring current evoked by rapid application of 10mM caffeine. (This current is completely inhibited by removal of  $Na_e$  and  $Ca_e$  or by application of Ni (Na/Ca exchange current)). Releasable SR Ca after RIs of 5 to 120s (cell volume = 30pl) was estimated to be  $57.8 \pm 5.7$  to  $25.7 \pm 4.5$   $\mu$ mol/l accessible cell volume respectively. There was an exponential decline in Ca released from the SR after RIs of 2 to 180s ( $t_{1/2} = 25$ s); thereafter a portion (56%) of releasable Ca remained. We found a similar exponential decay ( $t_{1/2} = 35$ s) of the size of rapid cooling contractions (RCCs) with increasing RI. The time-to-peak of Na/Ca exchange current in the presence of caffeine slowed at long rest intervals. Decreasing SR load by 50% increased the time-to-peak of the current by  $213 \pm 37\%$  ( $n=6$ ). The rate of generation of a RCC was faster after short rest intervals and was associated with a faster rise in the corresponding increase in Indo-1 fluorescence. Decreasing SR load by 50% decreased the rate of cell shortening to  $34 \pm 5\%$  and decreased the rate of change in fluorescence to  $54 \pm 2\%$  ( $n = 5$ ).

## Tu-P0236

**$Na^+$  CURRENT AND  $Ca^{2+}$  RELEASE FROM THE SARCOPLASMIC RETICULUM DURING ACTION POTENTIALS IN CARDIAC MYOCYTES** ((Karin R. Sipido, Edward Carmeliet, Achilles Pappano)) Lab. of Physiology, University of Leuven, Belgium, and Dept. of Pharmacology, University of Connecticut, Farmington CT 06030-6125.

It has been proposed that subsarcolemmal  $Na^+$  accumulation during the  $Na^+$  current, through reverse mode Na/Ca exchange, induces fast  $Ca^{2+}$  entry sufficient to trigger  $Ca^{2+}$  release from the sarcoplasmic reticulum (SR). We tested this hypothesis and asked whether the  $Na^+$  current contributes to triggering of  $Ca^{2+}$  release from the SR during action potentials. Experiments were performed on isolated guinea-pig ventricular myocytes in whole cell current clamp with fura-2 as a  $[Ca^{2+}]_i$  indicator. The pipette solution contained (in mM): KCl 140 (or K-aspartate 120 and KCl 20), NaCl 10,  $MgCl_2$  0.5,  $MgATP$  4, fura-2 0.05, HEPES 10, pH 7.20. The external solution contained NaCl 137, KCl 5.4,  $MgCl_2$  0.5,  $CaCl_2$  2.5, dextrose 10, HEPES 11, pH 7.40 ( $T = 23^\circ C$ ). Steady state loading of the SR was obtained by applying conditioning action potentials.

Increasing or decreasing the availability of  $Na^+$  channels by hyperpolarizing or depolarizing the resting membrane did not affect subsequent  $Ca^{2+}$  release. In contrast, a depolarizing current during the action potential slowed  $Ca^{2+}$  release, while a hyperpolarizing pulse improved  $Ca^{2+}$  release. These results can be attributed to changes in driving force for the  $Ca^{2+}$  current and/or the  $Na^+$  current.

Block of the  $Na^+$  current with TTX initially improved  $Ca^{2+}$  release. However, after a delay  $Ca^{2+}$  release from the SR eventually decreased. The block of the  $Na^+$  current typically reduced the peak and early plateau of the action potential. In the presence of TTX, loading of the SR with  $Ca^{2+}$  by conditioning action potentials was reduced, as evidenced by the reduction in caffeine-induced  $Ca^{2+}$  release. Substitution of external  $Na^+$  with  $Li^+$  did not decrease  $Ca^{2+}$  release, but induced  $Ca^{2+}$  overload.

In conclusion, we could not detect a role for the  $Na^+$  current in triggering  $Ca^{2+}$  release, but  $Na^+$  influx via the  $Na^+$  channel may modulate the  $Ca^{2+}$  content of the SR.

## Tu-P0238

**CALCIUM ENTRY THROUGH SODIUM CHANNELS CAUSES RELEASE OF CALCIUM FROM THE SARCOPLASMIC RETICULUM IN RAT VENTRICULAR CELLS.** ((G. Thomas, C.W. Balke, S.R. Shorofsky)) University of Maryland, Baltimore, MD.

Calcium entry into cardiac cells through the L-type  $Ca^{2+}$  channel is thought to cause the release of  $Ca^{2+}$  from the sarcoplasmic reticulum (SR). Recently, data has indicated that it is the rise in  $Ca^{2+}$  in a specific domain near the  $Ca^{2+}$  release channel not the total intracellular  $Ca^{2+}$  that is the trigger for release from the SR. This implies that an alteration in the manner in which  $Ca^{2+}$  enters the cell should alter the intracellular  $Ca^{2+}$  transient and subsequent contraction. The present experiments were designed to investigate the ability of  $Ca^{2+}$  entry through  $Na^+$  channels to release  $Ca^{2+}$  from the SR and cause contraction.

Experiments were performed on freshly isolated, adult rat ventricular cells using the whole-cell patch clamp technique. Intracellular  $Ca^{2+}$  transients were measured using Indo 1. All voltage protocols were performed from a holding potential of -90 mV in a  $Na$ -free extracellular solution containing 1 mM  $CaCl_2$ . With depolarizing pulses, an inward current activated at about -55 mV, with peak currents of between 50 and 200 pA at -45 mV. This current was eliminated in a reversible manner by either removing  $Ca^{2+}$  from or adding TTX (10  $\mu$ M) to the bathing solution. Additionally, this current was eliminated by adding 5  $\mu$ M  $Na^+$  to the bathing solution, whereas 10  $\mu$ M extracellular  $Na^+$  caused an inward current to reappear. These data indicate that this current is carried by  $Ca^{2+}$  entering via TTX-sensitive  $Na^+$  channels. Depolarizations to test potentials between -55 and -45 mV resulted in  $Ca^{2+}$  transients and contractions. These contractions had a delayed onset, slower upstroke and more gradual decline than those seen when the L channels were activated. We conclude that 1) in rat ventricular myocytes  $Ca^{2+}$  can enter through  $Na^+$  channels under certain experimental conditions, resulting in  $Ca^{2+}$  release and contraction, and 2) that the shape of the transient elicited suggests that these channels are not as tightly coupled to the  $Ca^{2+}$  release channel as the L-type  $Ca^{2+}$  channel, supporting the local control theory of E-C coupling.

## Tu-P0240

**RE-LOADING OF  $Ca^{2+}$  DEPLETED SARCOPLASMIC RETICULUM DURING REST IN GUINEA-PIG VENTRICULAR MYOCYTES.** ((C.M.N. Terracciano, R.U. Naqvi and K.T. MacLeod)) Nat. Heart & Lung Inst., Cardiac Medicine, Univ. London, Dovehouse St., London, SW3 6LY, U.K.

The effect of rest on Ca depleted sarcoplasmic reticulum (SR) in guinea-pig cardiac myocytes was investigated using rapid cooling contractions (RCC) and the fluorescent indicator Indo-1. Rapid cooling of the cell to  $1^\circ C$  produces a release of Ca from the SR; when rewarming is induced in the presence of 10 mM caffeine, SR uptake is not effective and Ca is extruded from the cytoplasm mainly via Na/Ca exchange. A second cooling period elicited during the continuous presence of caffeine fails to bring about an increase in Indo-1 fluorescence (IF) suggesting that the SR has been depleted of Ca. In such a condition we tested the SR Ca re-loading after different rest intervals during which we superfused the cells with normal Tyrode (NT) solution containing 2 mM Ca. A change in IF during rapid cooling was used again as an index of the Ca load of the SR. After 1 and 2 minutes of rest we could record an increase in IF (respectively  $53.3 \pm 9\%$  ( $n=12$ ) and  $104.2 \pm 33\%$  ( $n=5$ ) of the twitch). Such an increase was absent when Ca was removed from the NT solution. In addition, the increase in IF was larger after 1 and 2 minutes in the presence of 4 mM Ca. In absence of  $Ca_e$  and presence of 5 mM Ni, changes in IF during the RCC were not detectable. We conclude that in guinea-pig ventricular myocytes with depleted SR, Ca is re-accumulated during prolonged rest. Such a SR re-loading seems to arise from an extracellular source of Ca.

## Tu-Pos241

EFFECTS OF RYANODINE ON CALCIUM HOMEOSTASIS IN ISOLATED, ADULT RAT CARDIOMYOCYTES. ((M.J. Watson and P.J. Gengo)) Burroughs Wellcome Co., Dept. of Pharmacology, Research Triangle Park, NC 27709. (Spon. by D.G. Lang)

Single cell fura-2 fluorescence imaging was used to study the effects of ryanodine (Ry) on  $Ca^{2+}$  homeostasis in isolated, intact adult cardiomyocytes. In electrically driven (25Hz) cells, our data demonstrates an increase in resting (non-depolarized)  $[Ca^{2+}]_i$  at Ry concentrations from 10nM to 1mM. This increase was accompanied by a decrease in the magnitude of the  $Ca^{2+}$  transient induced by depolarization. Contraction was completely inhibited by concentrations of Ry  $\geq 10\mu M$ ; however, resting  $[Ca^{2+}]_i$  continued to rise when cells were exposed to concentrations of Ry up to 100 $\mu M$  and remained constant thereafter up to 1mM.

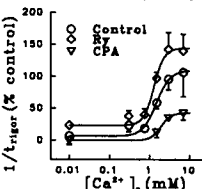
	10nM	1 $\mu M$	10 $\mu M$	100 $\mu M$	1mM
Resting $[Ca^{2+}]_i$ (% increase, pre-Ry $\pm$ SEM)	20.6 $\pm$ 4.8	41.7 $\pm$ 12.3	51.8 $\pm$ 11.0	76.6 $\pm$ 11.9	74.0 $\pm$ 7.3
Transient Magnitude (% of pre-Ry $\pm$ SEM)	95.2 $\pm$ 3.9	77.6 $\pm$ 16.1	21.3 $\pm$ 3.0	29.5 $\pm$ 2.9	24.8 $\pm$ 4.6

At the Ry concentrations used, cells remained viable as assessed by morphology and trypan blue exclusion. We did not encounter any Ry concentration which diminished  $[Ca^{2+}]_i$ , as might be expected with a blockade of the sarcoplasmic reticulum (SR) release channel. These results indicate that Ry (10nM to 1mM), in an intact, contracting cardiomyocyte, increases resting intracellular calcium and inhibits contraction likely by depleting SR calcium stores through a leaking SR-release channel.

## Tu-Pos243

RYANODINE AND CYCLOPIAZONIC ACID HAVE OPPOSITE EFFECTS ON THE RATE OF RIGOR DEVELOPMENT DURING METABOLIC INHIBITION IN RAT CARDIAC TRABECULAE. ((Yingming Zhang, Wei Dong Gao, Henk E.D.J. ter Keurs)) University of Calgary, Calgary, AB, Canada (Spon. by Henk E.D.J. ter Keurs)

Ryanodine (Ry) and cyclopiazonic acid (CPA) are known to interfere with the function of sarcoplasmic reticulum (SR). We investigated the effects of both agents on the rate of ATP depletion during metabolic inhibition. Trabeculae from rat right ventricles, mounted between a force transducer and a motor arm, superfused with Krebs-Henseleit solution (KH) at 30°C, were first depleted of intracellular glycogen reserve by exposure to CN<sup>-</sup>, glucose-free KH (CN-KH) for ~15 min. After full recovery, the trabeculae were exposed to CN-KH again at varied  $[Ca^{2+}]_i$ , while load was controlled at zero. The reciprocal value of the time to maximal rigor force ( $1/t_{rigor}$ ) was used as an index of overall rate of ATP depletion. 10  $\mu M$  Ry and 50  $\mu M$  CPA depressed twitch force (Ft) by 70-80%. Both agents prolonged the duration of contraction by 150%, but the time from peak Ft to half relaxation was prolonged much less by Ry than by CPA (15 $\pm$ 4% vs 57 $\pm$ 15%). Ry increased  $1/t_{rigor}$  while CPA decreased  $1/t_{rigor}$  at all  $[Ca^{2+}]_i$  as shown in the figure. Ry and CPA did not affect  $1/t_{rigor}$  in unstimulated trabeculae suggesting both had no effects on basal metabolism of myocardium. These results indicate that CPA reduces ATP consumption by blocking the SR- $Ca^{2+}$  pump, while Ry enhances ATP consumption by causing a leak of  $Ca^{2+}$  through the SR  $Ca^{2+}$  release channels and thereby increasing the rate of the SR- $Ca^{2+}$  pump.



## Tu-Pos245

EFFECTS OF  $\beta$ -ADRENERGIC AGONISTS ON CONTRACTILITY OF CARDIAC MYOCYTES ISOLATED FROM WILD-TYPE AND PHOSPHOLAMBAN (PLB) DEFICIENT MICE. ((Beata M. Wolska<sup>1</sup>, Wusheng Luo<sup>2</sup>, Evangelia G. Kranias<sup>3</sup> and R. John Solaro<sup>2</sup>)) <sup>1</sup>Univ. of Illinois, Chicago, IL, 60612 & <sup>2</sup>Univ. of Cincinnati, Cincinnati, OH, 45267.

We studied the role of PLB in regulation of cardiac contractility and  $Ca^{2+}$  transient using gene targeting methodology to disrupt the PLB gene in embryonic stem cells. Mice homozygous (-/-) and heterozygous (+/-) for the modified allele were generated. Cardiac myocytes were isolated from these mice and studied in comparison to wild type (+/+) cells. The time to peak contraction and time of relaxation were shorter in myocytes from -/- hearts compared to those from +/+ hearts. In the presence of 0.05  $\mu M$  isoproterenol (ISO), shortening of myocytes isolated from +/+ mice increased 3 fold compared to control contractions. However in myocytes isolated from -/- mice shortening increased only 1.5 times above control. Myocytes from -/- hearts fell into two populations with regard to effects of 0.05  $\mu M$  ISO. One population was similar to -/- myocytes and the other population similar to +/+. Under control conditions, the declining phase of the  $Ca^{2+}$ -transient measured in fura-2 loaded -/- myocytes was faster than that of +/+ myocytes. Moreover, in preliminary experiments, we observed an increase in the peak with little or no change in the kinetics of the  $Ca$ -transient in -/- myocytes responding to ISO. However, as expected, in the +/+ myocytes ISO significantly increased the rate of decline of the  $Ca^{2+}$ -transient.

## Tu-Pos242

OXIDATIVE EFFECTS OF SELENITE ON RAT VENTRICULAR CONTRACTION AND  $[Ca^{2+}]_i$ . ((B. Turan and M. Désilets)) Dept. of Biophysics, University of Ankara, Ankara, Turkey and Dept. of Physiology, University of Ottawa, Ottawa, Canada K1H 8M5.

Selenite ( $SeO_3^{2-}$ ) has been shown in some tissues to cause cell dysfunction that could be imputed to oxidative stress. This possible effect was studied in ventricular preparations from rat heart. Contractile measurements were performed at 35°C on papillary muscles stimulated at 0.1 Hz.  $Na_2SeO_3$  (1 mM) caused a small initial increase in developed force followed by a gradual decline, down to 31 $\pm$ 3% of control value after 20 min exposure (mean $\pm$ SEM, n=7). This decrease was paralleled by an augmentation of resting force (165 $\pm$ 2% of control after 20 min). Fura-2 loaded isolated ventricular myocytes were used to study the effects of selenite on  $[Ca^{2+}]_i$ . At 1 mM, it induced a rapid decrease of the amplitude of the  $Ca^{2+}$  transients (to 46 $\pm$ 8% of control after 5 min; n=10) together with a rise of resting  $[Ca^{2+}]_i$  (137 $\pm$ 7% of control after 5 min). These changes in contraction and  $[Ca^{2+}]_i$ , irreversible on washout of selenite, could be reversed by the disulfide reducing agent dithiothreitol (DTT). Thus, exposure to 1 mM DTT fully restored the  $Ca^{2+}$  transients amplitude and resting  $[Ca^{2+}]_i$ , while the measured tensions returned to within 80% of their initial values. Reducing the temperature to 22°C also entirely prevented the selenite-induced changes of both contraction and  $[Ca^{2+}]_i$ . The results indicate that selenite affects cardiac contractility through temperature-dependent oxidation of protein thiols and consequent alteration of  $[Ca^{2+}]_i$  regulation.

## Tu-Pos244

HYPERTROPHY AND SARCOPLASMIC RETICULUM FUNCTION IN HUMAN AND GUINEA-PIG CARDIOMYOCYTES. ((K. Davia, R. Naqvi, K.T. Macleod, and S.E. Harding)) Dept Cardiac Medicine, NHLI, Dovehouse St, London SW3 6LY, UK.

Cardiac hypertrophy is thought to contribute to diastolic dysfunction in human heart failure. We used enzymatically isolated myocytes from failing (F) and non-failing (NF) human ventricle and from the Goldblatt model of renal hypertension in the guinea-pig to investigate impaired sarcoplasmic reticulum (SR) function as a cause of prolonged relaxation in hypertrophy. We have previously shown that left ventricular myocytes from heart failure patients (F) have an increased time-to-peak contraction (TTP) and time to half relaxation (R50) compared with myocytes from non-failing (NF). Myocytes from NF were more sensitive to the SR  $Ca^{2+}$ -ATPase inhibitor, thapsigargin (TG) than those from F. TG (1 $\mu M$ ) increased TTP (42 $\pm$ 12% n=8, P<0.02, NF cf 17 $\pm$ 8% n=8, P=NS, F) and prolonged R50 (220 $\pm$ 94%, P<0.01, NF cf 41 $\pm$ 26%, P=NS, F). Myocytes from the hypertrophied left ventricle of Goldblatt guinea-pigs (H) exhibited prolonged relaxation compared with sham-operated animals (S): R50 (0.12  $\pm$  0.02 n=9, H cf 0.08  $\pm$  0.004 n=5, S P<0.001). Ventricular myocytes isolated from S were more sensitive to TG than those from H. Decreases in contraction amplitude (42 $\pm$ 6% n=4, P<0.01, S cf 19.2 $\pm$ 7% n=7, P<0.05, H) and increases in R50 (62 $\pm$ 8% n=4 P<0.01, S cf 4 $\pm$ 11% n=6, P=NS, H) with TG were smaller in H. Changes in contraction after rest periods were also used to investigate SR function. The amplitude of the first beat following 3 min rest was significantly decayed compared to steady-state levels in NF myocytes (26 $\pm$ 7% n=8) but not F (115 $\pm$ 18% n=19, P<0.001). However, post rest beats of myocytes from H and S were not significantly different, both showing decay. We conclude that hypertrophy mimics some, but not all, SR alterations seen in human heart failure.

## Tu-Pos246

MODULATION OF MYOCYTE CONTRACTILITY BY ARACHIDONIC ACID. ((D. Damron, B. Summers and M. Bond)) The Center for Anesthesiology Research and Dept. of Molecular Cardiology, The Cleveland Clinic Foundation, Cleveland, OH 44195

The release of arachidonic acid (AA) by phospholipases in response to cell surface receptor activation may be an important step in triggering non-cAMP-dependent inotropic responses in cardiac muscle. We previously showed that AA inhibited the transient outward  $K^+$  current ( $I_{TO}$ ) in rat ventricular myocytes resulting in prolongation of action potential duration (Damron et al., JBC, 1994). In this study, we used video edge detection of single, field stimulated (0.5 Hz) adult rat ventricular myocytes to examine the functional effects of AA on myocyte contractility. Superfusion of ventricular myocytes with AA (12.5  $\mu M$ ) resulted in a 34% increase in the amplitude of myocyte shortening. The AA-stimulated increase in myocyte shortening was reduced by 82% when the myocytes were first pretreated with staurosporine suggesting the involvement of a protein kinase in the inotropic actions of AA. A 28% increase in the amplitude of myocyte shortening was also observed when the myocyte was superfused with the  $K^+$  channel blocker 4-amino pyridine (2 mM, 4-AP). However, superfusion of the myocyte with 4-AP followed by AA had no additional effect on the amplitude of myocyte shortening. In contrast, superfusion of the myocyte with the  $Ca^{2+}$  channel agonist Bay K8644 following 4-AP resulted in a 13% increase in the amplitude of myocyte shortening above that observed with 4-AP alone. These results demonstrate that AA enhances myocyte contractility and suggest that protein kinase-dependent inhibition of  $K^+$  channels may be involved in mediating this inotropic event. We conclude that AA may be involved in the modulation of inotropic activity in cardiac muscle by inhibition of  $K^+$  channels, thus increasing  $Ca^{2+}$  entry into the cell and enhancing contractile function.



## Tu-Pos247

BETA ADRENERGIC RECEPTOR SUBTYPE MODULATION OF CALCIUM IN VENTRICULAR MYOCYTES. ((Michael A. Laflamme and Peter L. Becker)) Dept. of Physiology, Emory University, Atlanta, GA 30322.

The relative role of different  $\beta$ -adrenergic receptor subtypes in regulating cytosolic  $Ca^{2+}$  in the heart is controversial. We examined this issue by studying the effect of  $\beta$ -receptor activation on  $[Ca^{2+}]_i$  transients induced by depolarization in voltage clamped rat ventricular myocytes under conditions that controlled for chronotropic actions. Isolated myocytes were patch clamped in whole-cell mode with pipettes containing predominantly CsCl along with the calcium sensitive dye fura-2. Fluorescence was monitored with a high time resolution microfluorimeter to estimate  $[Ca^{2+}]_i$  changes. Cells were exposed to the mixed  $\beta$ -receptor agonist isoproterenol (ISO) or the selective  $\beta_2$  agonist zinterol (Zint) during repetitive 300 msec depolarizations imposed at 0.6 Hz to 0 mV from a holding potential of -40 mV. Consistent with the findings of others,  $10^{-6}$  M ISO increased peak  $I_{Ca}$  by  $85 \pm 30\%$  ( $n=4$ ) and the  $[Ca^{2+}]_i$  transient magnitude (estimated from 340/380 FI ratio) by  $28 \pm 17\%$  and accelerated the rate of  $[Ca^{2+}]_i$  fall (the time for FI ratio to fall from 75 to 25% of peak decreased to  $35.9 \pm 4.2\%$  of control).  $10^{-5}$  M Zint had only modest effects: in 5 cells there was  $27 \pm 6\%$  increase in peak  $I_{Ca}$  (with no significant alteration in the timecourse of inactivation) and a slight increase in the rate of  $[Ca^{2+}]_i$  fall (75-25% time decreased to  $66.5 \pm 6.1\%$  of control) although the  $[Ca^{2+}]_i$  magnitude was not significantly altered ( $106 \pm 12\%$  of control). Thus, our results suggest that  $\beta_2$  receptors have, at most, only a minor role in altering cardiac contractility via direct actions on calcium pathways.

## Tu-Pos249

ACIDOSIS INHIBITS  $Ca^{2+}$  LOADING AND  $Ca^{2+}$ -INDUCED  $Ca^{2+}$  RELEASE FROM THE SR IN SAPONIN-SKINNED RAT MYOCARDIUM ((J.C. Kentish and J-Z Xiang)) Dept. Pharmacology, U.M.D.S., St. Thomas' Campus, London SE1 7EH, U.K.

We investigated the actions of pH (7.4 - 6.5) on  $Ca^{2+}$  handling by the SR of cardiac muscle, using saponin-skinned trabeculae from rat right ventricle. The SR of the muscles was loaded at  $0.2 \mu M$   $Ca^{2+}$  for 3 min before (i) the  $Ca^{2+}$  loading of the SR was assessed by rapidly applying caffeine (10 mM), or (ii)  $Ca^{2+}$ -induced  $Ca^{2+}$  release (CICR) was triggered by flash photolysis of the "caged"  $Ca$ , nitr-5 (0.1 mM).  $Ca^{2+}$  release was measured with fluo-3. The caffeine-induced  $Ca^{2+}$  transient was maximal at the control pH of 7.1, where it reached  $0.87 \pm 0.08 \mu M$  (mean  $\pm$  S.E.,  $n=8$ ). It declined to  $40 \pm 4\%$  of control at pH 6.5 and to  $63 \pm 7\%$  at pH 7.4. The  $Ca^{2+}$  transient during CICR was  $0.46 \pm 0.07 \mu M$  ( $n=14$ ) at pH 7.1. This was not changed at pH 7.4, but was markedly reduced to  $19 \pm 9\%$  of control at pH 6.5. These results indicate that pH affects SR  $Ca^{2+}$  loading and CICR, though CICR is affected less than  $Ca^{2+}$  loading by alkalosis, and more than  $Ca^{2+}$  loading by acidosis. This suggests that the  $Ca^{2+}$  release mechanism of CICR is inhibited as pH falls. Our conclusion concurs with that from studies using  $Ca^{2+}$  channels in lipid bilayers (Rousseau & Pinkos, *Pflügers Arch.* 415, 645-647 [1990]) but disagrees with a previous skinned muscle study by Fabiato (*Cell Calcium* 6, 95-108 [1985]), who reported that pH affected CICR only as a result of altered SR  $Ca^{2+}$  loading. Supported by the British Heart Foundation.

## FOLDING-ASSEMBLY I

## Tu-Pos250

GroEL STABILIZES EARLY REFOLDING INTERMEDIATE OF GLYCERALDEHYDE 3-PHOSPHATE DEHYDROGENASE ((K.C. Wisser<sup>†</sup>, J.A. Schaeuete<sup>‡</sup>, D.G. Steel<sup>†§</sup> & A. Gafni<sup>†§</sup>)) <sup>†</sup>Instof Gerontology, <sup>§</sup>Deptof Biological Chemistry, <sup>§</sup>Dept of Physics and Electrical Engineering, University of Michigan, Ann Arbor, Mich. 48109

Refolding intermediates of Glyceraldehyde 3-Phosphate Dehydrogenase (GAPDH) observed during spontaneous and GroEL assisted renaturation from 4M GdCl<sub>3</sub> were characterized by extent of their regaining of activity and by room temperature phosphorescence - a sensitive indicator of protein structure. It is well known that UV radiation induces photochemical changes in proteins. Indeed, we observed that illumination by UV light (@290nm, deoxygenated conditions) during the early stages of spontaneous refolding inhibits the recovery of enzymatic activity of GAPDH. Native GAPDH or GAPDH at later stages in refolding were not as susceptible to the loss of activity caused by UV exposure. In addition, it was determined that GAPDH bound to the molecular chaperonin GroEL is locked in a refolding intermediate that remains susceptible to UV irradiation. We have previously shown that GroEL binds GAPDH irreversibly in the absence of Mg-ATP (and quickly releases it upon Mg-ATP addition). When the GAPDH/GroEL complexes were exposed to UV at different times after formation of the complex, and the complex was subsequently dissociated with Mg-ATP, it was observed that the UV exposed complexes had <25% activity of non-UV exposed samples independent of the time between complex formation and UV irradiation. This infers that the UV sensitive early folding intermediate of GAPDH is bound to GroEL but is not protected against UV irradiation and does not progress to the stage where UV sensitivity is lost. Binding to GroEL, while greatly enhancing the yield of GAPDH reactivation, arrests the intermediates in an early folding stage. [NIA grant #AG09761 and ONR N00014-91-J-1938]

## Tu-Pos248

DIFFERENTIAL PHOSPHORYLATION OF SERINE-16 AND THREONINE-17 OF PHOSPHOLAMBAN IN ISOLATED RAT AND FERRET VENTRICULAR MYOCYTES. ((K.L. Bennett, C.H. Orchard and J. Colyer\*)) Department of Physiology and \*Department of Biochemistry and Molecular Biology, University of Leeds, Leeds, LS2 9NQ, U.K.

Phospholamban is a protein, found in the cardiac sarcoplasmic reticulum membrane, which inhibits the activity of the  $Ca^{2+}$ -ATPase. When phospholamban is phosphorylated the inhibition is removed. Such phosphorylation can occur at two sites: serine-16 by PKA and threonine-17 by a  $Ca^{2+}$ -calmodulin-dependent protein kinase. We have investigated the possibility of differential phosphorylation of these phosphorylation sites. Rat and ferret ventricular myocytes were stimulated at 0.5 Hz and exposed to either: (i) physiological salt solution containing  $750 \mu M$   $Ca^{2+}$  (control); (ii)  $2 \times 10^{-7}$  mol/l isoprenaline or (iii) a bathing  $[Ca^{2+}]$  of 6mM. Protein samples were separated by SDS polyacrylamide gel electrophoresis and the phosphorylated forms of phospholamban detected using antibodies which are specific for phospholamban when phosphorylated at Serine-16 or Threonine-17 (Drago and Colyer, 1994, *J. Biol. Chem.* 269, in press). In rat cells there was no detectable phosphorylation of either site in control conditions or when bathing  $[Ca^{2+}]$  was increased. Isoprenaline resulted in the phosphorylation of Serine-16 alone. The addition of isoprenaline to ferret cells phosphorylated Serine-16 only, whereas increasing bathing  $[Ca^{2+}]$  caused the phosphorylation of Threonine-17 only. Since it is possible to detect the phosphorylation of Threonine-17 in homogenized rat heart with these antibodies these data suggest that there may be a species difference in the use of the Threonine-17 phosphorylation site of phospholamban. This in turn may affect the activity of the  $Ca^{2+}$ -ATPase of the sarcoplasmic reticulum. (Supported by the Medical Research Council, British Heart Foundation and Pfizer.)

## Tu-Pos251

ATP INDUCES A CONFORMATIONAL CHANGE IN BOVINE HSC70 AFTER INITIAL BINDING, BUT BEFORE HYDROLYSIS. ((J.-H. Ha, S. M. Wilbanks and D.M. McKay)) Beckman Laboratories for Structural Biology, Department of Structural Biology, Stanford University, Stanford, CA 94305. (Spon. by Lubert Stryer)

Hsc70 and dnaK have at least two distinct conformations: high peptide affinity state and the low peptide affinity state. The transition to low peptide affinity state can be induced by binding of ATP, but not by nonhydrolyzable ATP analogs. Consistent with this model, we observed ~10% change in trp fluorescence signal upon binding of ATP, but ~2% change upon binding of ATP analogs or of ADP. The rate constant increases with  $[hsc70]$  to a maximum value of  $0.7 \text{ sec}^{-1}$  at  $25^\circ\text{C}$ . This is more rapid than the ATP hydrolysis rate of  $0.003 \text{ sec}^{-1}$ , but slower than the rate of initial ATP binding determined by  $k_{on} = 2.7 \times 10^5 \text{ M}^{-1} \text{ sec}^{-1}$ . We propose that hsc70 undergoes conformational change after the ATP binding step, but before the chemical hydrolysis step of ATP:



A similar change in fluorescence upon ATP addition was observed with a 60 kDa truncated product (1-554). Small angle scattering experiment showed that ATP binding induces the decrease in an apparent radius of gyration ( $R_g$ ) of hsc70 and 60 kDa fragment, but not in  $R_g$  of the 44 kDa fragment which has peptide-independent ATPase activity. The change in  $R_g$  was not observed with association with ADP nor ATP analogs. These results suggest that the observed change in trp fluorescence signal may reflect a dramatic conformational change in hsc70 upon binding to ATP, and only to ATP.

## Tu-Pos252

STUDIES OF THE THREE DIMENSIONAL STRUCTURE OF THE PARTIALLY UNFOLDED INTERMEDIATE OF A THERMALLY LABILE MUTANT (M64L AND M98L) OF YEAST ISO-2-CYTOCHROME *c*. ((Alice R. Ritter\*, Ying Shi\*, Alice Fisher\*, James A. Ferretti\*, and Hiroshi Tanluchi\*) \*Laboratory of Biophysical Chemistry, NHLBI, and \*Laboratory of Chemical Biology, NIDDK, NIH, Bethesda, MD 20892.

We have cloned and expressed a mutant yeast iso-2-cytochrome *c* protein (M64L and M98L) which is destabilized with increasing temperature relative to the wild type protein (the phagemid containing the wild type gene was kindly provided by C. Mackinnon & B. Nall; the yeast strain by M. Smith & B. Hall). Circular Dichroism spectra at pH 6.0 show that the mutant protein begins to unfold at 25°C, exists as a partially unfolded intermediate up to 45°C, and globally unfolds at higher temperature. Additionally, we monitored the 695 nm Fe<sup>3+</sup>-S charge transfer band at pH 6.0 and observed analogous behavior. Examination of the one dimensional <sup>1</sup>H NMR spectra of the double mutant protein between 27°C and 42°C shows distinct changes. A number of resonances broaden with increasing temperature, including those of the heme and amino acid residues in the vicinity of the heme. We have used multidimensional NMR techniques coupled with distance geometry computations, back-calculation of NOE spectra, and minimum energy computations to obtain the secondary and tertiary structures of the intermediate state of the mutant protein. Our data suggest that the M98L mutation is primarily responsible for destabilization of the mutant protein relative to the wild type.

## Tu-Pos254

TEMPERATURE AND PRESSURE INDUCED UNFOLDING STUDIES WITH UNSTABLE MUTANTS OF *STAPHYLOCOCCAL* NUCLEASE. ((M.R. Eftink)) Department of Chemistry, University of Mississippi, University, MS 38677, and ((G.D. Ramsay)) AVIV and Associates, Lakewood, MD 08701

Nuclease conA (NCA) and nuclease V66W are mutant proteins that have reduced thermodynamic stability (NCA) and multi-state unfolding transitions (V66W). We have studied the temperature, pressure, and denaturant induced unfolding of these mutant proteins. For NCA we find a free energy change for unfolding,  $\Delta G^\circ_{un}$ , of ~1.5 kcal/mol at pH 7, 0.1 M NaCl, 20 °C, as compared to a value of 5.5-6 kcal/mol for wild type nuclease. NCA shows evidence of cold unfolding, having a  $\Delta C_p$  of 1.7 kcal/mol-K. Increased pressure unfolds NCA in what appears to be a two-state manner with an apparent  $\Delta V_{un}$  of about -100 mL/mol. From studies of the pressure induced unfolding of NCA as a function of temperature, we have constructed a P-T free energy surface for the unfolding reaction. Using a multi-dimensional CD/fluorescence instrument we find the guanidine-HCl induced unfolding of V66W to be well described by a three-state transition, in agreement with the work of Gittis et al. *J. Mol. Biol.* 232 718. We will report studies of the pressure induced unfolding of V66W, showing this mutant to have a lower  $-\Delta V_{un}$  than that found for the wild type nuclease. Although the pressure induced unfolding of V66W shows a bi-phasic transition, the smaller  $-\Delta V$  is consistent with a multi-state unfolding transition for this protein. This research was supported by NSF grant MCB 9407167.

## Tu-Pos256

RELATIONSHIP OF PROTEIN DESTABILIZATION BY DIAMIDE, ARSENITE AND OTHER SULFHYDRYL SPECIFIC AGENTS TO HSP INDUCTION. Senisterra G. and Lepock J. Department of Physics, University of Waterloo, Waterloo, Ontario, N2L 3G1, Canada

A number of chemicals agents which damage proteins are known to induce heat shock protein (HSP) synthesis. Chemical modification per se is not sufficient for induction even if it results in inactivation, but unfolding to some extent apparently is necessary. We use the Ca<sup>++</sup>-ATPase of sarcoplasmic reticulum as a model system for investigation of the effects of the sulfhydryl specific agents diamide and arsenite, both HSP inducers, on protein structure and compare these to the effects of other sulfhydryl specific agents. The Ca<sup>++</sup>-ATPase has 20 cys residues and denatures with a  $T_m$  of 50 °C as shown by differential scanning calorimetry (DSC). Treatment with diamide, arsenite, or NEM such as to titrate 6 to 8 cys residues destabilizes the protein ( $T_{ma}$  40 °C) resulting in denaturation at 37 °C. Treatment with higher concentrations of diamide and NEM, the more reactive agents, titrates nearly all cys residues and both denatures and inactivates the Ca<sup>++</sup>-ATPase. Both the thermally and chemically denatured proteins have increased exposure of hydrophobic residues, as shown by increased ANS fluorescence, which leads to aggregation. Labeling with the fluorescent probes Br-DMC (cys 344) or IAEDANS (cys 670 and cys 674) which react with only one or two cys residues neither destabilizes nor denatures the Ca<sup>++</sup>-ATPase. Thus, covalent attachment to several cys residues appears necessary to induce enough conformational strain in the Ca<sup>++</sup>-ATPase for sufficient destabilization to cause denaturation at 37 °C. The chemically denatured state has properties similar to that of the thermally denatured state.

## Tu-Pos253

THERMODYNAMIC STABILITY OF *STAPHYLOCOCCAL* NUCLEASES CONTAINING A CONSTRAINED TRYPTOPHAN ANALOG OR 5-HYDROXY-TRYPTOPHAN. ((C.Y. Wong)) Department of Biology, Johns Hopkins University, Baltimore, MD 21218 and ((M.R. Eftink)) Department of Chemistry, University of Mississippi, University, MS 38677.

A conformationally constrained tryptophan analog, WI (L-2,3,4,9-tetrahydro-1-H- $\beta$ -carboline-3-carboxylic acid), has been incorporated into *Staphylococcal* nuclease A. Although constrained amino acids, other than tryptophan, have been incorporated into proteins, they do not have the spectral characteristics necessary for a good probe. By choosing the appropriate constrained tryptophan analog, selected  $\phi$ ,  $\Psi$ ,  $\chi_1$ , and  $\chi_2$  angles can be imposed on local protein/peptide structure. We have constructed an *E. coli*/tryptophan auxotroph, strain UM1, that harbors the plasmid for *Staph* nuclease under the control of the  $\lambda$  P<sub>L</sub> promoter. Protein was expressed on these cells grown in the presence of WI or 5-hydroxy-tryptophan (5-HT, which was used as a control for tryptophan analog incorporation, due to its easily observed, red-shifted absorbance). Time-resolved fluorescence intensity and anisotropy data, CD and absorbance spectra were determined for WI-nuclease and 5-HT-nuclease. The guanidine-HCl induced unfolding of these forms of nuclease was monitored using a multi-dimensional spectrophotometer, which enables nearly simultaneous measurement of CD and fluorescence signals for the transition. A reversible, two-state transition is found for both WI-nuclease and 5-HT-nuclease. This research was supported by NSF grant MCB 9407167.

## Tu-Pos255

DETECTION OF A STABLE INTERMEDIATE IN THE THERMAL UNFOLDING OF A MUTANT FORM OF DIHYDROFOLATE REDUCTASE FROM *E. COLI*. ((J. Luo and C. R. Matthews)), Department of Chemistry, Center for Biomolecular Structure and Function, and Biotechnology Institute, The Pennsylvania State University, University Park, PA 16802

The reversible temperature-induced unfolding of a cysteine-free mutant (C85S/C152E) of dihydrofolate reductase from *E. coli* has been studied by absorbance and by both far and near ultraviolet circular dichroism spectroscopies. The non-coincidence of all three transition curves demonstrates the existence of a highly populated partially-folded form in the transition region. This intermediate retains substantial secondary structure but has lost specific tertiary packing around its tryptophan residues. Increases in enthalpy, entropy and heat capacity are observed for both the native/intermediate and intermediate/unfolded transitions; the majority of the changes in these parameters occurs in the first transition. The structure of the intermediate can be completely disrupted by addition of 0.5 M urea. These results suggest that the stable intermediate detected in the thermal unfolding reaction of this double mutant of dihydrofolate reductase resembles a molten globule. This work is supported by NSF grant MCB 9317273 to CRM.

## Tu-Pos257

CHEMICAL DENATURATION OF BOVINE PANCREATIC RIBONUCLEASE A: MONOHYDRIC ALCOHOL-MEDIATED DENATURATION. ((S. Subbiah, J. Vargas, S. Arora, and R. G. Biringer)) San Jose State University, San Jose, CA 95192-0101

The importance of the various factors that contribute to the stability of proteins has been the subject of controversy for many years. It is apparent from the vast amount of experimental work that both hydrogen bonding and the hydrophobic effect are the major contributors, but the relative importance of each has yet to be determined. We have examined the concentration-mediated denaturation of bovine pancreatic ribonuclease A (RNase A) with monohydric alcohols at constant protonic activities of 3 and 4. Transition midpoints decrease with increasing hydrophobicity of the alcohol. The higher alcohols show coincident fluorescence and CD transitions. The CD-monitored methanol-mediated transition shows an increase in the signal amplitude at 222 nm followed by the expected decrease. Such results indicate the formation of non-native secondary structure in the early portion of the denaturation transition. The effect of methanol on the urea-mediated and guanidinium ion-mediated denaturation of RNase A at pH\* 4 has also been examined. Methanol serves to lower the transition midpoints for all denaturants examined. The effect is inversely related to the denaturant strength suggesting that methanol and the respective denaturants compete for the same binding sites on the protein.

## Tu-Poe258

**DIFFERENTIAL STABILITIES OF RECOMBINANT AND NATIVE MYOGLOBINS.** ((M. S. Hargrove, E. M. Scott, and J. S. Olson)) Dept. of Biochemistry and Cell Biology, Rice University, Houston, TX, 77251.

The overall stability of myoglobin is a function of apoglobin stability and heme affinity, and the factors governing these two phenomena are not necessarily related. Heme is held in ferric myoglobin by a weak covalent bond between His93 and the Fe atom, steric interactions between the porphyrin and key residues along the C, E, F, and G helices, and a polar interaction involving the heme propionates. When heme dissociates, the resulting apomyoglobin loses some secondary structure but remains a fairly compact globular protein. Upon unfolding, apomyoglobin passes through a partially folded intermediate state in which the heme pocket is unfolded, and the A, G, and H helices remain as a folded core region. Each step in the unfolding of apomyoglobin can be visualized by monitoring fluorescence emission as a function of denaturant. Some abnormally stable apomyoglobins have been constructed and show an additional early unfolding event. Structural and functional studies of these mutants suggest that their apoglobins are more tightly folded than wild type apomyoglobin.

Rates of heme loss from myoglobins of different species are nearly identical. However, apoglobin stabilities vary markedly in spite of relatively conservative sequence differences. Some residues in sperm whale myoglobin have been mutated in an effort to determine which individual residues are responsible for the species differences. Regions of interest include the A helix and the E-F corner. Mutations in this region appear to have a large effect on both apoglobin unfolding transitions. Supported by NIH GM08280 (MSH), GN35649 (ISO), the Robert A. Welch Foundation, and the W. M. Keck Center for Computational Biology.

## Tu-Poe260

**REFOLDING AND REACTIVATION OF ACID-DENATURED AND EDTA INACTIVATED *E. COLI* ALKALINE PHOSPHATASE STUDIED BY PHOSPHORESCENCE SPECTROSCOPY.** ((V. Subramaniam)) Applied Physics Program & Inst. of Gerontology, University of Michigan, Ann Arbor, MI 48109.

Room temperature phosphorescence (RTP) spectroscopy is an exquisitely sensitive probe of the protein environment surrounding the emitting residue. We recently demonstrated that when *E. coli* alkaline phosphatase (AP) is refolded from chaotropically denatured (GuHCl) states, the structural rigidity of the protein core, measured by the RTP lifetime, returns to native-like levels long after the recovery of enzymatic activity, reflecting a process akin to annealing in the protein interior. In contrast, when AP is renatured following denaturation at low pH (50mM phosphate, pH 2), which disrupts the electrostatic interactions that help stabilize the folded state, the RTP recovers faster than in the GuHCl denatured case, though still lagging recovery of enzyme activity. Distribution analysis of the RTP decays using the maximum entropy method clearly reveals the presence of at least two intermediates characterized by short RTP lifetimes, indicating softer protein cores with diminished global stability. We also reactivate AP inactivated in EDTA by adding excess  $Zn^{2+}$  and  $Mg^{2+}$ . EDTA chelates the 2  $Zn^{2+}$  and 1  $Mg^{2+}$  ions per monomer in AP that are required for RTP and enzyme activity, but does not cause extensive unfolding of the protein. Thus reactivation by the addition of excess metal ions should restore both activity and RTP immediately. Our results support this hypothesis; both enzymatic activity and RTP return within the dead time of the mixing. Interestingly, while the addition of  $Mg^{2+}$  alone restores native-like RTP, there is no return of activity. Addition of  $Zn^{2+}$  alone restores both RTP and enzyme activity; however, the RTP lifetime slowly increases, indicating annealing of an initially soft core. The data reflect the different roles played by the metal species in the structural rearrangements which lead to increased rigidity of the structure around the phosphorescent residue, Trp 109. [NIA AG09761; ONR N00014-91-J-1938]

## Tu-Poe262

**PROTEIN FOLDING: ELECTROSTATIC AND THERMODYNAMIC PROPERTIES OF TRANSIENT CONFORMATIONS IN THE FOLDING PATHWAY.** ((Mikael Oliveberg and Alan R. Fersht)) CPE, MRC Centre, Cambridge CB2 2QH, UK

By kinetic and thermodynamic methods we have investigated the acid-titration behaviour and thermodynamic properties of 4 conformations in the folding pathway of barnase: the denatured state (D), an apparent folding intermediate (I), the major transition barrier ( $\ddagger$ ) and the native state (N).

Some of the highly anomalous  $pK_A$  values found in  $\ddagger$ , but salt-accessible surface interactions appear to be lost and the overall protection of titrating residues is weakened. The heat capacity of  $\ddagger$  is similar to that of N. The transition barrier for unfolding is both enthalpic and entropic, whereas the barrier for refolding is predominantly entropic. Our results suggest that  $\ddagger$  is an expanded form of the native state with loosened-up peripheral parts, and a "swollen" but non-hydrated core.

The folding intermediate (I) shows a heat capacity closer to that of N than of D, suggesting the presence of a non-hydrated core or non-hydrated hydrophobic elements. At pH 6.3, the thermal unfolding transition of I takes place between 30 °C and 50 °C, and it is shifted only to a small extent at pH 1.5. Hence, the titration properties of I appear similar to those of D, so that at low pH and 25 °C I does not unfold completely but constitutes the acid-denatured state.

The  $pK_A$  values of the (thermally) denatured state (D) are on average 0.4 units lower than those of model compounds, suggesting that also this state is compact (or partly structured) and involves intra-molecular interactions (charge repulsions).

## Tu-Poe259

**THERMODYNAMIC STABILITY OF CHYMOTRYPSINOGEN A,  $\alpha$ -CHYMOTRYPSIN AND RIBONUCLEASE A IN GLYCEROL.** ((Paul W. Chun)) Dept. of Biochem. and Mol. Biol., University of Florida, Gainesville, FL 32610-0245

We describe a method of evaluating the temperature-invariant chemical bond energy,  $\Delta H^0(T_0)$ , for chymotrypsinogen A and ribonuclease A in aqueous glycerol solution in the standard state in order to determine the effect of glycerol on the thermodynamic stability of these two proteins. Benzinger's definition (1) is applied to measure the temperature-invariant chemical bond energy,  $\Delta H^0(T_0)$ . Using the Planck-Benzinger thermal work function, it is possible to determine the different types of thermodynamic compensation operating in these systems. (i) For chymotrypsinogen A, in the absence of glycerol, no thermodynamic compensation between  $\Delta H^0(T)$  and  $\Delta S^0(T)$  is observed nor is any  $\langle T_0 \rangle$  observed. In the presence of glycerol, the magnitude of  $\Delta H^0(T)$  and  $\Delta S^0(T)$  are equivalent between  $\langle T_0 \rangle$ , the harmonic temperature at which  $\Delta G^0(T)$  and  $\Delta C_p^0(T)$  approach zero and  $\Delta H^0(T)$  and  $\Delta S^0(T)$  intersect, and  $\langle T_0 \rangle$ . (ii) In  $\alpha$ -chymotrypsin dimerization, where  $\langle T_0 \rangle$  ranges from 220-325°K, enthalpy-entropy compensation takes precedence. (iii) In ribonuclease A in the absence of glycerol,  $\langle T_0 \rangle$  ranges from 50-325°K, and the process operating seems to be one of entropic compensation: this widening temperature range is typical of the unfolding process. In the presence of glycerol at concentrations of 20% or higher,  $\langle T_0 \rangle$  ranges from 220-325°K, and enthalpy-entropy compensation is operating. This work was supported by a Faculty Development Award, DSR, University of Florida.

## Tu-Poe261

**Polyamines Stabilizes the Folding of Ca binding protein Parvalbumin** ((K. Sudhakar, J. M. Vanderkooi & M. Erecinska)) Dept. of Biochem. & Biophys., & Dept. of Pharmacology, School of Medicine, University of Pennsylvania, Philadelphia, PA 19104. (Spon. by J. M. Vanderkooi).

The determinants of Ca homeostasis in cells is the subject of continuing interest. Polyamines and the Ca binding protein parvalbumin are found specifically in particular actively metabolizing nerve cells, and their function and possible interrelations are unknown. The interaction of spermine, spermidine and putrescine with the parvalbumin, was studied with the help of the fluorescence, phosphorescence and circular dichroism spectroscopy. At physiological concentrations these polyamines interact with the Ca-free form or denatured form of parvalbumin, while no interaction with Ca-bound form was observed. These studies indicate that the polyamines protect against the unfolding of the protein and stabilizes the Ca bound protein. The binding affinities to the Ca-free form are 3 mM for spermine, 10 mM for spermidine and >25 mM for putrescine, as detected by a change in the fluorescence emission of tryptophan. CD spectroscopy reveals the polyamines increase in the ellipticity of Ca-free parvalbumin, showing that binding produces a conformational change of the protein. (Supported by NIH GM 34448).

## Tu-Poe263

**FAST REFOLDING OF COLD UNFOLDED PROTEIN** ((Bengt Nölting and Alan R. Fersht)) Cambridge Centre for Protein Engineering, MRC Centre, Hills Road, Cambridge CB2 2QH, U.K. (Spon. by Keiko Hirose)

Using a combination of cold unfolding, double temperature jump and fluorescence detection we have discovered, at pH 2, 3-5 M urea and temperatures between less than 4 °C and more than 16 °C a fast refolding phase in bovine  $\beta$ -lactoglobulin A. Its unusually fast rate constant increases with temperature, reaching about 300 s<sup>-1</sup> at 16 °C. The observed amplitude of the fast refolding kinetics was only about 0.5% change in relative fluorescence for an 8 K jump. After incubating lactoglobulin at -4 °C in 4.5 M urea for several hours the amplitude of the kinetics decayed following a single exponential with a rate constant of 10<sup>-4</sup> s<sup>-1</sup>, indicating that the fast transition is located before the 6 orders of magnitude slower, main transition of unfolding. The high speed and small amplitude of the kinetics of the fluorescence signal indicate that it reflects only small change in structure, or a fast transition between states of similar energy separated by a low barrier or both of that. This early step of cold unfolding might represent a transition between native-like substates.

## Tu-Poe264

**A SOLUBLE FRAGMENT FROM THE ASPARTATE RECEPTOR DISPLAYS PROPERTIES OF A MOLTEN GLOBULE STATE** ((S.K. Seeley, G.K. Wittrock, R.M. Weis, and L.K. Thompson)) University of Massachusetts, Amherst, MA 01003. (Spon. by L.K. Thompson)

The transmembrane aspartate receptor is central to bacterial chemotaxis and is organized into a periplasmic ligand-binding domain, two transmembrane helices, and a cytoplasmic signaling domain. We are seeking insights into the mechanisms of signaling and adaptation by investigating the changes which occur in a 31 kDa cloned fragment that encodes the cytoplasmic domain (c-fragment). Point mutations in the cytoplasmic domain have been found which lead to either of the two behavioral extremes of constant tumbling or constant smooth-swimming, providing evidence for two signaling states of the receptor. Recent studies have revealed a monomer-oligomer equilibrium and correlated the smooth-swimming behavioral phenotype with the tendency to form oligomers. We have characterized the association/dissociation process by studying the dissociation kinetics for two oligomer-forming c-fragment proteins using gel filtration chromatography and circular dichroism. We have also studied the secondary structure of isolated monomer and oligomer forms using far-UV CD. These studies indicate the dissociation process proceeds through a highly unfolded intermediate and that the c-fragment monomeric proteins are partially unfolded. A model is used to describe these results where intermolecular coiled-coil interactions in the oligomer are substituted by intramolecular contacts in the monomer. NMR and near-UV CD reveal unusually dynamic properties for both the monomeric and oligomeric forms of the c-fragment and indicate that they share structural characteristics with the "molten globule" state. Results from these studies raise the question of whether or not the dynamic, molten globule-like structure is relevant to signaling.

## Tu-Poe266

**STUDIES OF LYSOZYME FOLDING BY SYNCHROTRON SMALL-ANGLE X-RAY SCATTERING** ((Lingling Chen, Sebastian Doniach and Keith O. Hodgson)) Department of Chemistry and Department of Applied Physics, Stanford University, Stanford, CA 94305

The folding of lysozyme was studied by both static and time-resolved small-angle x-ray scattering (SAXS). Lysozyme was denatured in concentrated urea solution with the disulfide bonds intact. Equilibrium measurements were performed over a series of urea concentrations and at different pH conditions. The radius of gyration increases with urea concentration from ~14 Å to ~22 Å. At pH ~2.9 the most rapid increase of  $R_g$  occurs at 4M urea, consistent with published CD spectra observations. Distance distribution  $P(r)$  functions were evaluated for the native and denatured states.  $P(r)$  function for the native state is characteristic of a globular protein, and correlates well with  $P(r)$  computed from the crystal structure. The shape of  $P(r)$  function for the denatured state indicates that the molecules are partially unfolded: the form is distinct from a random coil. The maximum intramolecular distance is enlarged substantially from ~44 Å to ~75 Å. The presence of a well defined peak in the Kratky plot of the native state demonstrates again a compact globular structure of the folded molecule. The peak diminishes in the denatured state, indicating a partial loss of compactness of the unfolded molecules.

Time-resolved SAXS investigations of lysozyme folding were carried out using a stopped-flow method. The refolding is initiated by rapid dilution of the unfolded lysozyme in concentrated urea solution with a buffer containing no denaturant. A decrease is observed in  $R_g$ , with the final value corresponding well to the  $R_g$  obtained from equilibrium measurements. The time constants for refolding (on the scale of seconds) are consistent with those reported from optical measurements. The forward intensity remains fairly constant throughout refolding, indicating that no significant dimer intermediate occurs in contrast to that observed in the refolding of myoglobin.

## Tu-Poe268

**CONTRIBUTIONS OF TRYPTOPHAN SIDE CHAINS TO THE CIRCULAR DICHROISM OF GLOBULAR PROTEINS: EXCITON COUPLETS AND COUPLED OSCILLATORS.** ((Irina Grishina and R.W. Woody)) Department of Biochemistry and Molecular Biology, Colorado State University, Fort Collins, CO 80523.

We have applied exciton theory to estimate the CD contribution of the Trp  $B_\pi$  transition to the far-uv circular dichroism (CD) of globular proteins. Strong exciton couplets are predicted for a number of proteins, including dihydrofolate reductase (DHFR), chymotrypsin and chymotrypsinogen. These predicted CD spectra are dominated by the contributions of the closest pair, W47/W74 in DHFR, W174/W215 in chymotrypsinogen. The sign and magnitude of the predicted couplets are consistent with experimental data for DHFR and its W74L mutant, and with the previously unexplained CD changes upon chymotrypsin activation. More extensive coupled-oscillator interactions among all aromatic and peptide chromophores are described for DHFR and barnase. The total far-uv CD spectra predicted for these proteins agrees poorly with experiment, but difference spectra calculated between the wild-type spectrum and that of mutants in which aromatic residues are replaced with non-chromophoric side chains show satisfactory agreement with experiment in most cases. (Supported by GM 22994)

## Tu-Poe265

**VOLUMETRIC CHARACTERIZATION OF GLOBULAR PROTEIN STATES AND THE TRANSITIONS BY WHICH THEY INTERCONVERT: CYTOCHROME C** ((T.V. Chalikian, V.C. Gindikin, K.J. Breslauer and A.P. Sarvazyan)) Dept. of Chemistry, Rutgers Univ., New Brunswick, NJ, 08903. \*Perm. address: Inst. of Theoretical and Exper. Biophys., Russian Acad. of Sciences, Pushchino, Russia.

At acidic pH, cytochrome c adopts native (N), molten globule (MG), or unfolded (U) conformations, with the specific state depending on the solution pH and ionic strength. We have used high precision ultrasonic and densimetric techniques to measure volume and compressibility changes accompanying the transitions from N to MG and from N to U. For the N-MG transition that occurs upon acidification to pH 2 in the presence of 200 mM CsCl, we find a volume increase of  $0.014 \text{ cm}^3 \text{ g}^{-1}$  and a compressibility increase of  $3.2 \times 10^{-6} \text{ cm}^3 \text{ g}^{-1} \text{ bar}^{-1}$ . For the N to U transition that occurs upon acidification to pH 2 in the absence of salt, we find a volume increase of  $0.010 \text{ cm}^3 \text{ g}^{-1}$  and a compressibility decrease of  $2.4 \times 10^{-6} \text{ cm}^3 \text{ g}^{-1} \text{ bar}^{-1}$ . We interpret these results to reach the following conclusions: (i) In the molten globule state, the solvent inaccessible core is preserved, with the volume of the core being about 40% of the intrinsic volume of the native cytochrome c; (ii) In the MG state, the coefficient of the adiabatic compressibility of the preserved core is equal to  $58 \times 10^{-6} \text{ bar}^{-1}$ . This value is over 4 times higher than that of the interior of the native protein, and is consistent with the interior of the preserved MG core being liquid like; (iii) In the unfolded state, only 70 to 80% of the surface area of the fully unfolded conformation is exposed to the solvent; (iv) The relative volume fluctuations of the solvent inaccessible interiors of cytochrome c in the native, molten globule, and unfolded conformations are equal to 0.6%, 1.9%, and 3%, respectively. These results will be discussed in terms of the nature of the three states of cytochrome c and the transitions through which they interconvert.

## Tu-Poe267

**PHOSPHOLIPASE A<sub>2</sub> REFOLDING AND ASSIGNMENT BY MULTIDIMENSIONAL NMR.** ((P.F.F. Almeida, R. Jerala\*, G.S. Rule, Q. Ye, B.K. Lathrop and R.L. Biltonen)) Univ. Virginia, Depts. Pharmacology and Biochemistry, Charlottesville, VA 22908. \*On leave from IJS, Ljubljana, Slovenia. (Spon. by G.S. Rule)

Recombinant phospholipase A<sub>2</sub> (PLA<sub>2</sub>) from *Agkistrodon piscivorus piscivorus* (D-49) has been prepared by expressing a synthetic gene in *E. coli*. The protein is produced in the form of inclusion bodies in the bacteria and has to be renatured in order to generate the active enzyme. The refolding strategy consisted essentially of a sequential reduction of the concentration of guanidium hydrochloride from 6M → 2M → 0.8M → 0, the disulphide bridges being allowed to reform in the presence of a mixture of reduced and oxidised glutathione at the stage of 0.8 M guanidium hydrochloride. The refolding process yielded maximum in active enzyme after about 20 hrs with an yield of about 50%. A large yield was particularly important in view of the preparation of <sup>13</sup>C and <sup>15</sup>N - labelled PLA<sub>2</sub> for multidimensional NMR studies. Due to severe resonance overlap we had been previously unable to complete the assignment using the <sup>15</sup>N labelled PLA<sub>2</sub> spectra only. Using the doubly labelled protein in a series of triple resonance NMR experiments in combination with specifically labelled <sup>15</sup>N PLA<sub>2</sub> spectra, we were now able to achieve the resonance assignment, leading to the determination of a solution structure. (Supported by NIH and NSF, R.J. partially supported by MZT).

## Tu-Poe269

**APPLICATION OF A MULTI-DIMENSIONAL CD-FLUORESCENCE SPECTROPHOTOMETER TO STUDY THE GUANIDINIUM AND PH INDUCED UNFOLDING OF APOMYOGLOBIN AND SOME OF ITS MUTANTS.** ((R. Ionescu, M. R. Eftink)) Department of Chemistry, University of Mississippi, University, MS 38677, and ((M. S. Hargrove, and J. S. Olson)) Department of Biochemistry and Cell Biology, Rice University, Houston, TX 77251.

We have developed a fully automated, combined CD-fluorescence instrument to perform denaturant induced titration and to perform pH titrations, with use of a feedback procedure to control the amount of delivered titrant. We will present data using this instrument to characterize the guanidine-HCl and pH induced unfolding of sperm whale apomyoglobin (apoMb) and a couple of its mutants. Using CD, Barwick and Baldwin (Biochemistry 32, 3790) have shown that, at low pH, an equilibrium unfolding intermediate is significantly populated for apoMb. DeYoung et al (Biochemistry 32, 3877) have presented fluorescence data showing that apoMb undergoes a urea-induced pre-denaturation transition at neutral pH, but found an apparent two-state transition as monitored by CD. Using our combined instrument we find that the guanidine-HCl induced unfolding of apoMb at neutral pH is a three-state process, with  $\Delta G^\circ_{un}$  of 3.2 and 1.5 kcal/mol for the successive transitions. We have also performed automated pH titrations, by simultaneously monitoring CD and fluorescence signals. The pH transition is multi-phasic for both types of signals and a global analysis of the data sets was performed to obtain the pK<sub>a</sub> shifts that occur for the transition. This research was supported by NSF grant MCB 9407167.

## Tu-Pos270

LIGAND-PROTEIN BINDING CONSTANTS AND ENTHALPIES FROM THE GLOBAL FIT OF CD THERMAL UNFOLDING CURVES. ((D. D. Muccio, C. L. Jones, and F. Fish)) Department of Chemistry, University of Alabama at Birmingham, Birmingham, AL 35294.

Brandts and Lin (*Biochemistry*, 1990, 29, 6927) and Straume and Freire (*Anal. Biochem.*, 1992, 203, 259) have shown that accurate binding constants and enthalpies can be determined from the fit of several DSC thermal unfolding curves of RNase A with different concentrations of 2'CMP. We have undertaken a similar study using CD spectroscopy to monitor the protein unfolding. The thermal unfolding curves of a single concentration of RNase A (29  $\mu$ M) in the absence and presence of 2'CMP at four different ligand concentrations (14 to 120  $\mu$ M) were measured in 50 mM KOAc buffer (pH 5.5). Additionally, the temperature scan of a buffer background and the optically active ligand at one concentration was also included in the data set. Together, these seven temperature curves were fit by a global analysis using a simple coupled equilibrium model:  $N = U$  and  $NL = L + N$ ; where N and U are the native and unfolded proteins and L and NL are the free and protein-complexed ligand. The binding constants and enthalpy change of the ligand step compared well to literature data determined from DSC and titration calorimetry. Some advantages and limitations of using spectroscopy will be discussed.

## Tu-Pos272

CONFORMATIONAL STUDIES OF GLYCATED  $\alpha$ -CRYSTALLIN AND  $\gamma$ -II-CRYSTALLIN FROM THE BOVINE LENS. ((C. Sullivan and T. Schleich)) Dept. of Chemistry and Biochemistry, University of California, Santa Cruz, CA 95064.

Glycation has been proposed to cause structural changes in lens proteins which disrupt their close packing and short range order critical for lens transparency. In this report,  $\alpha$ - and  $\gamma$ -II-crystallin, major structural proteins of the lens, were glycosylated *in vitro* and their secondary structures examined by far ultraviolet (UV) circular dichroism (CD). Secondary structural compositions were estimated using deconvolution methods. Both methods showed that ribosylated  $\gamma$ -II-crystallin had a lower amount of  $\alpha$ -helix, increased random structure and had less contributions to the far UV CD from aromatic residues and disulfides compared to the incubation control. The results for ribosylated  $\alpha$ -crystallin indicated no change in secondary structural composition whereas those of glucosylated  $\alpha$ -crystallin were less clear. Small changes in tertiary structure were evident in glycosylated crystallins from near UV CD. Ribosylated  $\alpha$ - and  $\gamma$ -II-crystallin showed a large decrease in tryptophan fluorescence accompanied by an increase in non-tryptophan fluorescence and the formation of non-disulfide crosslinks. Two types of cross-linked ribosylated  $\gamma$ -II-crystallin were apparent from the results of boronate affinity chromatography and SDS gel electrophoresis. The importance of these results and their relevancy to cataract will be discussed. (Supported by NIH grant EY 04033.)

## Tu-Pos274

PHYSICAL PROPERTIES OF  $\delta$ -ENDOTOXINS FROM *BACILLUS THURINGIENSIS*. ((Q. Feng and W.J. Beckett)) Biochemistry, The Ohio State University, 484 W. 12th, Columbus, OH 43210.

Crystalline proteins (Cry) isolated from different strains of *Bacillus thuringiensis* (BT) have been studied by means of HPLC and optical spectroscopy. The proteins studied include Cry IAa, Cry IAb, Cry IAc, and Cry IIIA. The conformation of each of these proteins has been determined as a function of pH and solution composition. The Cry IA family of proteins undergo a conformational change when the pH of the solution is varied from neutral to basic. The proteins become more helical as the pH is increased. The Cry IA proteins also undergo a conformational change upon increasing the ionic strength of the solutions. In contrast, Cry IIIA does not undergo a conformational change upon either an increase in pH or in ionic strength. If the pH of the solution is, instead, decreased, Cry IIIA eventually undergoes acid denaturation while proteins in the Cry IA family are not affected by a decrease in pH to as low as 2. These conformational changes are relevant to the biological activity of each family of toxins. In addition, it has been observed that the Cry IA toxins spontaneously form oligomers in solution while the wild type Cry IA does not. [This research was sponsored by the National Science Foundation, DMB9004902, WJB]

## Tu-Pos271

STUDY OF RNASE UNFOLDING PROCESSES BY STRUCTURE-INTERPRETED ORDER PARAMETER OBTAINED FROM THE ESR LINE SHAPE. ((N.N. Vylegzhanina, V.I. Shlenkin, D.A. Fushman\*, L.O. Yagolina, A.E. Altshtuler)) Kazan Institute of Biology, POB 30, 420503, Kazan, Russia; \*The Rockefeller University, 1230 York Ave., New York, NY 10021, USA

We have recently considered the processes of electron-spin relaxation in spin-labeled proteins in solution utilizing the two-motion model of spin label mobility. The transverse relaxation rate is shown to be sensitive to the generalized order parameter S, characterizing a degree of restriction of the spin label mobility. This provides a new basis for ESR applications to structural aspects in proteins. We report here the application of this approach for studying the process of thermal denaturation of spin-labeled bacterial RNase *Bacillus intermedius* 7P (binase) and pancreatic RNase A. The ESR spectra were recorded over the temperature range 0-100°C for several values of pH (2.5-7.0). The values S were determined from the correlation between the dynamic parameter  $\tau_R S^2$  of spin-labeled proteins and experimentally obtained half-widths and intensities of the hyperfine components of the ESR spectrum. The correlation times used were deduced in our laboratory from the method of Time Domain Dielectric Spectroscopy. For both proteins the observed features of the order parameter behaviour are interpreted as due to both global unfolding of protein molecules and its predecessors, local transitions in the protein structure, in particular, in the vicinity of the spin label binding site. In the case of RNase A the values of S for thermally denatured state demonstrate that this protein can exist in two types of denatured substates. The increase of the amplitudes of intermolecular motions (as result, the order parameter decreases) in high-temperature substate supports the view that thermal unfolding process of this protein is two-stage one.

## Tu-Pos273

CIRCULAR DICHROISM OF THE WT AND THREE TYR $\rightarrow$ PHE MUTANT fd GENE 5 PROTEINS COMPLEXED WITH ssDNA AND POLY[d(A)]. ((B.L. MARK, M. VAUGHAN, D.M. GRAY<sup>1</sup> AND T.C. TERWILLIGER<sup>2</sup>)) Program in Molecular and Cell Biology, University of Texas at Dallas, Richardson, TX 75083-0688<sup>1</sup> and the Genomics and Structural Biology Group, Los Alamos National Laboratory, Los Alamos, NM 87545<sup>2</sup>.

The bacteriophage fd produces gene 5 protein (g5p) that sequesters the fd genome during part of its life cycle. The g5p binds in a nonspecific, cooperative manner to the ssDNA genome forming a left-handed helical complex. WT g5p and three mutant g5ps (Y26F, Y34F, and Y41F) were used to carry out titrations of, and salt dissociations from, fd ssDNA and poly[d(A)]. Fd ssDNA was similarly perturbed when titrated with any of these four proteins. Two binding modes were found for WT, Y26F, and Y34F g5ps, while previously only one binding mode was evident from CD studies of WT g5p binding to fd ssDNA. Poly[d(A)] also was similarly perturbed by each of the four proteins. Two modes of binding were evident for all four proteins in binding to poly[d(A)], as previously shown for WT g5p. Salt dissociations of the g5ps from either fd ssDNA or poly[d(A)] showed that the dissociation from the weaker secondary binding mode was essentially the same for each of the four proteins. This suggests that Tyr-26, Tyr-34 and Tyr-41 do not add to the stability of the secondary binding mode. However, the primary binding modes of the four proteins showed differences in salt-sensitivity. In complexes with fd DNA, the order of salt-stability, from least stable to most stable was Y41F < Y34F < Y26F < WT, while the order of stability of complexes with poly[d(A)] was Y41F < Y34F < Y26F  $\approx$  WT. The protein with the mutated Tyr-41 residue, purportedly located at the dimer-dimer interface, formed the most salt-labile complex.

This research was supported by NIH Research Grant GM38714, Grant MCB-9405683 from the National Science Foundation, and Grant AT-503 from the Robert A. Welch Foundation.

## Tu-Pos275

COMPARISON OF THE BIOPHYSICAL CHARACTERISTICS OF HUMAN AND MURINE TNF- $\alpha$ . ((L.O. Narhi, J. Wen, J. Philo, M. Zhang, S.J. Prestrelski, T. Arakawa)) Amgen Inc., Amgen Center, Thousand Oaks, CA 91320.

Human TNF- $\alpha$  and murine TNF- $\alpha$  are 80% identical and over 90% homologous, and yet have different effects *in vivo*. To begin to understand these differences, we have compared the biophysical characteristics of these two proteins. Circular dichroism, fluorescence and Fourier transform infrared spectroscopies revealed that the secondary and tertiary structures of the two proteins are essentially identical. There are, however, major differences in the stability of the two species to thermal denaturation, in the solubility of the unfolded forms of these proteins and in their trimer association constant. The human TNF- $\alpha$  begins to melt at 50°C, and precipitates concurrent with unfolding such that there is no protein in solution at 60°C. The murine TNF- $\alpha$  begins to melt at 60°C, to a soluble form which contains  $\alpha$ -helix, and has a midpoint transition temperature of 66°C. The murine TNF- $\alpha$  forms a very stable trimer that elutes as a single trimer peak under conditions where the human molecule elutes primarily as a monomer. Trifluoroethanol induces substantial  $\alpha$ -helix in both molecules, indicating that in the absence of long range interactions the TNF- $\alpha$  sequence has  $\alpha$ -helical propensity.

## Tu-Poe276

TEMPERATURE DEPENDENCE STUDY OF THE REACTION OF HUMAN OXYHEMOGLOBIN A WITH 5, 5' - DITHIOBIS (2 - NITROBENZOIC ACID). Christopher O. Aboluwoye\*, Ali. A. Moosavi - Movahedi<sup>†</sup> and A. Kh. Bordbar<sup>†</sup>.

\* Department of Chemistry, Ondo State University, Ado - Ekiti, Nigeria.

+ Institute of Biochemistry and Biophysics, University of Tehran, Tehran, Iran.

The temperature - dependence study of the reaction of human oxyhemoglobin A (O<sub>2</sub>HbA) with 5, 5' - dithiois (2 - nitrobenzoic acid), DTNB, as a function of pH has been studied.

The quantitative analysis of the pH dependence of the apparent second order rate constant shows that two ionizable groups are electrostatically linked to the reaction. Their pK<sub>a</sub> values are 5.5 and 8.7. These are assigned to His HC3 (146) β and to the CysF9 (93) β sulphhydryl.

The intrinsic activation parameters for these ionizable groups have been determined using the Arrhenius and Eyring equations. The intrinsic activation entropies of His HC3 (146) β and Cys F9 (93) β have confirmed that the two ionizable groups are electrostatically linked. Negative value of activation entropy for CysF9 (93) β shows that there is an increase in the polarity around the reactive centre. Large and positive intrinsic activation entropy of His HC (146) β further confirm that the salt bridge between His F 3 (146) β and Asp FG1 (93) β plays a major role in the reaction.

The variation of apparent parameters as a function of pH could be attributed to the effect of salt bridge, hydrogen bonding, van der waal forces and hydrophobicity of oxyhemoglobin A.

## Tu-Poe278

# CONFORMATIONAL PREFERENCES OF THE PENTAPEPTIDE REPEAT FROM A HIGH-SULPHUR WOOL PROTEIN BY 1H NMR.

((Mark I. Liff)) Philadelphia College of Textiles and Science, Philadelphia, PA 19144, (sponsored by Tobin Sosnick)

The properties of the elastic protein matrix from wool fibers are explained by peculiar conformational behavior of the pentapeptide repeat of the following structure: C-X-P-Y-C, where X is Gln or Arg, Y is Ser or Thr, C is Cys and P is Pro. It has been shown (R. Fraser, et al. *Int. J. Biol. Macromol.* 1989,106) that this repeat has a high propensity for reverse turns with X in position 1: the initial Cys in the repeat might form an intrachain disulphide linkage with the last one to stabilize the turn. However, another line of evidence (R. Zhang, *J. Biol. Chem.*, 1989, 18472) leads to the suggestion, that disulphide bonds are unlikely to occur in this sequence. In order to experimentally determine the structural implications of this repeat we used NMR to study conformational preferences of a nine residue peptide which is a common fragment of a B2 family of wool proteins, NH-Thr-Ser-Ser - Cys-Qln-Pro-Thr-Cys -Leu-NH<sub>2</sub> (the repeat is underlined). Under the reducing conditions, the NOEs and JNH-αH couplings of peptide in DMSO and water solutions are characteristic of unfolded structure. The oxidation of the Cys residues in pairs, which we performed in very dilute solutions of 5 μM, resulted in polymerization of the peptides, but not in the intramolecular cycles. These data also support the conclusion that the turns are unlikely. Therefore an alternative model for description of the protein matrix is needed.

## Tu-Poe280

DESIGN OF A SOLUBLE EQUIVALENT OF BACTERIORHODOPSIN ((C. J. Gibas and S.Subramaniam)) University of Illinois at Urbana-Champaign, Urbana, IL 61801. (sponsored by A.R. Crofts)

Membrane proteins pose difficult challenges for three dimensional structure determination and therefore it would be valuable if these could be solubilized in polar solvents. One of the few proteins whose structures are available is bacteriorhodopsin. The structure obtained from cryo-electron microscopy is at a very low resolution. On examination of the bacteriorhodopsin structure and structures of soluble helical proteins we found that the interhelical packing in bacteriorhodopsin is similar to that in four-helix bundles and in some larger helical proteins. We have studied pairwise preferences of amino acid occurrence in several types of soluble helical proteins, as well as preferential location and proportion of polar residues in various alpha-helix environments. We have used molecular modeling techniques to modify the structure of Bacteriorhodopsin, to create blueprints for a monomeric, soluble 7-helix bundle protein. While preserving residues shown to be necessary for BR function, we made modifications to the rest of the sequence, distributing polar and charged residues over the surface of the protein to achieve an amino acid composition as akin to that of soluble helical proteins as possible, and attempting to increase apolar contacts in the interior of the protein. Replacements gleaned from the sequences of helical proteins by BLAST were given preference in building the model, though in some cases we resorted to arbitrary replacements based on data for positional preference of amino acids in helices. We show that the modeled structures display good soluble protein profiles. [supported in part by NSF].

## Tu-Poe277

CONTRIBUTION OF ELECTROSTATIC FORCES TO THE HYPERTHERMOSTABILITY OF RUBREDOXIN FROM *PYROCOCCUS FURIOSUS*. ((S. Cavigner<sup>†</sup>, M.W.W. Adams<sup>†</sup> and S.I. Chan<sup>†</sup>)) <sup>†</sup>Arthur Amos Noyes Laboratories of Chemical Physics, California Institute of Technology, Pasadena, CA 91125 and <sup>†</sup>Department of Biochemistry, University of Georgia, Athens, GA 30602

As part of our study of the physical bases of protein hyperthermostability, we have investigated the contribution of electrostatic interactions by spectroscopically detecting the effects produced by environmental changes on Rubredoxin from *Pyrococcus Furiosus*. We used high ionic strength and pH extremes to show that the overall secondary and tertiary structure of the protein is substantially unchanged when all the individual ion pairs have been broken. This minimizes the importance of ion pairing to the stability of this hyperthermophilic Rubredoxin. Further assessment of the coulombic contribution to the stability is given by calculations of surface electrostatic potential under different simulated experimental conditions. Ionic strength has also been found to modulate the structure of Rubredoxin at very low pH by promoting differential exposure of hydrophobic groups.

## Tu-Poe279

A 3<sub>10</sub>-HELICAL PEPTIDE WITH A DEFECT IN THE HYDROGEN-BONDING PATTERN: IMPLICATIONS FOR THE CONFORMATIONAL PREFERENCES OF AIB. ((Adrienne Pettijohn<sup>†</sup>, Gautam Basu<sup>‡</sup> and Atsuo Kuki<sup>§</sup>)) <sup>§</sup>Cornell University, Ithaca, NY 14853 and <sup>‡</sup>Kyoto University, Kitashirakawa, Sakyo-ku, Kyoto 606, Japan.

The Aib-rich peptide 'Boc-Aib-Aib-Aib-Ala-Ala-Aib-Aib-Aib-NHMe (4,5-AA) has been synthesized and the solution-phase conformation in CDCl<sub>3</sub> and DMSO has been determined by NMR using both 1-dimensional perturbation techniques and 2-dimensional ROESY. The peptide in CDCl<sub>3</sub> has been sequence-assigned and is fully 3<sub>10</sub>-helical as expected. In contrast, three amide protons with high temperature coefficients were observed in DMSO-d<sub>6</sub>. Although this behavior is characteristic of an α-helix, the sequence assignment from ROESY reveals that only two of these amides are N-terminal while the third temperature-dependent amide belongs to Aib<sup>6</sup>. Additional three dimensional information from ROESY reveals that the peptide adopts a 3<sub>10</sub>-helical conformation with only a slight defect in DMSO-d<sub>6</sub>. There is no evidence indicative of an α-helical component. This observation calls for caution in assigning an α-helical conformation to peptides based solely on the results of 1-D perturbation experiments. Evidence is presented for the predominant effect of steric hindrance over hydrogen-bonding in the determination of Aib-containing peptide conformations. The effect of contiguous L-amino acids on the conformation of Aib-containing peptides, and the role of DMSO as a perturbant of structure, are also discussed.

## Tu-Poe281

IN VIVO AND IN VITRO RECONSTITUTION OF ACTIVE "OCTAMERIC" MITOCHONDRIAL CREATINE KINASE FROM THE TWO GENETICALLY ENGINEERED DOMAINS

((M. Gross, M. Wyss, T. Wallimann, and R. Furter)) Swiss Federal Institute of Technology, Institute for Cell Biology, CH-8093 Zurich, Switzerland

Creatine kinase is thought to be a flexibly-hinged two-domain enzyme, similar to 3-phosphoglycerate kinase. We genetically dissected the mitochondrial creatine kinase (Mi-CK) polypeptide into two fragments near a putative domain boundary defined by a protease-sensitive site found for M-CK (Morris & Jackson, *Biochem.J.* 280, 809, 1991). The 18.8kDa N-terminal and the 24.4kDa C-terminal fragment were expressed separately in *E.coli* and isolated from inclusion bodies with high purity and yield. In contrast, co-expression of both fragments from a single plasmid yielded soluble, enzymatically active Mi-CK (V<sub>max</sub> reduced by 50%), which formed an oligomer of the same 340kDa molecular weight as native octameric Mi-CK. The protein contained the two polypeptides in a 1:1 stoichiometry, suggesting that the domains formed a 16mer. This mosaic Mi-CK had lost the synergistic substrate binding characteristic of the native enzyme, and GdnHCl-induced inactivation was no longer cooperative. This indicates that both synergistic substrate binding and unfolding cooperativity depend on the covalent domain connectivity. The two isolated fragments significantly differed with respect to their structural integrity: while the C-terminal peptide was globular and showed the far- and near-UV CD characteristics of the wild-type protein, the N-terminal segment was largely unfolded, barely containing any secondary structure. CK enzyme activity could also be reconstituted *in vitro* by mixing both fragments under non-denaturing conditions, suggesting that the folded C-terminal domain supports the folding of the associated N-terminal domain.



## Tu-Pos282

DESIGN OF A PROTEIN OLIGOMERIZATION SCAFFOLD BASED ON LAC REPRESSOR. ((R. Fairman, H.-G. Chao, L. Mueller, S.-Y. Shaw, L. Shen, J. Novotny and G. Matsueda)) Division of Macromolecular Structure, Bristol-Myers Squibb Pharmaceutical Research Institute, P.O. Box 4000, Princeton, NJ 08543-4000.

We report the design of a protein oligomerization scaffold based on the tetramerization domain of Lac repressor. Peptides, whose sequences are derived from the carboxy-terminal amino acid sequence of Lac repressor, were synthesized to characterize the secondary, tertiary, and quaternary structures of this domain. We show that these peptides form well-folded anti-parallel four-helix bundles whose stabilities depend strongly on  $\alpha$ -helix length. The dissociation constants for bundles that contain  $\alpha$ -helices 21, 28, and 35 amino acids in length are  $3.1 \times 10^{-12}$ ,  $6.7 \times 10^{-23}$ , and  $1.0 \times 10^{-38}$  M<sup>3</sup>, respectively. These correspond to tetramer stabilities (in terms of the peptide monomer concentration) of 180  $\mu$ M, 51 nM, and 280 fM, respectively. Also, in contrast to many previous design attempts, the tertiary fold of a highly stable variant of the Lac repressor four-helix bundle appears to be well defined. Finally, to extend the design to include functionality, we characterized the structural effect of tethering the maltose binding protein to the amino terminus of this highly stable variant.

## Tu-Pos284

MOLECULAR AGGREGATION STUDIES USING SCANNING TWO PHOTON FLUCTUATION CORRELATION SPECTROSCOPY. ((Keith Berland, Peter T. C. So, W. W. Mantulin and Enrico Gratton)) Laboratory for Fluorescence Dynamics, University of Illinois at Urbana-Champaign

There are many problems in biology and biochemistry in which it is interesting to know whether proteins, lipid probes, or other small molecules are in an aggregated state. Several researchers have previously demonstrated the promise of scanning correlation spectroscopy (SCS) for detecting aggregated states. Such techniques perform quite well for large brightly labeled probes, but suffer greatly for small or singly labeled molecules. The major noise source is Rayleigh and Raman scattered laser excitation. We have recently used two-photon fluorescence correlation spectroscopy to accurately measure particle motion in 3D bulk solutions, and in cellular interiors. Two powerful advantages of the two-photon technique include the inherent excitation of only a small subvolume of bulk samples, and improved background rejection of scattered laser light. These features can greatly improve the performance of SCS methods and should make aggregation measurements possible for very small particles, with only single fluorescent labels. The separation between two-photon excitation and emission wavelengths is great enough that optical filters can eliminate scattered light. Particularly important for detecting low light levels is the rejection of Raman scattered light, which overlaps with the fluorescence spectrum for one photon excitation. We have constructed a scanning two-photon system. We have accurately measured particle concentrations for molecular assemblies as small as 7 nm radius latex beads. We have also demonstrated that our system can detect single fluorescein molecules. We are currently working to demonstrate the feasibility of protein aggregation measurements using SCS. This work was supported by NIH (RR03155).

## Tu-Pos286

CALCIUM BINDING TO THE EGF DOMAIN IN GLA-EGF MODULE PAIR OF COAGULATION FACTOR X INDUCES DOMAIN INTERACTIONS ((M. Sunnerhagen, G. A. Olah, J. Stenflo, J. Trehellia, and T. Drakenberg)) Physical Chemistry 2, University of Lund, P.O.B. 124, S-221 00 Lund, Sweden; Los Alamos National Laboratory, Los Alamos, NM 87545

Coagulation factor X is a serine protease with three non-catalytic modules: two Epidermal Growth Factor (EGF)-like domains and one  $\gamma$ -carboxyglutamic acid (Gla) domain at the N-terminus. Calcium binding to the Gla domain is important for binding the coagulation factor to the plasma membrane surface of activated platelets. In addition, recent mutation studies have shown that calcium binding to EGF domains is also necessary for biological activity. Therefore, we used NMR and X-ray scattering to determine the solution structure of the Gla-EGF module pair from coagulation factor X in the absence of calcium and with calcium bound to the EGF module only. Contrary to previous opinion, NMR and scattering data show the Gla domain not to be disordered in the absence of calcium but to have similar secondary structure and global fold as the calcium bound structure. Furthermore, calcium binding induces the two domains to fold toward each other via a rearrangement of helix 3 (residues 33-44) in the Gla domain which connects the two domains resulting in a decrease in the radius of gyration and maximum linear dimension of the Gla-EGF module pair.

## Tu-Pos283

ASSOCIATION STATES OF CHIMERIC GLYCOPHORIN A/STAPHYLOCOCCAL NUCLEASE IN NONIONIC DETERGENT SOLUTIONS STUDIED BY SAXS ((Zimei Bu, Raphael Lamed and Donald M. Engelman)) Department of Molecular Biophysics & Biochemistry, Yale University, New Haven, CT 06511

Glycophorin A (GpA) is a single helix transmembrane protein. Its chimeric construct, made by fusing the transmembrane domain of glycophorin A to the C-terminal of staphylococcal nuclease (SN), forms a dimeric complex in SDS micelles. A highly specific hydrophobic motif in the transmembrane helix is found to be responsible for the dimerization of (Lemmon et al., *Biochem J*, 12719-12725 (1992); Lemmon et al., *Nature Struct Biol*, 1, 157-163 (1994)). Here, we use small angle x-ray scattering to measure the association states of this chimeric protein dissolved in a mild nonionic detergent environment. Guinier plots show that in 1-O-octyl  $\beta$ -D-glucopyranoside GpA/SN is polydispersed, but in  $\beta$ -D-dodecyl maltoside ( $\beta$ -DM) GpA/SN has only two distinct sizes when the detergent to protein concentration ratios are about 5. We are using the zero angle scattered intensity to calculate the GpA/SN association constant and will extend this method to measure the effect of GpA transmembrane domain amino acid sequence variation on the association state of GpA/SN.

## Tu-Pos285

THERMODYNAMIC ANALYSIS OF THE TETRAMERIZATION DOMAIN OF HUMAN p53. ((M.S. Lewis,\* K. Sakaguchi, H. Sakamoto, E. Appella and P.W. Chun\*\*)) \*BEIP, NCR and LCB, NCI, NIH, Bethesda, MD 20892 and \*\*Dept. Biochem. and Mol. Biol., U. of Florida, Gainesville, FL 32610.

Human p53 is a tumor-suppressor gene product associated with cell cycle control and growth suppression, and is known to form homotetramers in solution. Using synthesized peptides corresponding to carboxyl-terminal sequences in human p53, we have demonstrated by equilibrium ultracentrifugal analysis that peptides 319-393 and 319-360 exhibit reversible tetramer formation and that successive deletion of amino- and carboxyl-terminal residues from peptide 319-360 reduced tetramer formation (H. Sakamoto, et al., PNAS USA (1994) 91:8974-8978). We present here an analysis of the temperature dependence of the standard Gibbs free energy changes of tetramerization at pH 7.5 of six of these peptides, using the Planck-Benzinger thermal work function and extrapolating to 0 K to obtain the temperature-invariant enthalpy,  $\Delta H^0(T_0)$ , which is postulated to be the primary source of the chemical bond energy for the reaction (P.W. Chun, J. Phys. Chem. (1994) 98: 6851-6861). The values of  $\Delta H^0(T_0)$  for the peptides are: 303-393: 140.4 kcal/mol; 319-393: 203.2 kcal/mol; 303-360: 49.7 kcal/mol; 319-360: 62.7 kcal/mol; 319-351: 29.7 kcal/mol; 319-347: 10.9 kcal/mol. No  $\Delta H^0$  dominated thermodynamic compensation was observed. With the exception of the 319-347 peptide, which exhibited TAS<sup>o</sup> driven thermodynamic compensation, the remaining peptides exhibited the  $\Delta H^0$ -TAS<sup>o</sup> thermodynamic compensation that is found to be characteristic of many self-associating systems.

## Tu-Pos287

ASSEMBLY AND MELTING TRANSITIONS OF  $\lambda$  cI REPRESSOR MUTANTS. ((D.S. Burz, E. Merabet & G.K. Ackers)) Department of Biochemistry & Molecular Biophysics, Washington University School of Medicine, St. Louis, MO 63117.

We have used sedimentation equilibrium (SedEq) and differential scanning calorimetry (DSC) to assess the strength and stoichiometry of higher order protein-protein interactions in single-site mutants of bacteriophage  $\lambda$  cI repressor. SedEq experiments suggest that dimers of mutant repressors EK102 & EK188 assemble to a stoichiometry greater than two as is observed with wild type repressor [Sencar et al. (1993) *Biochemistry* 32, 6179], whereas other C-terminal domain mutants do not assemble beyond dimers. PT158 self-associates from monomers to a stoichiometry greater than two with no evidence of a dimeric intermediate. The concentration at which these higher order assembly processes occur is similar for wild type, EK102 & PT158, but greater for EK188. DSC profiles are best described by three transitions attributed to the melting of the N-terminal and C-terminal domains and the linker region between domains. Mutations in the C-terminal domain consistently decrease the  $T_M$  of the C-terminal domain transition and increase the  $T_M$  of the N-terminal domain transition. Stoichiometries obtained from the ratio of calorimetric to van't Hoff enthalpies confirm results elucidated using SedEq in the absence of operator DNA and further suggest that the linker region interacts more strongly with the C-terminal domain of the protein. These stoichiometries change in the presence of operator DNA. Results demonstrate that cooperativity mutants previously shown to exhibit an altered conformation in solution [Burz et al. (1994) *Biochemistry* 33, 8399] are likely to have an altered structure based upon the changes in thermal stability, assembly stoichiometry and denaturation enthalpy. Supported by NIH grants GM-39343 & R37-GM24486.

## Tu-Pos288

EVIDENCE FOR DISULFIDE BOND FORMATION IN RECA PROTEIN FROM *ESCHERICHIA COLI*. ((D.M. Budzynski and A.S. Benight)) Department of Chemistry, University of Illinois, Chicago, IL, 60607. (Spon. by R.F. Goldstein)

RecA protein was studied by denaturing gel electrophoresis under reducing and non-reducing conditions. Results demonstrated the presence of intramolecular disulfide bonds and intermolecular disulfide bonds that could be induced by a variety of agents including ATP-γS, GTP-γS, MgCl<sub>2</sub> and H<sub>2</sub>O<sub>2</sub>. These observations suggest the association process of RecA may not be entirely reversible. Under mildly denaturing conditions (established by 2.0 M guanidinium hydrochloride) the solution hydrodynamics of RecA samples with and without disulfide bonds were investigated by dynamic light scattering. Under mildly denaturing conditions the presence of disulfide bonds induced by ATP-γS significantly effects the hydrodynamic behavior of the protein. In contrast, under non-denaturing conditions the light scattering behaviors of RecA with or without disulfide bonds were identical. These results suggest disulfide bond formation may restrict substantially internal (sub-global) motions of RecA protein filaments. (Supported by NSF)

## Tu-Pos290

CHARACTERIZATION OF A HYDROPHOBIC SITE IN CALSEQUESTRIN FROM RABBIT SKELETAL MUSCLE SARCOPLASMIC RETICULUM ((C. Yang<sup>1</sup>, C.A.R. Wesson<sup>1</sup>, W. R. Trumble<sup>2</sup>, & A. K. Dunker<sup>3</sup>)) <sup>1</sup>Dept. Biochem/Biophys., Washington State University, Pullman, WA 99164; <sup>2</sup>Dept. Microbiol., Mol. Biol. & Biochem., University of Idaho, Moscow, ID 83844

Calsequestrin (CS) is a Ca<sup>2+</sup>-binding protein (Kd ~ 1 mM, 40 - 50 sites/CS) located within the terminal cisternae of the sarcoplasmic reticulum. Previously we suggested a two step model for Ca<sup>2+</sup>- or K<sup>+</sup>-induced folding of CS and more recently suggested the creation of a hydrophobic binding site concomitant with the folding induced by either ion (He et al., J. Biol. Chem. 268: 24635-24641, [1993]; He et al., Biophys. J. 66: A398 [1994]). Here we report further characterization of this hydrophobic site using several probes, including 1-anilino-naphthalene-8-sulfonate (ANS), N-phenyl-1-naphthylamine (P65), 6-propionyl-2-dimethyl aminonaphthalene (prodan) and p-dimethylamino benzylidenemalononitrile (D443), coupled with fluorescence quenching measurements. Comparative studies using the same probes with four proteins having hydrophobic sites of differing character provide additional information. The overall comparisons suggest that the hydrophobic site is most like the heme site in apo-myoglobin, less similar to the hydrophobic binding site in bovine serum albumin and rather unlike the hydrophobic clusters of molten globular protein forms. Further comparisons suggest that the hydrophobic site is indeed created by the ion-induced unfolding, but that Ca<sup>2+</sup>-induced aggregation of CS causes displacement of the bound probe. Given that surface-accessible hydrophobicity has been shown to have a very high correlation with protein recognition (Young et al., Protein Sci. 3: 717-729 [1994]), these data suggest that the hydrophobic site in CS merits additional characterization.

## Tu-Pos292

PHYSICAL CHARACTERIZATION OF THE ASSOCIATION OF Ca<sup>2+</sup> TO MIXED AND UNMIXED HALF MOLECULES OF CALBINDIN D9. ((D. W. Kupke; J. Sherman & F. C. S. Tsai; K. Alessi & L. A. Marky)). Dept. of Biochem., Univ. of Virginia, Charlottesville, VA 22908; Dept. of Chem., Univ. of British Columbia, Vancouver, Canada V6T 1Z1; Dept. of Chem., New York Univ., New York, NY 10003

We have synthesized the peptides that correspond to each half of calbindin D9 and have studied their interaction with Ca<sup>2+</sup> by circular dichroism, titration calorimetry and density techniques. We wished to determine upon adding Ca<sup>2+</sup>, a) whether the N-terminal peptide containing the pseudo or non-archetypal calcium binding loop exhibits properties which differ from those of the C-terminal peptide containing the archetypal binding loop, and b) if the 1:1 non-covalent mixture of the two half molecules show cooperativity in binding of Ca<sup>2+</sup>. These experiments were done in 20 mM Pipes, 0.1 M KCl, pH 7 at 20°. All 3 observables, CD(θ<sub>222</sub>), volume expansions (ΔV) and heat change (ΔH), indicated little, if any, Ca<sup>2+</sup> uptake by the N-terminal peptide, whereas similar studies on the C-terminal one clearly suggested a positive uptake. The mixtures, however, showed much greater uptake than did the sum of the individual peptides—the ΔV data exhibiting a similar total expansion to that of the intact calbindin, but a steeper initial slope, (ΔV/Δ[Ca<sup>2+</sup>]), suggesting enhanced cooperativity. Lower concentrations of KCl have shown greater Ca<sup>2+</sup> uptake by each peptide and of the mixture, indicating a significant electrostatic effect.

(Supported by Grants GM-34938 and GM-42223 from the NIH.)

## Tu-Pos289

CHARACTERIZATION OF LACTOSE REPRESSOR PROTEINS CONTAINING SINGLE TRYPTOPHAN INSERTIONS ((J.K. Barry and K.S. Matthews)) Dept. of Biochemistry and Cell Biology, Rice University, Houston, TX, 77251.

The influence of environment on tryptophan fluorescence properties allows this amino acid to be used as a probe for local environment in a protein. Native lac repressor contains two tryptophans, W201 and W220, both in its core domain. Previous characterization of single tryptophan mutants (W201Y and W220Y) indicates that W220 is located in the inducer binding site while W201 is buried within the core. W210Y and W220Y both have a slightly reduced affinity for operator, and W220Y binds inducer with 30-fold lower affinity (Gardner and Matthews, (1990) J Biol. Chem. 265, 21061). This data indicates that the tryptophan residues can be replaced with tyrosine while maintaining repressor structure and functional properties. A mutant lactose repressor containing no tryptophan (W201Y/W220Y) was generated by site-directed mutagenesis. This tryptophan-less repressor creates a background upon which tryptophans can be inserted to probe the environment of different regions in the lactose repressor. Four sites were chosen for tryptophan insertion; Y7, K62, Y282 and L323, for the following reasons: Y7 is in the N-terminal domain responsible for DNA binding; K62 is in the hinge region which connects the core domain and the N-terminus; Y282 is located in the dimeric subunit interface; and L323 is in the area between the core domain and the C-terminal oligomeric region. All of these insertion mutants have been characterized by MCD and fluorescence spectroscopy, operator and inducer binding properties, and measurement of oligomeric state as well. Supported by NIH GM22441 (KSM), the Robert A. Welch Foundation C-576 and the Claire Luce Boothe Foundation (JKB).

## Tu-Pos291

INCLUSION BODIES OF INTERLEUKIN-2 AND INTERFERON-γ ARE FORMED FROM PARTIALLY-FOLDED INTERMEDIATES.

((Sangita Seshadri\*, William C. Channing†, Mei Zhang†, Tsutomu Arakawa† and Anthony L. Fink\*)) \*University of California, Department of Chemistry and Biochemistry, Santa Cruz, CA 95064 and †Amgen Inc., Thousand Oaks, CA 91320.

Attenuated total reflectance (ATR) FTIR has been used to study the structure of inclusion bodies (IBs) of human IL-2 and IFN-γ. These proteins are all-α proteins with six helices in IL-2 and IFN-γ. The secondary structure composition of native IL-2 and IFN-γ, determined by ATR-FTIR, is in agreement with that previously determined by X-ray crystallography: namely 62% and 65% helix respectively. In the inclusion bodies, IL-2 and IFN-γ showed 21% and 10% less helix than the native conformation, respectively, and a 20 - 25 % increase in β-structure. The structures of the two IBs are clearly different, that from IFN-γ being significantly more native-like. The increase in the β-structure is attributed to intermolecular interactions in the formation of the aggregated protein in the inclusion body. The presence of substantial native-like secondary structure in the IB indicates that the IBs are formed from partially-folded intermediates. Comparison of the protein conformation in the IB with that in folding aggregates will be discussed. These observation support the idea that most aggregated proteins arise from partially-folded intermediates.

## Tu-Pos293

FAST EVENTS IN PROTEIN FOLDING: LASER T-JUMP/TIME-RESOLVED IR STUDY OF THE HELIX-COIL TRANSITION. ((S. Williams<sup>1</sup>, T.P. Causgrove<sup>1</sup>, R. Gilmanshin<sup>2</sup>, R. Callender<sup>3</sup>, W. H. Woodruff<sup>1</sup>, and R. Brian Dyer<sup>1</sup>)) <sup>1</sup>CST-4, Los Alamos National Laboratory, Los Alamos, NM 87545, <sup>2</sup>Department of Physics, City College of New York, New York, NY 10031. (Spon. by R. B. Dyer)

Our goal is to capture the fast events in protein folding/unfolding with structural specificity. To date key hurdles in studying these events have been the rapid initiation of the folding/unfolding and the availability of a probe capable of monitoring dynamics on short (10<sup>-10</sup>-10<sup>-3</sup> s) time scales. Near-IR pulsed excitation (10 ns or 50 ps) of water overtone absorbances at 5000 cm<sup>-1</sup> is used to increase the temperature of a small volume of peptide/protein solution by 10 °C. Subsequent unfolding reactions are monitored in the mid-IR using transient absorption spectroscopy. We have used this method to study the unfolding (helix-coil transition) of a *de novo* synthetic peptide, Suc-A5-(A3-R-A)3-A-NH<sub>2</sub>, and a protein, apomyoglobin, in a molten globule state. Static FTIR spectra of both systems show changes characteristic of the helix-coil transition in the amide I region (1630-1650 cm<sup>-1</sup>) with temperature. Time-resolved IR spectra indicate that all of the absorbance changes exhibited in the static measurements occur faster than the present detector time-resolution of 1 μs indicating that the helix-coil transition rate of both systems is greater than 1 x 10<sup>6</sup> s<sup>-1</sup>. Measurements on shorter time scales (10<sup>-10</sup>-10<sup>-7</sup> s) are in progress.

## Tu-Pos294

A Spectroscopic Study of Four Single-Tryptophan Mutants of *E. coli* Adenylate Kinase

Tim Fulmer<sup>1,2</sup>, Tim Bilderback<sup>1</sup>, Michael Glaser<sup>1</sup>, William Mantulin<sup>1,2</sup>  
University of Illinois at Urbana-Champaign, <sup>1</sup> Dept. of Biochemistry & <sup>2</sup> Laboratory for Fluorescence Dynamics, Dept. of Physics, Urbana, IL, 61801

*E. coli* adenylate kinase (AK) catalyzes the synthesis and interconversion of adenosine nucleotides by the following reaction:  $Mg^{2+}ADP + ADP \rightleftharpoons Mg^{2+}ATP + AMP$ . The enzyme is a single subunit, globular protein of MW 23,000 Daltons. It has been cloned and over-expressed, and its x-ray crystal structure has been solved to high resolution (Berry, et al., *Proteins*, 1993). Furthermore, the x-ray structure shows evidence of a large degree of conformational flexibility. The wild-type enzyme is devoid of tryptophan. Through the use of site-directed mutagenesis techniques, tryptophans can be selectively placed in various regions of the protein, providing optical probes of local AK dynamics and the protein-solvent microenvironment. Finally, the fluorescence properties of the tryptophans can be studied as a function of chemical denaturant and temperature to provide insights into the global structural and dynamic changes which occur during protein folding and unfolding. Additionally, CD spectroscopy serves as a benchmark for these global processes. We have constructed, over-expressed, and purified four single-tryptophan mutants (S41W, F86W, Y133W, and F137W). To gain a better understanding of AK conformational dynamics we have studied their native-state and equilibrium-unfolding properties using a battery of fluorescence techniques: steady-state and time-resolved fluorescence, steady-state and time-resolved polarization, and fluorescence-intensity and lifetime quenching. Additionally, we have carried out an extensive statistical and global analysis of several fluorescence lifetime and anisotropy models. The four mutants show a significant diversity of fluorescence response in their folding properties as well as in their native states (e.g., in the native state, emission maxima vary from 328 nm to 356 nm, and intensity-averaged lifetimes range from 2 ns to 6 ns). This diversity can be correlated with the location and the dynamic environment of the tryptophan residue.

## Tu-Pos296

CHARACTERIZATION OF THE SLOW FOLDING REACTIONS IN THE TRP APOREPRESSOR FROM *E. COLI*. (Xiao Shao and C. Robert Matthews) Department of Chemistry, The Pennsylvania State University, University Park, Pennsylvania 16802.

The refolding of the dimeric trp aporepressor from *E. coli* has previously been shown to involve three slow phases whose relaxation times are independent of urea concentration below 3 M urea at pH 7.6 and 25°C [M. S. Gittelman & C. R. Matthews (1990) *Biochemistry* 29, 7011-7021]. The role of cis/trans proline isomerization in these phases was tested by constructing four single proline mutations, P6H, P37A, P45G, and P93G, and the quadruple mutant, des-Pro and examining their folding behaviors. Similar to wild type repressor, three urea-independent slow folding phases are observed for all five mutant proteins. To test whether these phases are influenced by proline isomerization reactions in a more subtle way, the rates were measured in the presence of cyclophilin which is known to accelerate such reactions. The rates of the slowest phases for wild type, P6H, P37A, and P96G repressors were increased by a factor of ~3 at 500 nM cyclophilin while the rates of the des-Pro and P45G remained unchanged. This result shows that cis/trans isomerization at the T44/P45 peptide bond is coupled to another type of slow folding reaction which limits folding in the slowest reaction for P45G and des-Pro proteins. The activation energy for the slowest folding phase in wild type repressor was found to be  $16.3 \pm 0.6$  kcal/mol and that in the des-Pro repressor was  $15.7 \pm 1.1$  kcal/mol. Taken together, these results show that proline isomerization is not ultimately responsible for the three slow folding phases in trp aporepressor. Some other type of reaction with a high activation energy and which is independent of the denaturant concentration is involved. This work was supported by the NIH through grant GM 23303.

## Tu-Pos298

## Approaching Critical Aggregation Concentrations in Chaperonin Assisted Protein Folding: Confirmation of the release and rebinding mechanism. K.E. Smith and M.T. Fisher, Department of Biochemistry and Molecular Biology, University of Kansas Medical Center, Kansas City, KS 66160

The Chaperonins, groEL and groES, are known to assist in the folding of protein both *in vitro* and *in vivo*. Recent evidence suggests that Chaperonin bound proteins fold via complete release from and rebinding to the Chaperonin. This mechanism has been criticized on the grounds that released folding intermediates would still have the propensity to misfold and aggregate yet this has generally not been observed. Since aggregation is concentration dependent, the release and rebinding mechanism predicts that aggregation may be observed at higher concentrations of released folding intermediates. groEL-rhodanese complexes were formed at 2:1 and 1:1 molar ratios (groEL oligomer:rhodanese monomer) and concentrated using centrifugal ultrafiltration. With groE in excess, ATP induced renaturation yielded high recoveries ( $\geq 90\%$  of original) at initial unfolded rhodanese concentrations as high as 500  $\mu$ g/ml. However, at stoichiometric ratios, a decrease in reactivable rhodanese was observed at less than 100  $\mu$ g/ml. Addition of excess groEL to the latter solution showed a marked effect on the final renaturation yields. Our results support the rebinding and release mechanism and indicate that the critical aggregation concentration of Rhodanese is dependent on the groE concentration. Supported by NIH grant GM49309.

## Tu-Pos295

## THE PROTEIN FOLDING TRANSITION IN STAPHYLOCOCCAL NUCLEASE IS CHARACTERIZED BY A POSITIVE ACTIVATION VOLUME

((Gediminas Vidugiris\*, Dagmar Truckses<sup>o</sup>, Ken Prehoda<sup>o</sup>, Andrew Hinck<sup>o</sup>, Stuart Loh<sup>o</sup>, John Markley<sup>o</sup> and Catherine A. Royer\*)) University of Wisconsin-Madison, \*School of Pharmacy, <sup>o</sup>Department of Biochemistry

Pressure jump relaxation kinetics measurements of the unfolding and refolding of staphylococcal nuclease reveal that the rates of both transitions are diminished as pressure is increased. For example, at pressures near 1.5 kbar, both the unfolding and refolding transitions occur on a timescale of near ten minutes, compared to timescales of near one second for pH or denaturant jump kinetics at atmospheric pressure. This simple observation leads to the conclusion that the activation volume for both transitions is positive. Refolding transitions fit well to a simple monoexponential decay. At pressures below the transition midpoint,  $\log \tau$  vs pressure yields an activation volume for the refolding transition of +70 ml/mole. Such an increase in system volume can be interpreted as arising from a transition state structure that excludes solvent, yet is not well packed. Unfolding transitions were complex and good fits were obtained with a double exponential decay, implying at least two steps to the unfolding. Nonetheless, the average relaxation time increased with increasing pressure, indicating a positive activation volume of unfolding. Mutant nucleases were investigated as a means of identifying the basis for the value of the activation volume and the complex unfolding profiles.

## Tu-Pos297

## DYNAMICS OF SECONDARY STRUCTURE FORMATION IN A MODEL SYSTEM

((Anne Gershenson, Ari Gafni and Duncan G. Steel)) Institute of Gerontology, University of Michigan, Ann Arbor, MI 48109

The formation of secondary structure is believed to occur early in the folding of globular proteins. However, experimental information on the dynamics of this process is minimal due to the difficulty in obtaining data on short time scales. We are using polyglutamic acid (PGA) as a model system for studying secondary structure formation. PGA undergoes a coil to  $\alpha$  helix transition upon lowering the pH from neutral to acidic. The two conformations have been extensively studied under steady state conditions using intrinsic PGA optical activity as well as the fluorescence and optical activity of dyes bound to PGA. To investigate the kinetics of the PGA conformational change on the millisecond time scale we jump the pH via stopped flow and monitor the changes in fluorescence of bound dyes due to the coil-helix transition. The information from stopped flow experiments provides a baseline for looking at conformational changes on shorter time scales using light induced transient pH jumps. Transient changes in the pH result from the fact that the pKs of aromatic alcohols are much lower in the excited singlet state than in the ground state. Thus, by using a UV laser pulse to excite an aromatic alcohol we can transiently increase the hydrogen ion concentration by orders of magnitude and monitor the fluorescence and optical activity of dyes bound to PGA. The dependence of folding rates on polymer chain length and the magnitude of the pH change employed to induce the coil-helix transition are being studied.

Supported by NIA grant #AG09761 and ONR contract #N00014-91-J-1938

## Tu-Pos299

PREPARATION, CHARACTERIZATION AND AGGREGATION KINETICS OF TWO ASSOCIATED STRUCTURES OF RECA PROTEIN FROM *ESCHERICHIA COLI*. ((D.M. Budzynski and A.S. Benight)) Department of Chemistry, University of Illinois, Chicago, IL, 60607.

Conditions that led to isolation of homogeneously pure, milligram quantities of two distinctly different RecA associated structures were identified. These protein species (the large and small structures) were studied by dynamic and total intensity light scattering. The large structure had an average translational diffusion coefficient,  $D_{90}(L) = 8 \pm 2 \times 10^{-8}$  cm<sup>2</sup>/s, a molecular weight,  $M_r = 1.8 \pm 0.2 \times 10^6$ , and radius of gyration,  $R_g = 465 \pm 29$  Å. The small structure had  $D_{90}(S) = 20.5 \pm 2.5 \times 10^{-8}$  cm<sup>2</sup>/s,  $M_r = 6.8 \pm 0.5 \times 10^5$ , and  $R_g = 300 \pm 20$  Å. The small structure could be converted to the large structure by heating. The large structure could be converted to the small structure by prolonged incubation at 4°C. Temperature dependence of the kinetics of MgCl<sub>2</sub> induced aggregation of the freshly prepared large and small structures and the large structure prepared from the small structure was investigated. Results provided an evaluation of the activation thermodynamics for MgCl<sub>2</sub> induced aggregation of the RecA structures. For the freshly prepared large structure,  $E_a = 358$  kcal/mol, four times higher than that of the freshly prepared small structure, and eight times higher than that of the large structure prepared from the small structure. These measurements provide new insights into mechanisms of RecA aggregation. (Supported by NSF)